CHARACTERIZATION AND PERFORMANCE OF ZERO-CEMENT CONCRETE

PREPARED BY:

Eslam Gomaa
Simon Sargon
Cedric Kashosi
Ahmed Gheni
Mohamed ElGawady, Ph.D.
William Schonberg, Ph.D., PE
Missouri University of Science and Technology

PREPARED FOR:
Missouri Department of Transportation
Construction and Materials Division Research Section

TECHNICAL REPORT DOCUMENTATION PAGE

1. Report No. cmr 18-011	2. Government Accession No.	3. Recipient's Catalog No.	
4. Title and Subtitle Characterization and Performance of Zero-Cement Concrete		**5. Report Date** May 2018 Published: December 2018	
		6. Performing Organization Code	
7. Author(s) Eslam Gomaa https://orcid.org/0000-0002-8748-8867 Simon Sargon Cedric Kashosi Ahmed Gheni https://orcid.org/0000-0001-9042-869X Mohamed ElGawady, Ph.D. https://orcid.org/0000-0001-6928-9875 William Schonberg, Ph.D, PE https://orcid.org/0000-0002-6405-349X		**8. Performing Organization Report No.**	
9. Performing Organization Name and Address Department of Civil, Architectural and Environmental Engineering Missouri University of Science and Technology 1401 N. Pine St., Rolla, MO 65409		**10. Work Unit No.**	
		11. Contract or Grant No. MoDOT project # TR201614	
12. Sponsoring Agency Name and Address Missouri Department of Transportation (SPR) Construction and Materials Division P.O. Box 270 Jefferson City, MO 65102		**13. Type of Report and Period Covered** Final Report (January 2017-April 2018)	
		14. Sponsoring Agency Code	

15. Supplementary Notes

Conducted in cooperation with the U.S. Department of Transportation, Federal Highway Administration. MoDOT research reports are available in the Innovation Library at https://www.modot.org/research-publications.

16. Abstract

This study has investigated the feasibility of using five different types of class C fly ashes (FAs) sourced from Labadie, Jeffrey, Kansas City, Thomas Hill, and Sikeston power plants in the state of Missouri to synthesize zero-cement concrete (ZCC) for different structural and repair applications. Alkali activator (Alk) consisting of sodium silicate (SS), Na_2SiO_3, and sodium hydroxide (SH), NaOH were used to synthesize the ZCC. Slag, crumb rubber, and air-entraining admixture (AEA) were used in a few mixtures as additives to improve the durability of the ZCC. Approximately 300 mortar and concrete mixtures were prepared during this study to investigate the mixing procedure, water/FA, Alk/FA, SS/SH, curing regime, fresh properties, mechanical properties, durability, repair applicability, and cost analysis of the ZCC. A 5000 psi MoDOT conventional concrete (CC) mixture was also prepared and tested for comparison purposes. This study revealed that ZCC can be used as a replacement for CC. ZCC showed good workability and adequate compressive strength for structural applications ranging from 3,660 psi to 7,465 psi based on the curing regime and source of FA. Some ZCC mixtures successfully passed 300 cycles of freeze and thaw per ASTM C666-15 procedures A and B. Furthermore, the drying shrinkage values of the ZCC specimens at all ages were significantly lower than those of the corresponding CC specimens. ZCC also presents higher corrosion resistance compared to CC. ZCC mixtures have a low to moderate permeability and chloride ion penetrability, while the CC mixture showed a high permeability and chloride ion penetrability. Finally, ZCC can be used as a repair material for existing concrete structures. The bond between ZCC as a repair material and CC as a host material was adequate and comparable to the bond between CC and CC.

17. Key Words Admixtures; Binders; Bridge decks; Concrete; Fly ash; Girders; Hydration; Portland cement		**18. Distribution Statement** No restrictions. This document is available through the National Technical Information Service, Springfield, VA 22161.	
19. Security Classif. (of this report) Unclassified.	**20. Security Classif. (of this page)** Unclassified.	**21. No. of Pages** 327	**22. Price**

Form DOT F 1700.7 (8-72) Reproduction of completed page authorized

FINAL REPORT

Characterization and Performance of Zero-Cement Concrete

Prepared for

Missouri Department of Transportation

By

Eslam Gomaa
Simon Sargon
Cedric Kashosi
Ahmed Gheni
Mohamed ElGawady, Ph.D.
William Schonberg, Ph.D, PE

Missouri University of Science and Technology, Rolla, Missouri

May 2018

COPYRIGHT STATEMENT

Authors herein are responsible for the authenticity of their materials and for obtaining written permissions from publishers or individuals who own the copyright to any previously published or copyrighted material used herein.

DISCLAIMER STATEMENT

The opinions, findings, and conclusions expressed in this document are those of the investigators. They are not necessarily those of the Missouri Department of Transportation, U.S. Department of Transportation, or Federal Highway Administration. This information does not constitute a standard or specification

ACKNOWLEDGMENTS

EXECUTIVE SUMMARY

This study has investigated the feasibility of using locally available fly ashes (FAs) to synthesize zero-cement concrete (ZCC) for different structural and repair applications. Using ZCC made of 100% FA reduces global CO_2 emissions, saves energy, and decreases raw material consumption during the production process of ordinary Portland cement. Class C FAs, sourced from Labadie, Jeffrey, Kansas City, Thomas Hill, and Sikeston power plants in the state of Missouri, were used to synthesize the ZCC. Two different alkali activators (Alk) were used in this study: sodium silicate (SS), Na2SiO3, and sodium hydroxide (SH), NaOH. Slag, crumb rubber, and air-entraining admixture (AEA) were used in a few mixtures as additives to improve the durability of the ZCC. The mixing procedure, water/FA, Alk/FA, SS/SH, curing regime, fresh properties, mechanical properties, durability, repair applicability, and cost analysis of the ZCC were investigated in this study. Approximately 300 mortar and concrete mixtures were tested. A 5000 psi MoDOT conventional concrete (CC) mixture was prepared and tested for comparison purposes. Three curing regimes (oven, ambient, and moist) were applied to the ZCC.

This study revealed that ZCC can be used as a replacement for CC. ZCC showed good workability and adequate compressive strength for structural applications ranging from 3,660 psi to 7,465 psi based on the curing regime and source of FA. Some ZCC mixtures successfully passed 300 cycles of freeze and thaw per ASTM C666-15 procedures A and B. Furthermore, the drying shrinkage values of the ZCC specimens at all ages were significantly lower than those of the CC specimens. ZCC also presents higher corrosion resistance compared to CC. ZCC mixtures have a low to moderate permeability and chloride ion penetrability, while the CC mixture showed a high permeability and chloride ion penetrability. Finally, ZCC can be used as a repair material for existing concrete structures. The bond between ZCC as a repair material and CC as a host material was adequate and comparable to the bond between CC and CC.

The relationships between the compressive strength of ZCC and splitting tensile strength, flexural strength, and modulus of elasticity are similar to those used by current codes and standards such ACI 318-14. Finally, ZCC is cost competitive; the cost of ZCC ranged from \$59/yd^3 to \$105/yd^3.

Table of Contents

List of Figures

xviii

List of Tables

Chapter 1:   Introduction

1.1 Background

The annual global concrete production amounts to four tons per capita and about 1.7 tons in the United States [1]. The U.S. consumed about 230 million m^3 of ready mixed concrete during 2014 [1]. These tremendous numbers are due to the multiple construction applications of concrete, including buildings, bridges, tunnels, pavement, and dams. It was estimated that more than 70% of the bridges and 50% of the low rise buildings throughout the U.S. are constructed using concrete [1], which makes it the most consumed material after water in the world [2].

Concrete is a composite material that includes cement, aggregates, and water. Cement acts as the binder of the concrete, so it is one of the most important concrete components. The volume of cement represents between 7% to 14% of the total volume of the concrete mixture [1]. The global production of the cement industry has had a massive growth; in 1950 the production was 133 million tons and increased to 4.2 billion tons in 2014 [3]. The U.S. consumed 86.5 million metric tons of Portland cement (OPC) in 2014 [1]. However, the production of one ton of ordinary Portland cement causes about one ton of CO_2 emissions, which represents about 8% of the global CO_2 emissions [4-7]. In addition, 1.7 tons of raw materials are required for the production of one ton of cement. Furthermore, the consumed energy during the cement production is about 3000 kJ for each kg of clinker during the cement production. Therefore, finding a more environmentally friendly alternative to cement is an urgent need.

One way to reduce cement usage is to partially replace it with by-product or natural pozzolanic materials such as fly ash (FA), ground granulated blast furnace slag (GGBFS), and metakaolin (MK). Utilizing fly ash in the concrete industry has not only a good impact on the environment

but also improves the rheology, mechanical strength, durability, and economy of concrete production [8, 9]. However, FA has a negative effect on the concrete's early strength, especially with a high replacement ratio [10].

Another way to improve the sustainability of concrete is totally replace the cement by these by-products or natural pozzolanic materials, producing zero-cement concrete (ZCC) [6, 11]. The ZCC is synthesized by reacting a material rich in silica and alumina such as FA with alkali solutions such as sodium silicate and/or sodium hydroxide that induce the formation of strong binding phases. ZCC possess attractive characteristics such as sustainability [12], lower shrinkage [13], better fire and acid resistance, durability [14], lower creep [15], and better resistance to sulphuric acid attack [16].

1.2 Fly Ash (FA)

FA is a by-product of coal combustion during energy generation in power plants. The FA production in the U.S. reached 53.4 million tons in 2013 [17]. According to a forecast study prepared by the American Road and Transportation Builders Association, FA production will reach 54.6 in 2033 with two 95% confidential intervals as shown in Fig. 1.1, which assure the sustainability of FA production for long term usage [17]. There will be a relatively unchanged amount of electrical power generated from coal in the next few decades due to several socioeconomic factors [17].
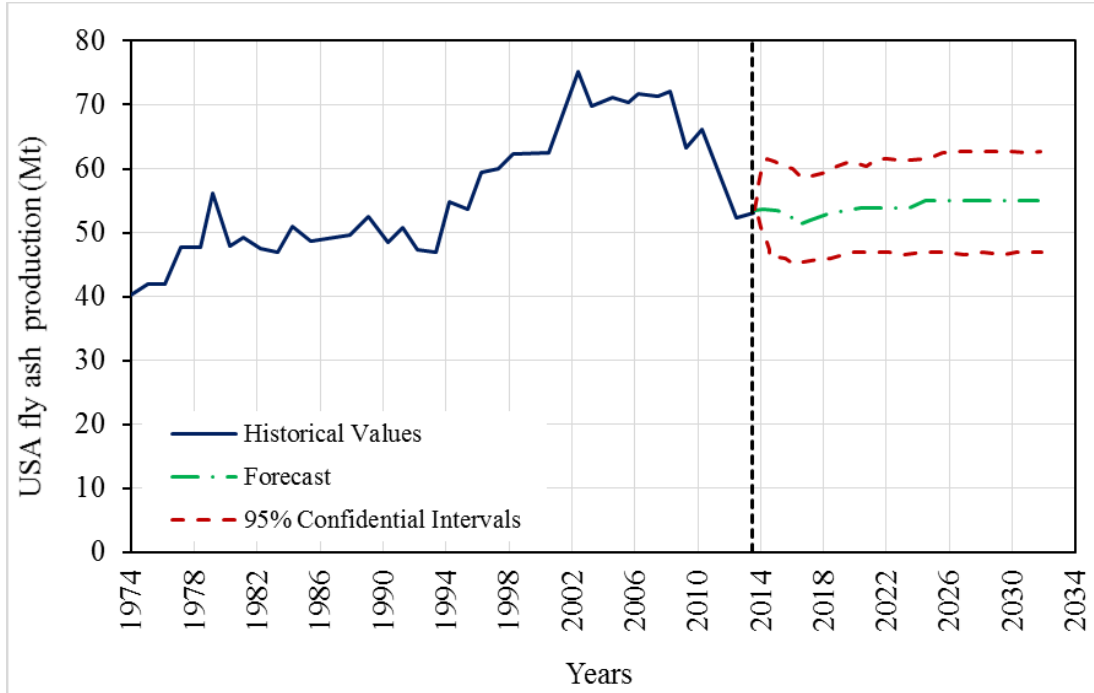
Figure 1.1: FA production [17].

Missouri is the fourth largest coal consumer in the U.S. [18]. Coal-fired power plants generate 6,679 thousand MWh or 81.3% of the electricity in the state of Missouri which generate about 2.7 million tons of coal combustion residuals (CCRs) annually. The CCR disposal issue is not limited to Missouri; rather, it is a national issue with CCRs being the second largest waste stream in the U.S. One-hundred and forty million tons of fly ash, a byproduct of coal combustion, is generated annually in the U.S. Only 50 million tons are reused, and the remaining fly ash is stored in landfills at dry storage and ponds, where water is added to stabilize the fly ash [17]. Embankment collapses in these ponds may lead to destruction of nearby areas and leaching of heavy metal into soil [19]. On December 22, 2008, a dike which was holding back an 84 acre pond of wet coal ash collapsed at the Tennessee Valley Authority's Kingston plant, filling the Emory River with ash and creating huge mounds of toxic waste (Fig. 1.2) [20, 21].

Figure 1.2: A failed impoundment at the Kingston plant in eastern Tennessee [20].

1.2.1 Chemical properties

The binder in ZCC consists of an alumina-silicate rich material such as FA and alkali activators. FA is a combination of coal impurities and flue gases, and hence there is strong variability in the physical and chemical properties of FA. The FA chemical composition is affected by the type of burned coal that is used to produce it. Table 1.1 summarizes the chemical composition of the FAs derived from different coals sources [22].

Table 1.1: Chemical Composition of the FAs Derived from Different Coal Sources (%) [22].

Chemical composition	Bituminous	Sub-bituminous	Lignite
SiO_2	20-60	40-60	15-45
Al_2O_3	5-35	20-30	10-25
Fe_2O3	10-40	4-10	4-15
CaO	1-12	5-30	15-40
MgO	0-5	1-6	3-10
Na_2O	0-4	0-2	0-6
K_2O	0-3	0-4	0-4
SO_3	0-4	0-2	0-10
LOI[*]	0-15	0-3	0-5

[a]LOI: Loss on ignition

ASTM C618-15 [23] classifies FA into two types, class C and class F, based on the summation of the oxide content. In the case of class F, the oxides' content is higher than or equal to 70% of

4

the total weight of the FA while it has to be between 50% and 70% of the total weight of the FA in the case of class C. Despite the importance of the calcium content on the characteristics of FA, ASTM C618-15 doesn't consider that. However, it is more common to find that class F has a low calcium content while class C has high calcium content. Other standards, such as CSA A3001 [24], considers the calcium content when classifying a FA. CSA A3001 [24] classifies FA into three classes. Class F, which has CaO up to 8%, class CI, which has CaO from 8% to 20%, and class CH, which has CaO more than 20%. Fig. 1.3 presents a correlation between ASTM C618-15 and CSA A3001 classifications.
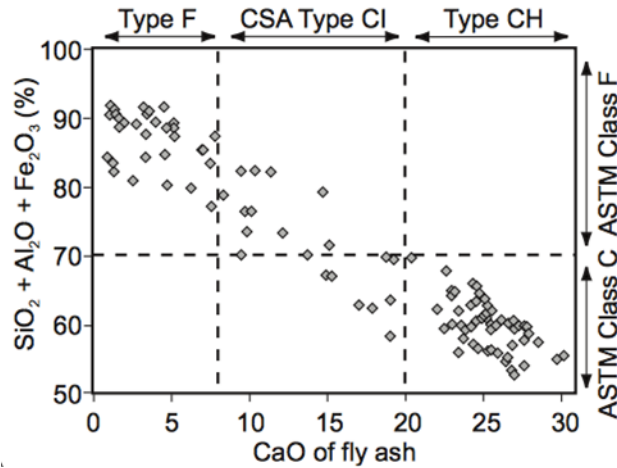
Figure 1.3: Correlation between the ASTM C618-15 [23] and CSA A3001 [24] classifications.

1.2.2 Physical properties

FA particles have either a solid or hollow spherical shape. The majority of the FAs are amorphous (glassy) material in nature [22]. The particle size distribution of most of the bituminous FAs is smaller than 0.0029 in (sieve no. 200) [22], while those derived from sub-bituminous coals have slightly coarser particles. The FA specific gravity ranges from 2.1 to 3.0 depending on its chemical composition[22]. The FA surface area ranges from 119522 to 703070 in^2/lb (170 to 1000 m^2/kg) [22]. Increasing the surface area of FA by grinding resulted in higher

strength [25]. However, grinding FA increases the production cost. Similarly, the particle size distribution of FA affects the performance of ZCC [26].

1.3 Constituents of Zero-Cement Concrete (ZCC)

ZCC is a relatively new type of concrete where the Portland cement binder in conventional concrete is replaced with other binders. In the 1970s, Davidovits developed a new class of concrete material called geopolymer concrete (GC) in which 100% of OPC is replaced with aluminosilicate-rich material such as fly ash that is polymerized using an alkaline solution. The chemical reaction, which is called geopolymerization, takes place between the aluminosilicate and alkaline solution resulting in an inorganic amorphous three-dimensional polymeric chain and ring structure consisting of Si-O-Al-O bonds [27-30]. The geopolymerization process can be described by Eq. 1.1 [31]. The geopolymerization is quite different from the common hydration process that takes place in conventional concrete (CC).

$$n(Si_2O_5, Al_2O_2) + 2nSiO_2 + 4nH_2O + (Na^+, K^+) \rightarrow n(OH)_3 - Si - O - Al^- - O - Si - (OH)_3 \quad (1.1a)$$
$$|$$
$$(OH)_2$$

$$n(OH)_3 - Si - O - Al^- - O - Si \rightarrow (Na^+, K^+) - (-Si - O - Al^- - O - Si - O -)n + 4nH_2O \quad (1.1b)$$
$$|\quad\quad\quad| \quad\quad\quad\quad |\quad\quad |\quad\quad |$$
$$(OH)_2 \quad (OH)_3 \quad\quad\quad\quad O \quad\quad O \quad\quad O$$
$$|\quad\quad |\quad\quad |$$
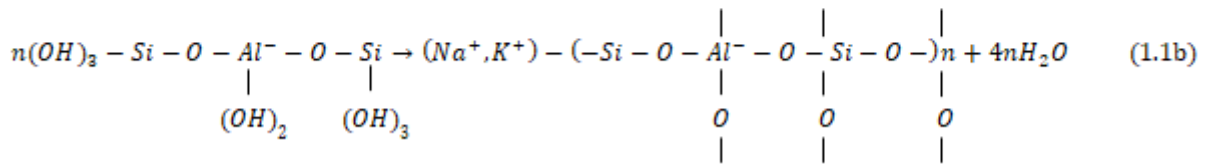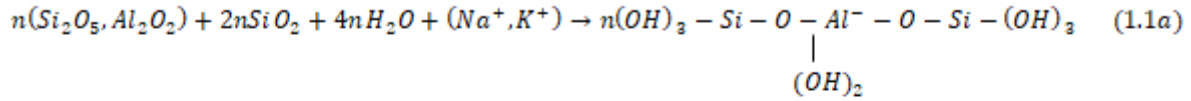
1.3.1 Precursors

Both class F and C FAs as well as slag were used to synthesize ZCC. FA has a finer particle size than slag; therefore, FA displayed higher reactivity [32]. Early research on ZCC focused on using Class F (low calcium) FA as a precursor due to its low calcium content [13, 33-39]. The calcium content in the case of FA class F is considered as a contamination, producing different

chemical assemblage that may cause lower strength and a lower reaction rate [32, 40, 41]. Recently, class C FA has been emerged as a promising precursor [5, 42-46]. The existence of calcium in class C FA forms calcium silicate hydrate (C-S-H) while the alumina and silicate go through the geopolymerization process. Therefore, as the fraction of calcium silicate hydrate increases, the setting time decreases, and the compressive strength increases [21]. Class F FA is generally used in production of ZCC cured at elevated temperatures where the geopolymerization process requires a higher temperature in order to take place [47], while class C FA is generally used in production of ambient-cured ZCC.

FA's chemical and physical properties have significant effects on ZCC. FA was sourced from 25 different sources (13 class F and 12 class C) to study the effect of the different chemical composition on the fresh and mechanical properties of ZCC [48]. The silica, alumina, and calcium oxide of the FAs ranged from 27.15% to 62.121%, 14.72% to 28.61%, 1.97% to 33.39%, respectively. The setting time of class F and class C FA ranged from 25 to 600 minutes and from 1.5 to 285 minutes, respectively, indicating that the setting time of FA class C is shorter than that of class F. Furthermore, a single ZCC mixture was prepared where each of these FA was used as a precursor. The mixture displayed a wide range of compressive strength ranging from 400 psi (2.73 MPa) to 11655 psi (80.37 MPa).

In another study, five FAs were investigated as ZCC precursors [21]. With increasing the calcium content in the FA, the compressive strength of the specimens cured for 3 days at 140° F (60° C) increased and the setting time decreased. The finer particle size of some FAs led to a higher surface area resulting in more reactive FA and higher compressive strength. Also, the compressive strength of ZCC increased with increasing the amorphous phase as it is easier to be dissolved by the alkali activator compared to the crystalline phase. It is worth noting that while

7

FA with fine particles displayed better reactivity [25, 49], in some cases this led to a very short setting time and hence bad workability and low strength [50].

1.3.2 Alkali activators

The performance of ZCC is affected by the type and concentration of the alkaline activator. Most of the used alkali activators are in liquid form [5, 44, 45, 51]. Two alkali activators are used to synthesize ZCC, sodium silicate (SS)/potassium silicate (PS) and/or sodium hydroxide (SH)/potassium hydroxide (PH). One of the advantages of the PS over the SS is its lower viscosity compared with that of SS [6] and hence the potassium-based ZCC displays higher workability and compressive strength. However, the potassium-based activators are more expensive [52]. Furthermore, Si and Al from the precursor become more soluble in the existence of SS [53]. However, the potassium-based activators are more expensive [52]. Therefore, commonly SS and/or SH are used to synthesize ZCC.

It is common practice to mix SH with SS producing aqueous alkaline where the existence of soluble silicate is important as it provides the species required to initiate the oligomers formation and polycondensation of silicate and/or alumina-silicate from the precursor material. There is no consensus on the optimum SH molarity and SS/SH. Molarity values ranging from 3M to 20M and SS/SH values ranging from 0.0 to 3.0 were reported to produce the highest compressive strength and workability. It should be noted that sodium silicate is generally more expensive than sodium hydroxide and hence optimizing SS/SH is crucial for the economical production of ZCC.

ZCC having SH molarity ratios ranging from 10M to 20M and SS/SH ranging from 0.67 to 3.0 were instigated for FA class F precursor [44]. Increasing the SH molarity from 10M to 20M and increasing the SS/SH from 0.67 to 3.0 decreased the workability. However, the effect of the SH

molarity between 10M and 20M on the compressive strength was small. The highest compressive strength was achieved at SS/SH of 0.67-1.0 (Fig. 1.4).

Other researchers [45] found that the highest compressive strength for FA class F precursor was obtained with SH with molarity of 15M and SS/SH of 1.0 and 2.0. Furthermore, for mixtures with SS/SH of 1.0, the setting time and workability decreased with increasing the SH molarity. However, the setting times and workability values of mixtures having SS/SH of 2.0 and SH of 10M and 15M were not consistent (Table 1.2). Similar recommended values of SH molarity of 14M [13, 51] and SS/SH of 2.5 [13, 54] were found to result in the highest ZCC compressive strength and good workability of class F FA precursor and a binary binder system consisting of class F FA and slag (Figs. 1.5 and 1.6) (Table 1.3) [13, 51, 54]. Other researchers [55], however, recommended a much smaller molarity of 6M combined with SS/SH of 2.0 (Fig. 1.7) for FA class F precursor.
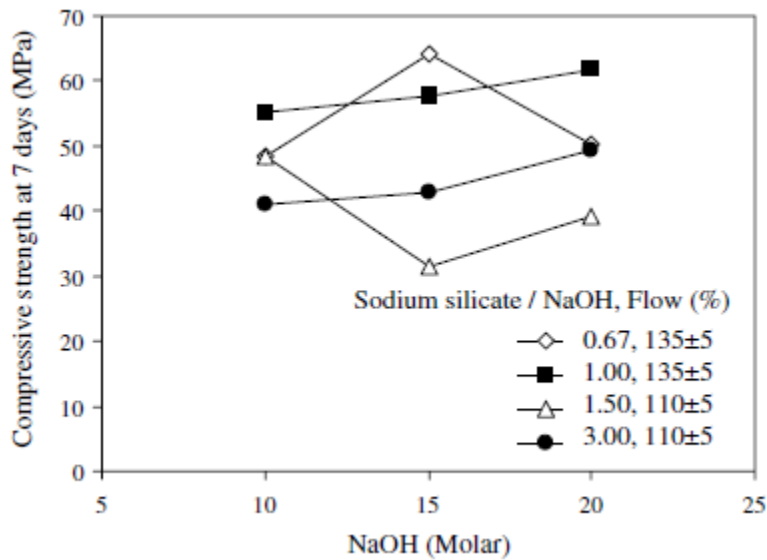
Figure 1.4: Effect of SS/SH on 7-day compressive strength [44].

Table 1.2: Flow (workability) and Setting Time of ZCC [45].

Mixes	Flow (mm)	Setting time (min)
S:H 1-10M	580	50
S:H 1-15M	560	36
S:H 1-20M	470	28
S:H 2-10M	500	52
S:H 2-15M	550	68
S:H 2-20M	530	58
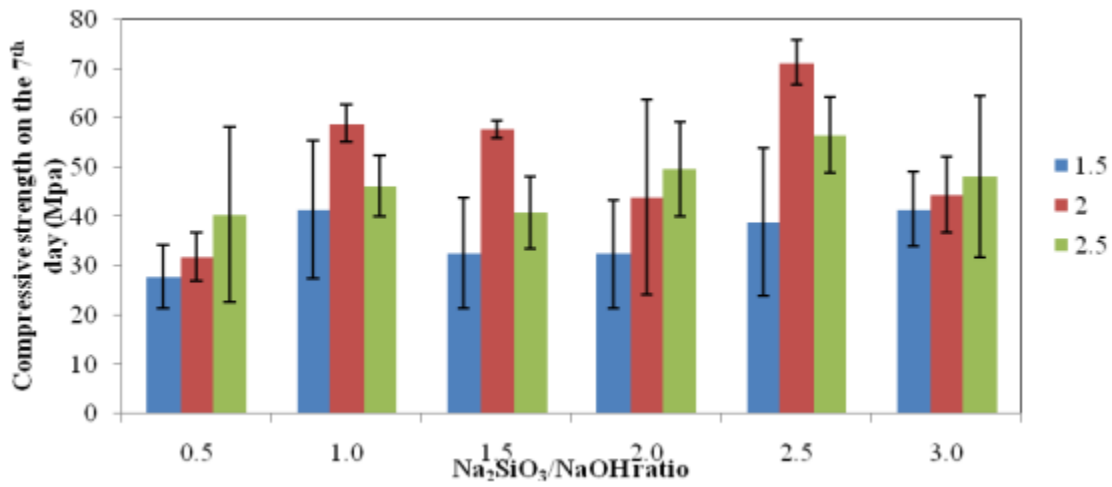
Figure 1.5: Effect of SS/SH on the compressive strength of ZCC for FA/Alk of 1.5. 2, and 2.5 [54].

Table 1.3: Effect of SH Molarity and SS/SH on Compressive Strength [13].

Mixture	Concentration of NaOH liquid in molarity (M)	Sodium silicate/NaOH liquids ratio by mass	7-day compressive strength after curing at 60 °C for 24 h, MPa
A-1	8M	0.4	17.3
A-2	8M	2.5	56.8
A-3	14M	0.4	47.9
A-4	14M	2.5	67.6
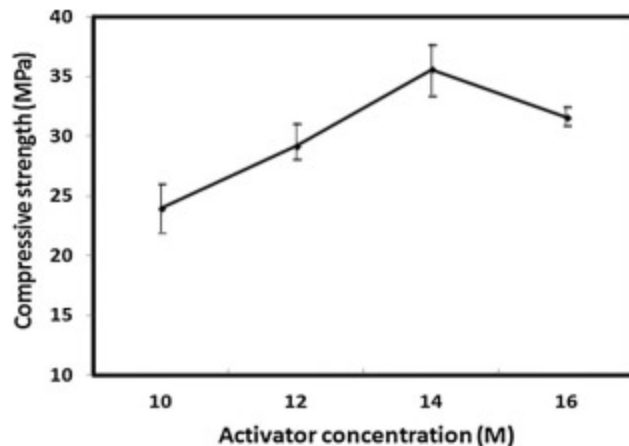
Figure 1.6: Effect of SH molarity on the compressive strength [51].
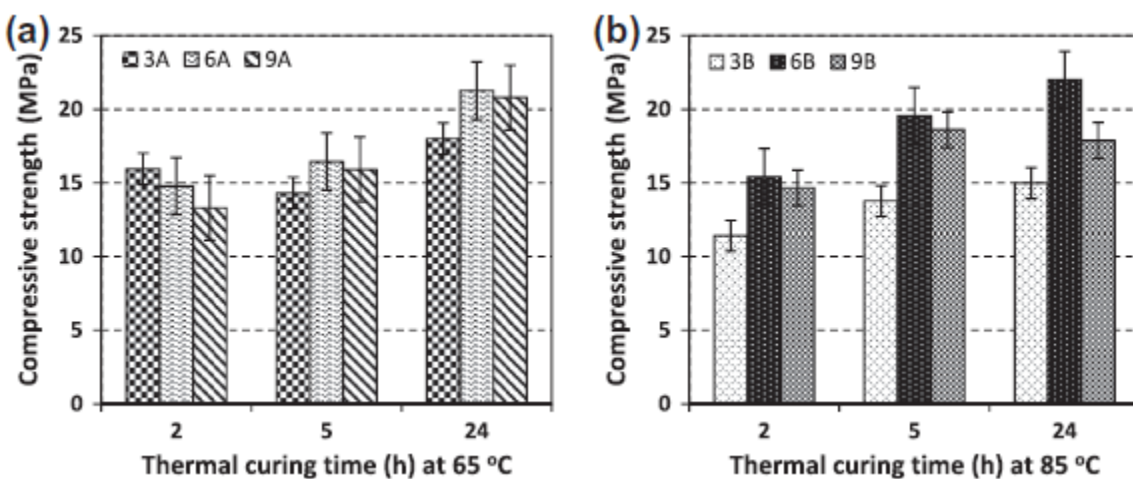
Figure 1.7: Effect of SH molarity on the compressive strength of ZCC at different curing temperatures and durations [55].

As shown in this review, there is no consensus on the required SH molarity and SS/SH in a ZCC system that yields a reasonable setting time, workability, compressive strength, and cost. These differences in the recommended values are related to the differences in the chemical and physical properties of the precursors. Therefore, it is crucial to determine the required SS/SH and molarity to synthesize a structural ZCC using local FA precursors.

1.4 Mixing and Curing Zero-Cement Concrete (ZCC)

1.4.1 Mixing procedure and energy

Different mixing procedures were used by different researchers to synthesize ZCC [38, 56-59]. The mixing procedures can be grouped as follows.

Procedure no.1 was used for ZCC or ZC mortar using class F FA [32, 59], class C FA [56], slag [57], and class F FA and slag [38, 58] precursors. This procedure includes adding the dry ingredients including the coarse aggregate, sand, and FA to the mixer; then, mixing them for one to three minutes. Then, the SS and SH that had been mixed were added to the mixer over one to five minutes. Lastly, the water and superplasticizer (if needed) were added over one minute. Once all ingredients were added, mixing continued up to four minutes.

Procedure no. 2 was used for ZCC or ZC mortar using FA class F precursors [42, 45, 60]. The FA and SH were added to the mixer over five minutes. Then, the aggregates were added to the mixer over five minutes. Lastly, the SS was added to the mixer and mixed for five minutes.

Procedure no. 3 was used for ZCC or ZC mortar using class F and class C [48], and class F [61] precursors. The FA and SH were added to the mixer over 30 seconds to five minutes. Second, the SS was added to the mixer and mixed over one minute. Lastly, the aggregates were added to the mixer over one to three minutes.

Procedure no. 4 was used for ZCC or ZC mortar using FA class F [34, 37, 62] and class C [37]. All the dry materials were mixed together for two to four minutes. Then, the alkali activators, water, and superplasticizer (if needed) were added and mixed for two to eight minutes.

Procedure no. 5 was used for ZCC or ZC mortar using FA class F with additives such as nano-silica, rice husk, nano-alumina [63], and FA class C [64]. All the dry materials were mixed

together for 1 minute or until a homogenous mixture was obtained. Then, the alkali activators were added separately. Either the SH was added first until a homogenous mixture was obtained followed by adding the SS and mixing for a further five minutes for FA class F with additives such as nano-silica, rice husk, and nano-alumina [63] or the SS was added first and mixed for two minutes followed by adding the SS which was in solid form and mixed for ten minutes for FA class C [64].

Another factor that affects the performance of ZC systems is the mixing time. A study was carried out on slag pastes and mortars to study the effectiveness of mixing time [65]. Four mixing times were used to mix the mortars including 1, 3, 10, and 30 minutes. The results revealed that increasing the mixing time from 3 to 30 minutes resulted in an increase in the initial and final setting time by 2 hours and 8 hours, respectively. Also, mixing for 30 minutes resulted in the highest workability, compressive strength, and flexural strength (Fig. 1.8). In addition, an improvement in the cohesion and compactness in the mortar mixture, which reduced the porosity and drying shrinkage of the mixture, was observed.
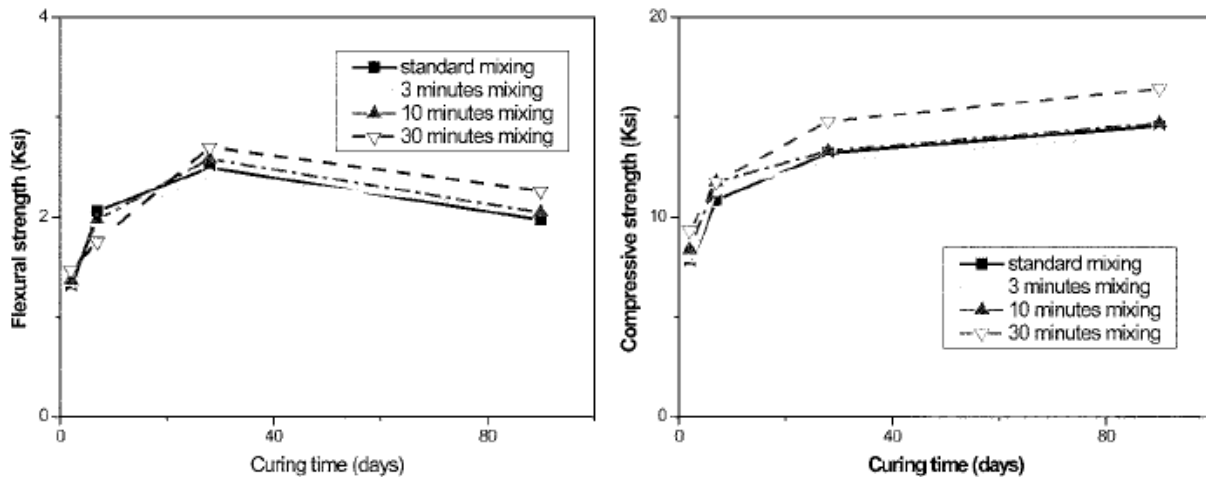
Figure 1.8: Flexural and compressive strength of ZC mortar mixed for different times [65].

Another factor that affects the performance of ZC systems is the mixing energy [66]. Mixing periods of 1, 3, and 6 minutes were used with a mixing speed of 1000 rpm to prepare ZC paste using class C FA precursor. Another mixing period of 10 minutes was used with a mixing speed of 140 rpm. Increasing the mixing time from 1 minute to 10 minutes while decreasing the mixing speed increased the initial and final setting times (Fig. 1.9). Also, mixing at a higher speed for only one minute resulted in a higher compressive strength compared with mixing at lower speed for 10 minutes, where the compressive strength increased from 9080 psi (62.6 MPa) to 10890 psi (75.1 MPa). High speed mixing resulted in uniform mixing of raw materials which is important for initial dissolution of the fly ash [67]. Furthermore, increasing the mixing speed improved the workability of the materials [63].

The presented literature showed that there is no consensus on the best approach to mix ZCC or the mixing duration and speed. Therefore, more research is required to determine the optimal ZCC mixing approach, duration, and speed.
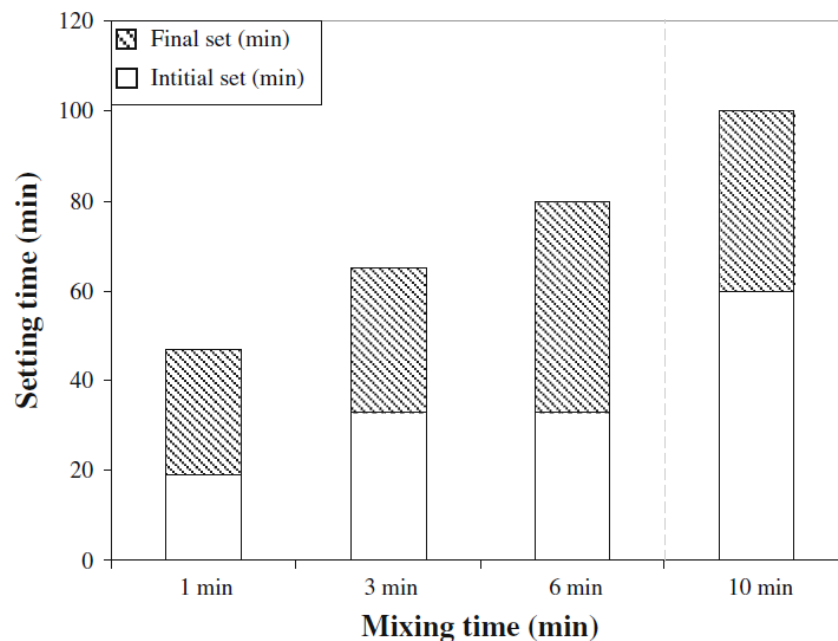
Figure 1.9: Initial and final setting time of ZC paste mixed for different times [66].

14

1.4.2 Rest time for oven-cured ZCC

The resting time can be defined as the time between the start of mixing the alkali activators with the FA and the time of placing the specimens in the oven to be cured at the assigned temperature. The rest time is an important factor that affects the strength of the mixture. Based on a study of ZC mortar synthesized using FA class F and sustaining different rest times ranging from 0 to 6 hours, the highest compressive strength was achieved after a rest time of 1 hour and curing the specimens at a temperature of 60° C (Fig. 1.10) [44].
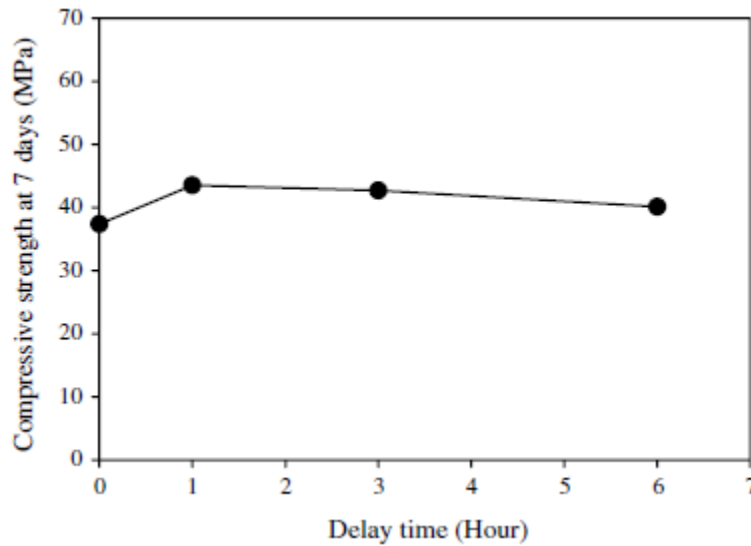
Figure 1.10: Effect of resting time on the compressive strength of ZC mortar [44].

In a different study on ZC paste with class F FA precursor [33], three curing regimes were studied. (1) The specimens were cured at room temperature for 2 hours followed by curing them at a temperature of 75° C for one month. (2) The specimens were cured at room temperature for 24 hours followed by curing them at a temperature of 75° C for 24 hours. (3) The specimens were cured at room temperature for 24 hours followed by curing them at a temperature of 75° C for 6 hours. The results revealed that a rest time of 24 hours was beneficial to strength development.

1.4.3 Curing temperature

Depending on the chemical composition and physical properties of the FA precursor, a different curing regime maybe required. Class F FA requires high-temperature curing while class C FA can be cured at ambient or high temperatures [25, 44, 68]. High temperature curing was either in a dry atmosphere, i.e., an oven, or in saturated atmosphere with RH 95 ± 5%. Ambient curing was either in a dry atmosphere; i.e., an oven, or in saturated atmosphere with RH 95 ± 5%.

Studies on FA class F based ZCC investigated the effects of different temperatures and curing periods on the compressive strength of ZCC [13]. Curing temperatures ranging from 86° F $(30^o$ C) to 194° F $(90^o$ C) were investigated. The curing time ranged from 6 to 96 hours for ZCC mixtures that cured at 140° F $(60^o$ C). Increasing the curing temperature from 86° F $(30^o$ C) to 194° F $(90^o$ C) increased the compressive strength; however, the compressive strength beyond a threshold curing temperature ranging from 140° F $(60^o$ C) to 167° F $(75^o$ C) either remained constant or decreased (Figs. 1.11 and 1.12). Furthermore, with increasing the curing time, the compressive strength increased; however, the increase in the compressive strength beyond 48 hours of curing time was not significant (Figs. 1.13 and 1.14) [44, 69, 70].
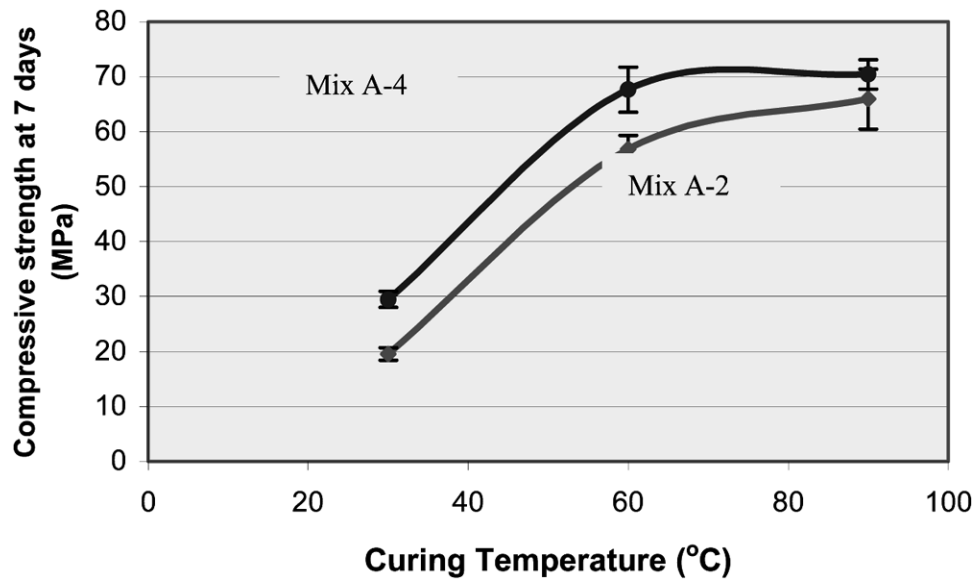
Figure 1.11: Effect of curing temperature on the compressive strength of ZCC [13].
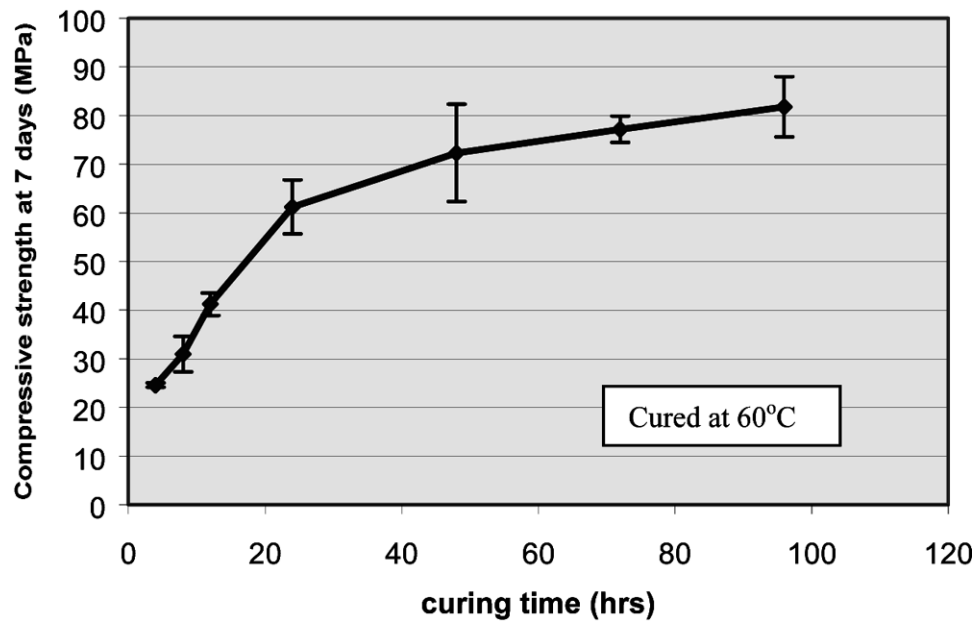
Figure 1.12: Effect of curing temperature on the compressive strength of ZCC [13].
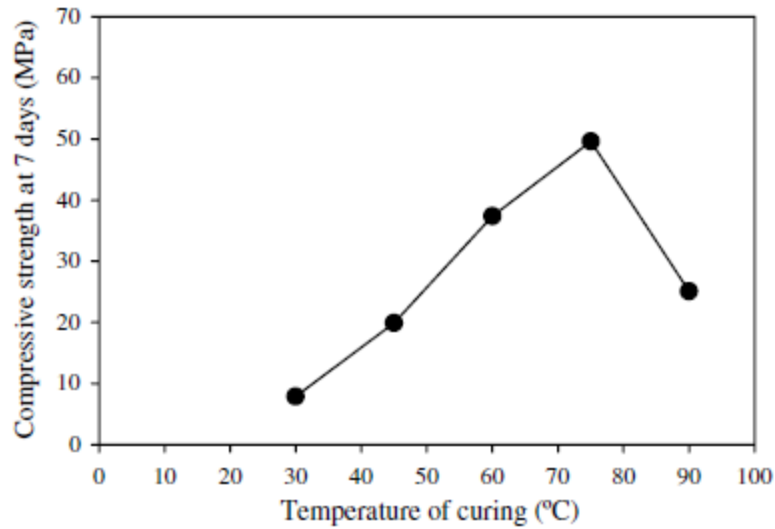
Figure 1.13: Effect of curing temperature on the compressive strength of ZC mortar [44].
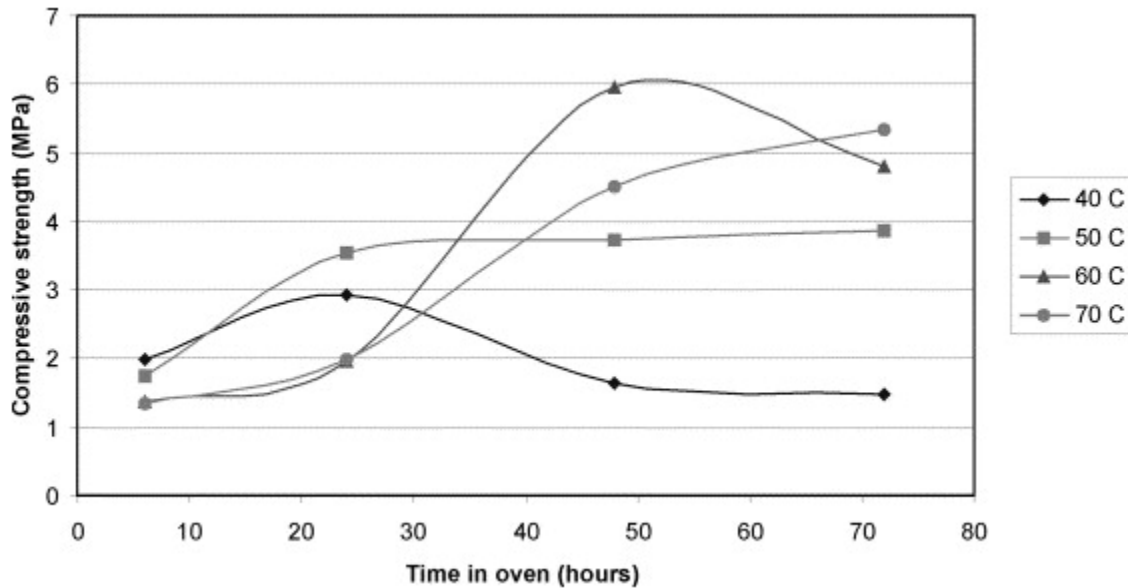
Figure 1.14: Effect of curing temperature and time on the compressive strength of ZC paste [69].

A study on the effect of two different curing regimes on the compressive strength of class F FA based ZCC was conducted [45]. Two curing regimes were applied: (1) oven curing at a temperature of 140° F (60° C) for 24 hours and then storing the specimens in the laboratory until the testing date, and (2) curing in a controlled room at a temperature of $73 \pm 3^\circ$ F ($23 \pm 3^\circ$ C). In both curing regimes, the cylinders were encased in a with vinyl sheet and stored at the

temperature of $73 \pm 3^{\circ}$ F ($23 \pm 3^{\circ}$ C). Compressive strengths ranging from 2885 psi (19.89 MPa) to 3345 psi (23.06 MPa) and from 4900 psi (33.80 MPa) to 6770 psi (46.69 MPa) at the ages of 7 and 28 days, respectively, were measured for the specimens cured at the temperature of $73 \pm 3^{\circ}$ F ($23 \pm 3^{\circ}$ C). Compressive strength ranged from 5465 psi (37.69 MPa) to 6225 psi (42.91 MPa) and from 5815 psi (40.09 MPa) to 7890 psi (54.40 MPa) at the ages of 7 and 28 days, respectively, for the specimens cured at the temperature of 140° F (60° C).

Based on the reviewed results, specimens cured at higher temperatures displayed higher compressive strengths compared to those cured at lower temperatures. However, a comprehensive study on class C FA based ZCC is required.

1.4.4 Curing regime

Three curing regimes were applied to ZC mortar having FA class F precursor including ambient, oven, and heat curing. For ambient curing, the specimens were left in the laboratory at a temperature of $86 \pm 3.6^{\circ}$ F ($30 \pm 2^{\circ}$ C). For oven curing, the specimens were covered by vinyl sheets and subjected to $140 \pm 3.6^{\circ}$ F ($60 \pm 2^{\circ}$ C) for 24 hours followed by ambient curing until the age of testing. The heat-cured specimens were covered with gunny bags and exposed to heat rays of sunlight at a temperature of approximately $95 \pm 3.6^{\circ}$ F ($35 \pm 2^{\circ}$ C) for almost 6 hours during the daytime [56]. The results revealed that at the early ages, the oven curing regime displayed higher strength compared with the other curing regimes (Fig. 1.15). However, at later ages such as 28 and 60 days, the heat curing regime displayed the highest compressive strength, which indicated that the continuous application of heat to specimens kept under external exposure curing resulted in higher compressive strength.
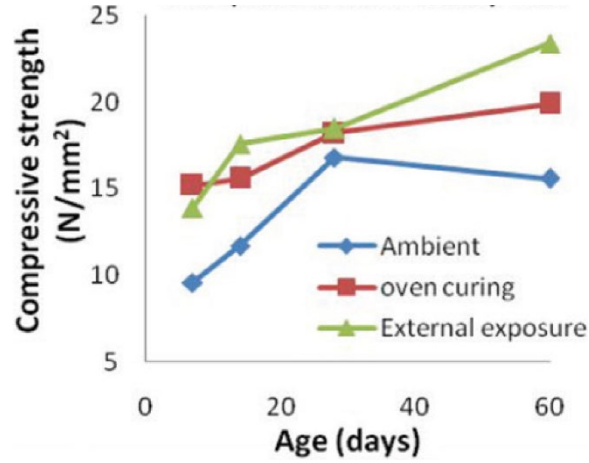
Figure 1.15: Effect of curing regime on the compressive strength of ZCC [56].

1.5 Mechanical Properties of ZCC

The other mechanical properties of ZCC, such as splitting tensile strength, flexural strength, and

modulus of elasticity were studied in the literature. Several researchers studied the splitting

tensile strength of ZCC synthesized using class F FA [36], class C FA [45], slag [57], and a

combination of class F FA and slag [35, 38]. Researchers also studied the flexural strength of

ZCC that was synthesized using class F FA and class C FA [48], slag [57], and a combination of

class F FA and slag [35]. These previous studies suggested empirical equations in the form of

Eq. 1.2 to correlate the splitting tensile strength of concrete, f_{ct}, or the flexural strength of

concrete, f_r, to its compressive strength, f_c', where k and n are constants obtained from

regression analyses of experimental data.

$$f_{ct} \text{ or } f_r = k(f_c')^n \tag{1.2}$$

Furthermore, researchers studied the modulus of elasticity of ZCC synthesized using class F FA

and class C FA [48], slag [57], class C FA and slag [46], and combination of class F FA and slag

[38]. These previous studies suggested empirical equations in the form of Eq. 2 to correlate the

modulus of elasticity of concrete, E_c, to its compressive strength, f_c', where k, n, and a are

20

constants obtained from regression analyses of experimental data and w_c is the concrete density. The modulus of elasticity of the ZCC ranged from 1450 ksi (10 GPa) to 5800 ksi (40 GPa), which is in the same range as that of the CC [71].

$$E_c = k \, (w_c)^m \, (f_c'/a)^n \tag{1.3}$$

1.6 Drying Shrinkage

Drying shrinkage of mortar and concrete can cause micro cracks where moisture and external harmful agents such as chlorides and sulfates can penetrate the structures, reducing their durability [1, 34]. The drying shrinkage of the ZC mortars and concretes were investigated in few studies. For ZC mortar synthesized using slag cured at room temperature, the dry shrinkage values were similar to those of the corresponding OPC specimens [39]. However, for the slag mortar specimens cured at room temperature with RH of 95%, the shrinkage increased compared with the specimens cured in a dry environment. Also, a high shrinkage took place at the early ages for RH conditions (Fig. 1.16). This contradicted the results of the reference OPC specimens (Fig. 1.17).

21
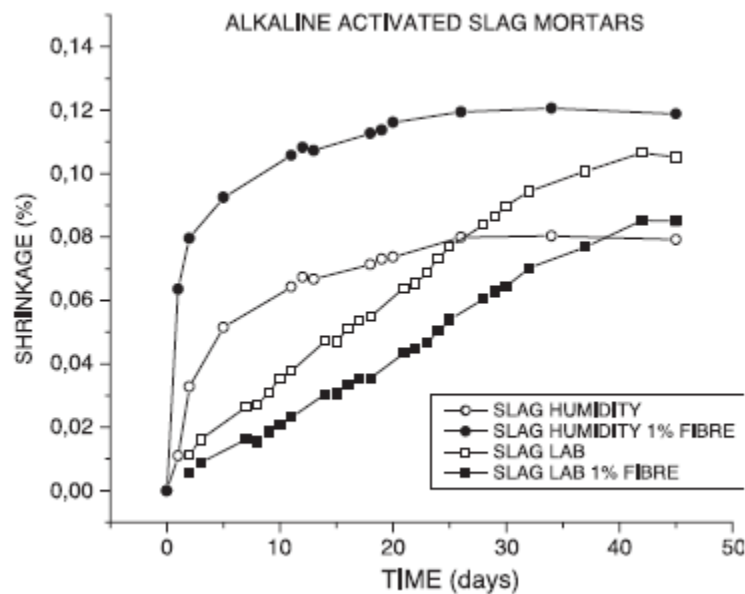
Figure 1.16: Effect of fibers and storing condition on the shrinkage over time for slag specimens [39].
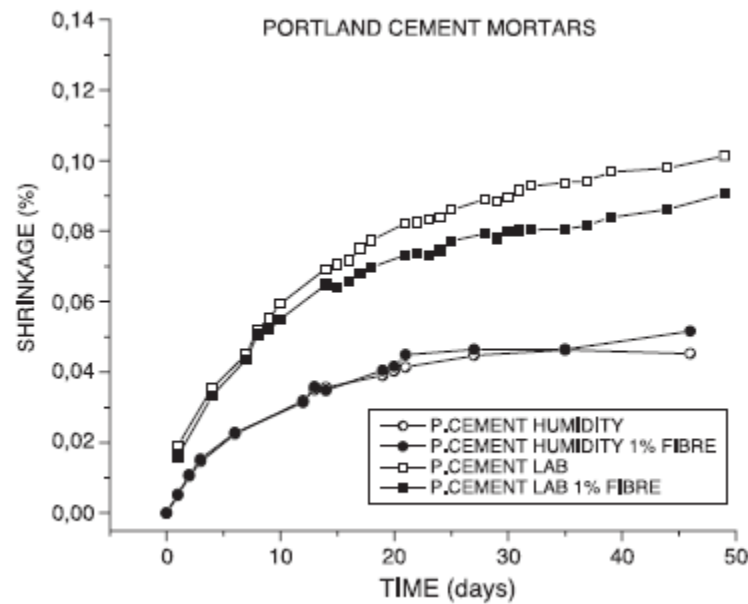
Figure 1.17: Effect of fibers and storing condition on the shrinkage over time for OPC specimens [39].
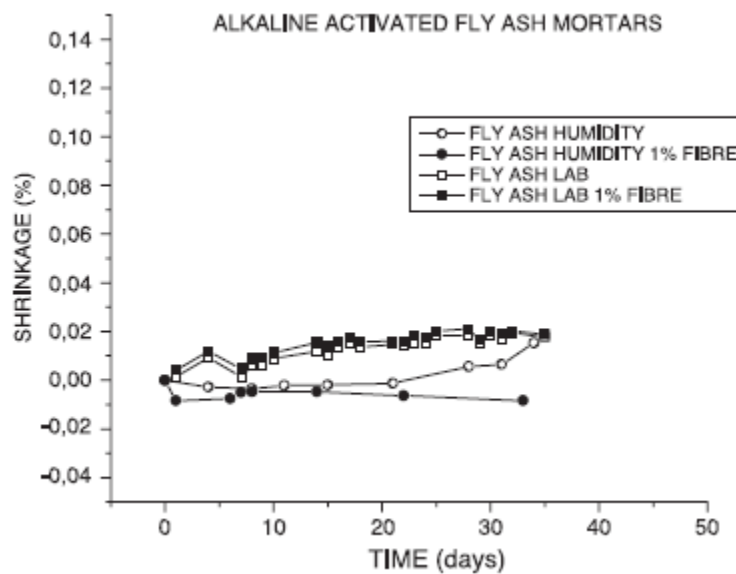
Figure 1.18: Effect of fibers and storing condition on the shrinkage over time for FA specimens [39].

ZC mortar synthesized using class F FA and thermally cured displayed approximately 80% lower shrinkage values than those of the corresponding OPC specimens (Figs. 1.19 and 1.20)

[34, 39]. Placing the ZC mortar synthesized using class F FA in 95% RH, i.e., where free water was available, decreased the shrinkage slightly compared with dry conditions [39]. Similarly, using 1% fiber did not significantly change the shrinkage [39].
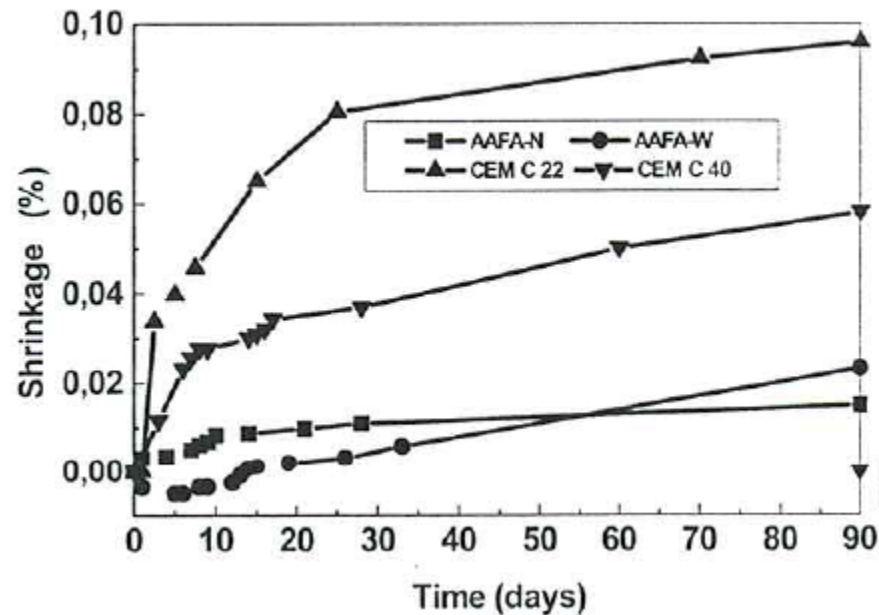
Figure 1.19: Drying shrinkage in ZC and OPC mortars [34].
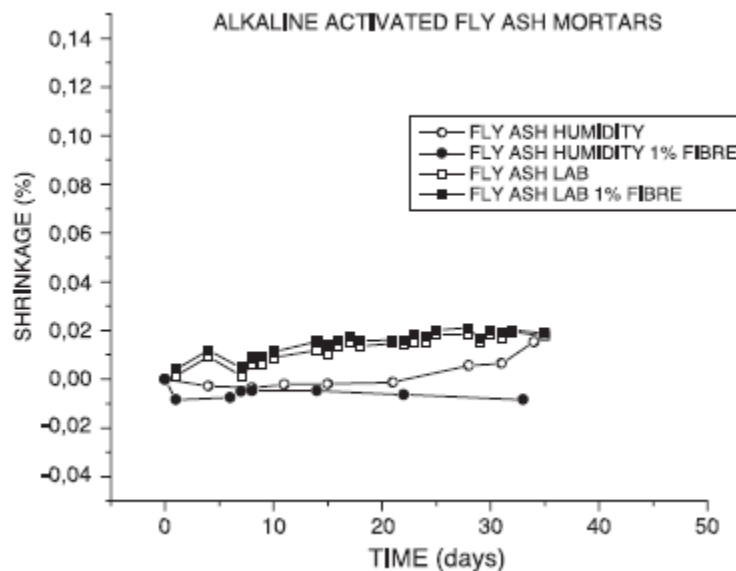
Figure 1.20: Effect of fibers and storing condition on the shrinkage over time for FA specimens [39].

23

The drying shrinkage of ZC mortar synthesized using class C FA was much lower than that of the corresponding OPC specimens [42]. Furthermore, decreasing the FA particle size through grinding did not significantly change the shrinkage values.

The limited studies on dry shrinkage of ZC focused on class F FA as precursor for ZC mortar. Therefore, the shrinkage of ZCC synthesized using class C FA needs to be investigated.

1.7 Durability of ZCC

The durability of ZCC is one of the important properties that needs to be studied. One of the factors that represents the durability of the concrete is the freeze and thaw resistance. There is no consensus on the freeze and thaw performance of ZCC [72]. The reported freeze and thaw resistances of the ZCC were excellent to fair. This variation is mainly due to the significant change of the chemical and physical properties of the precursors used to synthesize the ZCC.

ZCC synthesized using slag and air entraining admixtures displayed high freeze and thaw resistance (Table 1.4) [73]. The relative dynamic modulus of elasticity of the four mixtures was approximately 100% after 500 freeze and thaw cycles. One mixture displayed relative dynamic modulus of elasticity lower than the ASTM C666-15 [74] specified limit of 60% after 300 freeze and thaw cycles. That lower resistance of that particular mixture was linked to the lower SS/slag.

Table 1.4: Properties of Slag-Based ZCC and Summary of Test Results after 500 Cycles of Freezing and Thawing [73].

	Concrete mixtures				
	1	2	3	4	5*
Sodium silicate/slag	0.48	0.48	0.39	0.37	0.33
Air content, fresh concrete (%)	6.2	5.2	7.3	7.2	5.7
Voids in hardened concrete (%)	3.9	4.2	4.5	6.2	4.7
Spacing factor of air bubbles (μm)	270	325	336	286	377
Initial compressive strength (MPa)	30.2	29.7	30.7	32.1	33.7
After 500 freeze-thaw cycles*					
Length variation (%)	+0.03	+0.04	+0.07	+0.09	+0.18
Weight variation (%)	−3.7	−1.0	−2.7	−2.9	−2.6
Variation of resonant frequency (%)	+1.8	+3.4	−1.4	−0.1	−29.9
Variation of pulse velocity (%)	−1.0	+0.8	−3.6	−8.1	−29.0
Relative dynamic modulus of elasticity (%)	104	107	97	100	50
Residual flexural strength (%)	62	63	58	67	32

* Mixture 5: test terminated at 300 cycles.

Using OPC as an additive as well as air entraining admixtures improved the freeze and thaw resistance of class F based ZCC [75-78]. However, using limestone as an additive did not improve the freeze and thaw resistance. Generally, the compressive strength and relative dynamic modulus of elasticity of all the specimens decreased after subjecting them to the freeze and thaw cycles (Figs. 1.21 and 1.22). Other studies [79, 80] found that air entraining admixtures reduced the freeze and thaw resistance when used with lightweight class F FA based ZCC. However, the lightweight class F FA based ZCCs were able to sustain up to 300 cycles with and without air entraining admixtures (Fig. 1.23).
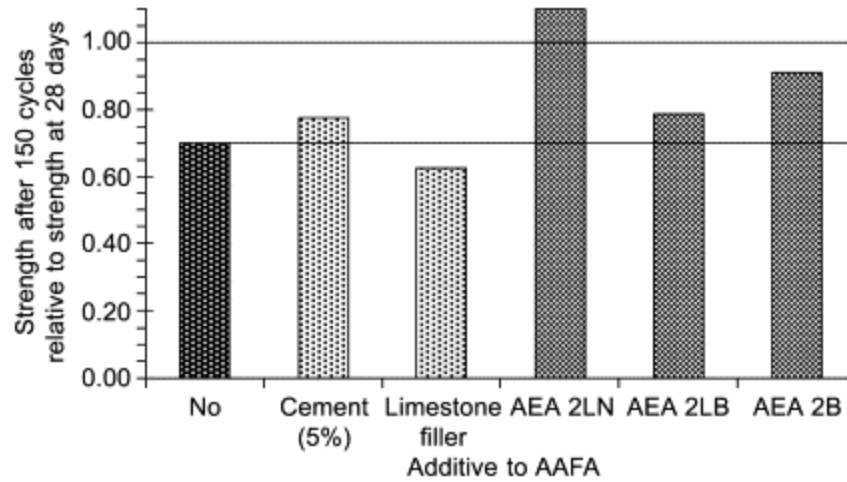
Figure 1.21: Compressive strength after 150 freeze-thaw cycles relative to 28 days of curing of mortars composed of activated fly ash, with and without additives [75, 76]. (Note: this figure was taken from [81].
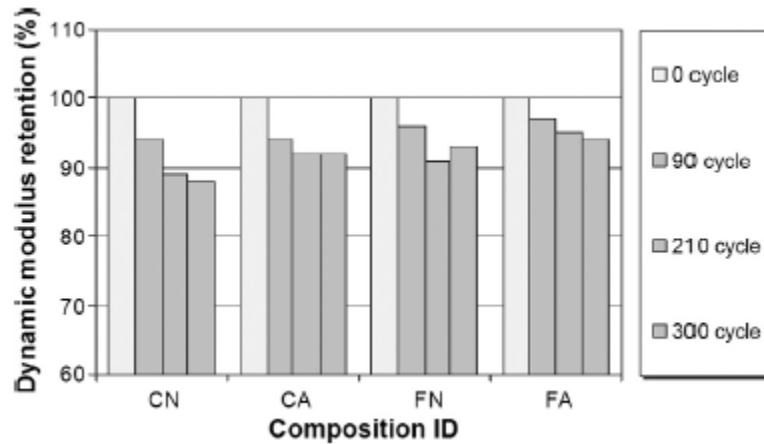
Figure 1.22: Dynamic modulus retention (%) after 90, 210, and 300 freeze–thaw cycles [77, 78]. (Note: CN = OPC mortar without air entraining agent, CA = OPC mortar with air entraining agent, FN = FA mortar without air entraining agent, and FAA = FA mortar with air entraining agent)
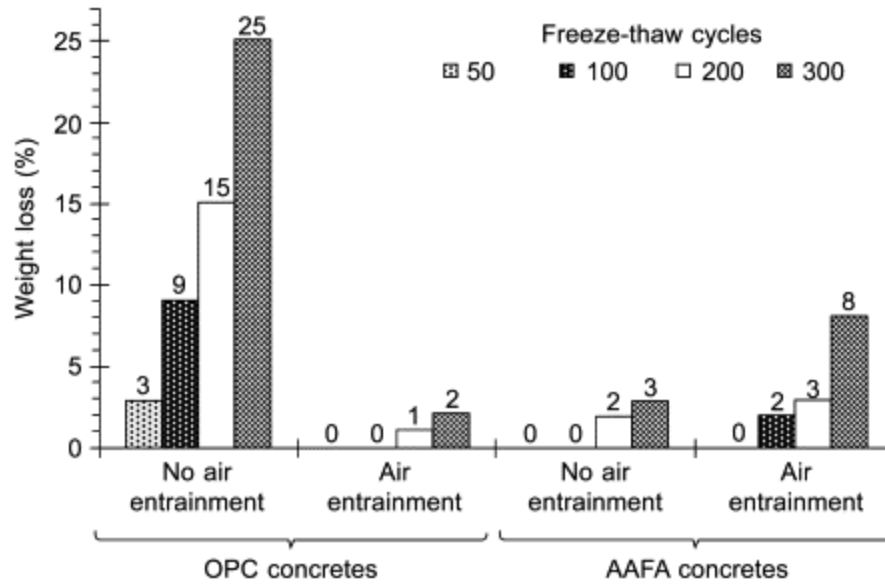
Figure 1.23: Weight loss after 50, 100, 200 and 300 freeze-thaw cycles of alkali-activated fly ash concretes compared to OPC concretes, with and without air entrainment [79, 80]. (Note: this figure was taken from [81].

The high freeze and thaw resistance of slag-based ZCC was also confirmed for mixtures with and without polypropylene fibers [39]. Furthermore, the freeze and thaw resistance of a binary system slag/class F FA based ZCC and a reference CC was investigated [39]. The slag mixtures and the slag/FA mixtures were cured at room temperature. However, the class F FA mixtures were cured at temperature of 85° C for 24 hours after casting. The compressive and flexural strengths of the specimens synthesized using slag and slag/FA after subjecting them to 50 cycles were higher than that of their reference specimens (Table 1.5). The increase in the strength for these mixtures indicated that the activation of the slag continued during the high humidity conditions while the reference specimens were cured at room temperature, hence the rate of increase in strength of the ambient-cured specimens was much lower. Furthermore, the mixtures synthesized using the class F FA displayed a significant decrease in compressive and flexural strengths after being subjected to freeze and thaw cycles. Furthermore, for CC specimens, the flexural strength decreased after the freeze and thaw cycles; however, the compressive strength

27

remained approximately constant. That could be related to the crack formations in the specimens due to the freeze and thaw which weakened the tensile strength of the specimens.

Table 1.5: Flexural and Compressive Strengths With and Without 50 Cycles of Freeze and Thaw [39].

Mortars	Fibre (%)	Without cycles		50 cycles	
		Flexural (MPa)	Compression (MPa)	Flexural (MPa)	Compression (MPa)
Slag	0	8.8	91.4	10.7	108.2
	0.5	8.2	89.2	10.5	104.6
Fly ash	0	6.6	38.1	3.3	29.1
	0.5	6.7	44.5	3.9	35.4
Fly ash/slag	0	4.7	30.9	6.9	33.8
	0.5	4.9	31.2	6.6	34.7
Cement	0	8.2	50.2	6.9	52.9
	0.5	8.2	48.4	6.9	47.2

More recently, the freeze and thaw resistance of ZC mortar synthesized using class F FA, ground granulated blast furnace slag (GGBS), and natural zeolite–clinoptilolite (NZ) were studied [82]. Mixtures synthesized using FA, GGBS, NZ, and combinations of them were tested. The combination mixtures were made of 50% of each of the two materials, by weight. The loss in the specimens' weights (Fig. 1.24) and compressive strengths (Fig. 1.25) of each specimen were determined. The results revealed that the specimens synthesized using GGBS displayed the highest freeze and thaw resistance. In addition, adding the GGBS to the FA or NZ improved their freeze and thaw resistance compared with those mixtures synthesized using only FA or NZ. The weakest mixtures were those synthesized using NZ. Furthermore, with increasing the SS/SH from 1.0 to 2.0 and 3.0, the freeze and thaw resistance increased for all mixtures.
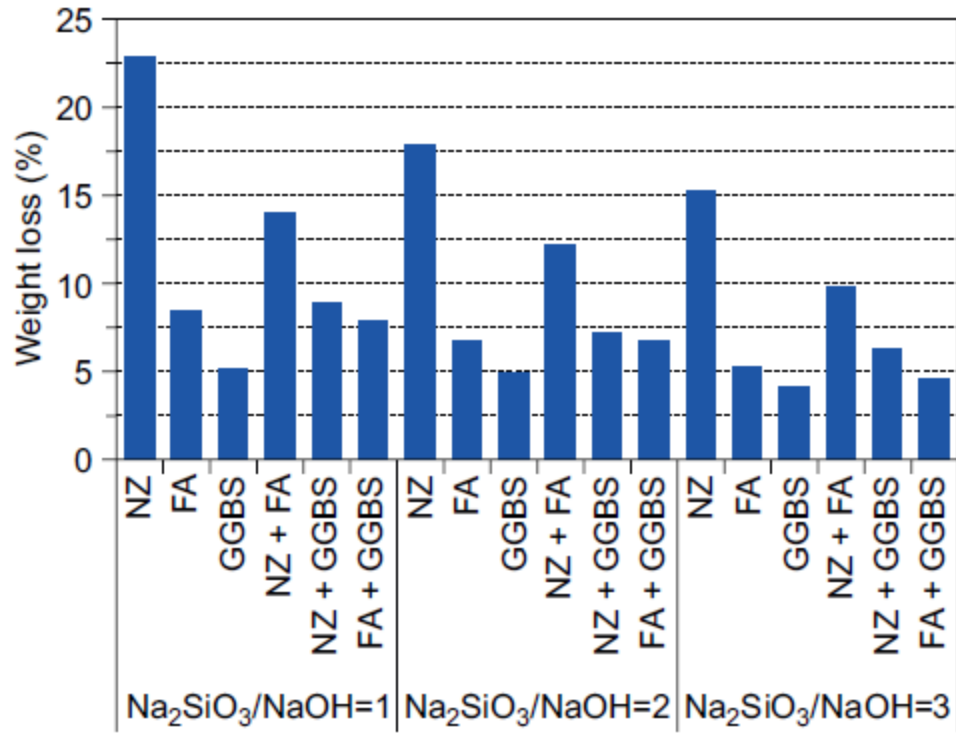
Figure 1.24: Weight loss of ZC mortars after 25 cycles of freeze-thaw [82].
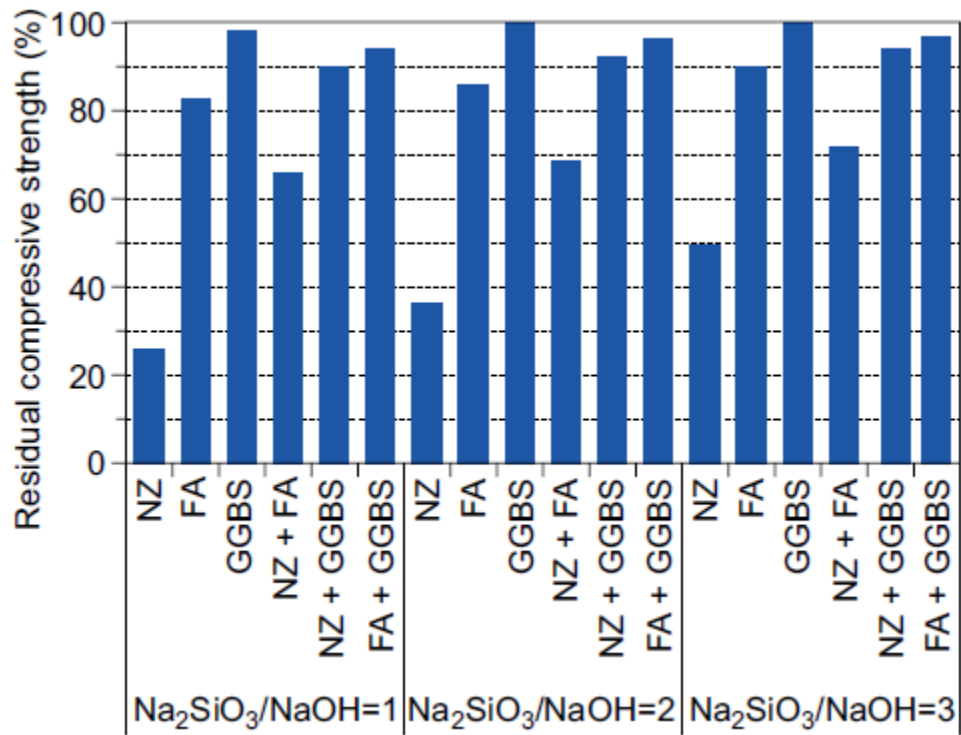
Figure 1.25: Residual compressive strength of ZC mortars after 25 cycles of freeze-thaw [82].

Studies on freeze and thaw resistance of class C FA based ZCC are very limited. The freeze and thaw of ZCC synthesized using two different radioactive high-calcium FAs were studied [5]. The two FAs, referred to as Shivee Ovoo and Baganuur, had calcium content of 30.19% and 14.24% and are classified as class C and class F, respectively. The results revealed that the ZCC synthesized using class C FA displayed higher compressive strength before and after sustaining 40 freeze and thaw cycles (Table 1.6). Furthermore, the specimens subjected to freeze and thaw cycles and prepared using SS/SH of 1.0 displayed lower compressive strength compared with those prepared using SS/SH of 0.0.

Table 1.6: Freeze and Thaw Resistance of ZCC [5].

Sample	Sample name	Freeze-thaw cycles	Compressive strength (MPa)	Compressive strength after freeze-thaw cycle (MPa)
1	Baganuur fly ash based concrete activated 8 M-NaOH, (80% gravel stone + 20% flyash)	> 40	23 (3.2)	20
2	Baganuur fly ash based concrete activated 8 M NaOH, (75% gravel stone + 25% flyash)	> 40	29 (4.1)	26.3
3	Shivee-Ovoo fly ash based concrete activated 8 M-NaOH, (80% gravel stone + 20% flyash)	≥ 40	10.6 (2.1)	6.8
4	Shivee-Ovoo fly ash based concrete activated with 8 M-NaOH, (75% gravel stone + 25% flyash)	30	14.1 (1.2)	*
5	Baganuur fly ash based concrete activated with solution (50% Na_2SiO_3/50% 10 M NaOH), (80%g stone + 20% flyash)	5	30.0 (4)	*
6	Baganuur fly ash based concrete activated with solution (50% Na_2SiO_3/50% 10 M NaOH), (75%g stone + 25% flyash)	5	30.5 (5.5)	*

*These samples were destroyed during the freeze-thaw cycles.

The previous studies displayed that the freeze and thaw resistance of the ZCC synthesized using slag were high and passed ASTM C666-15 limits [74]. In addition, adding slag to class F FA based ZCC improved its freeze and thaw resistance. However, the freeze and thaw resistance of ZCC synthesized using class F FA only was low. Furthermore, air entraining admixtures generally improves the freeze and thaw resistance of ZCC synthesized using class F FA. The freeze and thaw resistance of ZCC synthesized using class C FA has been little studied before [5]. Therefore, it is urgent to study the freeze and thaw resistance of ZCC synthesized using class C FA.

1.8 ZC Mortar/Concrete for Repair Applications

Infrastructure rehabilitation is a serious concern worldwide. It was estimated in 2012 that over 1.6 trillion dollars were needed for the U.S.'s infrastructure rehabilitation over the next five years [83, 84]. About 27% of all the U.S. highway bridges need to be repaired or replaced [83, 84]. An annual estimated cost of 215 million euro is required for maintenance, repair, and strengthening of the reinforced and prestressed bridges in the European Union [85]. Therefore, finding a cost effective and efficient repair material is necessary. The key points of repair materials to ensure structural compatibility between the old and repaired materials are the adhesion (bond strength), compressive strength, tensile strength, modulus of elasticity (Fig. 1.26) [84], and cost. ZCC is one of the candidate materials to be used in repair of infrastructure as it has the potential to overcome the limitations of existing repair material such as epoxy and different types of concrete. However, there are limited studies on using ZC mortar/concrete as a repair material.
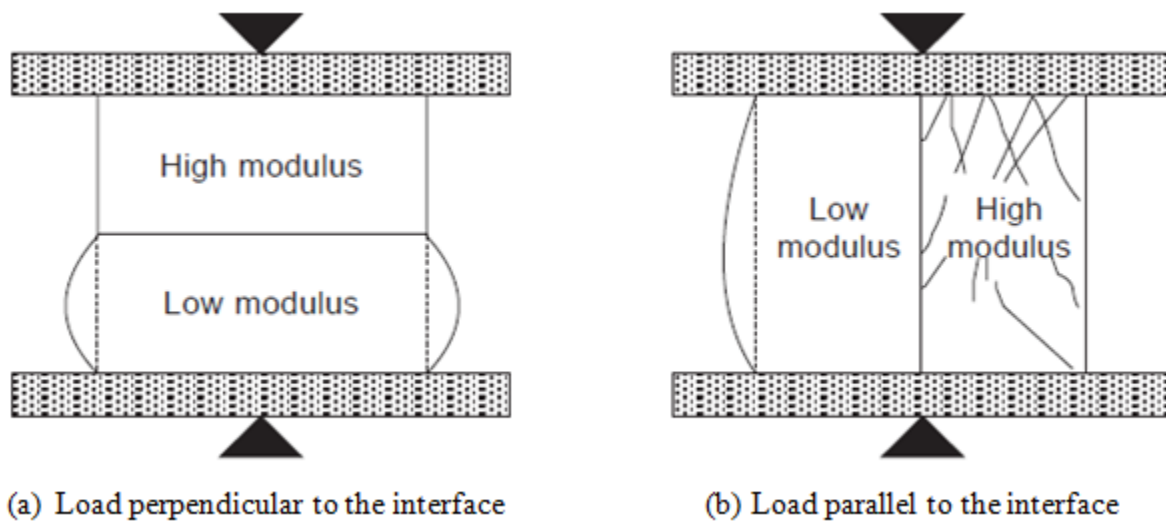
Figure 1.26: Mechanical behavior of materials with different modulus of elasticity: (a) load perpendicular to the interface, and (b) load parallel to the interface [84].

The adhesion (bond) strength between a concrete substrate-based OPC and different repair materials was assessed [86]. Three different repair materials included two commercially available pre-packed repair mortar mixtures, R1 and R2, and tungsten mine waste mud (TMWM). The first two had blended OPC, silica fume, fibers, graded aggregate with a maximum size of 2 mm, and other additives with 28-day compressive strength of approximately 6815 psi (47 MPa). The latter had 28-day compressive strength of 11355 psi (78.3 MPa). The slant shear was used to assess the bond strength between the conventional concrete substrate and each of the repair materials (Fig. 1.27).
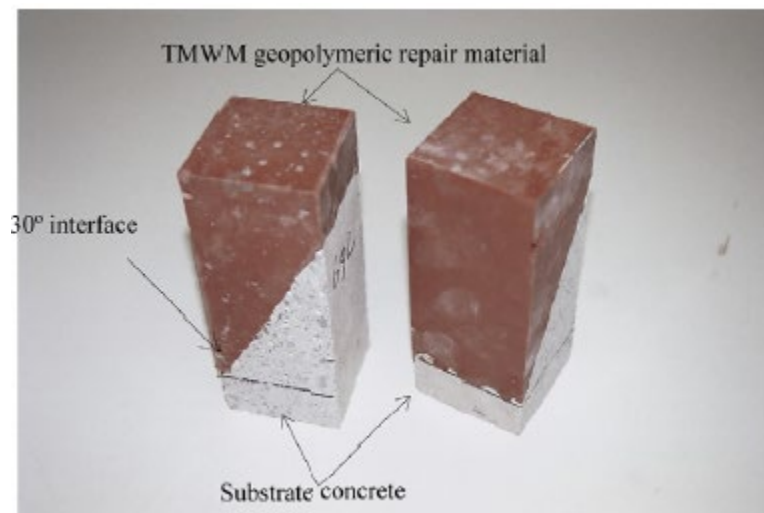
Figure 1.27: Slant shear specimens with interface line at 30° [86].

A surface treatment was applied to the concrete substrate surfaces of some specimens before placing the repair material. The surface treatment consisted of immersing the concrete substrate surface in 5% hydrochloric solution for 5 minutes followed by washing the surface. This etching process (ES) resulted in an increase in the specific surface of the concrete. Two failure modes occurred during testing: bond failure along the surface between the substrate and repaired materials (Fig. 1.28a) and monolithic failure (Fig. 1.28b). The adhesion (bond) strength was tested at the ages of 1, 3, 7, and 28 days. The bond strengths of the ZCC-based TMWM were

found to be higher than those of the commercial repair materials R1 and R2 (Fig. 1.29) either with or without surface treatment.
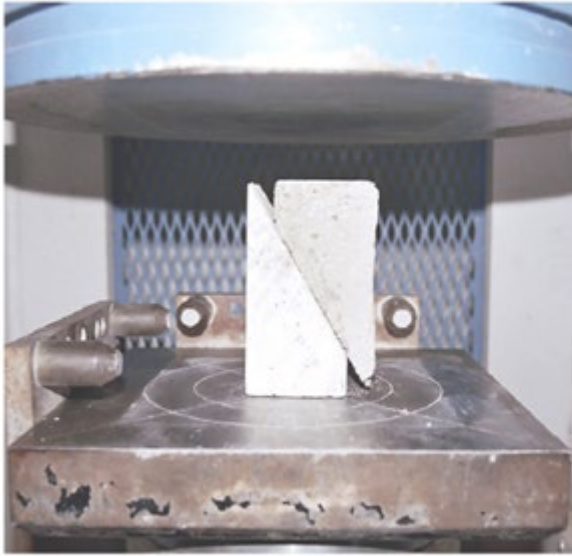
Figure 1.28: Failure modes; (a) adhesive failure, and (b) monolithic failure [86].
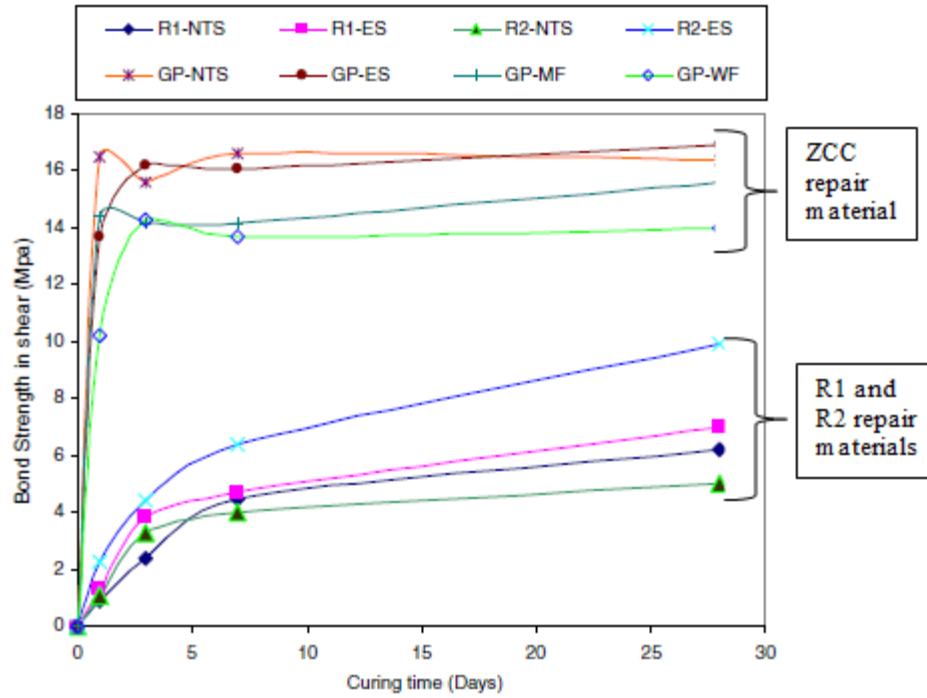
Figure 1.29: The bond strength results from the slant shear test [86].

Another study looked at the adhesion characterization between CC and five different materials, namely, ZC paste, three commercial repair materials (RMs), and CC [87]. In some ZC mixtures, the class C FA was partially replaced with Portland cement and calcium hydroxide. This replacement aimed to increase the calcium content in the mixture and potentially improve the interfacial between the ZC and substrate. The commercial repair material, RM-1, RM-2, and RM-3, were general purpose non-shrink grout mortar, multi-purpose non-shrink grout, and polymer modified repair mortar. The compressive strength of the three RMs were RM-1, RM-2, RM-3, 8990 psi (62 MPa), 10155 (70 MPa), and 5800 psi (40 MPa). The repair materials were cast with an interface line of 45° (Fig. 1.30). All of the samples were tested at the age of 28 days of curing at temperature of 25° C.

34
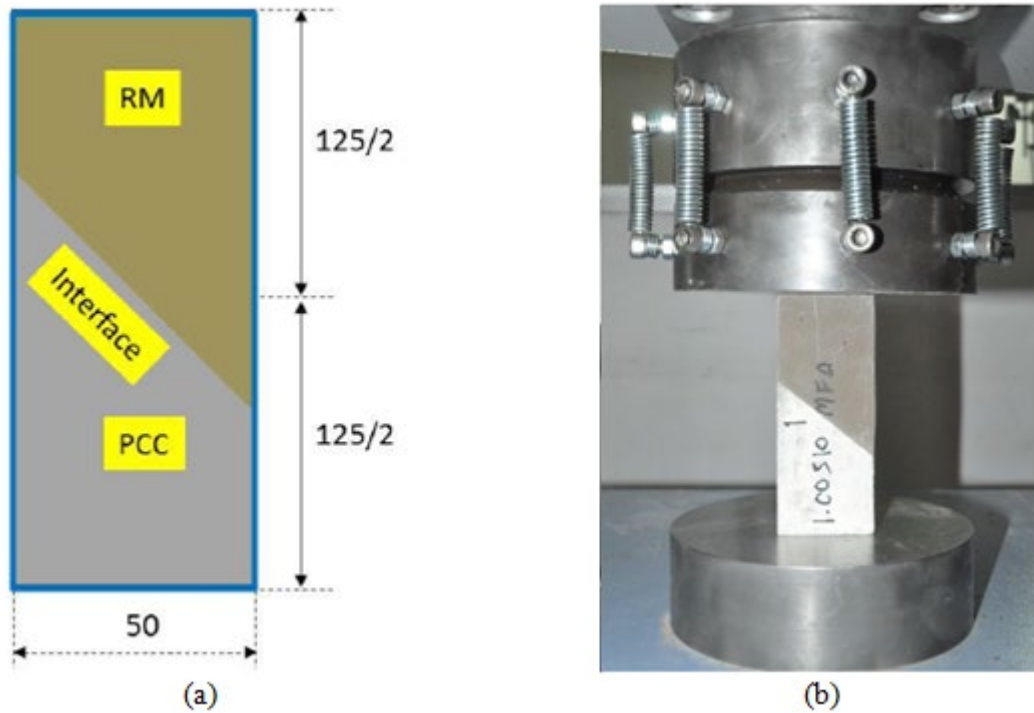
Figure 1.30: Tested specimens' (a) dimensions, and (b) compression test [87].

The bond strength between the substrate and the repaired CC was 1190 psi (8.2 MPa) which was the lowest among all repair materials (Fig. 1.31). Using the additives improved the bond strength of the ZC paste compared to using unmodified ZC paste. Replacing the FA with 15% of OPC or 10% of calcium hydroxide displayed the highest shear bond strength of 3700 psi (25.5 MPa) and 3570 psi (24.6 MPa), respectively, where the compressive strength of these two mixtures were 5510 psi (38 MPa) and 5510 psi (38 MPa), respectively. Therefore, while the compressive strength was not higher than the repair material, the bond was the highest. Replacing the FA with PC or calcium hydroxide formed calcium silicate hydrate (CSH) and/or calcium aluminate silicate hydrate (CASH) along with the sodium aluminate silicate hydrate (NASH). These reactions' products improved the bond strength between the two materials.
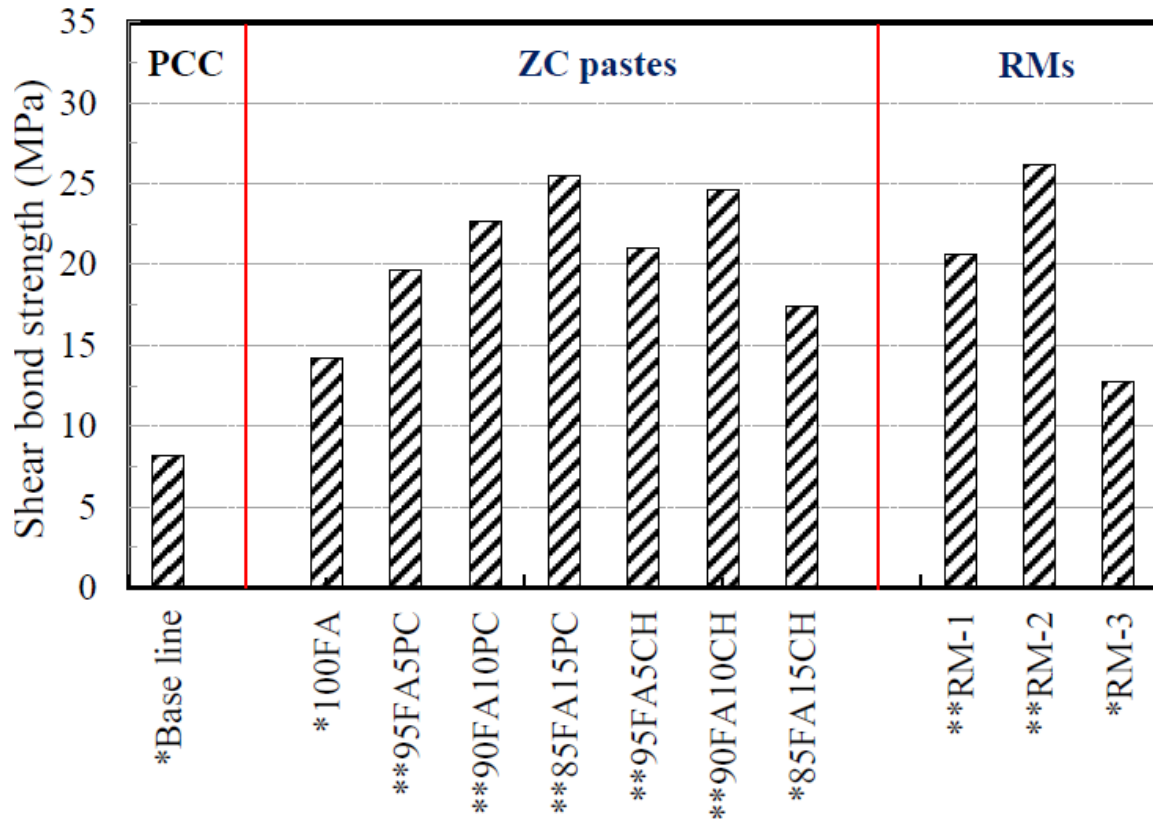
Note: * is shear failure mode whereas ** is compressive failure mode.

Figure 1.31: Bond strength between the substrate and repaired layers (note: PCC stands for CC repair) [87].

One of the drawbacks of this research was the inaccuracy in the comparisons. While the CC repair mixture was a concrete, the commercial RMs mixtures were mortars, and the ZC mixtures were pastes. Therefore, to compare them, all of them would need to be the same, i.e., either concrete, mortar, or paste.

1.9 Safety and Transportation of Alkali Activators

The SS and SH are alkali solutions having pH ranging from 10 to 13 based on the concentration of the liquid. Commonly used safety tools such impermeable gloves and safety glasses are required for the labors during handling, transporting, and mixing of these alkali solutions with the FA to make the ZCC. However, after placing the ZCC and curing it, it is totally safe to be

handled, moved, and tested using bare hands. The supplies for the personal safety tools are specified in the Materials Safety Data Sheets that are available with the commercial alkali activated materials are quite similar to those specified for the CC. Similar to CC, the tools such as mixer, wheelbarrow, scoop, rod, and mold that are used during the mixing and casting of the ZCC need to be cleaned using a running water. It does not require special drainage pipelines or cleaning process.

1.10 Cost and CO_2

The cost of raw material required for ZCC is comparable to that of CC. Large-scale usage of ZCC will likely lead to lower costs due to large orders of reagents, which is the most expensive component. Depending on the binder-source location, the energy source, and the mode of transportation, zero-cement concrete can be financially and environmentally efficient, leading to a potential reduction of 44% to 64% in CO_2 emissions while financial costs range from 7% lower to 39% higher compared to conventional concrete [88]. Furthermore, the embodied energy of FA-based zero-cement concrete was found to be 40% less than that of CC. The sodium hydroxide and sodium silicate contributed 34% and 21%, respectively, to the cost of the ZCC [89].

1.11 Objective and Organization of this Report

The overarching objective of this research is to study the feasibility of using the locally available fly ashes (FAs) to make zero-cement concrete (ZCC) for different structural and repair applications. ZCC is relatively new class of concrete that does not include any ordinary Portland cement (OPC) and relies on other alternative materials such as fly ash, slag, etc. as the binder. To

achieve the objectives of this research, different tasks were carried out (Fig. 32) and summarized in this report. The report is organized in the following chapters:

Chapter 1: Literature review

This chapter presents a brief overview of the literature available on precursors, alkaline activators, mixing, curing, performance, and cost of zero-cement concrete.

Chapter 2: Material properties

This chapter presents a comprehensive characterization for the materials that were used in this project. This includes the particle size distribution of the aggregates, chemical and physical properties of the fly ash sourced from five different power plants, and properties of the alkali activators.

Chapter 3: Trial mixtures and mixing procedures of zero-cement mortars and concrete

Using high calcium FAs to synthesized ZC mortar and concrete is relatively new. Therefore, finding the best mixing procedure for ZC mortar and concrete is essential. Chapter 3 presents the best mixing procedure for ZC mortar and concrete. In addition, the appropriate ranges of water/fly ash (W/FA), alkali activators/fly ash (Alk/FA), and sodium silicate to sodium hydroxide (SS/SH) to synthesize ZC mortar and concrete with acceptable workability and setting time as well as adequate strength for structural applications were investigated and presented.

Chapter 4: Fresh properties and strength of zero-cement mortar

The appropriate mixing procedure and ranges were determined and presented in Chapter 3. A fine-tuning and optimization procedure for ZC mortar was carried out and presented in Chapter

4. The purpose of this chapter was to study the effect of W/FA, Alk/FA, and SS/SH on the fresh properties and compressive strength of ZC mortars.

Chapter 5: Optimization of thermal curing temperature and duration of zero-cement mortar

This chapter investigates the effect of different curing durations and temperatures on the compressive strength of ZC mortar. Curing temperatures ranging from 185° F (85° C) to 86° F (30° C) applied over durations ranging from 4 hours to 168 hours were investigated. In addition, hot weather common during the summer in the state of Missouri was imitated using two different curing regimes.

Chapter 6: Mechanical properties and drying shrinkage of zero-cement concrete

This chapter presents the fresh and mechanical properties of ZCC. Five ZCC mixtures were prepared and subjected to three different curing regimes including oven, ambient, and moist curing. The fresh properties including the slump, unit weight, air content, and temperature are presented in Chapter 6. The mechanical properties including the compressive strength, splitting tensile strength, modulus of elasticity, flexural strength are also presented.

Chapter 7: Durability of zero-cement concrete

This chapter presents the durability of ZCC. Durability was investigated by testing the freeze and thaw resistance, surface resistivity, bulk electrical conductivity, and rapid chloride ion penetration. Also, the effects of adding slag, crumb rubber, and air entraining admixture (AEA) to ZCC mixtures was investigated and presented.

Chapter 8: Zero-cement concrete as a repair material

This chapter presents the results of slant shear and pull-off tests on ZCC used as a repair material. Specimens were constructed out of CC mixtures representing the host structure, i.e., the existing concrete structural elements. Then, ZCC was used as a repair material by placing it against the CC specimens. The repair procedures and results of both tests are presented.

Chapter 9: Cost analysis

This chapter presents a cost analysis for the ZCC and CC mixtures.

Chapter 10: Conclusions, recommendations, and future work

This chapter provides a summary of the main findings of this project. In addition, recommendations for synthesizing ZCC are presented, as well as suggestions for future studies on ZCC are presented as well.

Chapter 11: References

This chapter includes bibliographical references.

Chapter 2:   Material Properties

In this chapter, the properties of the materials that were used in this project are characterized.

2.1 Aggregates

2.1.1 Coarse aggregate

A MoDOT approved dolomite having a specific gravity of 2.76 per ASTM C127-15 was used in this project as the coarse aggregate [90]. The aggregate sieve analysis results showed that the dolomite particle grading was within the limits of ASTM C33-16 (Fig. 2.1) [91]. The coarse aggregate was prepared in the saturated surface dry condition prior to mixing.
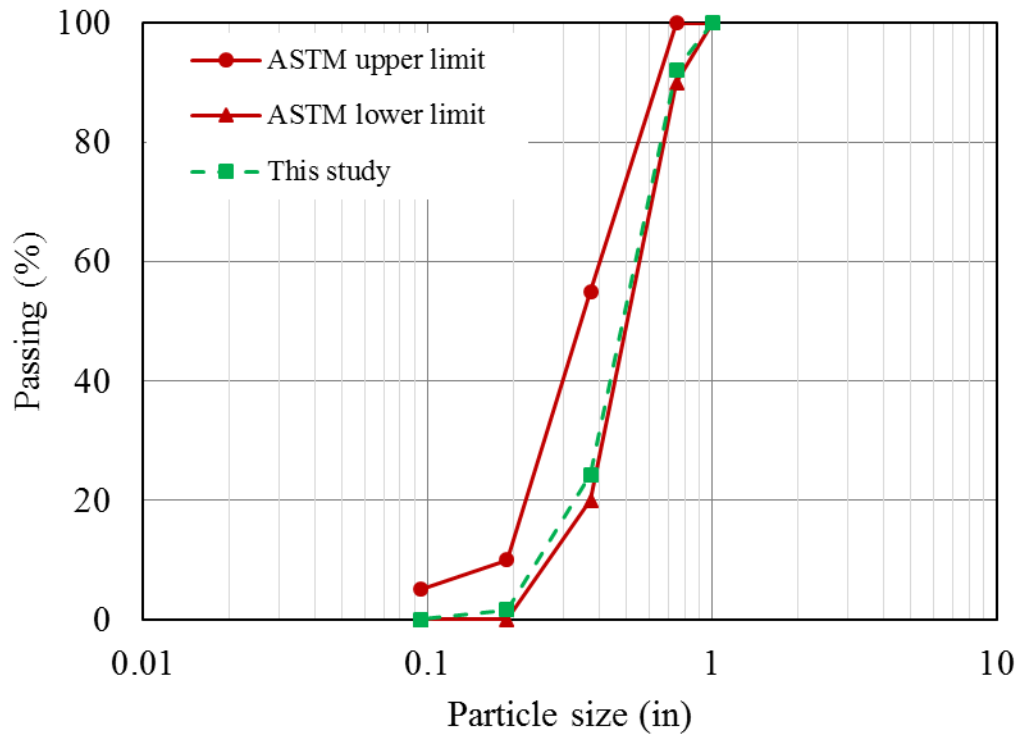
Figure 2.1: Sieve analysis of the coarse aggregate

2.1.1 Fine aggregate

An approved Missouri river sand with a specific gravity of 2.60 was used in this study as the fine aggregate per ASTM C128-15 standard procedures [92]. Two different sizes were used for mortar (Fig. 2.2) and concrete (Fig. 2.3) mixtures per ASTM C33-16 [91] and ASTM C778-13 [93], respectively. All sands were prepared in the saturated surface dry condition prior to mixing.
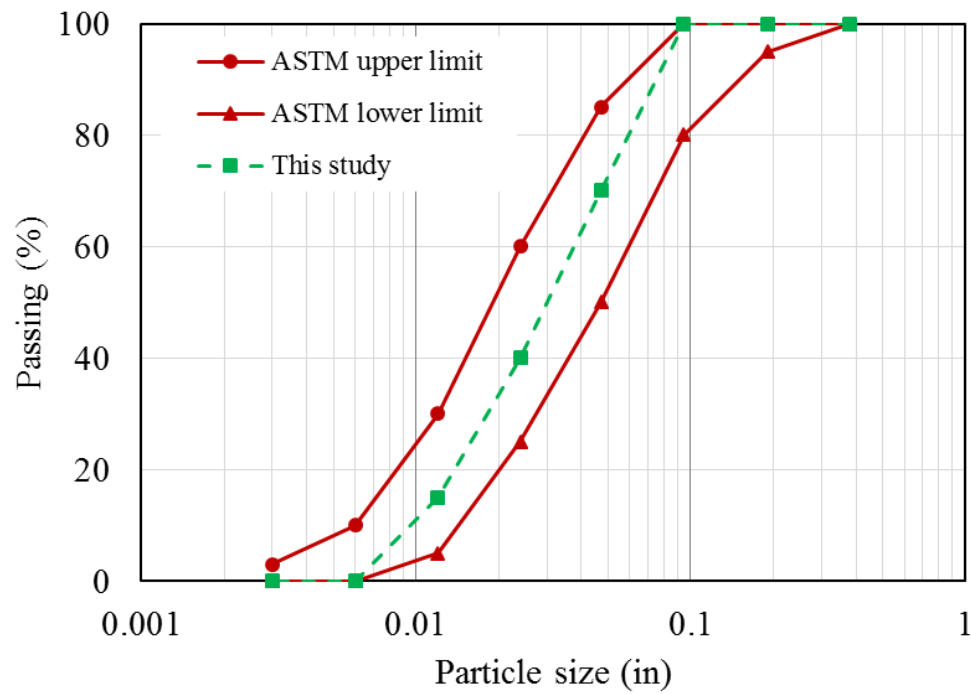
Figure 2.2: Sieve analysis of the sand used for mortar mixture.
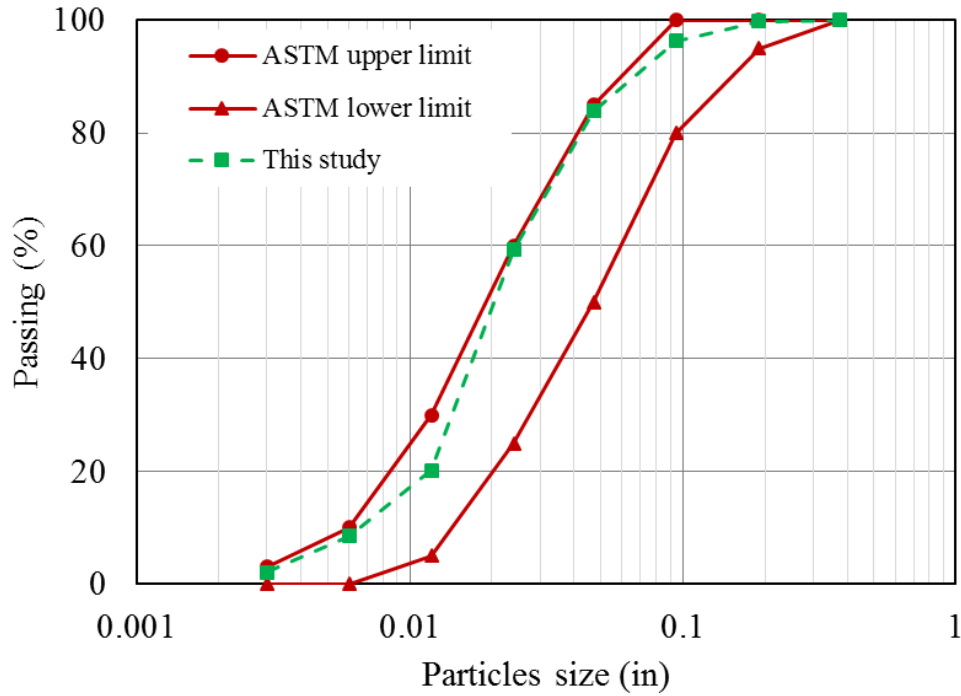
Figure 2.3: Sieve analysis of the sand used for concrete mixture.

2.2 Alkali Activators

Two different alkali activators were used in this study, namely sodium silicate and sodium hydroxide.

2.2.1 Sodium silicate

Two different types of sodium silicate (Na_2SiO_3) were used during the course of this study. Type one was obtained from PQ Corporation in 5 gallon buckets (Fig. 2.4a). The amount of Na_2SiO_3 in this solution was 44.1% (w/w) while the water content was 55.9% (w/w). The second type was shipped from China. The amount of Na2SiO3 in this solution was 43.5% (w/w) while the water content was 56.5% (w/w). Both types had a specific gravity of 1.53 g/cm3 at 20° C. The sodium silicate that was bought from China was shipped in 55 gallons barrels (Fig. 2.4b). Fig. 2.4c shows the sodium silicate solution color which was almost transparent.
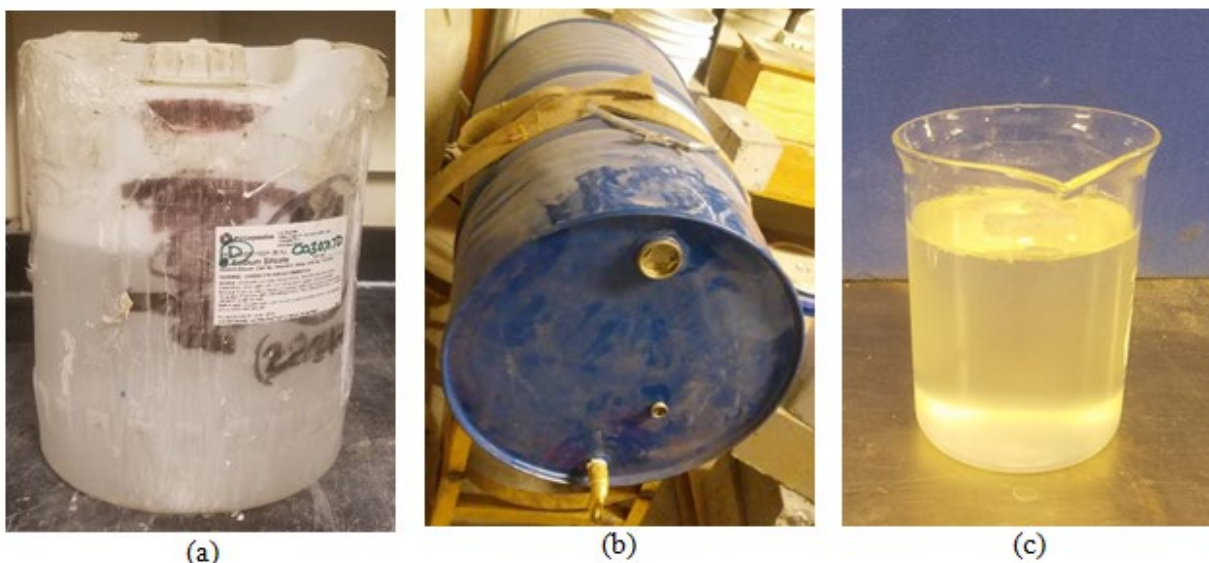
Figure 2.4: Sodium silicate solution (a) 5 gallon bucket, (b) 55 gallon barrel, (c) color.

2.2.2 Sodium hydroxide

The sodium hydroxide was obtained in solid pellet form from Bulk Apothecary Company (Fig. 2.5a). A sodium hydroxide solution with molarity of 10 M was prepared 24 hours prior to the mixing day to let the solution cool down to room temperature. It was not a necessary condition that the solution is prepared 24 hours prior to mixing, only that it was cooled to room temperature before mixing. The SH solution molarity was fixed at 10 M, which was obtained by mixing 314 gm of the SH solid pellets with 686 gm of distilled water (Fig. 2.5b).
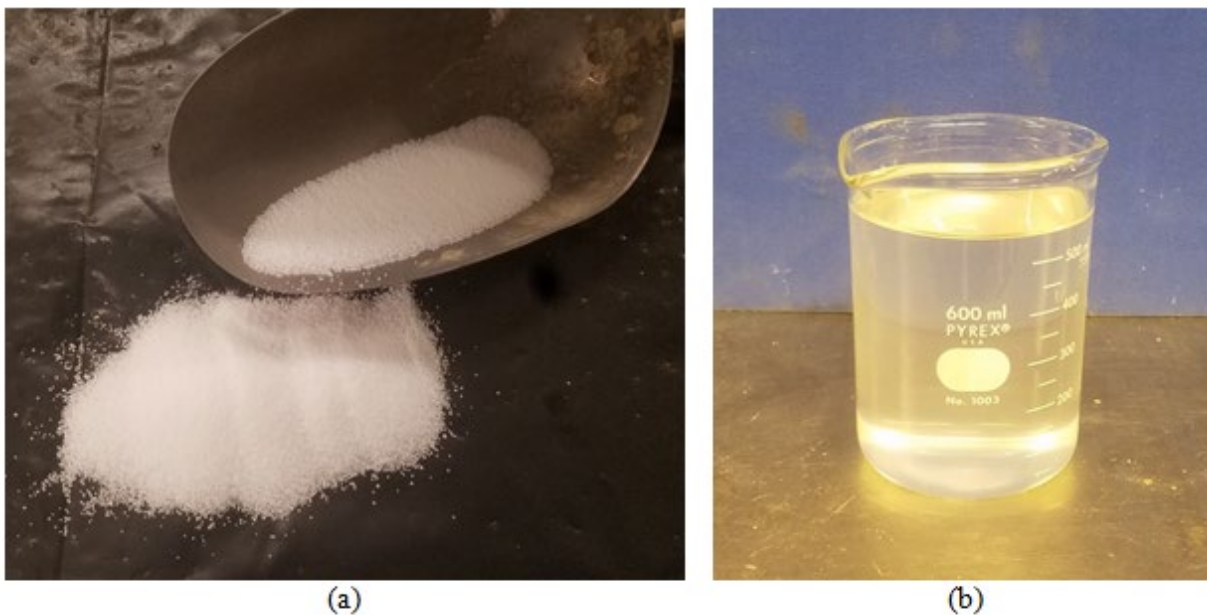
Figure 2.5: Sodium hydroxide (a) before preparation in solid pellet form and (b) after preparation in liquid form.

2.3 Fly Ash (FA) Characterization

Five different types of fly ash (FA) were used during the course of this study. These FAs were sourced from Labadie (FA37), Jeffrey Energy Center (FA29), Kansas City (FA26), Thomas Hill (FA24), and Sikeston (FA21) power plants (Fig. 2.6) located in different regions of Missouri. The chemical and physical properties of the five FAs are presented in the following sections.

The nomenclatures of the fly ashes start with the letters "FA" for fly ash followed by the calcium content percentage. For example, FA37 is a fly ash having a calcium content of 37%.

Figure 2.6: FA colors and sources.

2.3.1 X-ray fluorescence

The chemical composition of each FA was determined using X-ray fluorescence spectroscopy (XRF) per ASTM D4326-13 [94]. The XRF analyses were performed using a Thermo Scientific ARLTM Quantx spectrometer. The spectrometer was first calibrated using the results of analyzing 25 different certified standard reference materials obtained from the U.S. Geological Survey, National Institute of Standards and Technology, and Geological Survey of Japan. The spectrometer was operated under four separate conditions to optimize the sensitivity for different elements. These conditions were: (1) 4 kV with vacuum and no filter to measure Na2O, MgO, Al2O3, SiO_2, and P2O$_5$; (2) 8 kV with vacuum and cellulose filter to measure K2O and CaO; (3) 12 kV in air with Al filter to measure TiO_2 and MnO; and (4) 16 kV in air with a thin Pd filter to measure Fe2O3. Loss on ignition was determined by burning fly ash samples at 700° C for two hours.

A sample of each FA was prepared by placing approximately 5 grams of loose powder mixed with 1 ml of Elvacite binder into 30 mm diameter aluminum cups [95]. The powder samples were pressed into flat disks using a steel die and pressure of 56,000 psi. Table 2.1 shows the chemical properties of the different types of FAs. All the FAs are classified as FA class C according to the ASTM C618-15 classification [23].

It is of interest that ElGawady et al. (2020) found that there is a slight difference in the chemical compositions of FA from one batch to the next. Work is still in progress for the next two years to determine the standard deviation of such changes over time. For example, Table 2.2 shows the chemical composition of the five different types of FAs obtained from different batches.

As shown in the tables, four out of five FAs showed similar chemical compositions. The fifth FA, sourced from Labadie, displayed a different chemical composition. The first batch (Table 2.1) had lower calcium content compared with the second batch (Table 2.2). Generally, the first batch was used for preparing the mortar and concrete mixtures reported in Chapters 3 and 4. The second batch was used in the rest of the report. Two sources of ground granulated blast furnace slags (GGBFS), S1 and S2, were used in this study in the durability study (Chapter 7) and their chemical compositions were determined (Table 2.3).

Table 2.1: Chemical Composition of the First Batch of FAs Samples by XRF.

Chemical composition	FA27 (%)	FA29 (%)	FA24 (%)	FA25 (%)	FA21 (%)
SiO_2	38.02	38.68	41.80	38.83	43.94
Al_2O_3	18.67	17.10	18.34	18.07	20.93
Fe_2O3	4.86	3.80	4.87	3.80	4.78
$Sum(SiO_2 + Al_2O_3 + Fe_2O_3)$	61.55	59.58	65.01	60.7	69.65
CaO	27.14	29.06	24.12	24.91	21.26
MgO	7.40	8.29	6.21	10.12	5.08
Na_2O	1.22	0.70	2.03	0.46	1.39
K_2O	0.47	0.39	0.56	0.47	0.66
TiO_2	1.40	1.22	1.39	1.39	1.39
P_2O_5	0.80	0.74	0.66	0.87	0.54
MnO	0.02	0.04	0.03	0.02	0.03
LOI^*	0.60	1.14	0.19	1.09	0.58
MC^b	0.09	0.00	0.03	0.08	0.02

[a]LOI: Loss on ignition
[b]MC: Moisture content

Table 2.2: Chemical Composition of the Second Batch of FAs Samples by XRF (ElGawady et. Al 2020).

Chemical composition	FA37 (%)	FA29 (%)	FA26 (%)	FA24 (%)	FA21 (%)
SiO_2	36.89	37.94	42.25	40.43	43.91
Al_2O_3	13.99	17.44	17.91	17.53	20.12
Fe_2O3	3.52	3.67	4.73	4.72	4.96
Sum($SiO_2 + Al_2O_3 + Fe_2O_3$)	54.4	59.05	64.89	62.68	68.99
CaO	36.96	28.79	25.86	24.07	21.24
MgO	4.80	8.00	4.74	9.39	4.29
Na_2O	1.62	1.85	1.58	1.17	2.87
K_2O	0.62	0.39	0.56	0.48	0.70
TiO_2	0.87	1.17	1.44	1.40	1.36
P_2O_5	0.70	0.71	0.89	0.79	0.51
MnO	0.03	0.04	0.04	0.02	0.05
LOI[*]	0.50	0.82	0.12	0.62	0.40
MC[b]	0.07	0.02	0.04	0.10	0.01

[a]LOI: Loss on ignition
[b]MC: Moisture content

Due to the similar chemical compositions of the two batches of FAs, the other properties of the

FAs were carried out on the second batch of the FAs only.

Table 2.3: Chemical Composition of the Slag Samples by XRF.

Chemical composition	S1 (%)	S2 (%)
SiO_2	32.98	43.28
Al_2O_3	10.96	7.77
Fe_2O3	0.52	0.43
CaO	44.74	35.26
MgO	7.18	9.29
Na_2O	2.53	2.78
K_2O	0.59	0.47
TiO_2	0.28	0.25
P_2O_5	0.23	0.17
MnO	0.09	0.29
LOI[*]	0.03	0.02
MC[b]	0.00	0.01

[a]LOI: Loss on ignition
[b]MC: Moisture content

2.3.2 Physical properties

The surface area, particle size distribution, and relative density of the five FAs are presented in this section.

2.3.2.1 Surface area (BET)

A surface area and pore size analyzer, Nova 2000e, (Fig. 2.7) from Quantachrome Instruments was used to measure the surface area of the five FAs based on the Brunauer-Emmett-Teller (BET) theory. The theory aims to explain the physical adsorption of gas molecules on a solid surface and serves as the basis for an important analysis technique for the measurement of the specific area of materials. The test started with heating up the sample to ensure that it lost the moisture content before placing it in a long bulb followed by immersing it in liquid nitrogen.

Figure 2.7: BET surface area analyzer (Nova 2000e).

The instrument consists mainly of two units; the heating cells on the left hand side (Fig. 2.7) and the liquid nitrogen dewar on the right hand side (Fig. 2.7). The surface area results of the five FAs ranged from 1446 to 3124 m^2/kg with FA26 having the lowest and FA29 having the highest surface areas, respectively, as shown in Fig. 2.8.
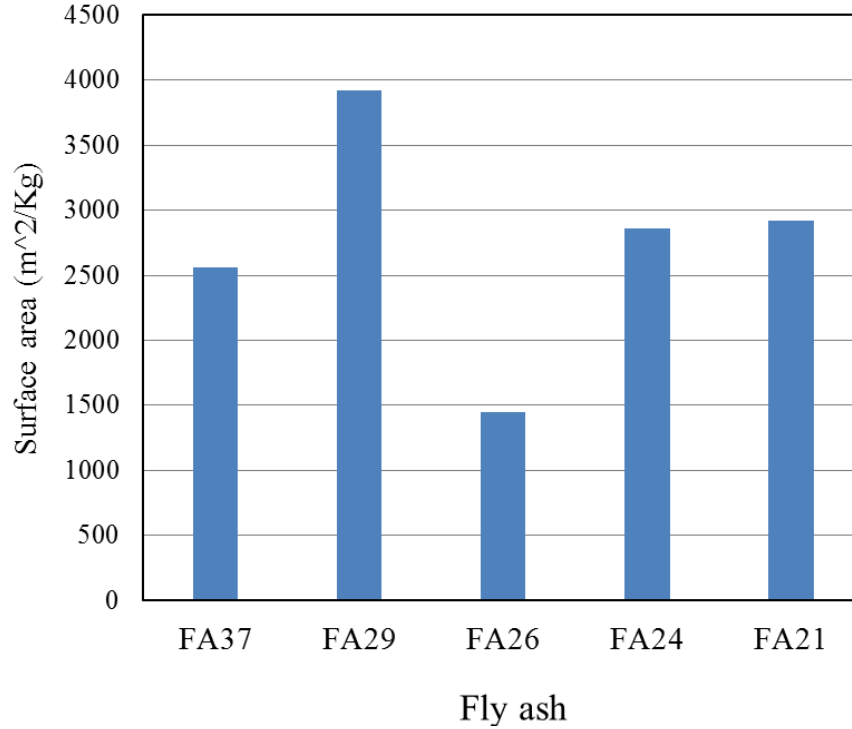
Figure 2.8: FAs surface areas

2.3.2.2 *Particle size distribution*

A particle size analyzer (Microtrac S3500) was used to measure the particle size distribution of the five FAs. The Microtrac S3500 is the first particle size analyzer that uses three precisely placed red laser diodes to accurately characterize particles as shown in Fig. 2.9. It utilizes the proven theory of Mie compensation for spherical particles and the proprietary principle of Modified Mie calculations for non-spherical particles. Isopropanol was used as the dissolved liquid in the test. The reactive index of the FAs was selected to be 1.65 as reported in the literature [96].
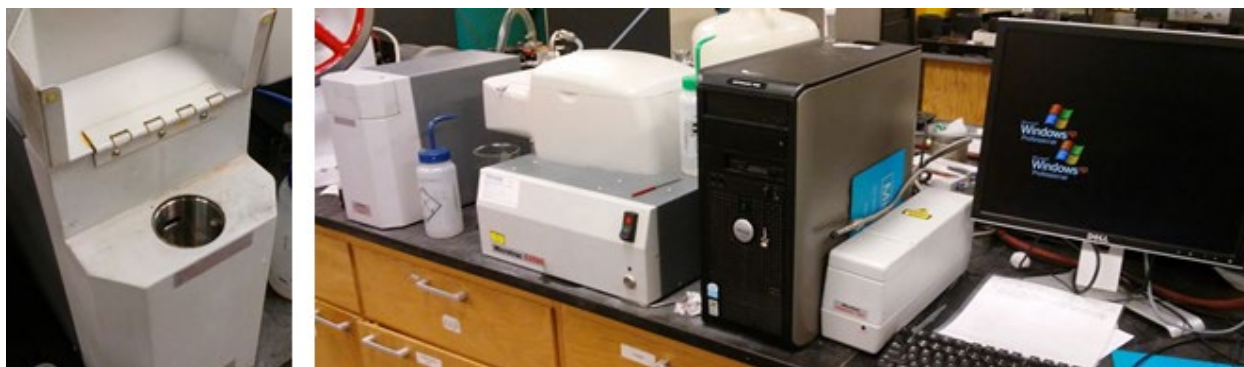
Figure 2.9: Particle size analyzer (Microtrac S3500).

Fig. 2.10 shows the results of the particle size distribution test. The diameters at which 50% of the particles passed (D_{50}) were 14.75, 14.87, 16.25, 16.13, and 12.81 μm for FA37, FA29, FA26, FA24, and FA21, respectively.
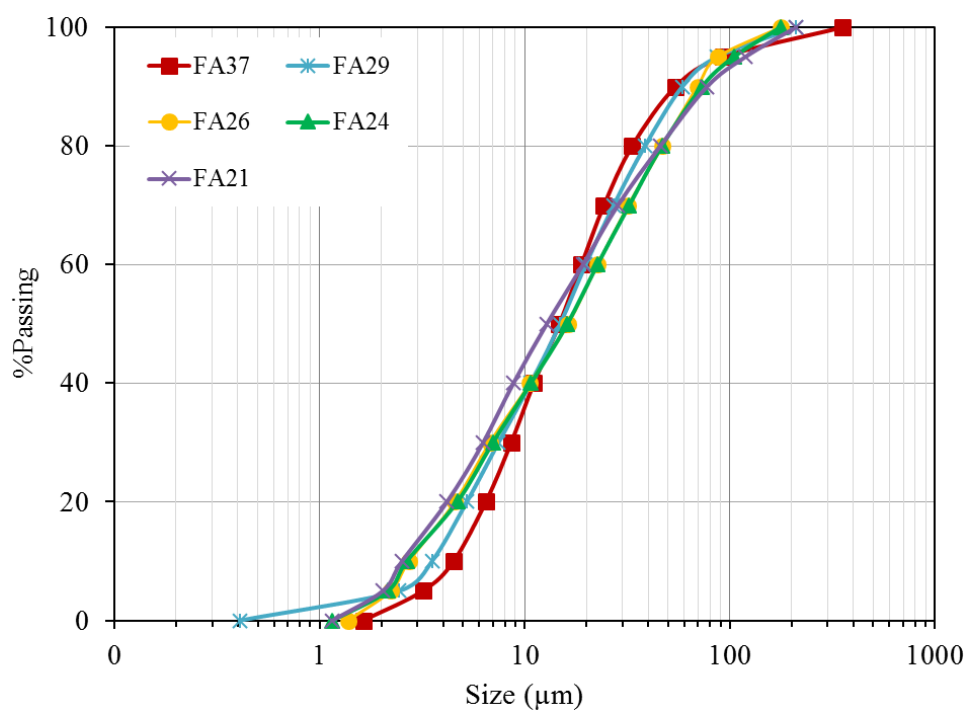
Figure 2.10: Particles size distribution of FAs.

2.3.2.3 *Specific gravity*

A pycnometer (Ultrapyc 1200e) was used to measure the specific gravity of the FAs by applying Archimedes' principle of fluid (gas) displacement and the technique of gas expansion (Boyle's

law) in accordance with the standard test method provided by ASTM C604-12 (Fig. 2.11) [97]. Helium gas was used in this instrument. The specific gravity of the different FA types ranged from 2.70 to 2.97 as shown in Table 2.4.

Table 2.4 summarizes the physical properties of the five FAs including the particle size distribution, relative density, and surface area (BET) tests results. D_{10} and D_{50} represent the corresponding diameters of 10% and 90% of the FA particle passed.

Figure 2.11: Pycnometer for measuring the specific gravity of the FAs.

Table 2.4: Physical properties of FAs.

Fly Ash Test	FA37	FA29	FA26	FA24	FA21
Particle size distribution D10%(μm)	32.98	43.28	2.73	2.66	2.523
Particle size distribution D50%(μm)	10.96	7.77	16.25	16.13	12.81
Particle size distribution D90%(μm)	0.52	0.43	69.32	73.16	77.34
Surface area (BET) m²/kg	44.74	35.26	1446	2858	2921
Specific gravity	7.18	9.29	2.70	2.89	2.82

Chapter 3: Trial Mixture and Mixing Procedures of Zero-Cement Mortar and Concrete

ZCC synthesized out of high calcium FA is a relatively new material that requires a thorough investigation. This chapter presents preliminary studies to determine the following aspects:

(1) What is the best mixing procedure for ZC mortar and ZCC? Four different mortar and eight different concrete mixing procedures were tried, investigated and are presented in this chapter.

(2) What are the appropriate ranges of Alk/FA, SS/SH, and W/FA to produce a structural mortar and concrete?

To address these issues, 215 mortar mixtures and 80 concrete mixtures were investigated. These mixtures were prepared using only one source of FA for mortar mixtures and four sources of FA for the concrete mixtures. Once the required ranges and appropriate mixing procedures were determined, a fine-tuning and optimization procedure was carried out and presented in Chapter 4, where the five sources of FA were used for mortar mixtures. The mixtures presented in this chapter evolved with the understanding of the effects of the different parameters and mixing procedures on the performance of ZC mortar and concrete. The criterion for accepting a structural mortar was a good workability higher than 40%. For concrete mixtures, the criteria were an adequate concrete strength exceeding 3000 psi and workability with a minimum slump of three inches.

3.1 Mortar

3.1.1 Materials

FA 24 was used in this chapter to synthesize the ZC mortar. A comprehensive characterization of the material used in this chapter is presented in Chapter 2.

3.1.2 Mixing procedures

All mixtures were carried out using a Hobart N50 commercial mixer at a room temperature of 73 $\pm\,3^{o}\,$F (23 $\pm\,2^{o}\,$C) (Fig. 3.1). In all the mortar mixtures, the required alkali activators, SS and SH, were mixed together prior to adding them to the mixture. Since there is no ASTM standard mixing procedure for ZC mortar, it was required to develop a mixing procedure that lead to homogeneous workable mortar. This challenging task went through different stages wherein the first phase two mixing procedures, procedures no. 1 and no. 2, were investigated. Based on the results of the first phase, the mixing procedure was improved and mixing procedures, procedures no. 3 and no. 4, were developed.

Figure 3.1: Two sizes of Hobart N50 mortar mixers.

3.1.2.1 *Preliminary mixing procedures*

This set included two mixing procedures, i.e., procedures no. 1 and no. 2. Mixing procedure no. 1 consisted of the following steps:

(1) The sand and FA were mixed together in a dry condition in the mixer at a mixing speed of 136 rpm for one minute to homogenously spread the ingredients particles.

(2) The alkali activators were gradually added over one minute while the mixing process continued.

(3) The water was gradually added over one minute while the mixing process continued, to better wet the FA and sand particles.

(4) Once all ingredients were added, mixing continued for another two minutes.

During this mixing procedure, mixing continued at each step until a homogenous mixture was observed. The mixing was not the best procedure. Adding the alkali activators before adding the mixing water resulted in agglomeration of the mixture. This was improved in mixing procedure no. 2.

Mixing procedure no. 2 consisted of the following steps:

(1) The sand and FA were mixed together for one minute at a mixing speed of 136 rpm.

(2) The water was gradually added over one minute to better wet the FA and sand particles while the mixing process continued.

(3) The alkali activators were gradually added over one minute while the mixing process continued.

(4) Once all ingredients were added, the mixing continued for another four minutes.

Although there was not any sign of agglomeration when using this mixing procedure, more iterations were carried out to improve the workability using the same amount of W/FA. Hence, mixing procedures no. 3 and no. 4 were investigated.

3.1.2.2 *Improved mixing procedures*

This phase included mixing procedures no. 3 and no. 4, which were improved procedures based on mixing procedure no. 2. Mixing procedure no. 3 was similar to mixing procedure no. 2 with one difference. During step no. 4, the mixer speed was increased to 281 rpm and the mixing continued for another four minutes. The higher mixing speed during step no. 4 increased the mortar slump flow and prevented the flash setting that occurred in some mixtures prepared using mixing procedure no. 2.

Mixing procedure no. 4 was similar to mixing procedure no. 3. However, steps no. 3 and no. 4 were changed as follows:

(1) The alkali activators were gradually added over five minutes while the mixing process continued.

(2) The mixing speed was increased to 281 rpm and the mixing continued for another five minutes.

Adding the alkali activators gradually over five minutes, rather than adding them over one minute only as in mixing procedure no. 3, enhanced the workability significantly allowing the use of a smaller W/FA. Hence, procedure no. 4 was selected to carry out the mortar mixtures presented in Chapter 5.

3.1.3 Trial mixtures

As discussed in detail later in this chapter, the results of the fresh properties of the ZC mortar showed that mixing procedures no.1 and no. 2 were not the best. Hence, not every single mixture was carried out using the four different mixing procedures. Rather, the best mixtures were selected for further improvements while less successful mixtures were discarded. Furthermore, some mixtures were not reported here as they suffered flash setting when mixed using procedures no. 1 and no. 2. Tables 3.1 and 3.2 show the mixture details that were mixed using procedures no. 1 and no. 2, respectively. The details of the mixtures prepared using mixing procedures no. 3 and no. 4 are shown in Chapters 4 and 5, respectively, as they were more successful and hence received more attention and testing. However, the results of a single mixture that was mixed using the three mixing procedures, i.e. 2, 3, and 4, are presented in this chapter for comparison purposes (Table 3.3).

For mixing procedures no. 1 and no. 2, a wide range of parameters were investigated. For example, the W/FA ranged from 0.400 to 0.600 for mixing procedure no. 1 and from 0.425 to 0.550 for mixing procedure no. 2. The Alk/FA ranged from 0.200 to 0.300 for mixing procedure no. 1 and from 0.300 to 0.400 for mixing procedure no. 2. The SS/SH ranged from 0.0 to 2.5 procedure no. 1 and from 0.5 to 2.5 for mixing procedure no. 2.

Table 3.1: ZC Mortar Mixtures Prepared Using Mixing Procedure no. 1.

Mix.	W/FA	Alk/FA	SS/SH	Sand/FA	Oven bag for heat curing
1	0.400	0.300	1.0	2	No
2	0.600	0.300	2.5	2	No
3	0.500	0.200	2.5	2	No
4	0.400	0.350	1.0	2	No
5	0.530	0.300	0.0	2	No
6	0.530	0.250	0.0	2	No
7	0.400	0.250	1.0	2	No
8	0.550	0.300	2.5	2	No
9	0.530	0.300	1.0	2	No

Table 3.2: ZC Mortar Mixtures Prepared Using Mixing Procedure no. 2.

Mix.	W/FA	Alk/FA	SS/SH	Sand/FA	Oven bag for heat curing
10	0.550	0.400	1.0	2.75	No
11	0.500	0.350	1.0	2.75	No
12	0.475	0.325	1.0	2.75	No
13	0.450	0.300	1.0	2.75	No/yes
14	0.425	0.300	1.0	2.75	No
15	0.400	0.300	1.0	2.75	No
16	0.500	0.400	1.0	2.75	No
17	0.450	0.300	0.5	2.75	No
18	0.450	0.300	1.5	2.75	No
19	0.450	0.300	2.5	2.75	No
20	0.450	0.325	1.0	2.75	No/yes
21	0.500	0.325	1.0	2.75	No/yes
22	0.475	0.300	1.0	2.75	No/yes
23	0.500	0.350	0.5	2.75	No
24	0.500	0.350	1.5	2.75	No
25	0.500	0.350	2.5	2.75	No

Table 3.3: ZC Mortar Mixtures Prepared Using Mixing Procedures no. 2 Through no. 4.

Mixing procedure	W/FA	Alk/FA	SS/SH	Sand/FA	Oven bag for heat curing
2	0.400	0.300	1.0	2.75	No
3	0.400	0.300	1.0	2.75	Yes
4	0.380	0.300	1.0	2.75	Yes

3.1.4 Fresh properties, casting, curing, and testing

3.1.4.1 Workability

The workability was measured using the flow table per ASTM C230-14 [98]. Two layers of the ZC mortar were cast in a standard brass cone (Fig. 3.2a), and each was compacted 20 times. Then, the brass cone was removed vertically leaving the ZC mortar on the table. Thereafter, the table was dropped 25 times in 15 seconds (Fig. 3.2b). The workability of each ZC mortar mixture was measured by calculating the percentage of the increase in the ZC mortar diameter to the initial base diameter of the cone per ASTM C1437-15 [99]. The reported workability of each mixture was the average of four perpendicular diagonal measurements of the cone.

(a)   (b)

Figure 3.2: Workability testing of ZC mortar (a) mortar filling the brass mold, and (b) the final workability of the mixture.

3.1.4.2 Setting time

A modified Vicat needle (Fig. 3.3), having a diameter of 0.08 in, was used to measure the initial and final setting times of the ZC mortar mixtures as per ASTM C807-13 [100]. The initial setting time was the time between adding the alkali activator to the FA and 0.4 in penetration of the needle into the mortar, while the final setting time was the time between adding the alkali activator to the FA and no remarkable needle penetration into the mortar.

Figure 3.3: Setting time testing of ZC mortar.

3.1.4.3 Casting of mortar cubes

The fresh ZC mortar was cast into 2 in cube brass molds per ASTM 109-16 [101] (Fig. 3.4). Molds made out of brass were used in this study due to their high thermal conductivity. The mortar was placed in two layers, and each layer was tamped 32 times.

Figure 3.4: Brass molds (a) before and (b) after placing the ZC mortar.

3.1.4.4 Curing regimes

After casting the ZC mortar in the brass molds, the specimens were allowed to have a rest time of two hours at an ambient temperature of $73 \pm 3^{\circ}$ F (23° C $\pm 2^{\circ}$ C) [44]. Then, two different curing regimes were used. The first regime included an elevated heat curing in an electric oven at 158° F (70° C) for 24 hours. The molds were either encased in oven bags before placing them into the oven or placed directly without the oven bags (Tables 3.1 and 3.2). Oven bags were used for all specimens that were prepared using mixing procedures no. 3 and no. 4, as during testing specimens from mixing procedures no. 1 and no. 2, it was found that encasing the molds with oven bags increased the compressive strength of the ZC mortar as it prevents moisture evaporation during curing. In addition to the built-in thermal controller in the oven, the temperature of the oven was monitored using thermocouples that were placed at different locations in the oven (Fig. 3.5). In the second curing regime, the specimens were cured at an ambient temperature of $73 \pm 3^{\circ}$ F ($23 \pm 2^{\circ}$ C) for 7 days.
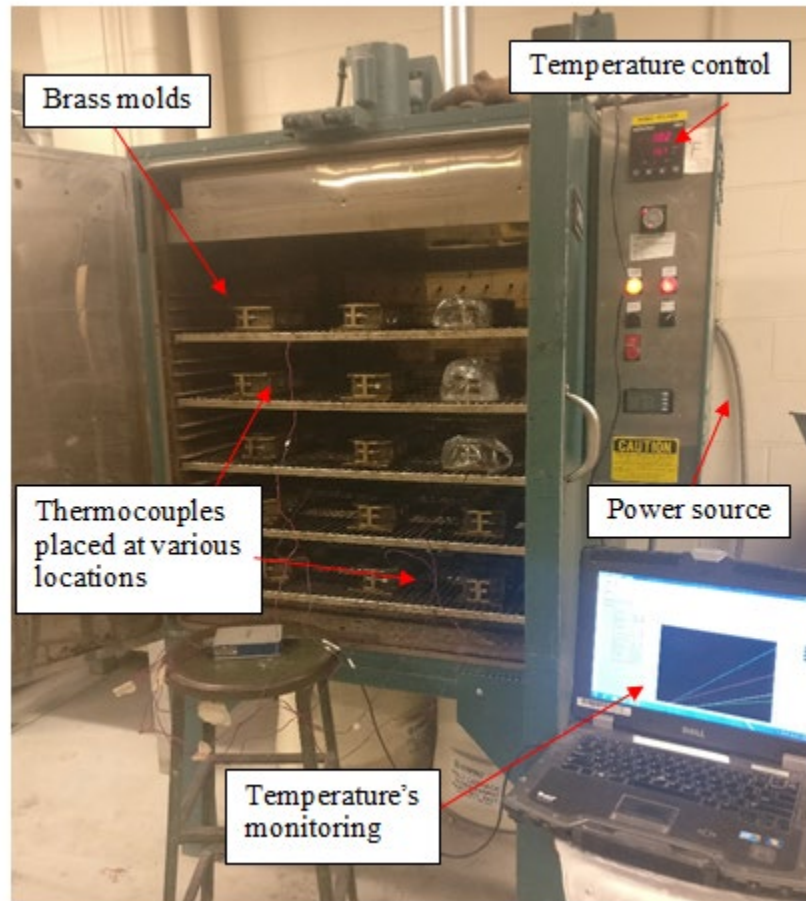
Figure 3.5: Thermocouples Setup.

All the oven-cured specimens were demolded after getting them out of the oven after at least 1 hour to let them cool down and avoid the sudden change in the temperature between the oven and the ambient temperature. The ambient-cured specimens were demolded after 24 hours or 48 hours depending on the observed setting times. Then, all the cubes were left at the ambient temperature until the testing day. All specimens were tested at the age of 7 days. It is worth noting that specimens prepared using the final mixtures presented in Chapter 6 were tested at different ages including 1 day and 28 days.

3.1.4.5 Compressive strength

The compressive strength of each mixture was determined using a Tinius Olsen loading machine (Fig. 3.6) using a loading rate of 200 lb/sec. The specimens were tested per ASTM C109-16 [101]. Each reported strength is the average of the results of three cubes per each mixture.
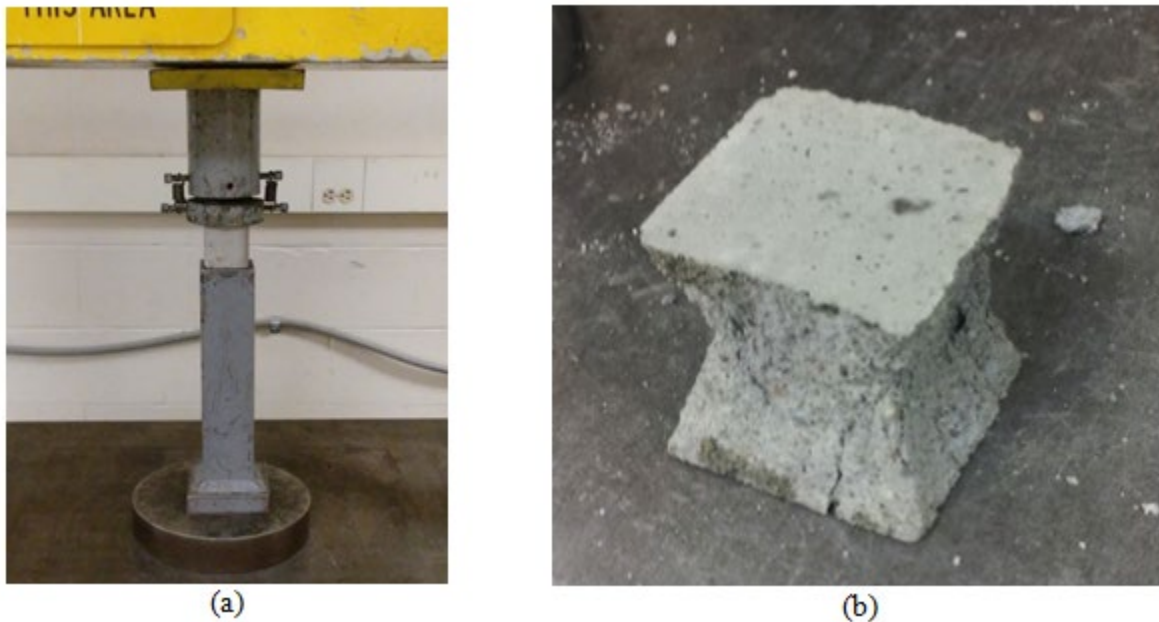
Figure 3.6: Compression test of ZC mortar cubes (a) during, and (b) after testing.

3.1.5 Results

Although there is no ASTM minimum required mortar workability, it is common practice to target a mortar mixture with workability higher than 40%. Similarly, there are no constraints on the setting times of the mortar mixtures tested by the modified Vicat needle per ASTM C807-13 [100]; however, the initial setting times of the investigated mortars were compared with the minimum and maximum initial setting times of the Portland cement paste per ASTM C150-16 [102], which are 45 minutes and 375 minutes, respectively. Furthermore, 3000 psi was selected to be the minimum acceptable compressive strength for the investigated mortar.

3.1.5.1 Results of mixing procedures no. 1

Table 3.4 shows the workability, initial setting time (In. Set.), final setting time (Fi. Set.), and compressive strengths of the specimens prepared using the nine mixtures and mixing procedure no. 1. The workability of the investigated mixtures ranged from 30% to 120% (Table 3.4). Three mixtures showed workability less than 40%. The initial setting times of the investigated mixtures ranged from 10 minutes to 165 minutes (Table 3.4) with four mixtures showed an initial setting time less than the minimum setting time limit of 45 minutes. The final setting times ranged from 25 minutes to 385 minutes with the nine mixtures showing an initial setting time less than the maximum setting time limit of 375 minutes (Table 3.4).

Table 3.4: Properties of ZC mortar mixtures prepared using mixing procedure no. 1.

Mix.	Workability (%)	In. Set. (min)	Fi. Set. (min)	$f_{c(ambient)}$ (psi)	$f_{c(oven)}$ (psi)	Acceptable
1	58	53	93	1780	3640	No ($f_{c(ambient)}$)
2	33	165	385	285	1920	No (workability, $f_{c(both)}$)
3	68	43	145	640	3650	No (In. Set., $f_{c(ambient)}$)
4	45	37	87	4315	4535	No (In. Set.)
5	30	10	25	920	1415	No (All)
6	35	32	32	680	1175	No (All)
7	58	55	95	1150	3790	No ($f_{c(ambient)}$)
8	71	164	378	1010	3095	No ($f_{c(ambient)}$)
9	120	55	121	115	1470	No ($f_{c(both)}$)

While mixing procedure no. 1 was not successful, a careful investigation of the obtained results can help in preliminary determinations of the required parameters to produce a structural mortar. The compressive strengths of the ambient-cured specimens, $f_{c(ambient)}$, were very low ranging from 115 psi to 1780 psi except for mix 4 which had 4315 psi. However, mix 4 displayed fast setting and was considered an inappropriate mixture. The compressive strengths of the oven-

cured specimens, $f_{c(oven)}$, were relatively higher than that of the ambient-cured with $f_{c(oven)}$ ranging from 1175 psi to 3790 psi except for mix 4 which had 4535 psi. Four mixtures showed $f_{c(oven)}$ less than 3000 psi. However, the compressive strength of all oven-cured specimens was less than 4000 psi except mix 4 which had 4535 psi. These low compressive strengths of the ambient and oven-cured specimens were mainly due to agglomeration of the mortar during mixing and low workability which resulted in inconsistent mortar mixtures. These results confirmed the visual inspection during the mixing that mixing procedure no. 1 was not appropriate for ZC mortar and had to be improved.

The best oven and ambient compressive strengths of the specimens that were mixed using procedure no. 1 were obtained at W/FA ranging from 0.400 to 0.550, Alk/FA ranging from 0.250 to 0.350, and SS/SH of 1.0 and 2.5. However, Alk/FA of 0.200 had $f_{c(oven)}$ of 3650 psi, $f_{c(ambient)}$ of only 640 psi; therefore, the Alk/FA of 0.200 was not considered for further investigation. Furthermore, in order to minimize the cost of the mixture, Alk/FA ratio of 0.35 was not considered for further study as it had a high alkali solution compared with Alk/FA of 0.250 and 0.300 that showed high compressive strengths with a lower alkali solution which would reduce the mixture cost. Although $f_{c(ambient)}$ of some specimens prepared using SS/SH of 0.0 were higher than that of some specimens prepared using SS/SH of 2.5, $f_{c(oven)}$ of the specimens prepared with SS/SH of 2.5 reached 3650 psi while that of the specimens synthesized with SS/SH of 0.0 reached 1415 psi. Hence, SS/SH of 0.0 was not considered for further investigation.

3.1.5.2 *Results of mixing procedure no. 2*

Table 3.5 shows the workability, setting times, and compressive strengths of the specimens prepared using mixing procedure no. 2. The workability of the sixteen investigated mixtures ranged from 35% to 150% (Table 3.5) with one mixture showing a workability of less than 40%

and hence considered unacceptable. The initial setting time of the investigated mixtures ranged from 50 minutes to 420 minutes (Table 3.5) while the final setting time ranged from 70 minutes to 490 minutes (Table 5). All the sixteen mixtures showed an initial setting time higher than 50 minutes. However, Mix. 21 exceeded the maximum initial setting time limit of 375 minutes and hence was considered unacceptable.

As shown in Table 3.5, the compressive strength of the ambient and oven-cured specimens ranged from 1185 psi to 3125 psi and 2865 psi to 5650 psi, respectively. For the ambient-cured specimens, one mixture displayed a compressive strength higher than 3000 psi, while thirteen mixtures displayed compressive strengths higher than 2000 psi. For the oven-cured specimens, fifteen mixtures displayed compressive strengths higher than 3000 psi. Therefore, mixing procedure no. 2 can be used as the basis to further improve the ZC mortar mixing procedure.

Table 3.5: Properties of ZC mortar mixtures prepared using mixing procedure no. 2.

Mix.	Workability (%)	In. Set. (min)	Fi. Set. (min)	$f_{c(ambient)}$ (psi)	$f_{c(oven)}$ (psi)	Acceptable
10	118	375	410	2005	5650	No ($f_{c(ambient)}$)
11	80	195	240	2000	5315	No ($f_{c(ambient)}$)
12	85	215	250	2470	5535	No ($f_{c(ambient)}$)
13	100	305	350	2300	4895	No ($f_{c(ambient)}$)
14	45	90	110	2610	4360	No ($f_{c(ambient)}$)
15	35	50	70	3125	4615	No (workability)
16	75	130	155	2645	4600	No ($f_{c(ambient)}$)
17	150	360	450	2220	2865	No ($f_{c(ambient)}$)
18	90	270	330	2655	4615	No ($f_{c(ambient)}$)
19	70	260	310	1940	4205	No ($f_{c(ambient)}$)
20	80	160	210	2535	4230	No ($f_{c(ambient)}$)
21	150	420	490	2635	4370	No (In. Set., $f_{c(ambient)}$)
22	110	360	420	1510	3175	No ($f_{c(ambient)}$)
23	120	220	270	2555	4125	No ($f_{c(ambient)}$)
24	105	250	305	2280	3765	No ($f_{c(ambient)}$)
25	70	195	260	1185	3510	No ($f_{c(ambient)}$)

As shown in Table 3.5, the mixtures that displayed an acceptable compressive strength while displaying good workability and setting times had W/FA ranging from 0.400 to 0.550, Alk/FA ranging from 0.250 to 0.400, and SS/SS ranging from 0.5 to 2.5. Furthermore, due to the cost of alkali activators, mixtures that had Alk/FA higher than 0.30 was not considered for further analysis. These ranges are similar to those obtained using mixture procedure no. 1.

3.1.5.3   Discussion of mixing procedures no. 1 and no. 2

This section presents qualitative comparison between the performances of mixtures prepared using mixing procedures no. 1 and no. 2. Fig. 3.7 shows comparisons between the workability, setting times, and compressive strengths of the mixtures prepared using procedures no. 1 and no. 2. The ambient compressive strength of mix 4 prepared using procedure no.1 was not included in Fig. 3.7e since it displayed fast setting. As shown in the figures, the workability, setting times, and compressive strengths of the oven and ambient-cured specimens prepared using mixing procedure no. 2 were better than those prepared using mixing procedure no. 1. During mixing procedure no. 2 there was no sign of agglomeration as was noticed in the specimens that were mixed following mixing procedure no.1. Using mixing procedure no. 2 increased the average workability (Fig. 3.7a), initial setting time ((Fig. 3.7b), final setting time (Fig. 3.7c), oven (Fig. 3.7d) and ambient (Fig. 3.7e) compressive strengths by 38%, 72%, 48%, 37%, and 47%, respectively.
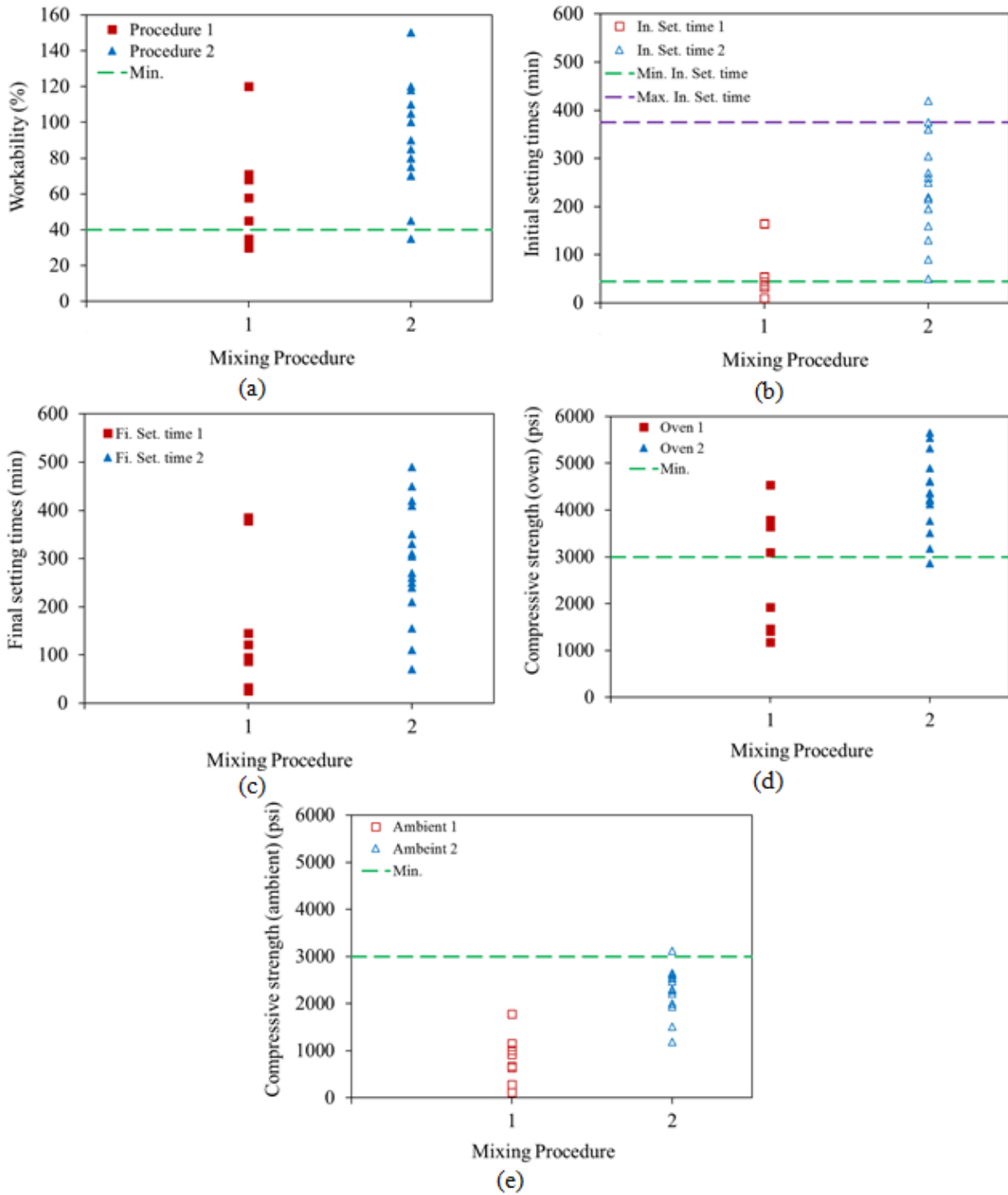
Figure 3.7: (a) Workability, (b) initial setting times, (c) final setting time, (d) oven-cured compressive strength, and (e) ambient-cured compressive strength of ZC mortars prepared using procedures no. 1 and 2.

3.1.5.4 Effect of W/FA

Figs. 3.8 and 3.9 show the effect of the W/FA, Alk/FA, and SS/SH on the workability, setting times, and compressive strength of the ZC mortars prepared using mixing procedures no. 1 and no. 2. The W/FA ranging from 0.40 to 0.550 showed workability higher than 40% (Fig. 3.8a) for all mixtures except one prepared using procedure no. 2. However, mixing procedure no. 1 did not have a consistent results, where mixtures having high values W/FA displayed very low workability. For W/FA of 0.40 and higher, all mixtures prepared using mixing procedure no. 2, but one, displayed an acceptable initial setting time. This was not the case for mixing procedure no. 1, where several mixtures didn't meet the minimum initial setting time (Fig. 3.8d). Furthermore, the W/FA ranging from 0.40 to 0.55 displayed compressive strength higher than 3000 psi for the oven-cured specimens prepared using mixing procedure no. 2. However, for this W/FA range, ambient-cured specimens prepared using mixing procedures no. 1 displayed very low strength while most of those prepared using mixing procedure no. 2 displayed strengths ranging from 1000 to 3000 psi (Fig. 3.9a).
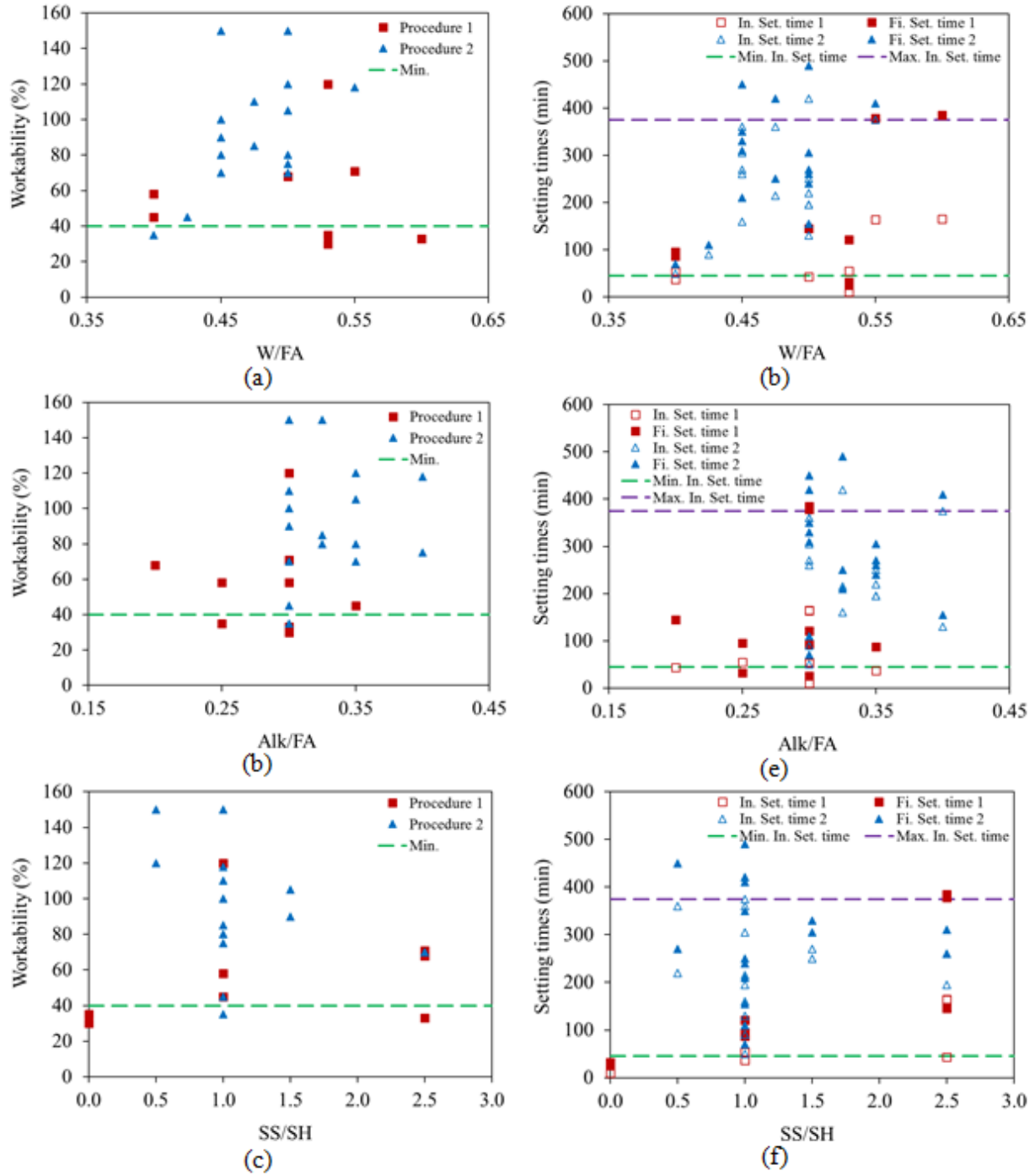
Figure 3.8: Effect of (a) W/FA on workability, (b) W/FA on setting times, (c) Alk/FA on workability, (d) Alk/FA on setting times, (e) SS/SH on workability, and (f) SS/SH on setting times of ZC mortars prepared using mixing procedures no. 1 and no. 2.
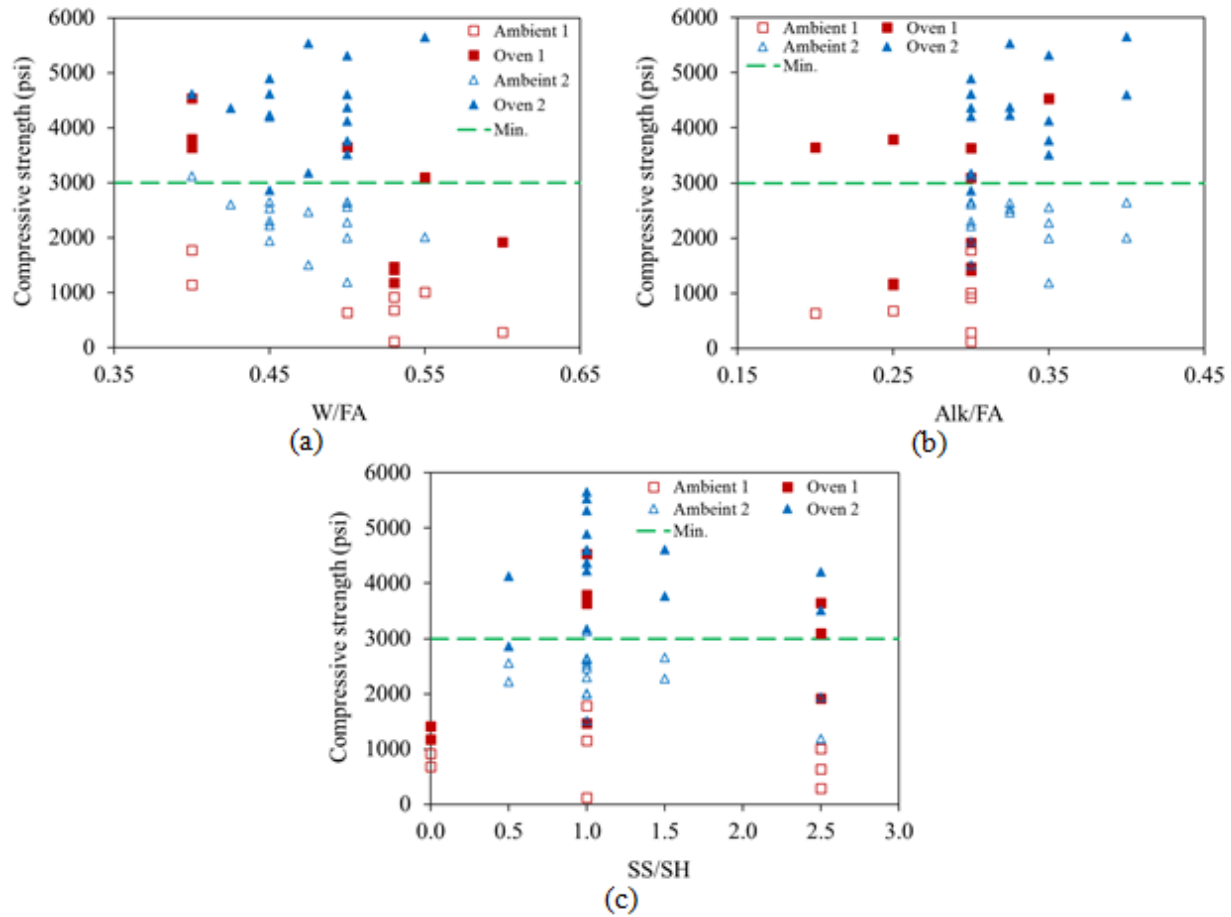
Figure 3.9: Effect of (a) W/FA, (b) Alk/FA, and (c) SS/SH on the compressive strengths of ZC mortars, respectively, prepared using mixing procedures no. 1 and 2.

3.1.5.5 Effect of Alk/FA

The Alk/FA ranged from 0.20 to 0.40 displayed workability higher than 40% (Fig. 3.8b). For all Alk/FA, all specimens that were prepared using mixing procedures no. 2, but one, met the acceptable range of initial setting time. However, those prepared using mixing procedure no. 1 either did not meet the minimum initial setting time or barely met it (Fig. 3.8e). For Alk/FA within 0.20 to 0.40, specimens prepared using mixing procedure no. 2 displayed ambient compressive strength of 2000 psi or higher, while those prepared using oven curing displayed 3000 psi or higher. For mixing procedure no. 1 for all Alk/FA values, all specimens, except five, displayed low strength (Fig. 3.9b).

3.1.5.6 Effect of SS/SH

The SS/SH ranging from 0.5 to 2.5 displayed workability higher than 40% (Fig. 3.8b). For the same range, all specimens prepared using mixing procedure no. 2, except one, displayed initial setting times within the acceptable range. However, regardless of SS/SH, numerous specimens that were prepared using mixing procedure no. 1 did not meet the setting time criterion regardless of SS/SH (Fig. 3.8f). The best compressive strengths also occurred at SS/SH of 1.0 for mixing procedures no. 1 and no. 2 (Fig. 3.9c).

3.1.5.7 Improved mixing procedures

Table 3.6 shows the workability, setting times, and compressive strength of the two improved mixing procedures and mixing procedure no. 2 for comparison. The workability, initial setting time, and final setting time of the mixture prepared using procedure no. 3 are 125%, 54%, and 53% higher than those of the same mixture prepared using procedure no. 2. Furthermore, the compressive strength of the oven-cured specimen prepared using procedure no. 3 is 26% higher than that of the specimen prepared using mixing procedure no. 2. However, the compressive strength of the ambient-cured specimens remained approximately constant. In mixing no. 3, after adding the alkali activator, the mixing speed was increased from 136 rpm to 281 rpm which increased the workability and homogeneity of the mixture, therefore increasing the compressive strength.

In the case of mixing procedure no. 4, adding the alkali activator gradually over five minutes instead of one minute enhanced the properties of the mixture significantly. The workability, initial setting time, and final setting time of the mixture prepared using procedure no. 4 are 122%, 219%, and 173% higher than those of the same mixture prepared using procedure no. 3. Furthermore, the compressive strength of the ambient-cured specimen prepared using mixing

72

procedure no. 4 was 129% higher than that of the specimen prepared using mixing procedure no. 3. However, the compressive strength of the oven-cured specimens remained approximately constant.

It was observed that after adding the alkali activator over one minute during mixing procedure no. 3, the mixture became more workable but the workability decreased significantly very quickly. However, when the same amount of alkali activator was added but over five minutes, the workability did not decrease at the same rate as with mixing procedure no. 3. It is worth mention that the ambient curing regime of mixing procedure no. 4 was set at a temperature of 86° F (30° C) to imitate hot summer temperatures in Missouri, which can partially explain the significant improvement in the ambient-cured compressive strength. Detailed discussion of curing effects is presented in Chapter 5 of this report.

Table 3.6: Properties of ZC Mortar Mixture Prepared Using the Improved Mixing Procedures.

Mixing procedure	W/FA	Alk/FA	SS/SH	Sand/FA	Workability (%)	In. Set. (min)	Fi. Set. (min)	$f_{c(ambient)}$ (psi)	$f_{c(oven)}$ (psi)
2	0.400	0.300	1.0	2.75	20	52	72	2300	4615
3	0.400	0.300	1.0	2.75	45	80	110	2310	5835
4	0.380	0.300	1.0	2.75	100	255	300	5280	5650

3.1.5.8 *Effect of the oven bag*

Table 3.7 shows comparisons between the compressive strengths of the two methods that were followed in the oven curing regime, where some molds were placed in oven bags and some were not. As shown in Table 3.7, the compressive strength of the specimens that were encased in oven bags showed an average compressive strength 18% higher than those that were not encased in oven bags.

Table 3.7: Compressive Strengths Results of the Oven-Cured Specimens With and Without Oven Bags.

Mix.	Mixing procedure	W/FA	Alk/FA	SS/SH	Sand/FA	$f_{c(oven)}$ without bags (psi)	$f_{c(oven)}$ with bags (psi)
13	2	0.450	0.300	1	2.75	4894	5179
20	2	0.450	0.325	1	2.75	4231	5420
21	2	0.500	0.325	1	2.75	4371	4768
22	2	0.475	0.300	1	2.75	3177	4320

3.2 Concrete

3.2.1 Materials

Four sourced FAs, FA27, FA24, FA25, and FA21, out of the first batch as discussed in Chapter 2, were used to prepare the ZCC mixtures presented in this section. All other materials used in this chapter are described in Chapter 2.

3.2.2 Mixing procedures

A gravity mixer (Fig. 3.10) having a capacity of 3 ft^3 was used in mixing the ZCC. The mixer relays on the rotating body of the mixer and the gravity of the mixture's ingredients to be mixed well.

Figure 3.10: Gravity mixer with a maximum capacity of 1.5 ft^3.

In all concrete mixtures, the required alkali activators consisting of SS and SH were mixed together prior to adding them to the mixture. Since there is no ASTM standard mixing procedure for ZCC, it was required to develop a mixing procedure that led to homogeneous workable concrete. To address this challenge, eight mixing procedures were investigated during this chapter.

3.2.2.1 Mixing procedure no. 1

The mixing procedure consisted of the following steps:

(1) The coarse and sand aggregates were mixed for one minute.

(2) The FA was added and mixed with the aggregates for one minute.

(3) The alkali activators were gradually added over one minute.

(4) The water was gradually added over one minute.

(5) Once all ingredients were added, the mixing procedure continued for another three minutes.

3.2.2.2   *Mixing procedure no. 2*

The first two steps are similar to mixing procedure no. 1. The other steps are as follows:

(3) The water was gradually added over one minute.

(4) The alkali activators were gradually added over one minute.

(5) Once all ingredients were added, the mixing procedure continued for another three minutes.

3.2.2.3   *Mixing procedure no. 3*

The first two steps are similar to mixing procedure no. 1. The other steps are as follows:

(3) The water was gradually added to the mix over one minute.

(4) The sodium hydroxide (SH) only was gradually added over two minutes.

(5) The sodium silicate (SS) was gradually added over one minute.

(6) Once all ingredients were added, the mixing procedure continued for another three minutes.

3.2.2.4   *Mixing procedure no. 4*

The first two steps are similar to mixing procedure no. 1. The other steps are as follows:

(3) Three quarters of the required water was gradually added over one minute.

(4) The alkali activators were gradually added over one minute.

(5) The remaining amount of water was gradually added over one minute.

(6) Once all ingredients were added, the mixing procedure continued for another three minutes.

3.2.2.5   Mixing procedure no. 5

The first two steps are similar to mixing procedure no. 1. The other steps are as follows:

(3) One half of the required water was gradually added over one minute.

(4) One half of the alkali activators were gradually added over one minute.

(5) The mixing was continued for two more minutes.

(6) The second half of the water was gradually added over one minute.

(7) The second half of the alkali activators was gradually added over one minute.

(8) Once all ingredients were added, the mixing procedure continued for another three minutes.

3.2.2.6   Mixing procedure no. 6

The mixing procedure consisted of the following steps:

(1) The coarse and sand aggregates were mixed for one minute.

(2) One half of the required water was gradually added over one minute.

(3) The FA was added and mixed with the aggregates for one minute.

(4) The second half of the water was gradually added over one minute.

(5) One half of the alkali activators were added over one minute.

(6) The mixing was continued for one more minute.

(7) The second half of the alkali activators was gradually added for one minute.

(8) Once all ingredients were added, the mixing procedure continued for another three minutes.

3.2.2.7 Mixing procedure no. 7

The first two steps are similar to mixing procedure no. 1. The other steps are as follows:

(3) The water was gradually added over one minute.

(4) One half of the alkali activators were gradually added over one minute.

(5) The mixing was continued for one more minute.

(6) The second half of the alkali activator was gradually added over one minute.

(7) Once all ingredients were added, the mixing procedure continued for another three minutes.

3.2.2.8 Mixing procedure no. 8

The first two steps are similar to mixing procedure no. 1. The other steps are as follows:

(3) The water was gradually added over one minute.

(4) The alkali activator was gradually added over five minutes.

(5) Once all ingredients were added, the mixing procedure continued for another five minutes.

3.2.3 Trial mixtures

In order to determine the required range of W/FA, FA content, coarse aggregate to sand ratio, and mixing procedure, numerous trial mixtures were investigated. The different mixing procedures were first investigated using FA25 (Table 3.8). Then, other sourced FAs were explored as well. Fine tuning of the concrete mixture is presented in Chapter 6. Tables 3.8 through 3.11 show the mixture details for FAs, FA25, FA27, FA24, and FA21, respectively.

Table 3.8: Design of ZCC Mixtures Prepared Using FA25 (lb/ft^3).

Mix.	W/FA	Alk/FA	SS/SH	Mixing Pro.	C.A.	Sand	FA	S.S.	S.H.	Water
1	0.400	0.300	1	1	60.7	50.6	25.0	3.75	3.75	5.91
2	0.550	0.250	1	2	70.6	48.6	19.0	2.38	2.38	8.11
3	0.425	0.250	1	2	92.6	63.7	25.0	3.12	3.12	7.52
4	0.350	0.300	1	2	56.2	56.2	25.0	3.75	3.75	4.66
5	0.450	0.300	1	2	56.2	56.2	25.0	3.75	3.75	7.15
6	0.500	0.300	1	2	59.9	49.9	25.0	3.75	3.75	8.40
7	0.425	0.300	1	2	59.9	49.9	25.0	3.75	3.75	6.52
8	0.400	0.300	1	2	60.7	50.6	25.0	3.75	3.75	5.91
9	0.375	0.275	1	2	62.2	51.8	25.0	3.43	3.43	5.68
10	0.400	0.275	1	2	61.4	51.2	25.0	3.43	3.43	6.30
11	0.390	0.250	1	2	62.2	62.2	25.0	3.12	3.12	6.44
12	0.425	0.300	1	2	49.9	49.9	29.3	4.40	4.40	7.52
13	0.450	0.300	1	2	50.6	50.6	28.1	4.21	4.21	7.93
14	0.425	0.300	1	2	51.4	51.4	28.1	4.21	4.21	7.24
15	0.425	0.300	1	2	60.7	50.6	25.0	3.75	3.75	6.53
16	0.400	0.300	1	3	60.7	50.6	25.0	3.75	3.75	5.91
17	0.400	0.300	1	4	60.7	50.6	25.0	3.75	3.75	5.91
18	0.400	0.300	1	5	60.7	50.6	25.0	3.75	3.75	5.91
19	0.400	0.300	1	6	60.7	50.6	25.0	3.75	3.75	5.91
20	0.400	0.300	1	7	57.3	47.8	28.1	4.21	4.21	6.55
21	0.400	0.300	1	7	60.7	50.6	25.0	3.75	3.75	5.91
22	0.380	0.300	1	8	58.2	48.4	28.1	4.21	4.21	5.99
23	0.350	0.300	1	8	59.8	49.9	28.1	4.21	4.21	5.17

Table 3.9: Design of ZCC Mixtures Prepared Using FA27 (lb/ft^3).

Mix.	W/FA	Alk/FA	SS/SH	Mixing pro.	C.A.	Sand	FA	S.S.	S.H.	Water
1	0.380	0.300	1.0	7	62.2	51.8	25.0	3.75	3.75	5.42
2	0.400	0.300	1.0	7	61.4	51.2	25.0	3.75	3.75	5.91
3	0.360	0.300	1.0	7	62.2	51.8	25.0	3.75	3.75	4.92
4	0.380	0.300	1.0	7	58.2	48.4	28.1	4.21	4.21	5.99
5	0.380	0.300	1.0	7	62.2	51.8	25.0	3.75	3.75	5.42
6	0.380	0.300	1.0	7	59.0	49.2	28.1	4.21	4.21	6.00
7	0.300	0.250	1.0	7	65.2	54.3	25.0	3.12	3.12	4.21
8	0.320	0.250	1.0	7	64.4	53.7	25.0	3.12	3.12	4.71
9	0.340	0.250	1.0	7	63.7	53.1	25.0	3.12	3.12	5.20
10	0.300	0.200	1.0	7	65.9	54.9	25.0	2.50	2.50	4.99
11	0.380	0.300	1.0	7	58.2	48.4	28.1	4.21	4.21	5.44
12	0.360	0.300	1.0	7	59.0	49.2	28.1	4.21	4.21	5.44
13	0.360	0.300	1.0	7	59.0	49.2	28.1	4.21	4.21	0.07
14	0.380	0.300	1.0	7	58.2	48.4	28.1	4.21	4.21	5.99
15	0.340	0.300	1.0	7	59.9	49.9	28.1	4.21	4.21	4.89
16	0.400	0.300	1.0	7	57.3	47.8	28.1	4.21	4.21	6.55
17	0.380	0.350	1.0	7	58.2	48.4	28.1	4.92	4.92	5.13
18	0.380	0.300	1.0	7	58.2	48.4	28.1	4.21	4.21	5.99
19	0.380	0.300	1.0	7	58.2	48.4	28.1	4.21	4.21	5.99
20	0.420	0.350	1.0	7	56.5	47.1	28.1	4.92	4.92	6.24
21	0.400	0.300	1.0	7	57.3	47.8	28.1	4.21	4.21	6.55
22	0.450	0.400	1.0	7	54.8	45.6	28.1	5.62	5.62	6.21
23	0.400	0.350	1.0	7	57.3	47.8	28.1	4.92	4.92	5.69
24	0.450	0.350	1.0	7	55.6	46.4	28.1	4.92	4.92	7.08
25	0.350	0.300	1.0	8	59.8	49.9	28.1	4.21	4.21	5.17

Table 3.10: Design of ZCC Mixtures Prepared Using FA24 (lb/ft^3).

Mix.	W/FA	Alk/FA	SS/SH	Mixing Pro.	C.A.	Sand	FA	S.S.	S.H.	Water
1	0.425	0.300	1.0	7	59.9	49.9	25.0	3.75	3.75	6.52
2	0.360	0.300	1.0	7	60.7	50.6	25.0	3.75	3.75	4.91
3	0.380	0.300	1.0	7	61.4	51.2	25.0	3.75	3.75	5.41
4	0.360	0.300	1.0	7	59.0	49.1	28.1	4.21	4.21	5.44
5	0.360	0.300	1.0	7	62.9	52.4	25.0	3.75	3.75	4.93
6	0.360	0.300	1.0	7	59.8	49.8	21.8	4.21	4.21	5.45
7	0.380	0.300	1.0	7	62.2	51.8	25.0	3.75	3.75	5.42
8	0.340	0.250	1.0	7	63.7	53.1	25.0	3.12	3.12	5.20
9	0.320	0.250	1.0	7	64.4	53.7	25.0	3.12	3.12	4.71
10	0.300	0.250	1.0	7	65.2	54.3	25.0	3.12	3.12	4.49
11	0.280	0.200	1.0	7	65.9	54.9	25.0	2.50	2.50	4.49
12	0.260	0.200	1.0	7	66.7	55.6	25.0	2.50	2.50	0.06
13	0.300	0.200	1.0	7	67.4	56.2	25.0	2.50	2.50	5.00
14	0.350	0.300	1.0	8	59.0	49.1	28.1	4.21	4.21	5.16

Table 3.11: Design of ZCC Mixtures Prepared Using FA21 (lb/ft^3).

Mix.	W/FA	Alk/FA	SS/SH	Mixing Pro.	C.A.	Sand	FA	S.S.	S.H.	Water
1	0.340	0.300	1	7	62.9	52.4	25.0	3.75	3.75	4.43
2	0.360	0.300	1	7	62.2	51.8	25.0	3.75	3.75	4.92
3	0.380	0.300	1	7	58.2	48.4	28.1	4.21	4.21	5.99
4	0.380	0.300	1	7	58.2	49.2	28.1	4.21	4.21	6.00
5	0.360	0.300	1	7	59.0	49.2	28.1	4.21	4.21	5.44
6	0.380	0.300	1	7	0.0	89.3	32.5	4.87	4.87	6.72
7	0.380	0.300	1	7	58.2	48.4	28.1	4.21	4.21	5.99
8	0.360	0.300	1	7	59.0	49.2	28.1	4.21	4.21	5.44
9	0.360	0.300	1	7	59.9	49.9	28.1	4.21	4.21	5.45
10	0.340	0.300	1	7	59.9	49.9	28.1	4.21	4.21	5.45
11	0.380	0.300	1	7	58.2	48.4	28.1	4.21	4.21	5.99
12	0.360	0.300	1	7	59.0	49.2	28.1	4.21	4.21	5.44
13	0.380	0.300	1	8	58.2	48.4	28.1	4.21	4.21	5.99
14	0.350	0.300	1	8	59.9	49.9	28.1	4.21	4.21	5.17

3.2.4 Fresh properties, casting, curing, and testing

3.2.4.1 Workability

The workability of each concrete mixtures was determined using a slump test per ASTM C143-15 [103] (Fig. 3.11).

Figure 3.11: Examples of slump tests of ZCC (a) 8 in (mix 11 of FA27), and (b) 6.5 in (mix 7 of FA25).

3.2.4.2 Casting of concrete cylinders

The concrete mixture that had an accepted slump was cast in 4 x 8 in plastic cylinders per ASTM C192-16 [104]. The concrete was placed in two layers and each layer was tamped 25 times.

3.2.4.3 Curing regimes

After casting the concrete in the plastic cylinders, each specimen had a rest time of two hours at an ambient temperature of 73 ± 3° F (23° C $\pm 2^{o}$ C) [44]. Then, two different curing regimes were used. The oven curing regime included an elevated heat curing in an electric oven at 158° F (70° C) for 24 hours. The molds were either encased in oven bags before placing them into the oven or placed directly in the oven without the bags (Tables 3.1 and 3.2). Oven bags were used for all specimens when it was found that encasing the molds in oven bags increased the compressive

strength of ZC mortar. As explained in the previous section, in addition to the built-in thermal controller in the oven, the temperature was monitored using thermocouples that were placed at different locations in the oven (Fig. 3.5). The ambient curing regime included leaving the specimens at an ambient temperature of $73 \pm 3^{\circ}$ F ($23 \pm 2^{\circ}$ C) for 7 days.

All the oven-cured specimens were demolded after letting them rest out of the oven for at least 1 hour to let them cool down and avoid sudden changes in the temperature between the oven and the ambient temperature. The ambient-cured specimens were demolded after 48 hours. With both curing techniques, two approaches were used to store the specimens after demolding them. First, specimens were stored directly in the laboratory at the room temperature of $73 \pm 3^{\circ}$ F ($23 \pm 2^{\circ}$ C) until the testing age. Second, specimens were encased in plastic bags to prevent moisture loss. The first storing approach was in conjunction with the mixing procedures no. 1 through 7. The second storing regime was followed for the specimens that were mixed according to mixing procedure no. 8. Furthermore, the two storing regimes were applied to a selected mixture of FA25 and FA21 that was prepared using mixing procedure no. 8 for comparison. All specimens were tested at the age of 7 days. It is worth noting that specimens prepared using final mixtures presented in Chapter 6 were tested at different ages including 1 day and 28 days.

3.2.4.4   *Compressive strength test*

The compressive strength of each mixture was determined using a Tinius Olsen loading machine at a loading rate of 500 lb/sec (Fig. 3.12). The specimens were tested per ASTM C39-16 [105]. The reported strengths are the average of the results of three cylinders per each mixture.

Figure 3.12: ZCC cylinders (a) before, and (b) after testing the compressive strength.

3.2.5 Results

The slump and compressive strength of each mixture are summarized in Tables 3.12 through 3.15 for mixtures synthesized using FA25, FA27, FA24, and FA21, respectively.

In mixing procedure no. 1, the alkali activator was added to the mixture before adding the water. That had a negative effect on the workability and caused the mixture to be stuck to the mixer even before adding the water. Therefore, this procedure was terminated and not used any more in this study.

In mixing procedure no. 2, high water content was used to synthesize the ZCC mixtures. However, the slump value was too high and bleeding was observed. Then, the water content was reduced significantly, but the mixture stuck to the mixer. So, the water content was increased again to increase the workability, but the corresponding compressive strength of both curing regimes was low and did not meet the minimum threshold of 3000 psi.

Table 3.12: Slump and Compressive Strengths of ZCC Mixtures Prepared Using FA25.

Mix.	W/FA	Alk/FA	SS/SH	FA (lb/ft^3)	Mixing Pro.	Slump (in)	$f_{c(oven)}$ (psi)	$f_{c(ambient)}$ (psi)
1	0.400	0.300	1	25.0	1	Stuck	N.A.	N.A.
2	0.550	0.250	1	19.0	2	bleeding	N.A.	N.A.
3	0.425	0.250	1	25.0	2	bleeding	N.A.	N.A.
4	0.350	0.300	1	25.0	2	stuck	N.A.	N.A.
5	0.450	0.300	1	25.0	2	8.5	3110	1395
6	0.500	0.300	1	25.0	2	7.0	2455	860
7	0.425	0.300	1	25.0	2	7.5	3475	1465
8	0.400	0.300	1	25.0	2	stuck	N.A.	N.A.
9	0.375	0.275	1	25.0	2	stuck	N.A.	N.A.
10	0.400	0.275	1	25.0	2	8.0	4040	2240
11	0.390	0.250	1	25.0	2	8.2	3225	1795
12	0.425	0.300	1	29.3	2	stuck	N.A.	N.A.
13	0.450	0.300	1	28.1	2	11.0	3175	1685
14	0.425	0.300	1	28.1	2	6.5	3435	2130
15	0.425	0.300	1	25.0	2	8.25	3880	2980
16	0.400	0.300	1	25.0	3	0.5	N.A.	N.A.
17	0.400	0.300	1	25.0	4	4.5	3055	1830
18	0.400	0.300	1	25.0	5	2.5	3410	1905
19	0.400	0.300	1	25.0	6	6.25	3405	1450
20	0.400	0.300	1	28.1	7	9.25	3520	1900
21	0.400	0.300	1	25.0	7	8.25	3545	1560
22	0.380	0.300	1	28.1	8	5.25	3590	2020
23	0.350	0.300	1	28.1	8	4.00	4540	4325

Table 3.13: Slump and Compressive Strengths of ZCC Mixtures Prepared Using FA27.

Mix.	W/FA	Alk/FA	SS/SH	FA (lb/ft^3)	Mixing Pro.	Slump (in)	$f_{c(oven)}$ (psi)	$f_{c(ambient)}$ (psi)
1	0.380	0.300	1.0	25.0	7	3.75	3770	2270
2	0.400	0.300	1.0	25.0	7	8.75	3280	1730
3	0.360	0.300	1.0	25.0	7	1.75	3900	1825
4	0.380	0.300	1.0	28.1	7	7.00	4390	4030
5	0.380	0.300	1.0	25.0	7	4.50	3845	3310
6	0.380	0.300	1.0	28.1	7	7.00	4005	3170
7	0.300	0.250	1.0	25.0	7	2.10	3760	1680
8	0.320	0.250	1.0	25.0	7	7.50	4130	1335
9	0.340	0.250	1.0	25.0	7	8.25	4770	2315
10	0.300	0.200	1.0	25.0	7	5.50	4270	1410
11	0.380	0.300	1.0	28.1	7	7.50	3690	2440
12	0.360	0.300	1.0	28.1	7	6.00	4075	3090
13	0.360	0.300	1.0	28.1	7	2.25	4075	3585
14	0.380	0.300	1.0	28.1	7	3.00	3850	3275
15	0.340	0.300	1.0	28.1	7	3.10	4915	2555
16	0.400	0.300	1.0	28.1	7	9.50	3520	555
17	0.380	0.350	1.0	28.1	7	0.50	N.A.	N.A.
18	0.380	0.300	1.0	28.1	7	3.00	4195	1915
19	0.380	0.300	1.0	28.1	7	2.00	3735	1735
20	0.420	0.350	1.0	28.1	7	5.63	3285	2370
21	0.400	0.300	1.0	28.1	7	8.50	3285	1170
22	0.450	0.400	1.0	28.1	7	1.00	2895	1810
23	0.400	0.350	1.0	28.1	7	3.75	4195	2405
24	0.450	0.350	1.0	28.1	7	9.25	3320	1065
25	0.350	0.300	1.0	28.1	8	9.00	4130	5265

Table 3.14: Slump and Compressive Strengths of ZCC Mixtures Prepared Using FA24.

Mix.	W/FA	Alk/FA	SS/SH	FA (lb/ft^3)	Mixing Pro.	Slump (in)	$f_{c(oven)}$ (psi)	$f_{c(ambient)}$ (psi)
1	0.425	0.300	1.0	25.0	7	10.00	N.A.	N.A.
2	0.360	0.300	1.0	25.0	7	3.75	2295	2550
3	0.380	0.300	1.0	25.0	7	6.50	3935	1440
4	0.360	0.300	1.0	28.1	7	1.75	3630	1545
5	0.360	0.300	1.0	25.0	7	2.00	3915	2910
6	0.360	0.300	1.0	21.8	7	1.00	3410	1055
7	0.380	0.300	1.0	25.0	7	5.75	4495	3605
8	0.340	0.250	1.0	25.0	7	6.50	4055	2315
9	0.320	0.250	1.0	25.0	7	4.75	4115	1585
10	0.300	0.250	1.0	25.0	7	1.75	4640	2965
11	0.280	0.200	1.0	25.0	7	3.00	4580	1125
12	0.260	0.200	1.0	25.0	7	Zero	N.A.	N.A.
13	0.300	0.200	1.0	25.0	7	5.63	2700	205
14	0.350	0.300	1.0	28.1	8	5.50	4570	4215

Table 3.15: Slump and Compressive Strengths of ZCC Mixtures Prepared Using FA21.

Mix.	W/FA	Alk/FA	SS/SH	FA (lb/ft^3)	Mixing Pro.	Slump (in)	$f_{c(oven)}$ (psi)	$f_{c(ambient)}$ (psi)
1	0.340	0.300	1	25.0	7	3.75	4320	1630
2	0.360	0.300	1	25.0	7	3.25	4735	1740
3	0.380	0.300	1	28.1	7	5.50	3940	1170
4	0.380	0.300	1	28.1	7	11.0	2180	410
5	0.360	0.300	1	28.1	7	5.50	4880	1560
6	0.380	0.300	1	32.5	7	11.0	5040	2090
7	0.380	0.300	1	28.1	7	9.00	5670	2170
8	0.360	0.300	1	28.1	7	1.50	5765	2880
9	0.360	0.300	1	28.1	7	7.50	4895	2575
10	0.360	0.300	1	28.1	7	9.50	4435	795
11	0.340	0.300	1	28.1	7	Stuck	1415	1015
12	0.360	0.300	1	28.1	7	7.50	4415	2530
13	0.380	0.300	1	28.1	8	8.00	4315	1795
14	0.350	0.300	1	28.1	8	7.50	4910	3325

In mixing procedure no. 3, the two alkali activators were not added together at the same time, but the sodium hydroxide was added first. That had a negative effect on the workability; the mixture had poor workability of only 0.5 in, and it was not possible to place the mixture in the molds for further testing.

In mixing procedure no. 4, not all the water was added before adding the alkali activator. That allowed adding less water content, but the strength was not improved, due to agglomeration of the mixture where not all the FA particles were wetted completely. Therefore, adding the alkali activators caused an agglomeration.

In mixing procedure no. 5, one half of the water and one half of the alkali activator were added first; then, the remaining amount of both were added later. That had a negative effect on the workability compared with adding all the water first before the alkali activator.

In mixing procedure no. 6, the water was added in two equal portions followed by adding the alkali activator in two equal portions. This change resulted in a significant improvement in the workability. However, the compressive strength was not improved due to the high W/FA that was necessary to avoid agglomeration.

In mixing procedure no. 7, the water was added in full followed by adding the alkali activator in two equal portions. This mixing procedure improved the workability, and the compressive strength exceeded the target of 3000 psi. However, more improvements in the workability and strength were desired.

In mixing procedure no. 8, the water was added at the beginning of the mixing procedure; however, the alkali activators were added gradually over five minutes which prevented the agglomeration and significantly improved the workability allowing the use of a lower water

content to achieve a given slump compared to other mixing procedures. This reduction in water content improved the strength of the ambient-cured specimens while it did not affect that of the oven-cured. It is worth noting that specimens that were prepared using this procedure were encased in plastic bags during the ambient curing which reduced the evaporation of water, allowing more effective curing and achieving higher strengths.

3.2.6 Discussion

3.2.6.1 *Mixing procedures*

This section presents qualitative comparisons between the performances of mixtures prepared using mixing procedures no. 1 through no. 8. Fig. 3.13 shows the effect of the mixing procedure on the slump and compressive strengths of ZCC. Furthermore, Table 3.16 presents comparisons between the performances of the same mixture design prepared using different mixing procedures. For the particular mixture presented in Table 3.16, mixing procedure no. 7 outperformed all other mixing procedures. For other mixtures, mixing procedures no. 2, 7, and 8 displayed the highest slump values (Fig. 3.13a). Although some of the specimens that were prepared using mixing procedure no. 7 showed very low workability (i.e. less than 3 in), those particular mixtures were prepared after the preliminary success of preparing ZCC mixtures using mixing procedure no. 7. Therefore, more mixtures were prepared where the W/FA was significantly reduced and/or the Alk/FA was significantly increased to obtain relatively higher strength ZCC having a good workability.

Table 3.16 shows that the compressive strength of the oven-cured specimens prepared using procedure no. 7 displayed the highest strength compared to those prepared using the other mixing procedures. However, the compressive strength of the ambient-cured specimens was low for all specimens. Qualitatively, the ambient and oven compressive strengths of the mixtures

prepared using procedure no. 7 were 8% and 19% higher than those of the mixtures prepared using procedure no. 2 (Fig. 3.13b). Similarly, the compressive strengths of the oven and ambient-cured specimens prepared using procedure no. 8 were 14% and 119% higher than those of the mixtures prepared using procedure no. 7. Therefore, mixing procedure no. 8 was used in the remainder of this project.
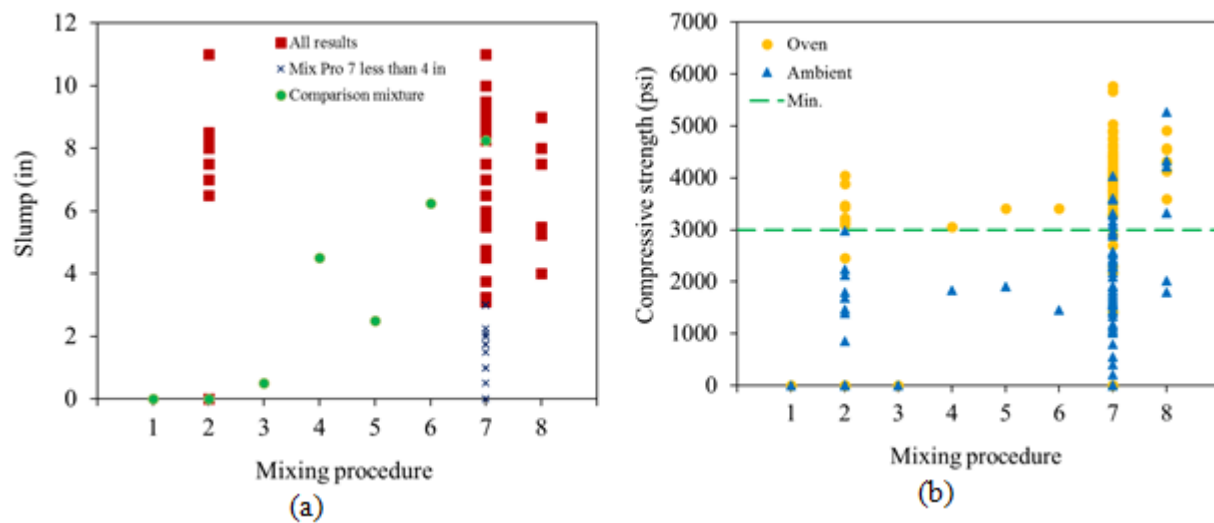
Figure 3.13: Effect of mixing procedure on (a) slump value and (b) compressive strengths of ZCC.

Table 3.16: Properties of ZCC Mixture Prepared Using Different Mixing Procedures.

Mix.	Mixing pro.	W/FA	Alk/FA	SS/SH	FA (lb/ft^3)	Slump (in)	$f_{c(oven)}$ (psi)	$f_{c(ambient)}$ (psi)
1	1	0.400	0.300	1	25.0	stuck	N.A.	N.A.
7	2	0.400	0.300	1	25.0	stuck	N.A.	N.A.
16	3	0.400	0.300	1	25.0	0.5	N.A.	N.A.
17	4	0.400	0.300	1	25.0	4.5	3055	1830
18	5	0.400	0.300	1	25.0	2.5	3410	1905
19	6	0.400	0.300	1	25.0	6.25	3405	1450
21	7	0.400	0.300	1	25.0	8.25	3545	1560

3.2.6.2   Effect of the storing system

Table 3.17 shows comparisons between the compressive strengths of specimens prepared using

FA25 and FA21 and stored using two different approaches during the curing period. One half of

the specimens were encased in plastic bags while the other half were stored at an ambient

temperature of $73 \pm 3^{\circ}$ F ($23 \pm 2^{\circ}$ C) without plastic bags. The specimens were prepared using

mixing procedure no. 8. As shown in Table 17, the compressive strength increased by 45% and

57% in the case of encasing them until the testing age. Therefore, in the remainder of this

project, all cylinders that were oven and ambient-cured were encased in plastic bags after

demolding them and remained encased until the testing day.

Table 3.17: Compressive Strengths of the Ambient-Cured Specimens With and Without
Encasing Them in Bags.

Mix.	FA	W/FA	Alk/FA	SS/SH	FA (lb/ft^3)	Mixing Pro.	$f_{c(ambient)}$ without bag (psi)	$f_{c(ambient)}$ with bag (psi)
22	FA25	0.380	0.300	1	28.1	8	2020	2920
13	FA21	0.380	0.300	1	28.1	8	1795	2820

3.2.6.3   Effect of W/FA, Alk/FA, SS/SH, and FA content

The fresh and hardened properties of ZCC depend on numerous parameters including the mixing

procedure, W/FA, Alk/FA, SS/SH, curing, and chemical and physical properties of the FA used.

Therefore, this section presents a qualitative comparison to determine the appropriate ranges of

W/FA, Alk/FA, and SS/SH. A more systematic investigation of the different parameters is

presented in Chapter 4 of this report.

Fig. 3.14 shows qualitative effects of the W/FA, Alk/FA, and FA content on the slump and

compressive strengths of ZCC. As shown in the Fig. 3.14, W/FA ranging from 0.32 to 0.50

displayed the highest slump values. However, the highest compressive strengths of the oven- and ambient-cured specimens were obtained at W/FA ranging from 0.340 to 0.380. For the Alk/FA and FA content, the highest slump value as well as compressive strength was obtained at Alk/FA of 0.300 and FA content of 28.1 lb/ft^3, respectively. Hence, it can be concluded that the W/FA ranging from 0.340 to 0.380 and Alk/FA of 0.300 showed high slump and compressive strengths.
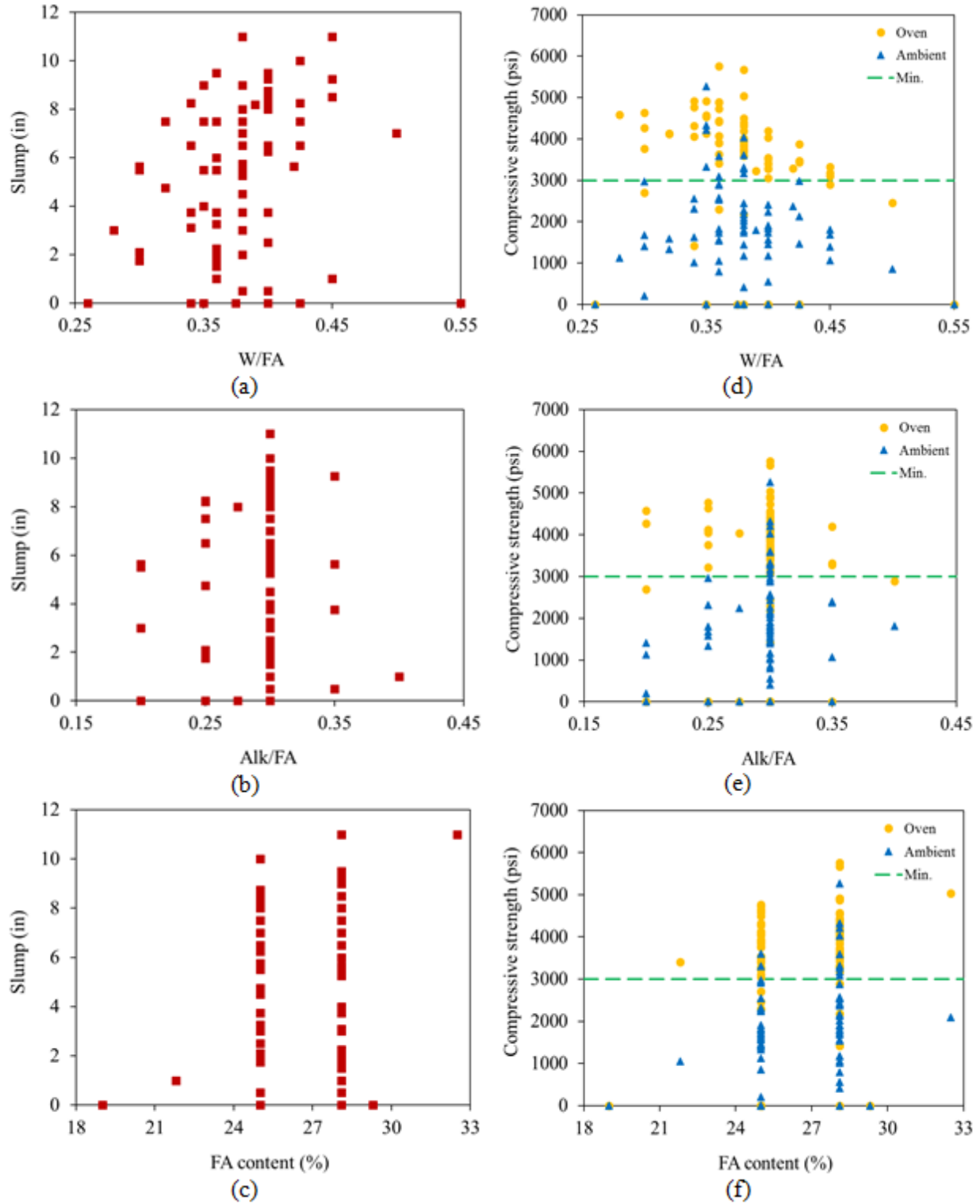
Figure 3.14: Effect of (a) W/FA on slump value, (b) W/FA on compressive strengths, (c) Alk/FA on slump value, (d) Alk/FA on compressive strength, (e) FA content on slump value, and (f) FA content on compressive strength of ZCC, respectively.

93

3.2.7 Findings and conclusions

3.2.7.1 Mortar trial mixtures

Based on investigating 27 ZC mortar mixtures using four different mixing procedures, the following conclusions can be drawn:

- ZC mortar having W/FA ranging from 0.400 to 0.550, Alk/FA ranging from 0.250 to 0.300, and SS/SH ranging from 0.5 to 2.5 resulted in a workable ZC mortar with a compressive strength adequate for structural applications. More refinement of these mixtures is presented in Chapters 4 and 5.

- Adding the alkali activator to the FA before adding the water caused a poor workability and a flash setting or required adding more water to prevent that phenomenon, which resulted in decreased compressive strength.

- Mixing the water with all ingredients before adding the alkali activator resulted in a good workability, setting time, and compressive strength.

- Mixing at a high speed of 281 rpm rather than 136 rpm after adding the alkali activator increased the workability, setting times, and the compressive strength.

- Adding the alkali activator gradually over five minutes rather than one minute improved the workability, setting times, and compressive strength.

3.2.7.2 Concrete trial mixtures

Based on investigating 76 ZCC mixtures using eight different mixing procedures and four different sourced FAs, the following conclusions can be drawn:

- ZCC having W/FA ranging from 0.340 to 0.380, Alk/FA of 0.300, and FA content of 28.1 lb/ft3 resulted in workable ZCC with a compressive strength adequate for structural applications.

- Adding the alkali activator to the FA before adding the water caused a poor workability and a flash setting or required adding more water to prevent that phenomenon, which resulted in a decrease of the compressive strength of the test specimens.

- Mixing the water with all ingredients before adding the alkali activator resulted in a good workability and compressive strength.

- Adding the alkali activator gradually over 5 minutes improved the workability significantly and allowed adding a lower W/FA ratio, which resulted in higher compressive strength.

- Encasing the concrete cylinders with plastic bags to prevent moisture loss during the curing at room temperature improved the compressive strength of the ambient-cured specimens significantly.

- Mixing procedure no. 8 displayed the highest strength among the rest of mixing procedures. Therefore, it was used in the rest of the project for mixing concrete.

Chapter 4: Fresh Properties and Strength of Zero-Cement Mortar

The effects of water to fly ash (W/FA), alkali activators to fly ash (Alk/FA), and sodium silicate to sodium hydroxide (SS/SH) ratios on the fresh properties and compressive strength of ZC mortar are presented in this chapter. This chapter also reports the optimum ratios of those parameters that resulted in structural ZC mortar.

4.1 Mix Properties and Mixing Procedures

As discussed in Chapter 2, two batches of FA were received and used during the course of this project. Five sourced FAs, namely FA27, FA29, FA24, FA25, and FA21, of the first batch, were used to prepare the mortar mixtures presented in this chapter. Detailed characterizations of the materials used for synthesizing the mortar mixtures are presented in Chapter 2 of this report.

To optimize the strength and workability of ZC mortar, thirteen mixtures were prepared (Table 4.1) with five different W/FA of 0.350, 0.375, 0.400, 0.425, and 0.450, three Alk/FA of 0.250, 0.275, and 0.300, and four SS/SH of 0.5, 1.0, 1.5, and 2.5. These ratios were selected based on the trial mixtures presented in Chapter 3. The sand to FA ratio remained constant at 2.75 for all mixtures. The W/FA presented in Table 4.1 included both the water in the alkali activator solution and the extra added water to the mix. Hence, the extra added water was adjusted for the different mixtures based on the amount of alkali activator. Mortar mixing procedure no. 3 described in Chapter 3 was used throughout this chapter. This set of thirteen mixtures was repeated for each source of FA. Hence, a total of 65 mixtures were prepared.

Table 4.1: Mix Design of ZC Mortars.

Mix No.	W/FA	Alk/FA	SS/SH	FA (lb/ft^3)	Sand (lb/ft^3)	SS (lb/ft^3)	SH (lb/ft^3)	Extra water (lb/ft^3)
1	0.35	0.25	1	34.5	94.9	4.31	4.31	6.75
2	0.375	0.25	1	34.1	93.7	4.25	4.25	7.56
3	0.4	0.25	1	33.6	92.3	4.19	4.19	8.25
4	0.4	0.3	1	33.5	92.1	5	5	7.25
5	0.425	0.3	1	33.1	91	4.94	4.94	7.94
6	0.45	0.3	1	32.6	89.8	4.88	4.88	8.69
7	0.4	0.275	1	33.6	92.3	4.63	4.63	7.75
8	0.4	0.25	0.5	33.6	92.5	2.81	5.63	8.13
9	0.4	0.25	1.5	33.6	92.3	5.06	3.38	8.38
10	0.4	0.25	2.5	33.6	92.3	6	2.38	8.5
11	0.45	0.3	0.5	32.6	89.8	3.25	6.5	8.5
12	0.45	0.3	1.5	32.6	89.8	5.88	3.94	8.75
13	0.45	0.3	2.5	32.6	89.8	7	2.81	8.88

W: Water
FA: Fly ash
Alk: Alkali activator
SS: Sodium Silicate
SH: Sodium Hydroxide

The nomenclatures of the ZC mortar mixtures start with the letter "M" for a mortar followed by the percentage of the calcium content of the FA that was used in that mortar mixture. For example, M27 is a ZC mortar synthesized using a FA having a calcium content of 27%.

4.2 Fresh and Hardened Properties of ZC Mortar

The workability, setting times, and compressive strength were selected to characterize the fresh and hardened properties of the ZC mortar in this chapter. The different testing procedures are discussed in detail in Chapter 3. The fresh ZC mortar was cast into 2 inch cube brass molds as per ASTM 109-16 [106]. The specimens were oven- and ambient-cured as explained in Chapter 3. The compressive strength of each mixture was determined by testing the mortar cubes after

curing 7 days from the casting day. The reported strength of each mixture is the average of three cubes cast out of that mixture.

4.2.1 Results of fresh properties

A summary of the results is presented in Tables 4.2 through 4.6 at the end of this chapter. The mean, range, variance, standard deviation (SD), and coefficient of variation (CV) of the results are also presented in the tables. As shown in the tables, 85% of the results had a CV less than 10% and the remaining 15% of the results had a CV less than 18%, which reflects the accuracy of the tabulated results.

There are no acceptance criteria for the workability or setting times of Portland cement mortar. However, ASTM C150-16 [102] limits the initial setting time (In. Set.), measured by the Vicat needle per ASTM C191-C [107], of Portland cement paste to a minimum of 45 minutes and a maximum of 375 minutes. This study adopted these acceptance criteria for the setting times. Furthermore, this report recommends a minimum workability of 40%.

The workability of the thirteen mixtures ranged from 50% to 150% for M21, 20% to 150% for M24, 42.5% to 150% for M25, 20% to 150% for M27, and 20% to 150% for M29 (Fig. 4.1). It is worth noting that the workability values are saturated at 150% corresponding to the diameter of the flow table. The initial set (In. Set.) time ranged from 35 minutes to 300 minutes for M21, 70 minutes to 395 minutes for M24, 35 minutes to 390 minutes for M25, 25 minutes to 250 minutes for M27, and 40 to 145 minutes for M29 (Fig. 4.2). The final setting (Fi. Set.) time ranged from 80 minutes to 410 minutes for M21, 110 minutes to 450 minutes for M24, 70 minutes to 490 minutes for M25, 40 minutes to 310 minutes M27, and 75 minutes to 195 minutes for M29 (Fig. 4.3).

The results revealed that the main factors that affect the workability and setting times of ZC mortar are the FA's chemical and physical properties such as the calcium content, surface area of the FA, W/FA, Alk/FA and, SS/SH.

4.2.2.1. Effect of calcium content and surface area.

Fig. 4.1 shows the relationship between the calcium content and workability of the different sourced FAs. Also shown in the figure is the correlation between workability and calcium content. Two coefficients of determination, R^2, are also shown on the figure. The first R^2 value of 0.11 is for all data and the second R^2 value of 0.24 is for all data points excluding the saturated points at workability of 150%. As shown in the figure, for all sourced FAs, except M24, increasing the calcium content decreased the workability. The workability of the M21 that has the lowest calcium content was the highest among all FAs while the workability of M29 and M27 that have the highest calcium contents was the lowest. For the M24, while it has an average amount of calcium content, it had a high workability due to its low surface area. As discussed in Chapter 2, FA24 has a surface area of 1446 m²/kg while FA21, FA25, FA27, and FA29 had surface areas of 2921, 2858, 2560, and 3925 m²/kg, respectively. However, the direct correlation between the surface area of FA and workability doesn't exist (Fig. 4.2).
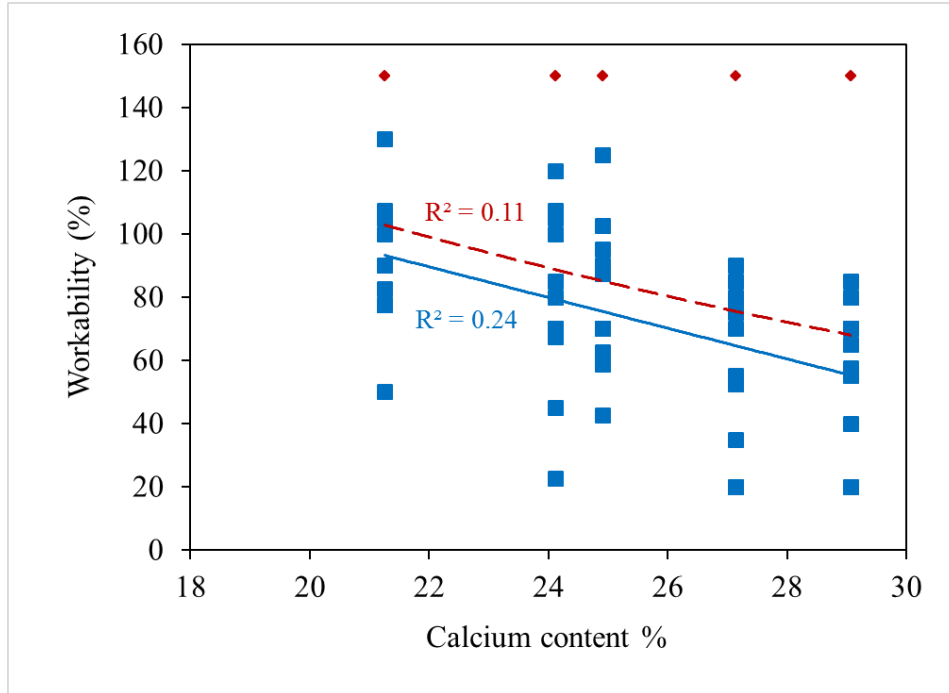
Figure 4.1: Effect of calcium content on the workability of ZC mortar.
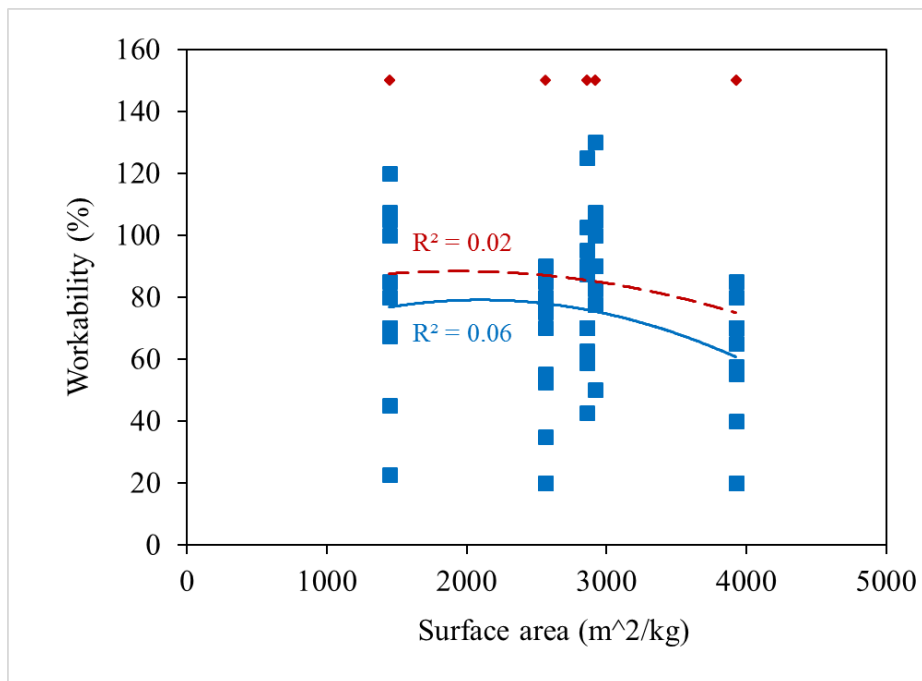
Figure 4.2: Effect of surface area on the workability of ZC mortar.

Figs. 4.3 and 4.4 show the relationship between the calcium content and setting times of the different sourced FAs. As shown in the figures, increasing the calcium content decreased the setting times. The coefficient of determination, R^2, is 0.32, representing a moderate correlation between calcium and setting time. The setting times of the M21 that has the lowest calcium content was the highest among all FAs while the workability of M29 and M27 that have the highest calcium contents was the lowest. The rapid formation of calcium silicate hydrate (CSH) and/or calcium aluminate silicate hydrate (CASH) caused low workability and short setting times. Furthermore, the setting times of M24 and M25 were relatively higher than those of the corresponding mixtures synthesized using the other FAs. The M24 had an average amount of calcium content; however, its surface area was relatively low, which decelerated the leaching and dissolution of the FA in the alkali activators which delayed and decelerated the geopolymerization and hydration process [49, 108]. Figs. 4.5 and 4.6 show the correlations between the surface area of the FA and the setting times. As shown in the figure, R^2 for both setting times was 0.24.
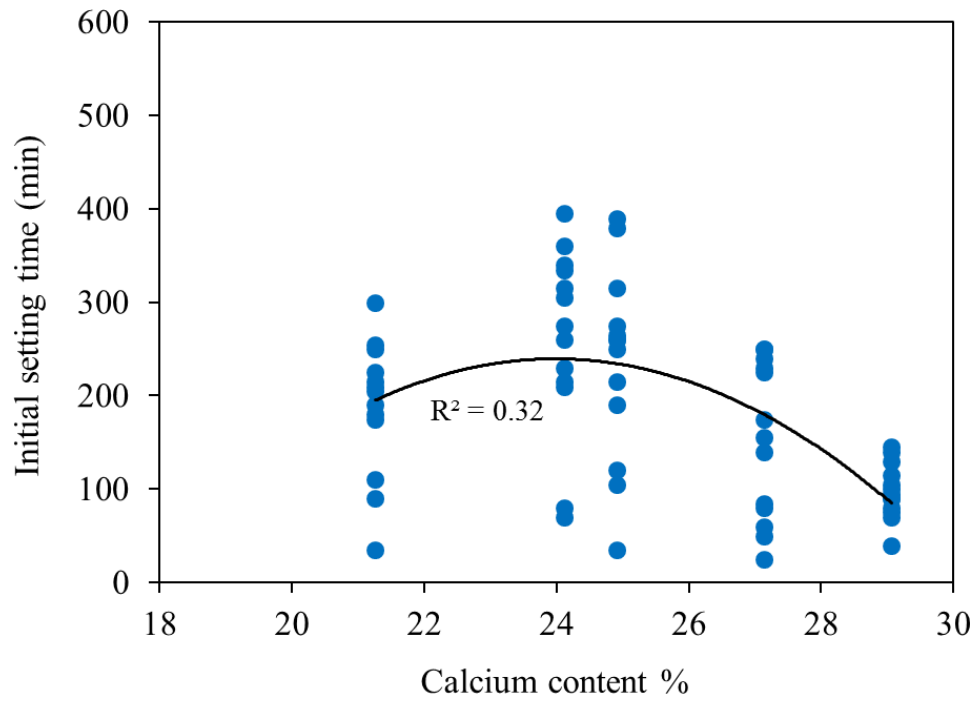
Figure 4.3: Effect of calcium content on the initial setting time of ZC mortar.
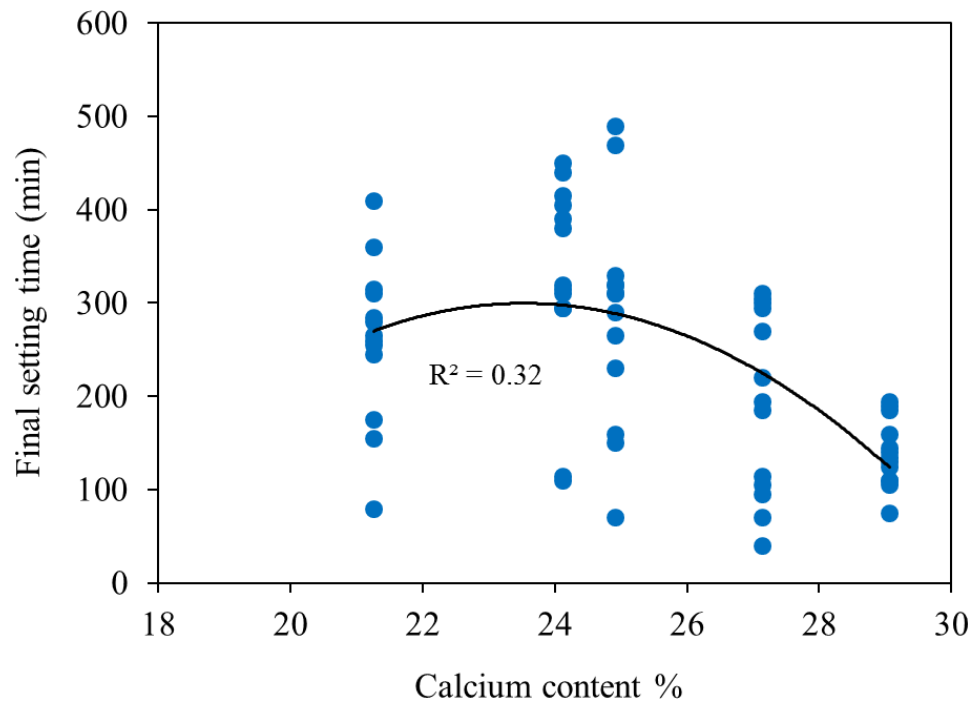
Figure 4.4: Effect of calcium content on the final setting time of ZC mortar.

102
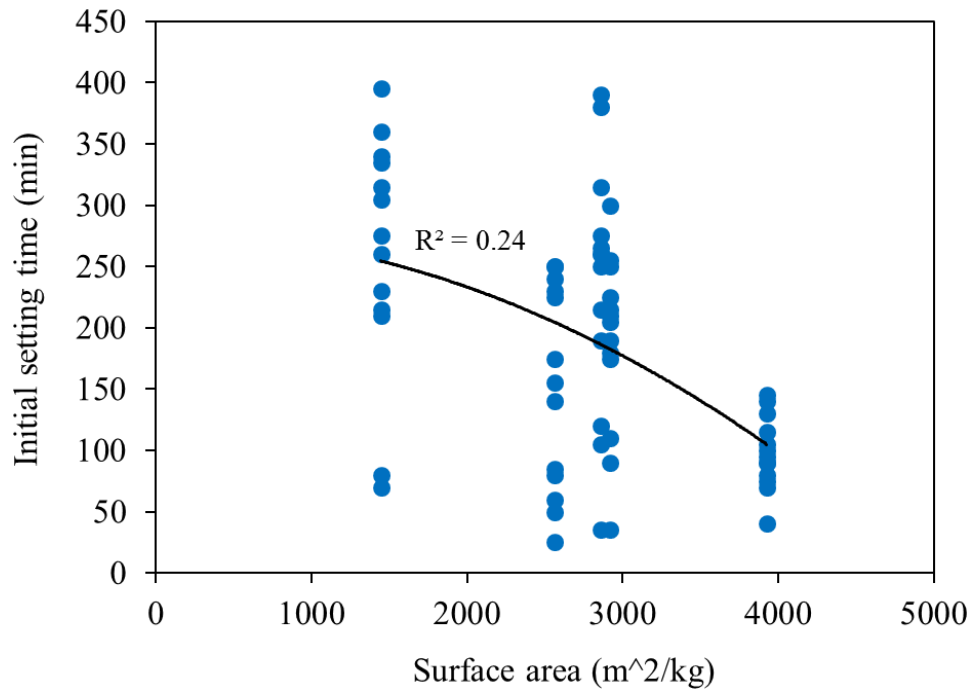
Figure 4.5: Effect of calcium content on the initial setting time of ZC mortar.
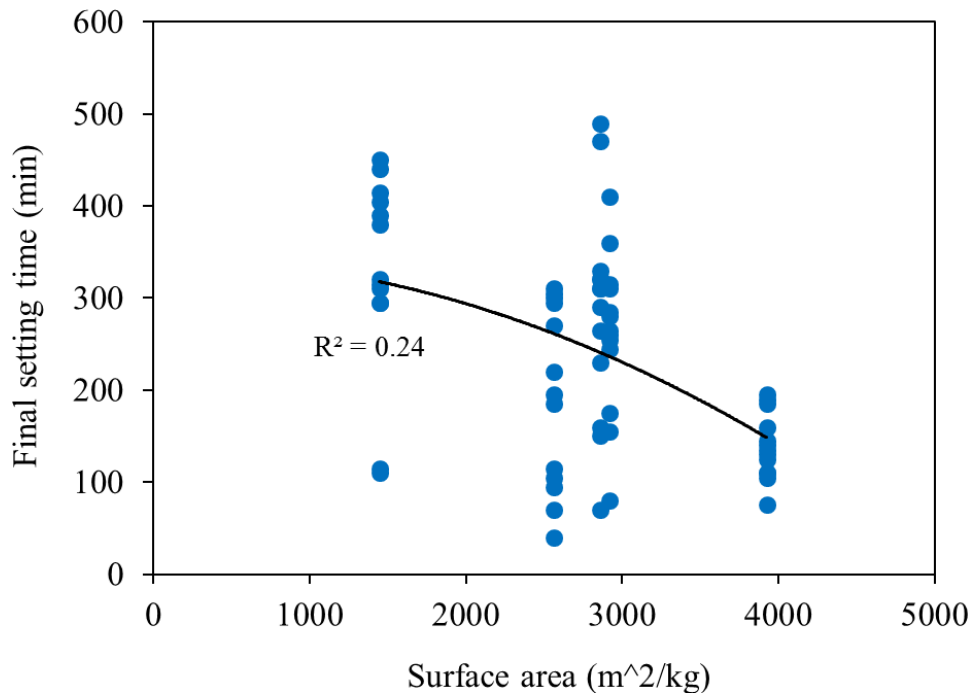
Figure 4.6: Effect of calcium content on the final setting time of ZC mortar.

M25 had a low amorphous phase content of 54.3% while FA21, FA24, FA27, and FA29 had

amorphous contents of 58.0%, 70.9%, 46.7%, and 54.7%, respectively. The amorphous (glass)

content of the FA is easier to be dissolved by the activators due to the disordered connection among the molecules of the materials. Therefore, rapid and higher geopolymer precursor species dissolve into the system [21]. Also, M25 has the highest MgO content of 10.12%. That possibly has an effect on delaying the setting time. More study is needed to investigate the effect of MgO on the fresh and hardened properties of the geopolymer mortar.

4.2.1.1 *Effect of W/FA on workability and setting times*

W/FA values ranging from 0.350 to 0.450 combined with SS/SH of 1.0 and Alk/FA of 0.250 or 0.300 were investigated. Figs. 4.7 through 4.9 show the effect of W/FA on the workability, initial setting time, and final setting time for Alk/FA of 0.250. Similarly, Figs. 4.10 through 4.12 show the effect of W/FA on the workability, initial setting time, and final setting times for Alk/FA of 0.300.
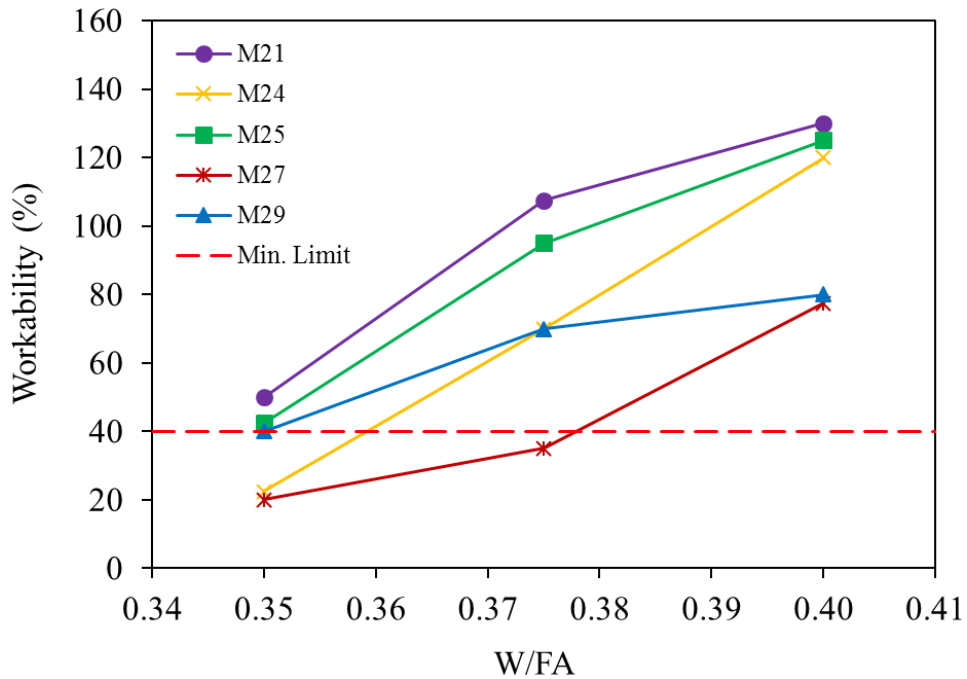
Figure 4.7: Workability of ZC mortar for Alk/FA of 0.250 and SS/SH of 1.0 for different W/FA.
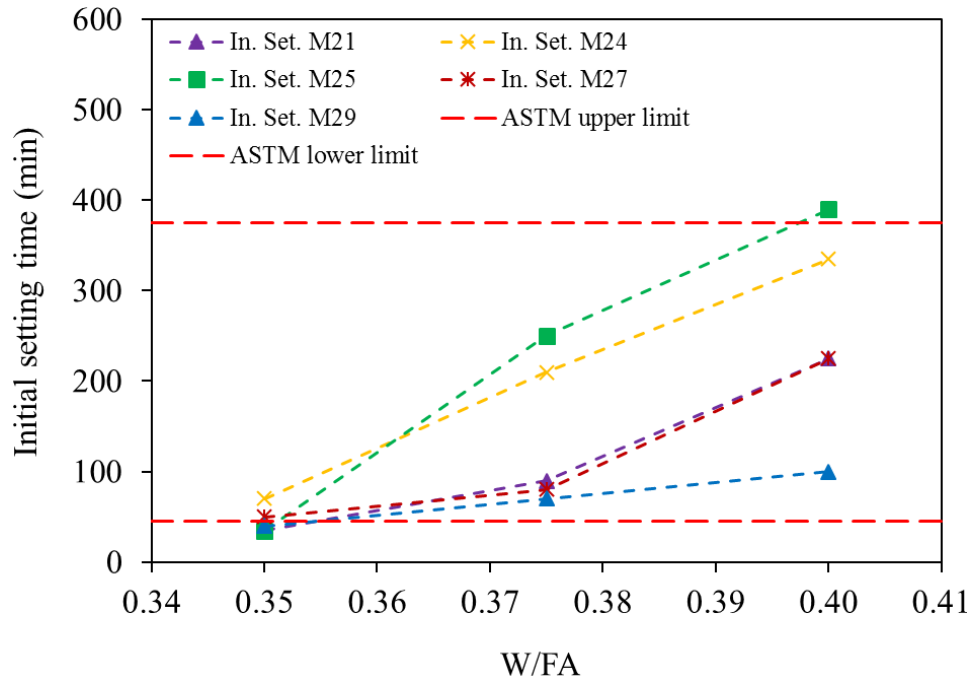
Figure 4.8: Initial setting time of ZC mortar for Alk/FA of 0.250 and SS/SH of 1.0 for different W/FA.
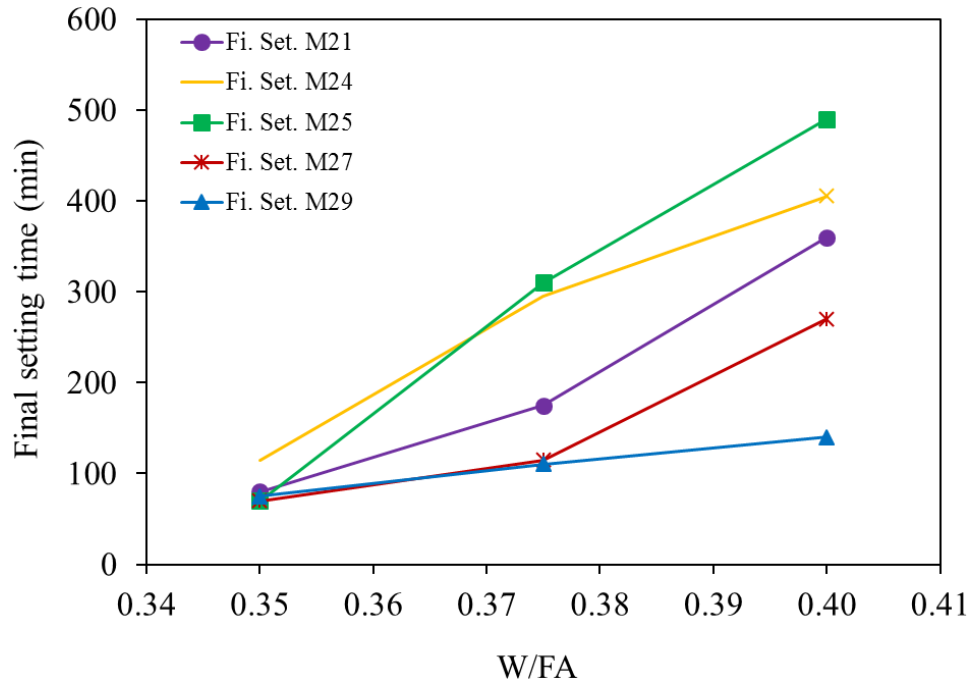
Figure 4.9: Final setting time of ZC mortar for Alk/FA of 0.250 and SS/SH of 1.0 for different W/FA.
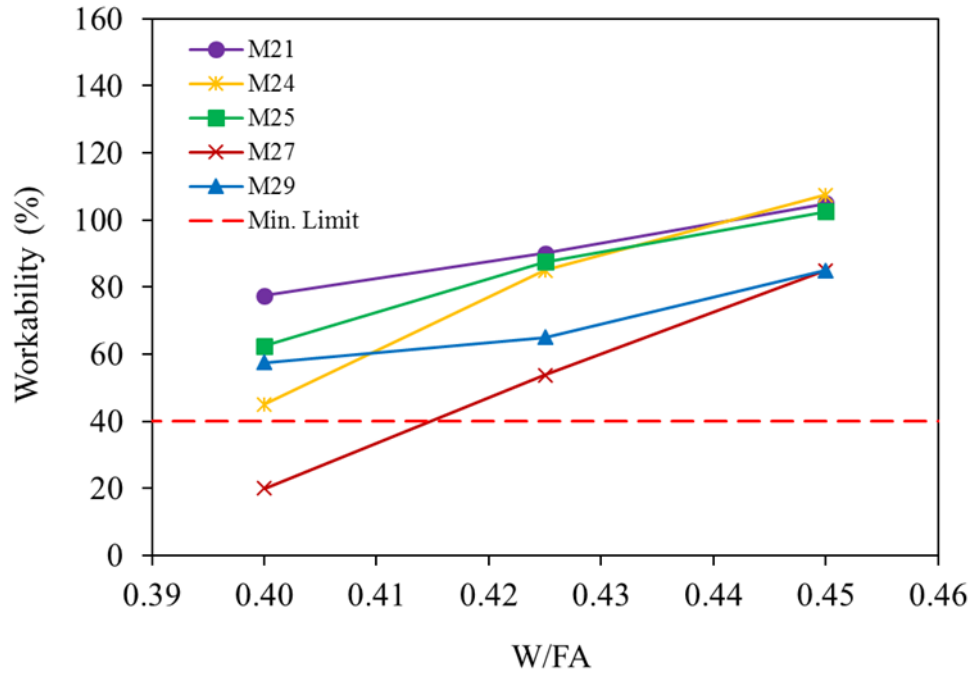
Figure 4.10: Workability of ZC mortar for Alk/FA of 0.300 and SS/SH of 1.0 for different W/FA.
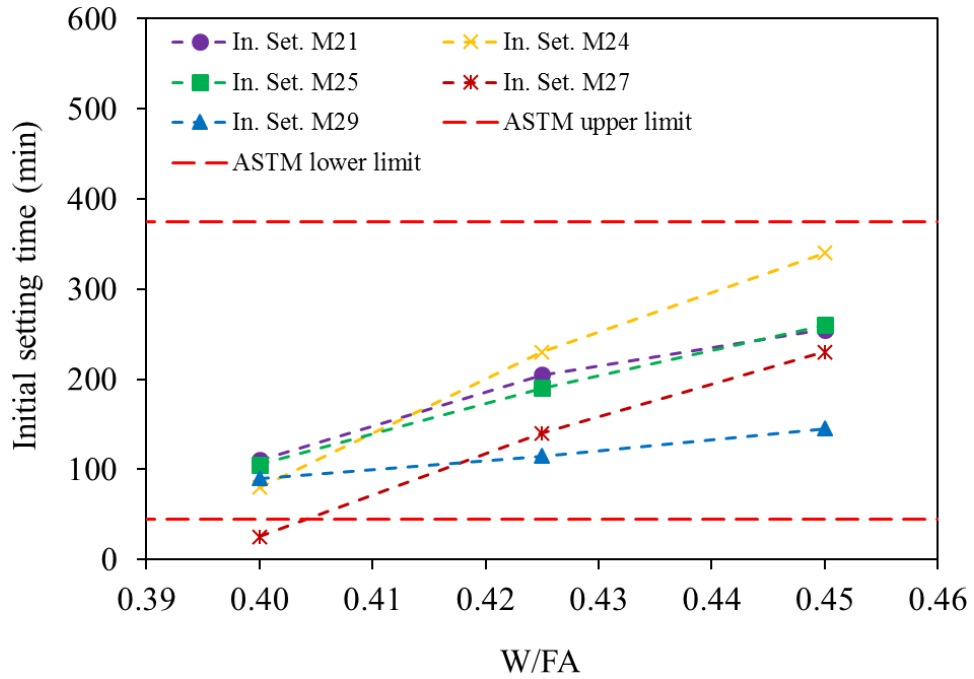
Figure 4.11: Initial setting time of ZC mortar for Alk/FA of 0.300 and SS/SH of 1.0 for different W/FA.
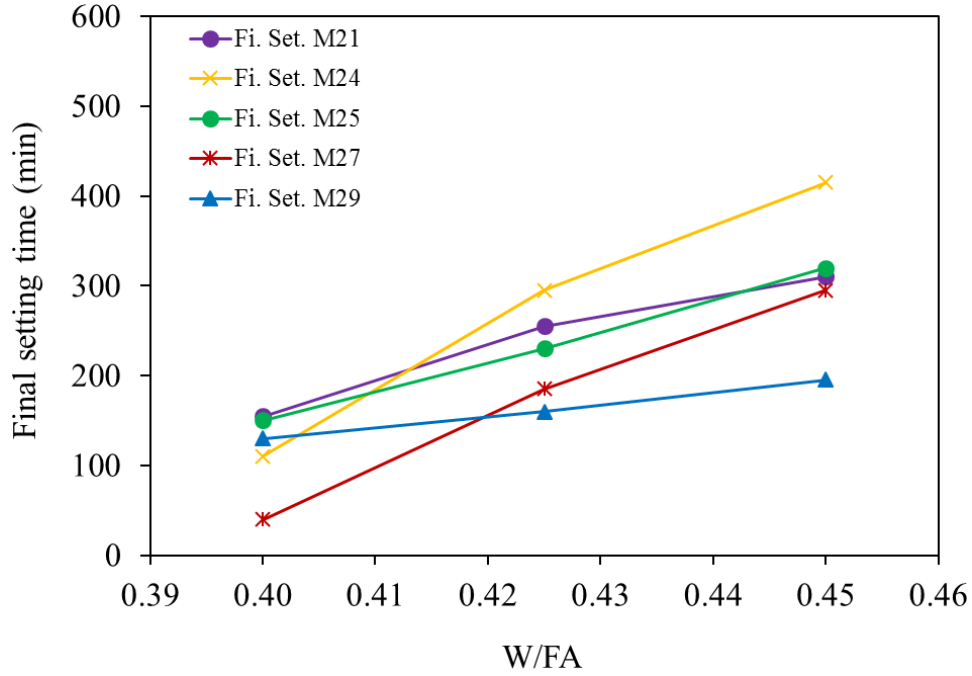
Figure 4.12: Final setting time of ZC mortar for Alk/FA of 0.300 and SS/SH of 1.0 for different W/FA.

As shown in Figs. 4.7 through 4.9, the workability ranged from 20% to 130%, the In. Set. ranged from 35 minutes to 390 minutes, and the Fi. Set. ranged from 70 minutes to 490 minutes. As shown in Figs. 4.10 through 4.12, the workability ranged from 20% to 108%, the In. Set. ranged from 25 minutes to 340 minutes, and the Fi. Set. ranged from 40 minutes to 415 minutes.

As shown in Figs. 4.7 through 4.12, for Alk/FA of 0.250 and 0.300, and SS/SH of 1.0, the workability and setting times of the five FAs increased with increasing the W/FA. The increase was more predominant for the mixtures made with Alk/FA of 0.250 than those mixtures made with Alk/FA of 0.300. The figures show also that the minimum W/FA that satisfies the setting times and workability limits are 0.375 and 0.425 for the mixtures synthesized using Alk/FA of 0.25, and 0.300.

4.2.1.2 Effect of Alk/FA on workability and setting times

Figs. 4.13 through 4.15 show the workability, initial setting time, and final setting time as a function of the Alk/FA while the W/FA and SS/SH remained constant at 0.400 and 1.0, respectively. As shown in the figures, the workability ranged from 20% to 130%, and the initial and final setting times ranged from 25 minutes to 100 minutes and 40 minutes and 140 minutes, respectively.
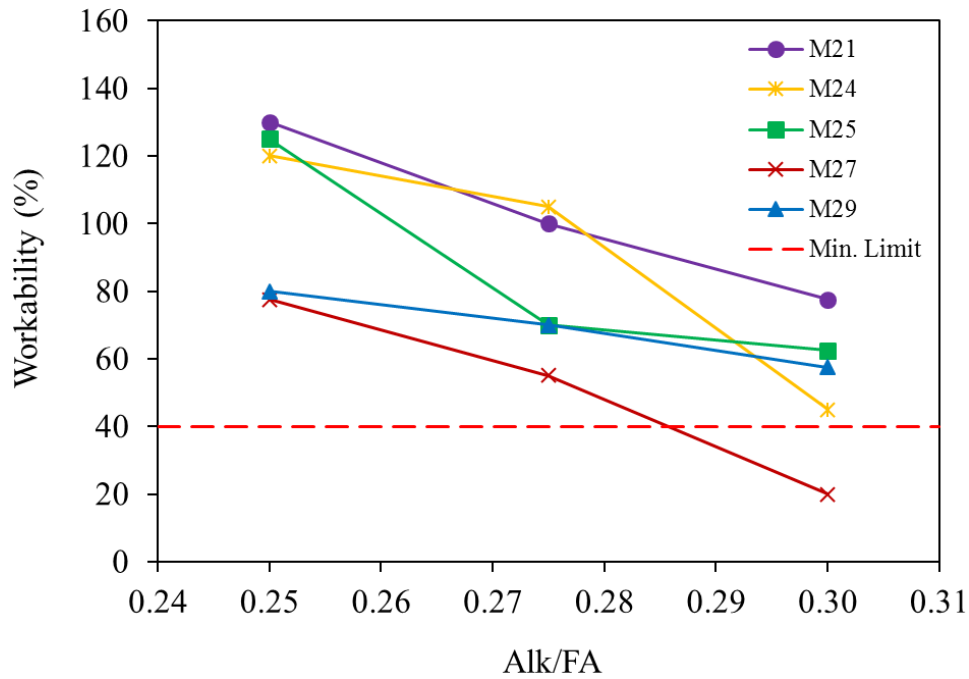
Figure 4.13: Workability of ZC mortar for W/FA of 0.400 and SS/SH of 1.0 for different Alk/FA.
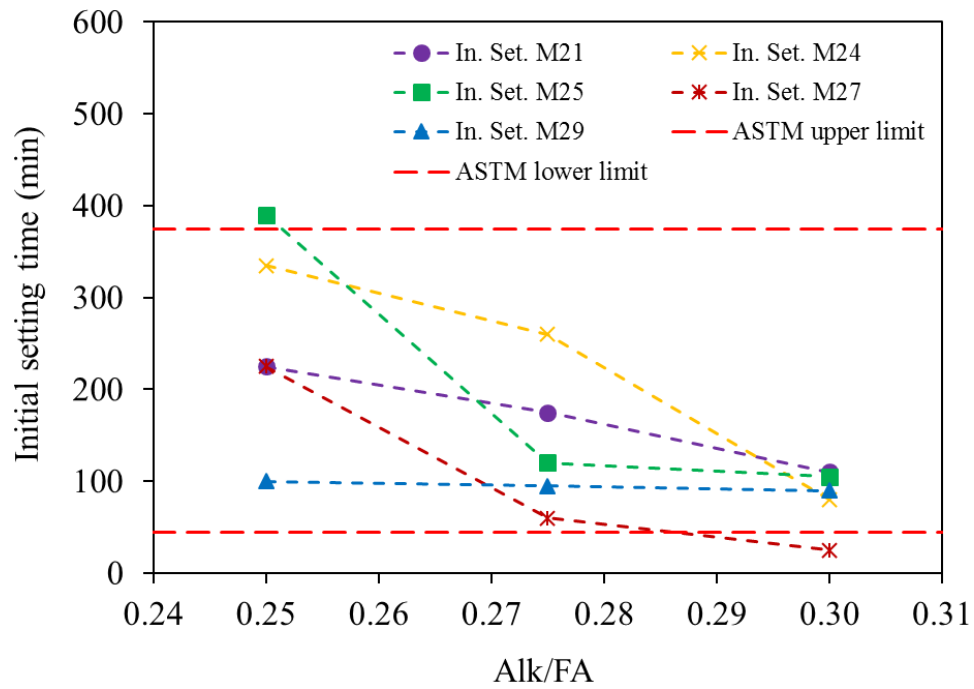
Figure 4.14: Initial setting time of ZC mortar for W/FA of 0.400 and SS/SH of 1.0 for different Alk/FA.
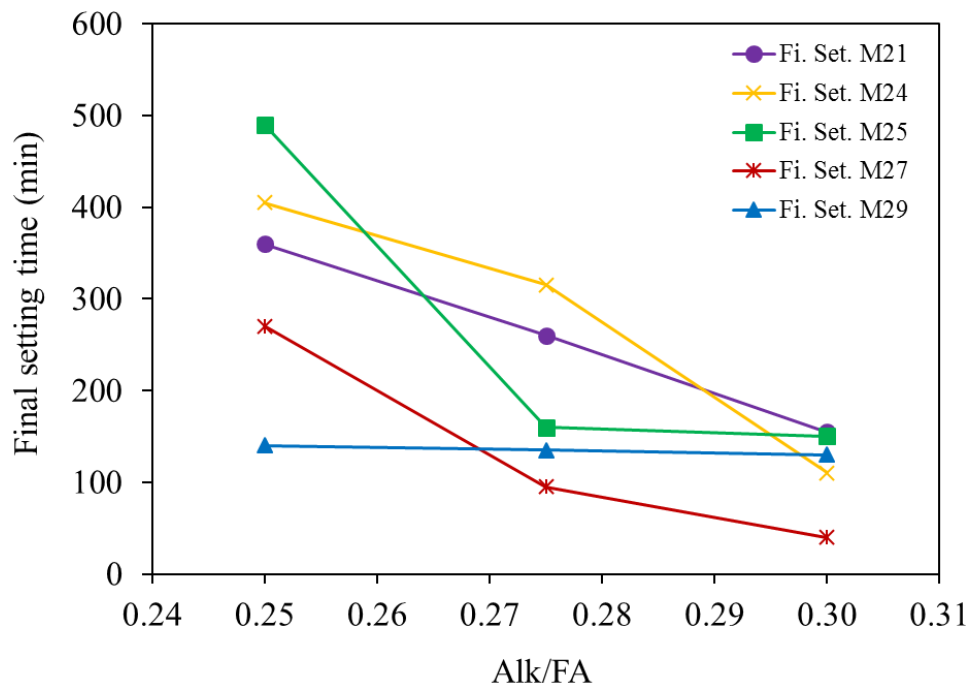
Figure 4.15: Final setting time of ZC mortar for W/FA of 0.400 and SS/SH of 1.0 for different Alk/FA.

For constant W/FA of 0.400 and SS/SH of 1.0, the workability and setting times decreased with increasing the Alk/FA (Figs. 4.13 through 4.15). Increasing the alkali activators in the mortar increased the viscosity of the aqueous, and accelerated the leaching and dissolution of the FA precursor which resulted in lower workability and shorter setting times [6, 45, 60]. The maximum Alk/FA that could be used with W/FA of 0.400 was 0.275 which passes the ASTM required value of the initial setting time and the workability lower limit of 40%.

4.2.1.3   Effect of SS/SH on workability and setting times

SS/SH ratios ranging from 0.5 to 2.5 combined with W/FA of 0.40 or 0.45, and Alk/FA of 0.250 or 0.300 were investigated. Figs. 4.16 through 4.18 show the effect of SS/SH on the workability, initial setting time, and final setting time for W/FA of 0.400 and Alk/FA of 0.250. Similarly, Figs. 4.19 through 4.21 show the effect of SS/SH on the workability and setting times for W/FA of 0.450 and Alk/FA of 0.300.
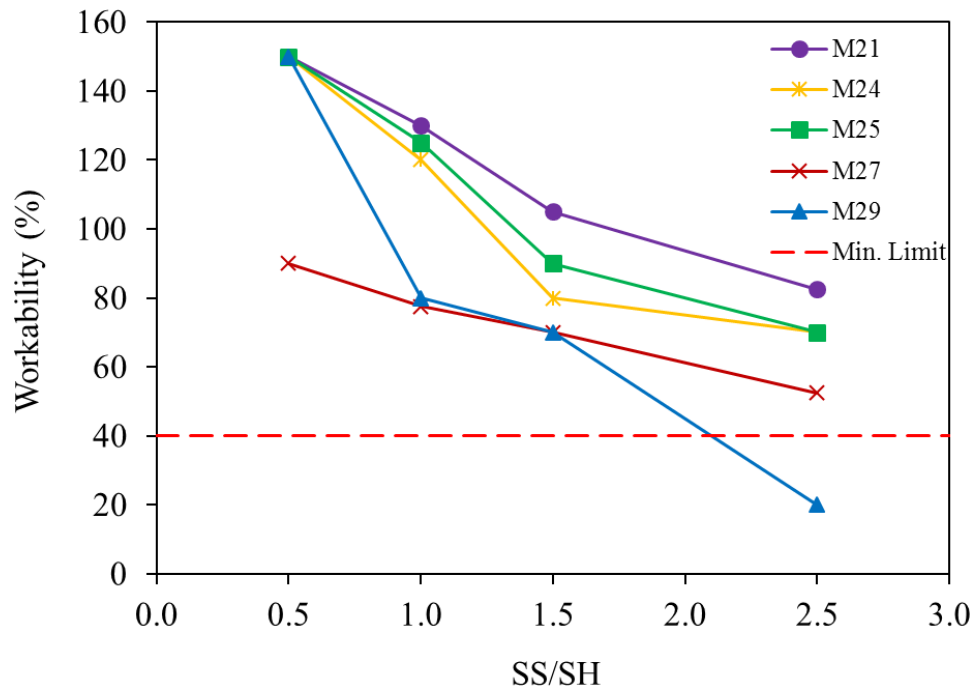
Figure 4.16: Workability of ZC mortar for W/FA of 0.400 and Alk/FA of 0.250 for different SS/SH.
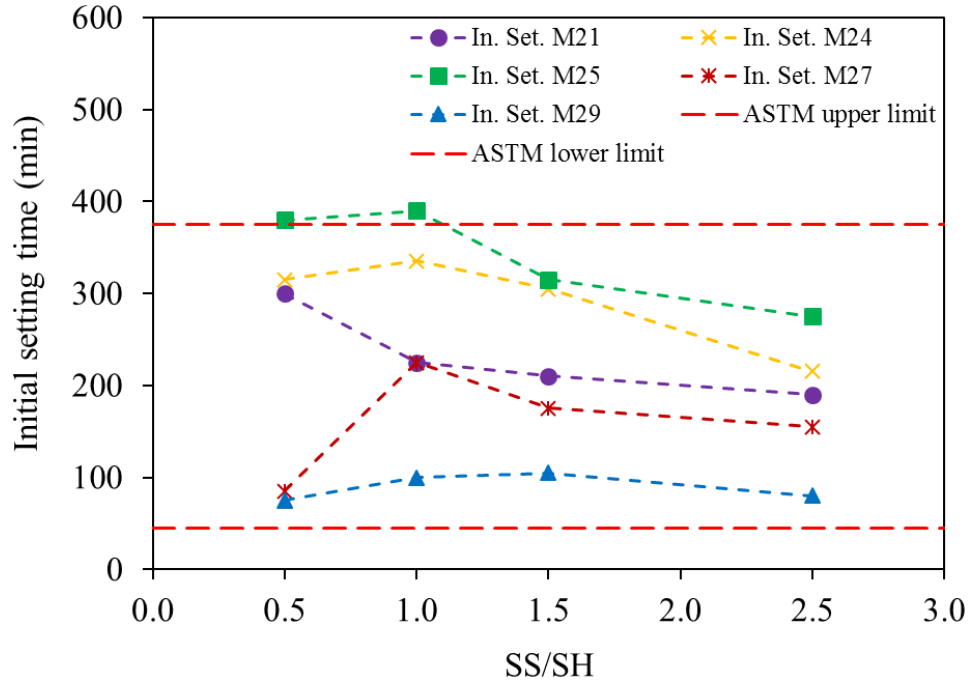
Figure 4.17: Initial setting time of ZC mortar for W/FA of 0.400 and Alk/FA of 0.250 for different SS/SH.
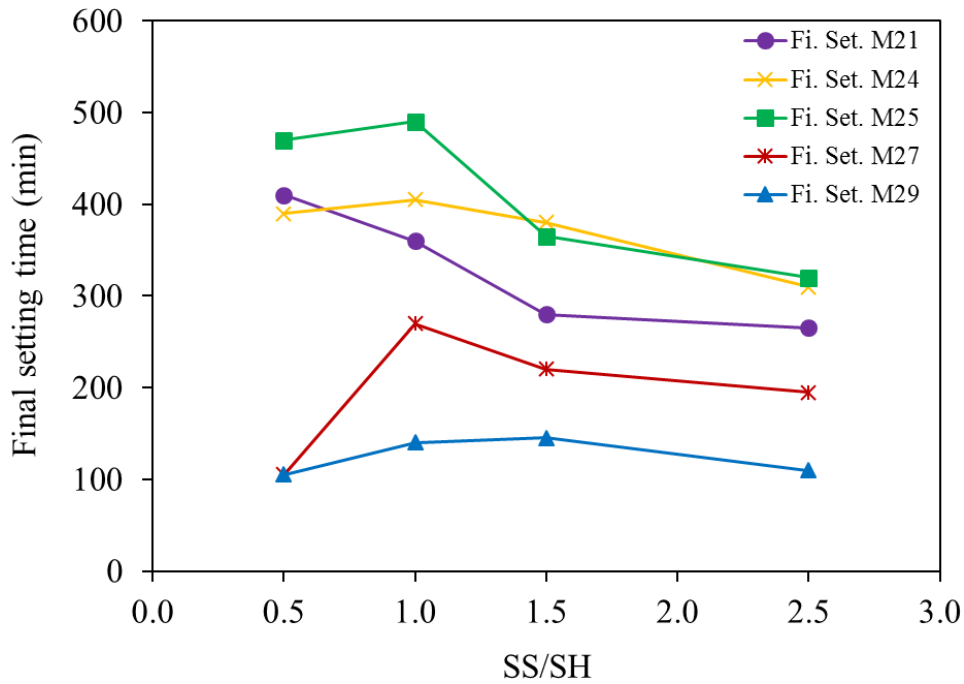
Figure 4.18: Final setting time of ZC mortar for W/FA of 0.400 and Alk/FA of 0.250 for different SS/SH.
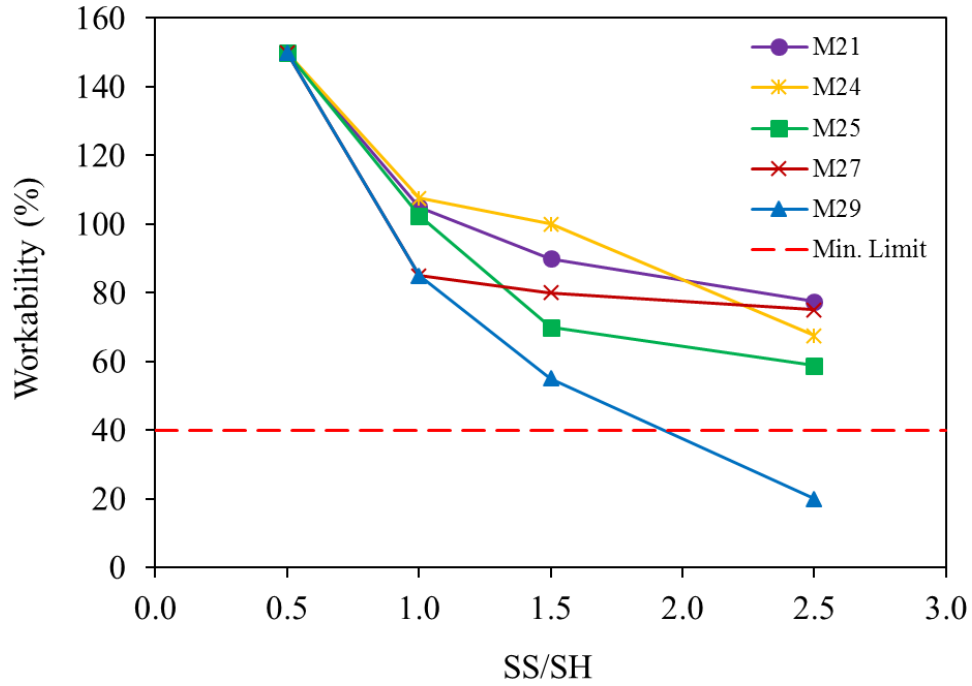
Figure 4.19: Workability of ZC mortar for W/FA of 0.450 and Alk/FA of 0.300 for different SS/SH.
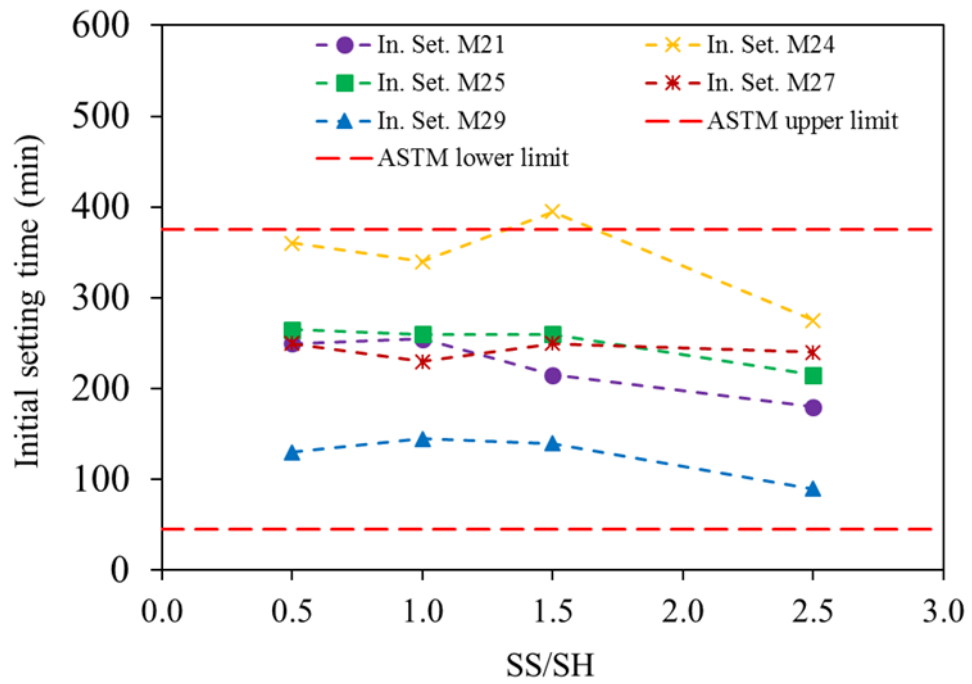
Figure 4.20: Initial setting time of ZC mortar for W/FA of 0.450 and Alk/FA of 0.300 for different SS/SH.
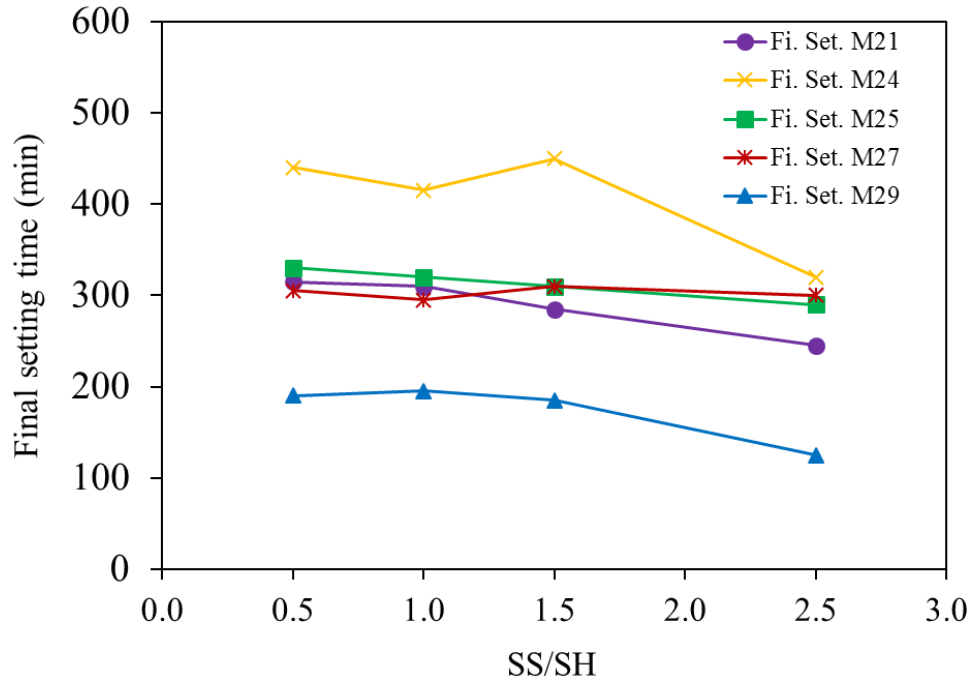
Figure 4.21: Final setting time of ZC mortar for W/FA of 0.450 and Alk/FA of 0.300 for different SS/SH.

As shown in Figs. 4.16 through 4.18, the workability ranged from 20% to 150%, the In. Set. ranged from 75 minutes to 390 minutes, and the Fi. Set. ranged from 105 minutes to 490 minutes. As shown in Figs. 4.19 through 4.21, the workability ranged from 20% to 150%, the In. Set. ranged from 90 minutes to 395 minutes, and the Fi. Set. ranged from 125 minutes to 450 minutes.

As shown in Figs. 4.16 through 4.21, for a given W/FA and Alk/FA, the workability and the setting time decreased with increasing the SS/SH from 0.5 to 1.0, 1.5, and 2.5. With increasing the SS the viscosity of the alkaline solution increased which resulted in lower workability [6]. Furthermore, increasing the SS/SH to 2.5 in the mixture increased the amount of soluble silica (SiO_2). Increasing the soluble silica enhanced the geopolymerization process and leaching and dissolution of the FA species in the mixture, causing a reduction in the setting time and

workability [63, 109]. The effect of SH content by moving from SS/SH of 0.5 to 1.5 was counterbalanced by the increase in the SS content within the mixture [110].

As shown in Figs. 4.16 through 4.21, all the mixtures passed the workability and setting time limits except one mixture for M24 and two mixtures for M25. Furthermore, it was not preferred to use a high SS/SH since the workability decreased with increasing SS/SH. In addition, among the four SS/SH ratios, the SS/SH of 1.0 showed a reasonable setting time, which is preferred to give enough time for casting and surfacing of the ZC mortar without any early setting. Using relatively small values of SS/SH would allow less W/FA to be added; therefore maximizing the strength of both hydration and geopolymerization mechanisms in the ZC mortar while displaying an acceptable In. Set. time. Therefore, SS/SH of one was found as the optimum ratio that satisfies the good workability and high setting times for all five FAs.

4.2.2 Results of compressive strength

The results of the compressive strength of all mixtures systems are shown in Figs. 4.24, 4.26, 4.28, 4.30, and 4.32 for oven curing specimens and Figs. 4.25, 4.27, 4.29, 4.31, and 4.33 for ambient curing specimens. The 7-day compressive strengths of ZC mortars ranged from 730 psi to 7900 psi depending on the curing regime, physical and chemical properties of the precursor, W/FA, Alk/FA, and SS/SH.

4.2.2.1. Effect of curing regime and calcium content on compressive strength

The strength of ZC mortar occurred due to two different mechanisms. (1) Geopolymerization, which generally needs elevated temperature. (2) Hydration, which occurs at ambient temperature. Generally, low calcium FA will have the higher contribution of the geopolymerization mechanism where high calcium FA has the higher contribution of the hydration mechanism.

114

The oven-cured specimens generally displayed higher compressive strengths than those of the 7-day ambient-cured specimens for all FAs except for some M29 mixtures (Fig. 4.22). The calcium content plays an important role in this behavior. Calcium could be regarded as a contamination during the geopolymerization process and alters the microstructure which causes a reduction in the compressive strength of the oven-cured mixtures [111]. However, the geopolymerization process is slow in the case of ambient curing system and requires elevated temperature to take place [33, 112]. The existence of the calcium compound in the FA would trigger the hydration process where the calcium and silica in the FA react with the water and form calcium silicate hydrate (CSH) which increased the compressive strength at the early ages at ambient temperature resulting in a relatively high compressive strength [43, 111, 113, 114].

Fig. 4.22 shows the relationship between the calcium content and compressive strength of the oven- and ambient-cured ZC mortars. As shown in the figure, the compressive strength of the oven-cured mixtures ranged from the 4180 to 7900 psi for M21, 2910 to 5810 psi for M24, 3070 to 6120 psi for M25, 3260 to 6640 psi for M27, and 2820 to 5830 psi for M29. Furthermore, the compressive strength of the ambient-cured mixtures ranged from 730 to 2650 psi for M21, 1160 to 3020 psi for M24, 1510 to 3580 psi for M25, 980 to 3000 psi for M27, and 3210 to 5460 psi for M29.

Presented also in Fig. 4.22 is the correlation between the calcium content and compressive strength as well as the coefficient of determination, R^2, of the oven- and ambient-cured ZC mortars. As shown in the figure, the correlation between the calcium content and strength is quite low in the case of oven curing with R^2 of 0.14 while it is much stronger in the case of ambient curing with R^2 of 0.55. The relatively small values of R^2 also confirm that the calcium content is not the only parameter that affects the compressive strength as explained earlier.

Generally, for all sourced FAs, except for M27, increasing the calcium content decreased the compressive strength of the oven-cured specimens and increased the compressive strength of the ambient-cured specimens. The oven-cured specimens of the M21 that have the lowest calcium content was the highest compressive strength among all FAs while the ambient-cured specimens of M29 that have the highest calcium contents was the highest compressive strength among all FAs. For the M27, while FA27 had the second-highest calcium content it had a low ambient compressive strength since it had the second-lowest surface area and amorphous content among all the FAs, as discussed in Chapter 2, which reduced the reactivity of the FA. Fig. 4.23 shows the effects of the surface area of each FA on the compressive strength of the different mixtures. Presented also in Fig. 4.23 is the correlation between the surface area and compressive strength as well as the coefficient of determination, R^2, of the oven- and ambient-cured ZC mortars. As show in the figure, the correlation between the calcium content and strength is quite low in the case of oven curing with R^2 of 0.08 while it is much stronger in the case of ambient curing with R^2 of 0.62.
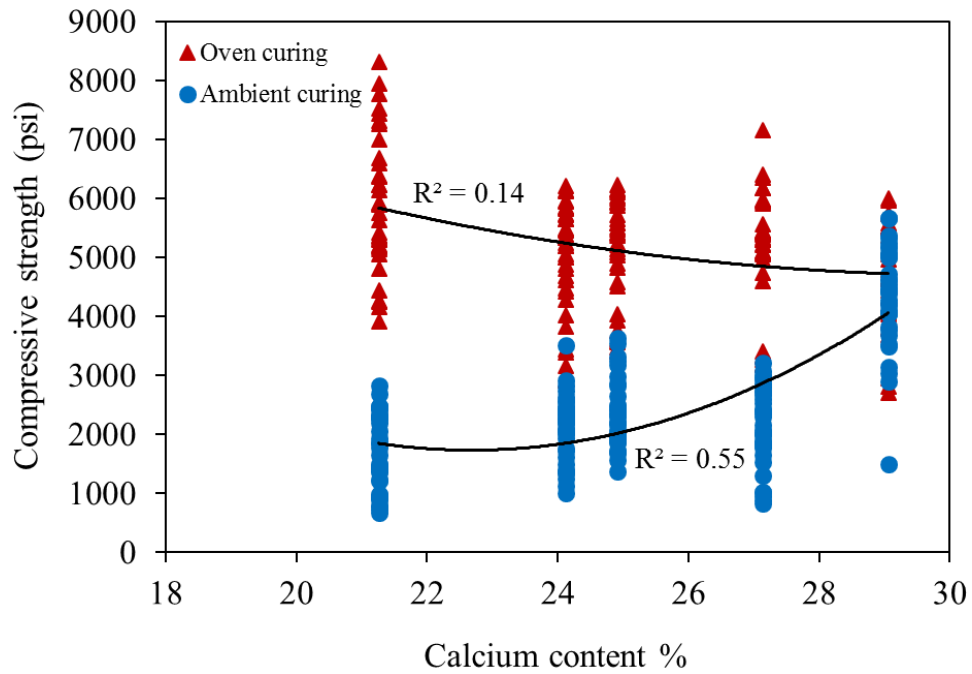
Figure 4.22: Effect of calcium content on the 7-day compressive strength of ZC mortar.
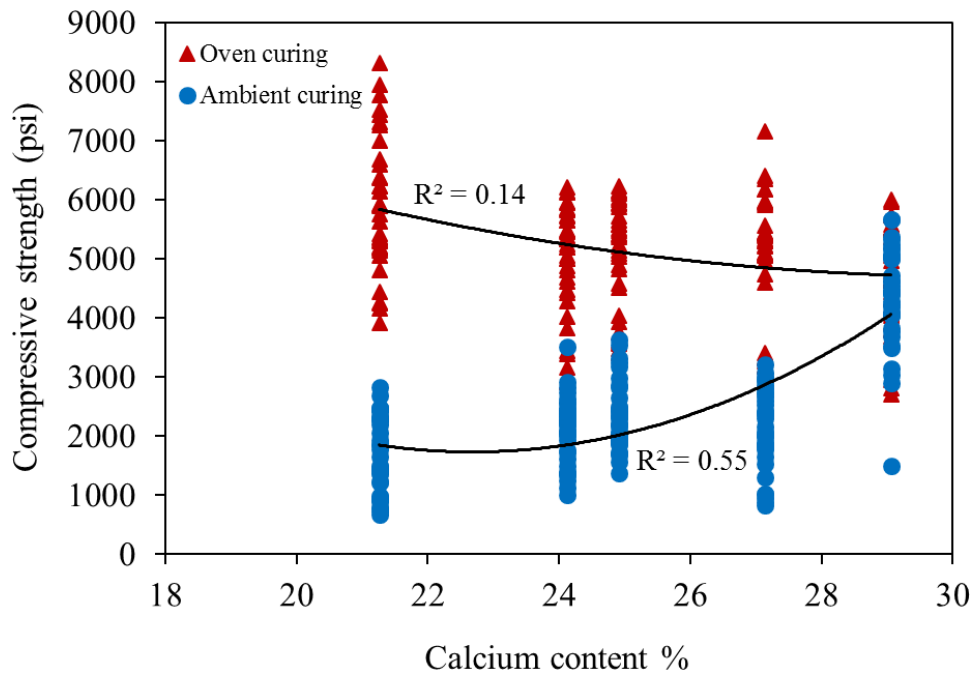
Figure 4.23: Effect of surface area on the 7-day compressive strength of ZC mortar.

117

4.2.2.1　*Effect of W/FA on compressive strength*

Figs. 4.24 and 4.25 show the compressive strength results of the oven- and ambient-cured specimens as a function of W/FA while keeping the Alk/FA and SS/SH constants at 0.250 and 1.0, respectively. Similarly, Figs. 4.26 and 4.27 show the compressive strength results of the oven- and ambient-cured specimens while keeping the Alk/FA and SS/SH fixed at 0.300 and 1.0, respectively.
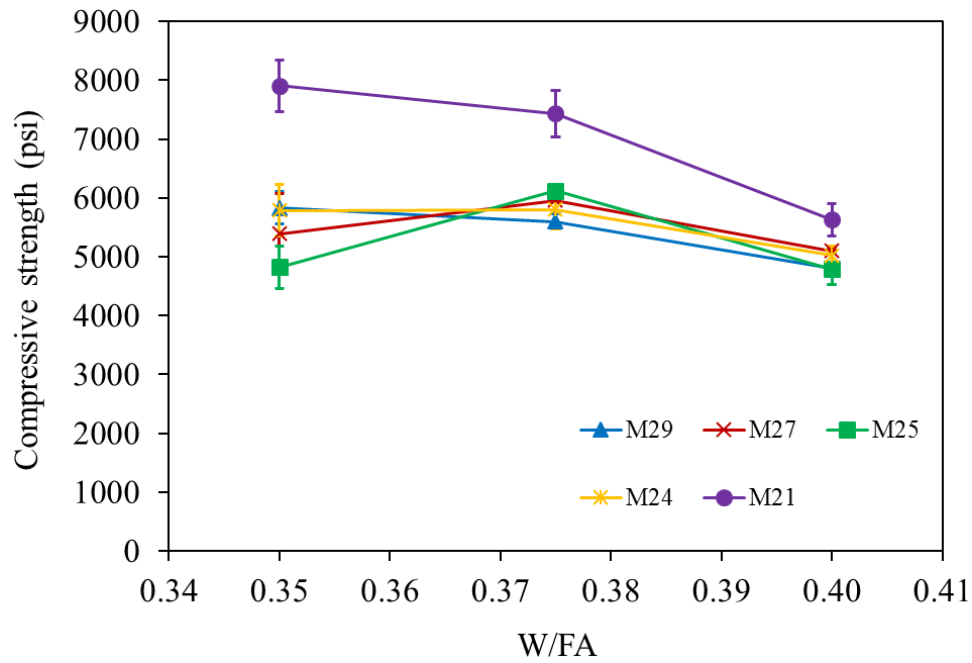
Figure 4.24: Compressive strength of the oven-cured ZC mortar for Alk/FA of 0.250 and SS/SH of 1.0 for different W/FA.
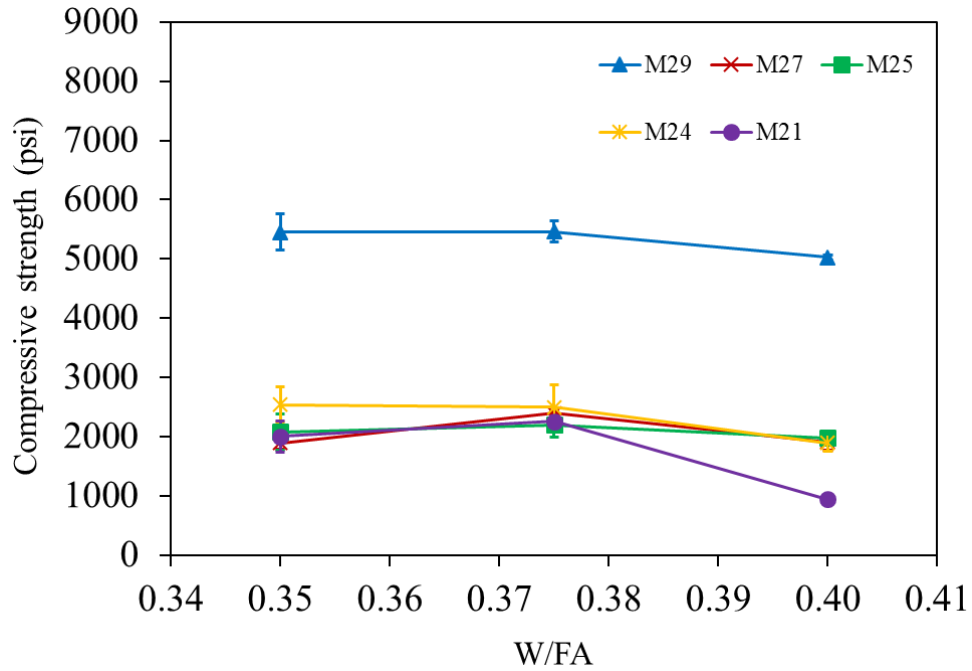
Figure 4.25: Compressive strength of the ambient-cured ZC mortar for Alk/FA of 0.250 and SS/SH of 1.0 for different W/FA.
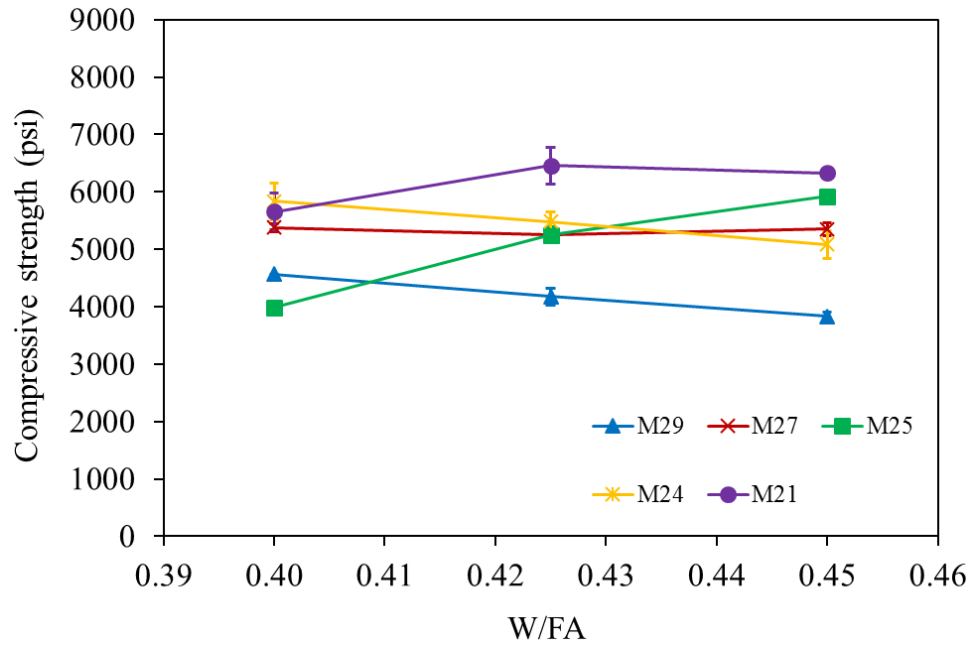
Figure 4.26: Compressive strength of the oven-cured ZC mortar for Alk/FA of 0.300 and SS/SH of 1.0 for different W/FA.
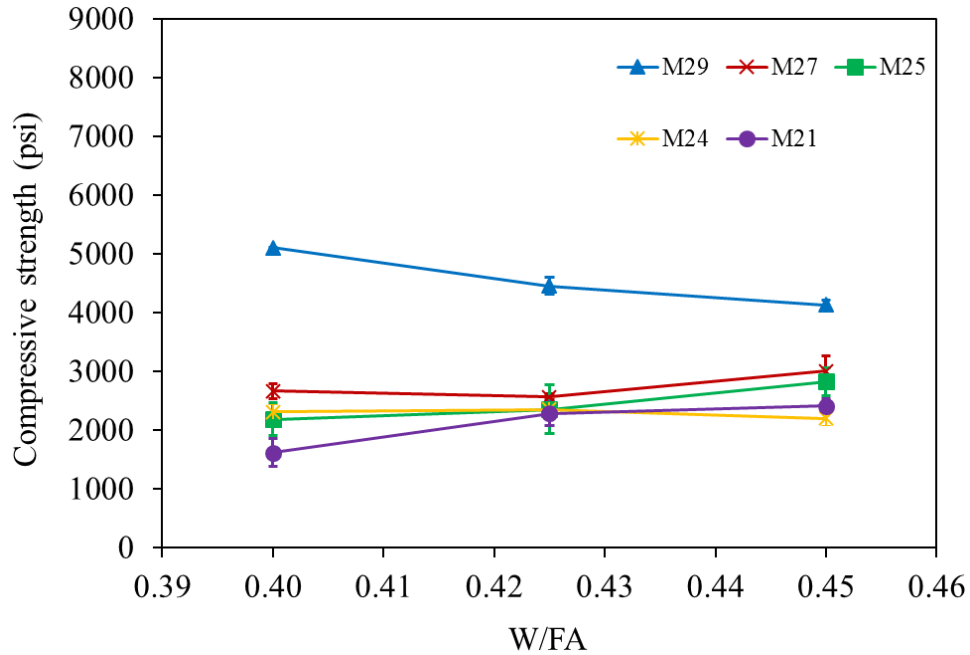
Figure 4.27: Compressive strength of the ambient-cured ZC mortar for Alk/FA of 0.300 and SS/SH of 1.0 for different W/FA.

As shown in Figs 4.24 and 4.25, with Alk/FA of 0.250 and SS/SH of 1.0, the compressive strength of all mixtures except those synthesized using FA25 and FA27 decreased with increasing the W/FA from 0.350 to 0.400. For M25 and M27, the strength slightly increased with increasing the W/FA from 0.350 to 0.400. Hence, the optimum W/FA was 0.350 for M21, M24, and M29 and 0.375 for M25 and M27.

For specimens having Alk/FA of 0.300, SS/SH of 1.0, and subjected to oven curing (Figs. 4.26 and 4.27), with increasing the W/FA, the compressive strength increased for M21 and M25 only. This is because in the case of high Alk/FA of 0.300, the presence of sufficient water content in the mixtures is necessary for geopolymerization to take place, which resulted in higher strength especially for mixtures synthesized using the FAs that had higher silica and alumina content. For specimens having Alk/FA of 0.300, SS/SH of 1.0, and subjected to ambient curing, adequate W/FA is important mainly for the hydration process; therefore, with low W/FA of 0.400, the

high alkaline triggers the geopolymerization process to take place. Therefore, the water was not free to be consumed in the hydration process as it was employed in the geopolymerization which is a slow process and produces weaker strength at ambient temperature. Furthermore, increasing the W/FA decreased the compressive strength of relatively high calcium FA mortar, i.e., M29 as the hydration process decreased.

4.2.2.2 *Effect of Alk/FA on compressive strength*

Figs. 4.28 and 4.29 show the compressive strength results of the oven- and ambient-cured specimens as a function of the Alk/FA while the W/FA and SS/SH constants at 0.400 and 1.0, respectively.
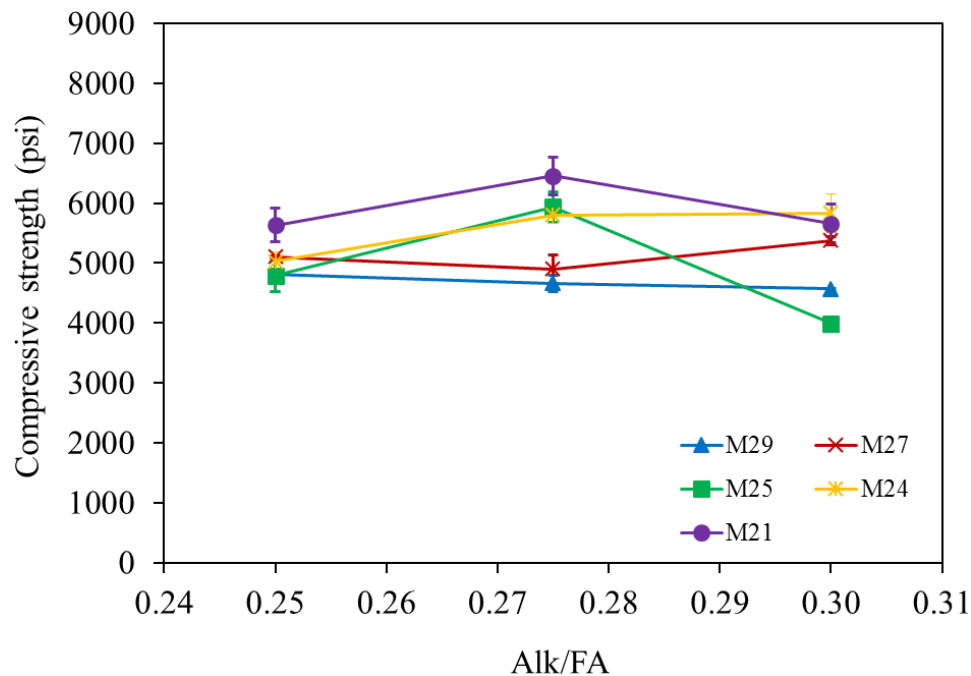
Figure 4.28: Compressive strength of the oven-cured ZC mortar for W/FA of 0.400 and SS/SH of 1.0 for different Alk/FA.
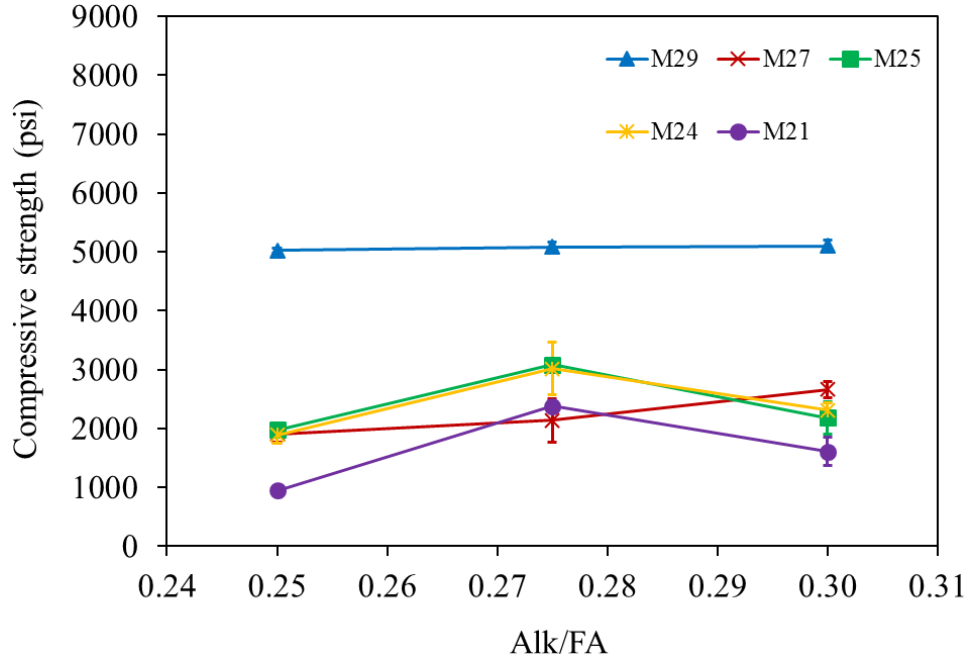
Figure 4.29: Compressive strength of the ambient-cured ZC mortar for W/FA of 0.400 and SS/SH of 1.0 for different Alk/FA.

As shown in Figs. 4.28 and 4.29, for W/FA of 0.400 and SS/SH of 1.0, the compressive strengths of the M21, M24, and M25 increased with increasing the Alk/FA from 0.250 to 0.275. With increasing the alkali concentration in the mixture, the solubility of the FA species increased [43]. Further increase of the Alk/FA from 0.275 to 0.300 accelerated the leaching and dissolution of the precursor at very early ages which resulted in incompletely dissolved and reacted FA particles; therefore, lower ambient and oven compressive strength. However, the compressive strength of the M27 increased with increasing the Alk/FA. As mentioned earlier, FA27 had the second-lowest surface area and amorphous content among all the FAs; therefore, higher Alk/FA was essential for dissolving the FA particles and resulted in higher compressive strength. Furthermore, the compressive strength of the M29 remained constant with changing the Alk/FA because the water content is the main parameter for the M29 that has the highest calcium content.

4.2.2.3 *Effect of SS/SH on compressive strength*

Figs. 4.30 and 4.31 show the compressive strength of the oven- and ambient-cured specimens as a function of the SS/SH while the W/FA and Alk/FA constants at 0.400 and 0.250, respectively. Similarly, Figs. 4.32 and 4.33 show the compressive strength of the oven- and ambient-cured specimens while the W/FA and Alk/FA constants at 0.450 and 0.300, respectively.
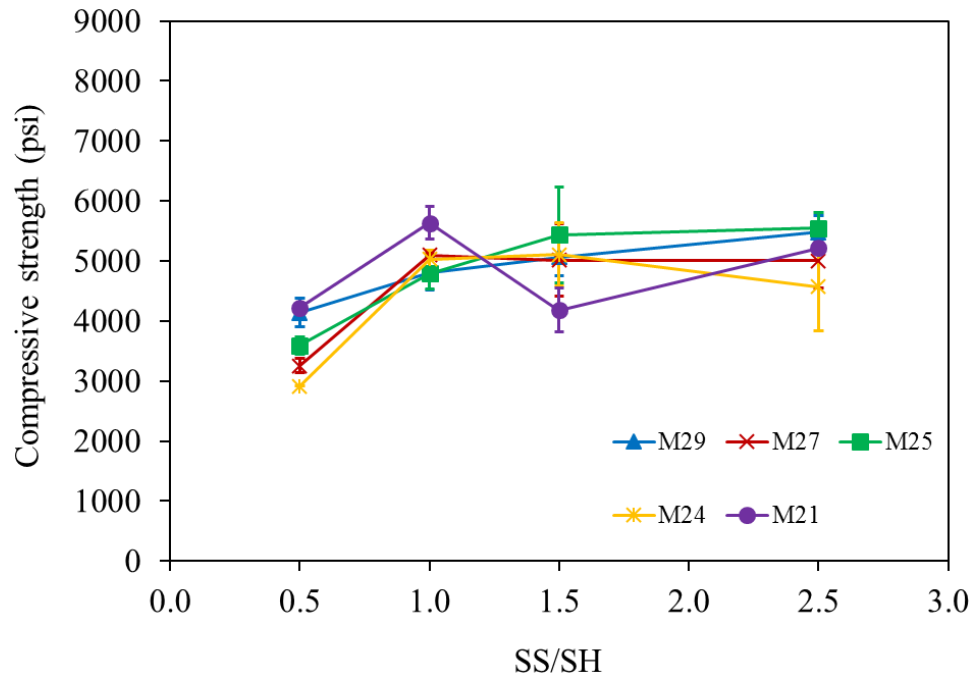
Figure 4.30: Compressive strength of the oven-cured ZC mortar for W/FA of 0.400 and Alk/FA of 0.250 for different SS/SH.
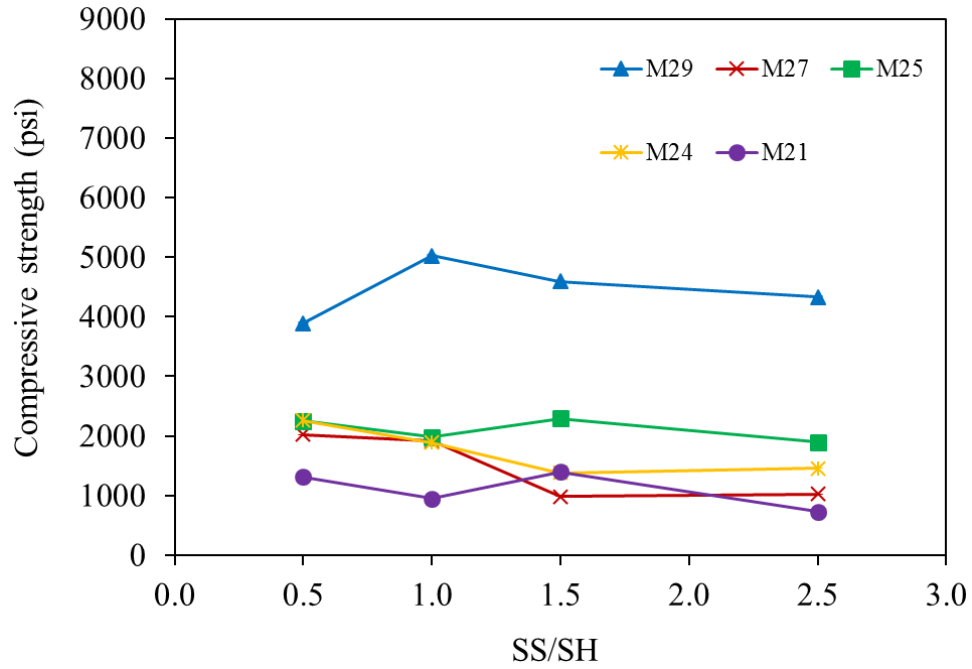
Figure 4.31: Compressive strength of the ambient-cured ZC mortar for W/FA of 0.400 and Alk/FA of 0.250 for different SS/SH.
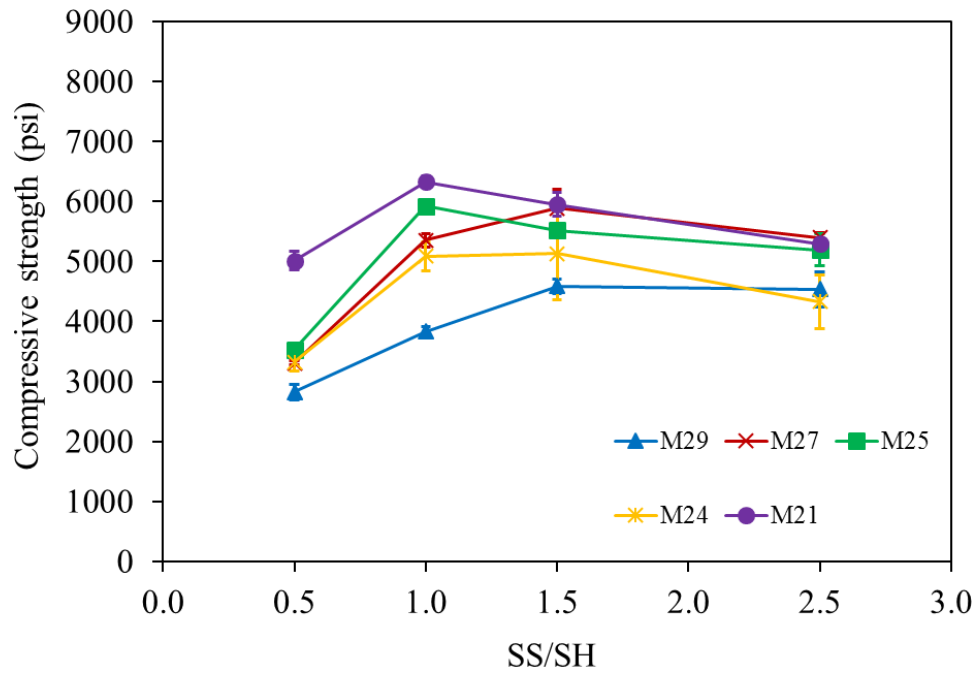
Figure 4.32: Compressive strength of the oven-cured ZC mortar for W/FA of 0.450 and Alk/FA of 0.300 for different SS/SH.
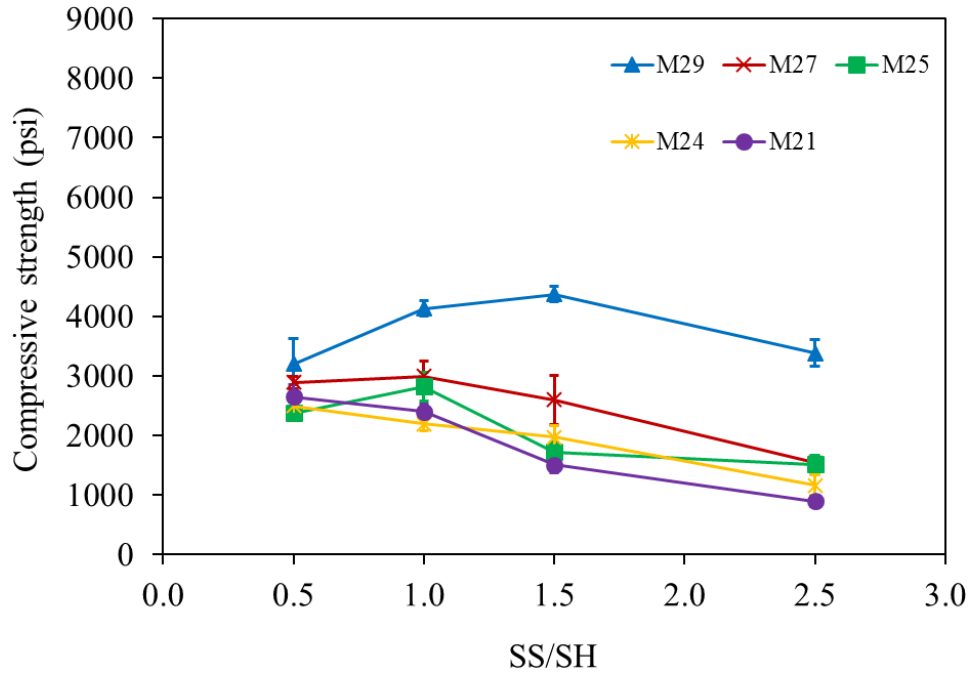
Figure 4.33: Compressive strength of the ambient-cured ZC mortar for W/FA of 0.450 and Alk/FA of 0.300 for different SS/SH.

For ambient-cured mixtures, the compressive strength slightly increased or remained constant with increasing the SS/SH from 0.5 to approximately 1.0. Beyond that, the strength gradually decreased with increasing SS/SH. This was due to the excessive soluble silica that was provided by the SS in the mortar that hindered the structure formation of the geopolymer products (aluminosilicate), reducing the compressive strength [63, 115]. The increase of the SH concentration in the mixture increased the hydroxide ions (OH⁻) and the alkali content (Na$_2$O) that enhanced the dissolution and leaching of the silica and alumina from the FA and resulted in higher strength at ambient temperature [45]. For M29, the high SH content released excessive hydroxide ions, and displayed a negative effect on the dissolution of the FA29 due to the highest calcium content.

For the ambient curing, the SS/SH of approximately 1.0 showed a good balance between the required hydroxide ions and alkali that provided by the SH and the soluble silica that is provided

by the SS, which resulted in high compressive strengths. SS/SH of 1.0 resulted in compressive strengths up to 2405 psi for M21, 2195 psi for M24, 2820 psi for M25, 3000 psi for M27, and 5025 psi for M29.

Specimens that were oven cured showed higher compressive strength with increasing the SS/SH from 0.5 to 1.0. Beyond that, the strength remained approximately constant. At elevated curing temperature, the geopolymerization process took place quicker than at ambient temperature. Therefore, with high SH content that released the hydroxide ions (OH$^-$) in the mixture, the leaching and dissolution of the FA compounds followed by precipitating the aluminosilicate gel were accelerated at early ages which resulted in incompletely dissolved and reacted FA particles, therefore resulting in lower compressive strength [63, 110, 116]. Oven-cured specimens having SS/SH from 1.0 to 2.5 displayed compressive strengths up to 6330 psi for M21, 5920 psi for M25, 5480 psi for M29, 6640 psi for M27, and 5130 psi for M24.

4.3 Discussion

Different combinations of W/FA, Alk/FA, and SS/SH were investigated. The study revealed that SS/SH of 1.0 is the most appropriate value to produce structural ZC mortar where it has good workability and compressive strength. Specimens having combinations of W/FA of 0.350 with Alk/FA of 0.250 and W/FA of 0.400 with Alk/FA of 0.300 did not pass the workability and setting time limits and hence this combination was excluded. To determine the best value of Alk/FA, Fig. 4.34 shows the peak strength for each mortar at SS/SH of 1.0 and two values of Alk/FA of 0.250 and 0.300. The figure presents the strength for oven- and ambient-cured specimens. As shown in the figure, the highest compressive strengths of the ambient-cured specimens in most cases occurred at Alk/FA of 0.30; this was used in the remaining chapters of this report.
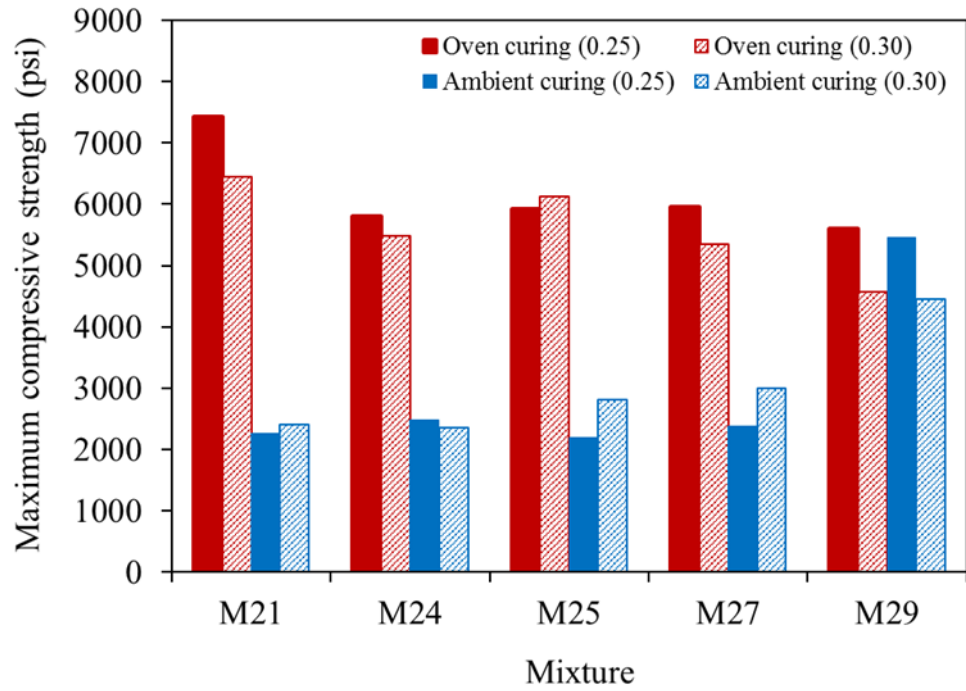
Figure 4.34: Peak strength for mortar at SS/SH of 1.0 and Alk/FA of 0.250 and 0.300.

Table 4.2: Details and Compressive Strength Results of Oven- and Ambient-Cured Mixtures of M21.

Oven-cured mixtures

Mix.	Compressive Strength (psi)	Range (psi)	Variance (ksi)	SD[a] (psi)	CV[b] (%)
1	7900	875	0.1927	439	5.55
2	7430	772	0.1558	395	5.31
3	5630	554	0.0768	277	4.92
4	5660	458	0.1049	324	5.72
5	6460	441	0.0972	312	4.83
6	6330	162	0.0084	92	1.45
7	7060	712	0.1590	399	5.65
8	4220	107	0.0032	56	1.33
9	4180	517	0.1336	366	8.74
10	5210	180	0.0085	92	1.77
11	5010	351	0.0318	178	3.56
12	5950	392	0.0385	196	3.30
13	5290	150	0.0056	75	1.42

Ambient-cured mixtures

Mix.	Compressive Strength (psi)	Range (psi)	Variance (ksi)	SD[a] (psi)	CV[b] (%)
1	2040	445	0.0569	238	11.69
2	2260	127	0.0081	90	3.97
3	950	64	0.0011	33	3.45
4	1610	333	0.0554	235	14.62
5	2280	411	0.0424	206	9.04
6	2410	212	0.0135	116	4.83
7	2230	504	0.0689	262	3.72
8	1310	270	0.0226	150	11.46
9	1400	49	0.0012	35	2.48
10	730	105	0.0028	53	7.27
11	2650	400	0.0414	203	7.68
12	1510	283	0.0203	142	9.43
13	890	171	0.0073	86	9.60

[a]SD: standard deviation

[b]CV: coefficient of variation

Table 4.3: Details and Compressive Strength Results of Oven- and Ambient-Cured Mixtures of M24.

Oven-cured mixtures

Mix.	Compressive Strength (psi)	Range (psi)	Variance (ksi)	SD[a] (psi)	CV[b] (%)
1	5790	864	0.1875	433	7.48
2	5800	672	0.1137	337	5.81
3	5030	312	0.0248	158	3.13
4	5830	646	0.1047	324	5.55
5	5490	314	0.0249	158	2.88
6	5090	447	0.0591	243	4.78
7	5810	253	0.0201	142	2.44
8	2910	210	0.0110	105	3.61
9	5110	1036	0.2707	520	10.18
10	4570	1365	0.5279	727	15.91
11	3330	288	0.0232	152	4.58
12	5130	1525	0.5928	770	15.01
13	4330	860	0.2009	448	10.35

Ambient-cured mixtures

Mix.	Compressive Strength (psi)	Range (psi)	Variance (ksi)	SD[a] (psi)	CV[b] (%)
1	5790	864	0.1875	433	7.48
2	5800	672	0.1137	337	5.81
3	5030	312	0.0248	158	3.13
4	5830	646	0.1047	324	5.55
5	5490	314	0.0249	158	2.88
6	5090	447	0.0591	243	4.78
7	5810	253	0.0201	142	2.44
8	2910	210	0.0110	105	3.61
9	5110	1036	0.2707	520	10.18
10	4570	1365	0.5279	727	15.91
11	3330	288	0.0232	152	4.58
12	5130	1525	0.5928	770	15.01
13	4330	860	0.2009	448	10.35

[a]SD: standard deviation

[b]CV: coefficient of variation

Table 4.4: Details and Compressive Strength Results of Oven- and Ambient-Cured Mixtures of M25.

Oven-cured mixtures

Mix.	Compressive Strength (psi)	Range (psi)	Variance (ksi)	SD[a] (psi)	CV[b] (%)
1	4830	508	0.1290	359	7.44
2	5920	65	0.0021	33	0.56
3	4790	206	0.0212	266	5.54
4	3990	98	0.0048	69	1.74
5	5250	202	0.0204	139	2.64
6	6125	185	0.0171	95	1.54
7	5930	351	0.0616	251	4.23
8	3600	190	0.0181	142	3.95
9	5430	572	0.1636	802	14.76
10	5550	354	0.0627	250	4.51
11	3530	170	0.0145	109	3.08
12	5520	106	0.0056	55	0.99
13	5190	187	0.0175	268	5.16

Ambient-cured mixtures

Mix.	Compressive Strength (psi)	Range (psi)	Variance (ksi)	SD[a] (psi)	CV[b] (%)
1	2140	435	0.0628	251	11.72
2	2200	431	0.0466	216	9.82
3	1980	31	0.0005	22	1.11
4	2180	522	0.0765	277	12.68
5	2350	785	0.1745	418	17.77
6	2820	342	0.0585	242	8.57
7	3080	84	0.0035	59	1.66
8	2250	142	0.0051	71	2.19
9	2290	140	0.0098	99	4.32
10	1890	64	0.00205	45	2.39
11	2370	178	0.0087	93	3.92
12	1720	321	0.0258	161	9.34
13	1510	280	0.0201	142	9.36

[a]SD: standard deviation

[b]CV: coefficient of variation

Table 4.5: Details and Compressive Strength Results of Oven- and Ambient-Cured Mixtures of M27.

Oven-cured mixtures

Mix.	Compressive Strength (psi)	Range (psi)	Variance (ksi)	SD[a] (psi)	CV[b] (%)
1	5390	1212	0.4553	675	12.5
2	5960	39	0.0004	20	0.3
3	5100	39	0.0005	22	0.4
4	5380	127	0.0043	65	1.2
5	5260	91	0.0041	64	21.9
6	5350	212	0.0130	114	2.1
7	4900	339	0.0575	240	4.7
8	3260	221	0.0150	122	3.8
9	5020	847	0.3587	599	11.2
10	6640	816	0.2078	456	6.9
11	3310	73	0.0014	37	1.1
12	5890	621	0.0971	312	5.3
13	5400	117	0.0068	83	3.8

Ambient-cured mixtures

Mix.	Compressive Strength (psi)	Range (psi)	Variance (ksi)	SD[a] (psi)	CV[b] (%)
1	1890	185	0.0102	101	5.34
2	2390	64	0.0011	33	1.37
3	1910	292	0.0217	147	7.71
4	2660	623	0.1024	320	12.03
5	2470	299	0.0245	157	1.90
6	3000	496	0.0654	256	8.52
7	1970	773	0.1561	395	17.45
8	2020	56	0.0016	40	1.96
9	980	148	0.0070	84	8.55
10	1030	461	0.0574	240	23.34
11	2890	196	0.0106	103	3.57
12	2600	809	0.1680	410	15.77
13	1540	210	0.0110	105	6.82

[a]SD: standard deviation

[b]CV: coefficient of variation

Table 4.6: Details and Compressive Strength Results of Oven- and Ambient-Cured Mixtures of M29.

Oven-cured mixtures

Mix.	Compressive Strength (psi)	Range (psi)	Variance (ksi)	SD[a] (psi)	CV[b] (%)
1	5830	492	0.0747	273	4.69
2	5600	224	0.0164	128	2.29
3	4810	504	0.0811	285	5.93
4	4570	4	0.0000	3	0.06
5	4180	290	0.0216	147	3.52
6	3840	128	0.0049	70	1.83
7	4660	257	0.0166	129	2.76
8	4140	136	0.0046	68	1.65
9	5060	213	0.0115	107	2.12
10	5480	203	0.0106	103	1.87
11	2820	256	0.0165	128	4.55

Ambient-cured mixtures

Mix.	Compressive Strength (psi)	Range (psi)	Variance (ksi)	SD[a] (psi)	CV[b] (%)
1	5450	431	0.0929	305	5.59
2	5460	326	0.0326	180	3.31
3	5030	61	0.0019	43	0.86
4	5100	141	0.0010	100	1.95
5	4450	432	0.0526	229	5.15
6	4130	231	0.0170	130	3.16
7	5090	161	0.0068	83	1.62
8	3890	284	0.0223	149	3.84
9	4590	325	0.0284	168	3.67
10	4330	352	0.0373	193	4.46
11	3210	789	0.1771	421	13.13
12	4380	259	0.0184	136	3.10
13	3390	389	0.0470	217	6.40

[a]SD: standard deviation

[b]CV: coefficient of variation

4.4 Summary and Conclusions

This chapter presents the effects of water to fly ash (W/FA), alkali activators to fly ash (Alk/FA), and sodium silicate to sodium hydroxide (SS/SH) ratios on fresh properties (workability and setting times) and compressive strength of ZC mortar. Based on this experimental work, a wide range of parameters including W/FA from 0.350 to 0.450, Alk/FA from 0.250 to 0.300, and SS/SH from 0.5 to 2.5 were investigated. The specimens were either cured in the oven for 24 hours or at ambient temperature for 7 days. Then, the compressive strength of the specimens was determined. The following can be concluded:

- The optimum values of Alk/FA and SS/SH were 0.300 and 1.0, respectively. These values resulted in a balance between the workability, setting times, and compressive strength for both curing regimes.

- The minimum W/FA that can be used was 0.425 with Alk/FA 0.300.

- The FAs that had a calcium content higher than 27% gave the highest compressive strength in the case of ambient curing regime.

- Mixtures that were synthesized using relatively low calcium content FAs displayed the highest compressive strength with oven curing while those synthesized using relatively high calcium content FAs displayed the highest compressive strength with ambient curing.

- The workability and setting times increased with increasing the W/FA and with decreasing the Alk/FA.

- The workability decreased with increasing the SS/SH from 0.5 to 2.5. For example, increasing the SS/SH from 0.5 to 2.5 increased the workability of the five sourced FAs from 150% to 60%.

- The initial and final setting times decreased with increasing the SS/SH. For example, increasing the SS/SH from 0.5 to 2.5 decreased the average initial setting time of the five sourced fly ashes from 251 minutes to 200 minutes while it decreased the average final setting time from 316 minutes to 256 minutes.

- FA29 showed the lowest workability and setting time among the other five FAs due to its high calcium content and surface area.

Chapter 5: Optimization of Thermal Curing Temperature and Duration of Zero-Cement Mortar

In this chapter, the effects of curing duration and temperature on ZC mortar mixtures were investigated. Five sourced FA were used to synthesize mortar mixtures. The mixtures were prepared using different alkaline and silicate contents. Therefore, the correlation between the alkaline, silicate, and curing characteristics can be evaluated. Curing temperatures ranging from 185° F (85° C) to 86° F (30° C) applied over durations ranging from 4 hours to 168 hours were used. Furthermore, hot weather curing was imitated using two different regimes. The energy required to achieve the different curing regimes was then calculated and correlated to the achieved compressive strength. Therefore, the compressive strength can be optimized based on the energy cost.

5.1 Material Properties

5.1.1 Fly ashes, sand, coarse aggregate, and alkali solutions

Five FAs were used in this part of the chapter to mix mortar; FA37, FA29, FA26, FA24, and FA21. The alkali activators, the sand for mortar was used in this chapter were mentioned in Chapter 2 of this report.

5.1.2 Mix design

Three different mixtures were selected as reference mixtures and prepared out of each of the five FA types, i.e., 15 mixtures were prepared during the course of this research. All three mixtures have a sand-to-binder (FA) ratio of 2.75 (Table 5.1). The first mixture, LA, had a relatively low Alk/FA of 0.275 with W/FA of 0.380. The silicate modulus, i.e., SS/SH in the alkali activator, was 1.0. The second mixture, HA, had a relatively high Alk/FA of 0.300 while keeping the

W/FA the same as mix 1. Both LA and HA mixtures had a SS/SH of 1.0. In the third mixture, HS, the SS/SH was increased to 2.0 since increasing the silicate content increases the dissolution rate of alkali activators [43]. However, the high viscosity of the silicate reduced the mixture's workability, and extra water was added to improve the workability of the mixture. The Na_2O of the Alk/FA in the different mixtures is shown in Table 5.2.

Table 5.1: Mix Designs.

MixNo.	LA	HA	HS
Alk/FA	0.275	0.300	0.275
W/FA	0.380	0.380	0.400
SS/SH	1.000	1.000	2.000
SH (lb/ft^3)	4.68	5.06	3.12
SS (lb/ft^3)	4.68	5.06	6.24
W (lb/ft^3)	7.12	6.62	7.99
Sand (lb/ft^3)	92.7	92.7	92.7
FA (lb/ft^3)	33.7	33.7	33.7

Table 5.2: Sodium/FA Ratios.

Mix	Sodium (Na_2O) Ratio (%)	Sodium (Na_2O) by weight (lb/ft^3)
LA	4.90	1.83
HA	5.30	1.99
HS	4.45	1.68

5.1.3 Mixing procedures

The mortars were mixed using mixing procedure no. 4, as described in Chapter 3.

5.1.4 Curing conditions

The mortar specimens were cured at different temperatures of 104° F (40° C), 131 (55° C), 158° F (70° C), and 185° F (85° C) for periods of 4, 8, 16, 24, and 48 hours. Furthermore, two different

hot weather curing scenarios were considered. The first scenario included curing at a constant temperature of 86° F (30° C) for 16, 24, 48, 96, and 168 hours. The second hot weather curing scenario included imitating a Missouri summer week using an environmental chamber where each specimen was subjected to curing temperatures ranging from 72° F (22° C) representing night time to 97° F (36° C) representing morning time (Fig. 5.1).
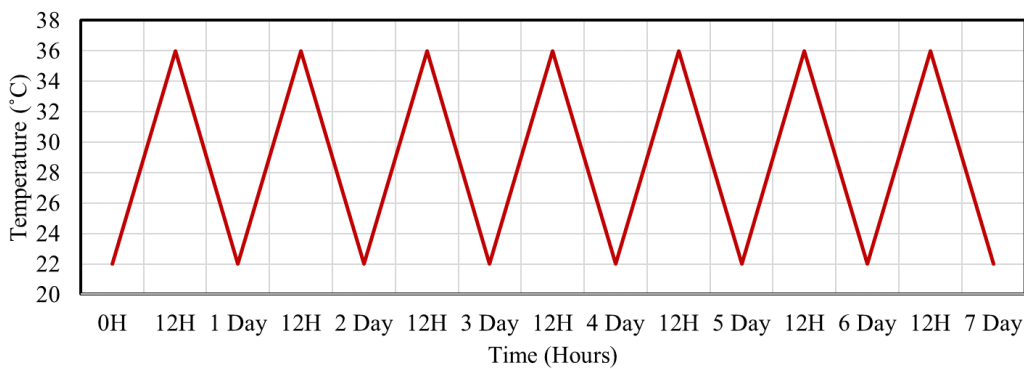
Figure 5.1: Environmental chamber temperature for one week.

5.2 Fresh Properties of the Mortar

The fresh properties were determined following the approach described in Chapter 3.

5.3 Results and Discussion

5.3.1 Setting time and workability

All the mixtures displayed initial setting times ranging from 75 minutes to 350 minutes and final setting times ranging from 100 minutes to 390 minutes (Fig. 5.2). While there is no ASTM standard for determining an acceptance criteria for the setting times of mortar, ASTM C191-13 [100] requires an initial setting time greater than 45 minutes and less than 375 minutes for paste mixtures. Hence, all mixtures satisfied the ASTM C191-13 [100] setting time requirements.

As shown in Fig. 5.2, doubling the amount of silicate in the HS mixtures compared to LA mixtures while keeping the total Alk/FA constant decreased the initial setting time by

approximately 42% for all FA sources. Higher soluble silicate in the system improves the geopolymerization process as it provides the ZC mortar with soluble silicate species that are important to trigger the formation of oligomers (monomers, dimers, trimers and tetramers) and the polycondensation of silicate and/or aluminosilicate oligomers. Such formations reduced the setting times. Furthermore, for silicate modulus of one, i.e., for LA mixtures, most oxygen sites on the silicate tetrahedrons are occupied by either hydrogen or sodium ions. Thus, in this case fewer amounts of negatively charged oxygen sites are available for calcium ions dissolved from the FA source, which resulted in a longer setting time for LA.

Increasing the alkaline content by approximately 10% from mixtures LA to HA reduced the initial setting time by approximately 25% (Fig. 5.2) due to the increased dissolution and leaching rates of the Si and Si–Al phases from the FA, which is necessary for triggering the formation of oligomeric precursors and polycondensation and accelerating the geopolymerization process.

The flowability results (Fig. 5.3) are consistent with the initial setting time of the respective mixtures. The flow results indicate that increasing the silicate in the ratio of alkali activators reduced the workability of the geopolymer mixtures by an average of 33%. This is attributed to the increase in the viscosity of the SS with increasing its modulus ratio. It is worth noting that the highest viscosity of SS occurred at a modulus of 2.0. Similarly, increasing the alkaline activators by 10% reduced workability by an average of 19%.
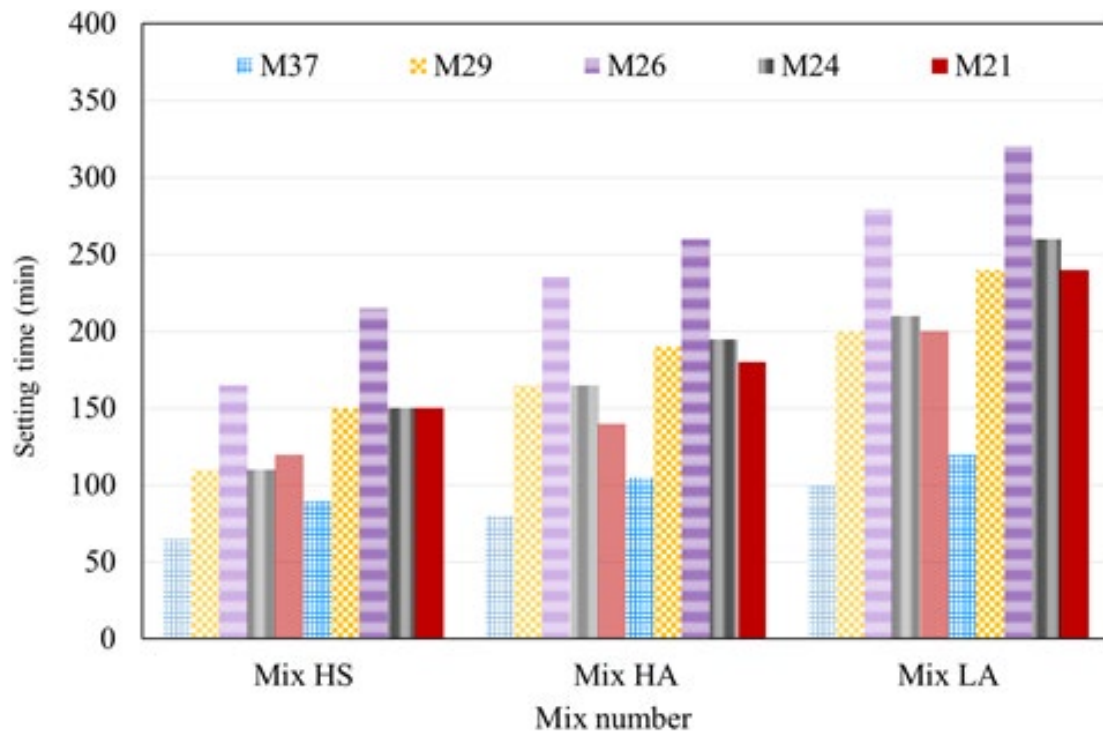
Figure 5.2: Setting times of ZC mortar mixes.
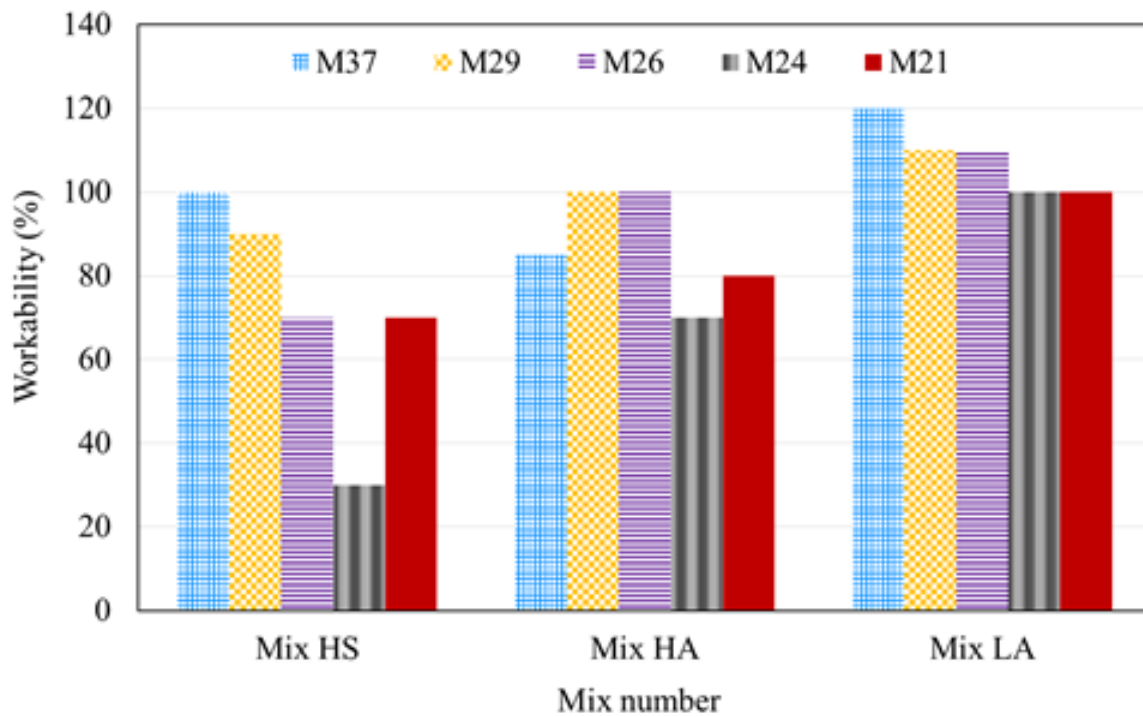
Figure 5.3: Workability of ZC mortar mixes.

5.3.2　Compressive strength

5.3.2.1　Oven-cured samples

Fig. 5.4 shows the compressive strength of each mixture after being cured for different periods at different temperatures. As shown in the figure, for a given mixture, it was possible to obtain different ZC mortar compressive strengths using different combinations of curing temperatures and durations. For example, it was possible to produce ZC mortar having compressive strengths in the range of 5000 psi – 5500 psi using numerous combinations such as curing at 104° F (40° C) for 48 hours or curing at 158° F (70° C) for 12 hours. These combinations granted flexibility to ZC producers to optimize the curing time and temperature for different project scenarios.

M37- Mix LA   M37-Mix HA   M37-Mix HS

M29- Mix LA   M29-Mix HA   M29- Mix HS

M26- Mix LA   M26- Mix HA   M26- Mix HS

M24- Mix LA   M24- Mix HA   M24- Mix HS

Temperature (Celsius)

86F 104F 131F 158F 185F

4 8 16 24 48 hrs

0-500 | 500-1000 | 1000-1500 | 1500-2000 | 2000-2500
2500-3000 | 3000-3500 | 3500-4000 | 4000-4500 | 4500-5000
5000-5500 | 5500-6000 | 6000-6500 | 6500-7000 | 7000-7500
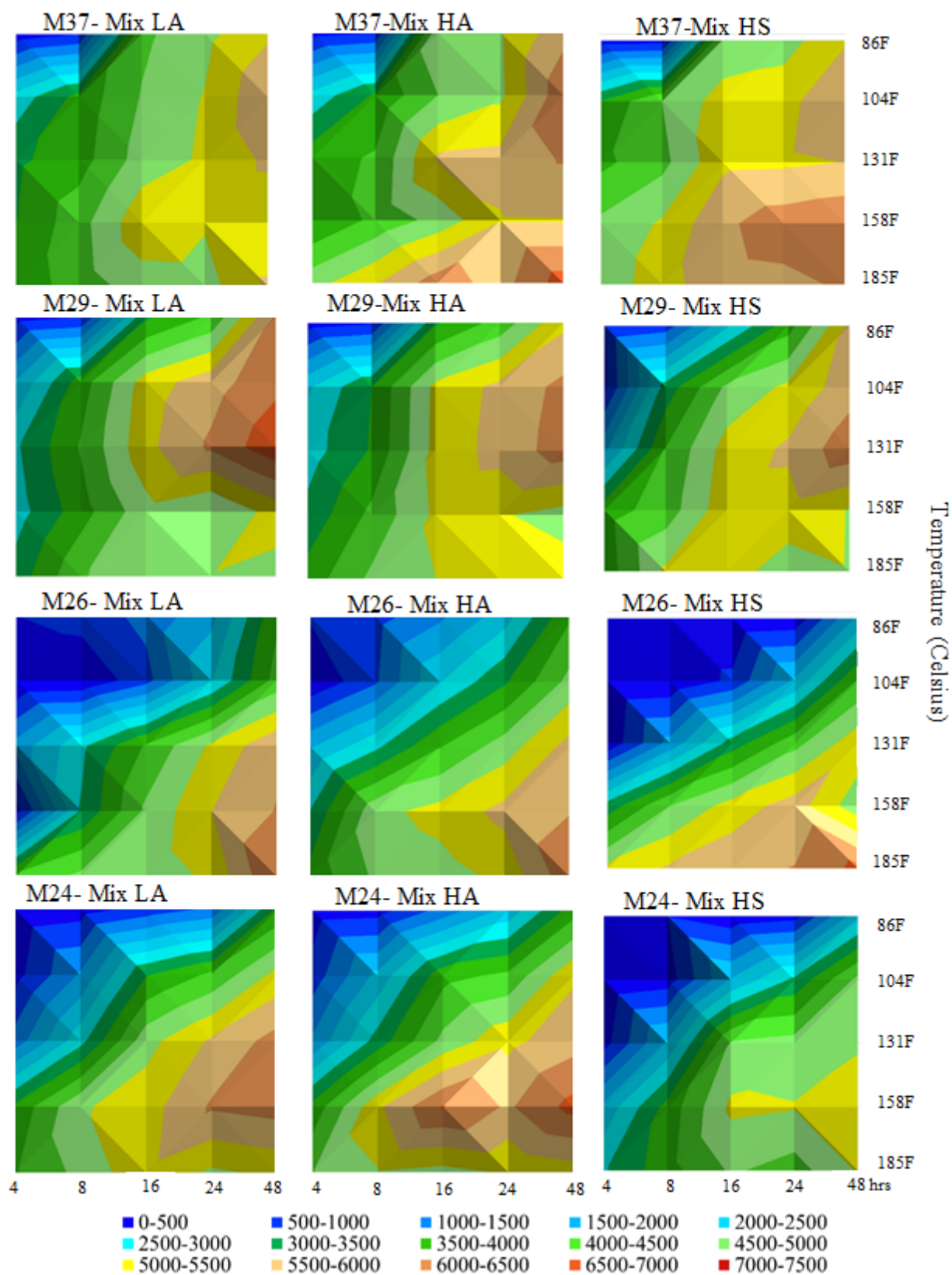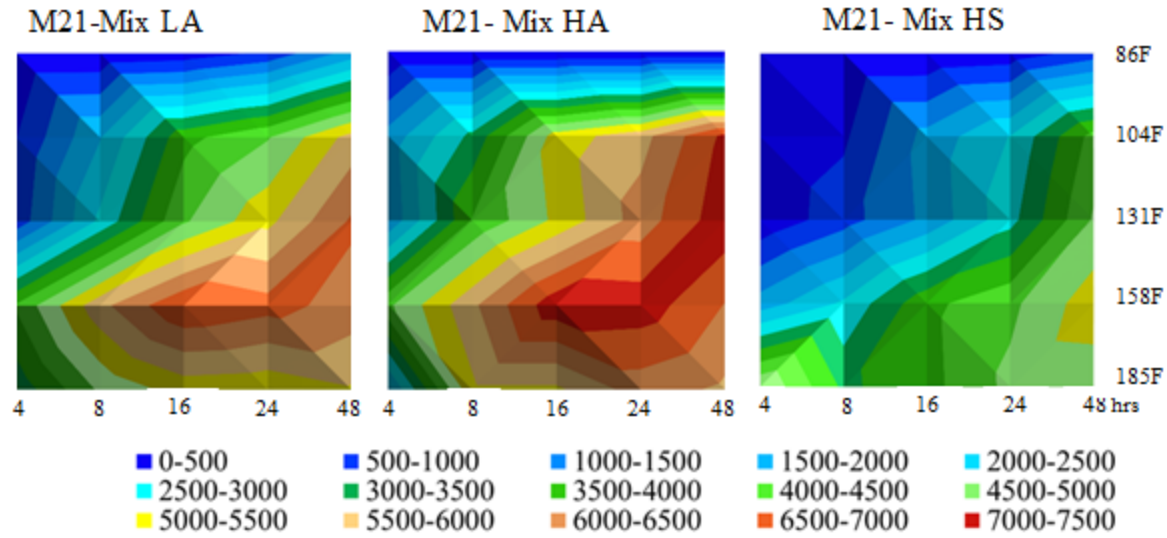
Figure 5.4: Compressive strength of different mixes at different temperatures and durations.

As shown in Fig. 5.4, the different mixtures that were synthesized using different FAs, alkaline contents, and silicate contents displayed different peak compressive strengths and required different curing temperatures and durations to achieve these peaks. For LA mixtures (left column of Fig. 5.4), the peak compressive strengths for the mixtures synthesized using high calcium FAs were generally lower than those of the mixtures synthesized using lower calcium FAs. For example, the peak strength for mixture M21 is 7350 psi (50.7 MPa), and it occurred after curing for 16 hours at 158° F (70° C) while that of mixture M37 is 5925 psi (40.9 MPa) and it occurred after curing for 48 hours at 104° F (40° C).

The calcium content in the FA source used in the ZC mortar also played an essential role in the peak strength of the LA mixtures. For all sourced FAs but FA26, decreasing the calcium content in the FA increased the region where relatively high compressive strength, i.e., higher than 5000 psi (34.5 MPa), can be achieved (the yellow and brown regions in the left column of Fig. 5.4). It should be noted that FA26 had a significantly lower surface area compared to all other FAs. Furthermore, decreasing the calcium content shifted the temperature required to achieve

142

relatively higher strength toward higher curing temperatures. The calcium content in the FA affects the geopolymerization process in the following three different aspects. 1) It forms $Ca(OH)_2$ and precipitates. The formation of $Ca(OH)_2$ will remove the OH^- ions which in turn reduce the pH of the alkaline solution and hence reduce the dissolution rate of the silicon and aluminum [117, 118]. 2) The free calcium ions react with the silica and alumina forming C-S-H gel. 3) The free calcium can replace a cation in the geopolymeric gel [43]. Increasing the curing temperature reduces the solubility of Ca in ZC mortar. For example, increasing the temperature from 73° F (23° C) to 167° F (75° C) reduced the leached calcium by 50% [43]. Reducing the solubility of calcium allowed more geopolymerization to take place and hence FA with a lower calcium content displayed higher compressive strength and vice versa. Table 5.3 shows an approximate summary of the required curing times and temperatures for each FA to display a compressive strength of 5000 psi (34.5 MPa) or higher. For example, curing at 86 to 185° F (30 to 85° C) for 24 to 48 hours produced the highest compressive strengths, ranging from 4795 to 5925 psi (33.1 to 40.9 MPa), for M37 mixtures which were synthesized using FA37 that had the highest calcium content (Fig. 5.4), while for M26 mixtures which were synthesized using a FA that had 30% lower calcium content than that used for M37 mixtures, curing at 131 to 185° F (55 to 85° C) for 24 to 48 hours produced the highest compressive strengths ranging from 5090 to 6520 psi (34.5 to 45.5 MPa).

Table 5.3: Summary of the Curing Temperatures and Periods Displayed Compressive Strength of 5000 psi or Higher.

Mixture	Period or Temp.	LA	HA	HS
M37	Temp. (^{o}C)	30-85	30-85	30, 40-55, 70-85,
M37	Period (hr)	24-48	24-48	48, 16-48, 8-48
M29	Temp. (^{o}C)	30, 40-85	30, 40-85	40-30, 55-85
M29	Period (hr)	48, 16-48	48, 16-48	48, 16-48
M26	Temp. (^{o}C)	55-85	55, 70-85	55, 70, 85
M26	Period (hr)	24-48	48, 24-48	48, 16-24, 4-48
M24	Temp. (^{o}C)	40, 55-85	40, 55, 70-85	55-85
M24	Period (hr)	48, 16-48	48, 24-48, 8-48	24-48
M21	Temp. (^{o}C)	40-55, 70-85	40-55, 70-85	70
M21	Period (hr)	24-48, 8-48	16-48, 8-48	48

The compressive strengths for HA mixtures (the middle column in Fig. 5.4) showed higher strengths compared to the corresponding LA mixtures (Table 5.3). Increasing the alkaline solution allowed higher strengths reached at relatively lower curing temperatures and/or shorter curing times. For example, the peak strength of HA M37 is 6740 psi (46.5 MPa) after 48 hours of curing at 86 to 185° F (30 to 85° C), while the peak strength for the corresponding LA mixture is 5925 psi (40.9 MPa) after 48 hours of curing at 86 to 185° F (30 to 85° C). Increasing the alkalinity triggers the occurrence different contradicting mechanisms. Increasing the surface hydroxylation which is proportional to the bulk concentration of hydroxyl ions (OH−) increases the dissolution rates of Si and Si-Al, and hence improves the geopolymerization process. However, increasing the alkaline content significantly increases the leaching rate of Ca that are available in the source FA and hence improves the hydration process [119]. However, the increased leached calcium ions hinder the geopolymerization process as explained earlier. Furthermore, the effects of increasing the alkaline were more prominent in the cases of FA with lower calcium content compared to those with FA having high calcium content. In the case of FA having low calcium content, the low level of calcium ions are dissolved and hence the

monomers and oligomeric of the silicate and aluminate will form geopolymer gel. Increasing the alkaline content in FAs having high calcium content leads to formation and precipitation of $Ca(OH)_2$ which reducing the alkalinity of the solution and hence hinder the geopolymerization process resulting in less increase in the strength at early age and high temperatures.

The compressive strengths for the HS mixtures (the right column in Fig. 5.4) which had a SS/SH of 2.0 while keeping the total alkaline activator the same as that of the LA mixtures, showed higher strengths compared to the corresponding LA mixtures for mixtures synthesized using high calcium FA while vice versa for low-calcium FA mixtures (Table 5.3). For example, the peak strength of M37 mix HS is 6410 psi (44.2 MPa) after 48 hours of curing at 86 to 185° F (30 to 85° C), and the peak strength for the corresponding LA mixture is 5925 psi (40.9 MPa) after 48 hours of curing at 86 to 185° F (30 to 85° C). However, the peak strength of M21 mix HS is 5300 psi (36.5 MPa) after 48 hours of curing at 158° F (70° C) while the peak strength for the corresponding LA mixture is 6295 psi (43.4 MPa) after 48 hours of curing at 158° F (70° C). This reduction in strength occurred for two interrelated reasons. 1) The LA mixture had lower SS and hence a higher pH than the HS mixtures. This higher pH led to higher dissolution of the FA and high geopolymer gel formation especially at high temperatures. 2) The difference in the extended chain conformation and its degree of polymerization in the two mixtures affect the geopolymerization formation with the LA mixtures having more favorable silicate conformations. Eighteen silicate conformations such as monomers, dimers, trimers, large rings, chain and cyclic trimers, and large rings generally coexist in silicate aqueous solution depending on the SS modulus [120]. An SS with modulus of one similar to that used in LA mixtures is typically richer in depolymerized lower-order species such as monomer and dimer which accelerate FA dissolution by reducing the reprecipitation of aluminosilicate gel particles onto the

FA surfaces as well as initiate the polycondensation of geopolymer gel. Furthermore, an SS with modulus of two similar to that used in HS mixtures is typically richer in more condensed and larger rings silicate species with few low-order uncondensed silicate monomers which reduce the speed of FA dissolution.

5.3.2.2 *Imitated hot weather (ambient Missouri summer)*

Fig. 5.5 shows the compressive strength results of the two hot weather imitating curing regimes. The figure shows that both curing regimes resulted in approximately equal 7 days compressive strengths for all M37 and M29 mixtures. However, the specimens subjected to a constant curing temperature of 86° F (30° C) displayed higher early strength up to approximately 4 days compared to those subjected to the imitated Missouri summer. Hence, the 7 days compressive strength of the different types of FA cured using the imitated Missouri summer week can be deduced from specimens cured at a constant temperature of 86° F (30° C) for a week.

As shown in Fig. 5.5, all mixtures but HA M21 displayed 7-day compressive strengths ranging from 5280 to 7305 psi (36.4 to 50.4 MPa). For the HA mixtures, the HA triggered the occurrence of different contradicting mechanisms. HA increases the dissolution rates of Si and Si-Al which improve the geopolymerization process, especially under high temperatures. Furthermore, increasing the alkaline content significantly increases the leaching rate of Ca that is available in the source FA and hence hinders the geopolymerization process and improves the hydration process [119]. For HA M21 and at imitated hot weather, the effects of these counter parameters cancel each other out, and the mixture developed a very low strength of approximately 23 psi.

(a)

(b)

147
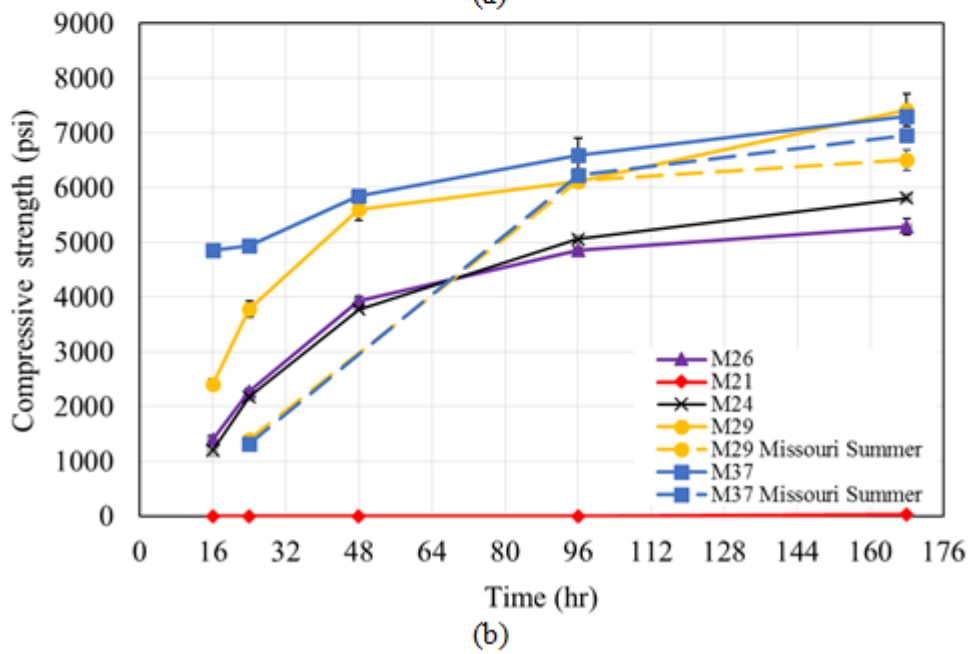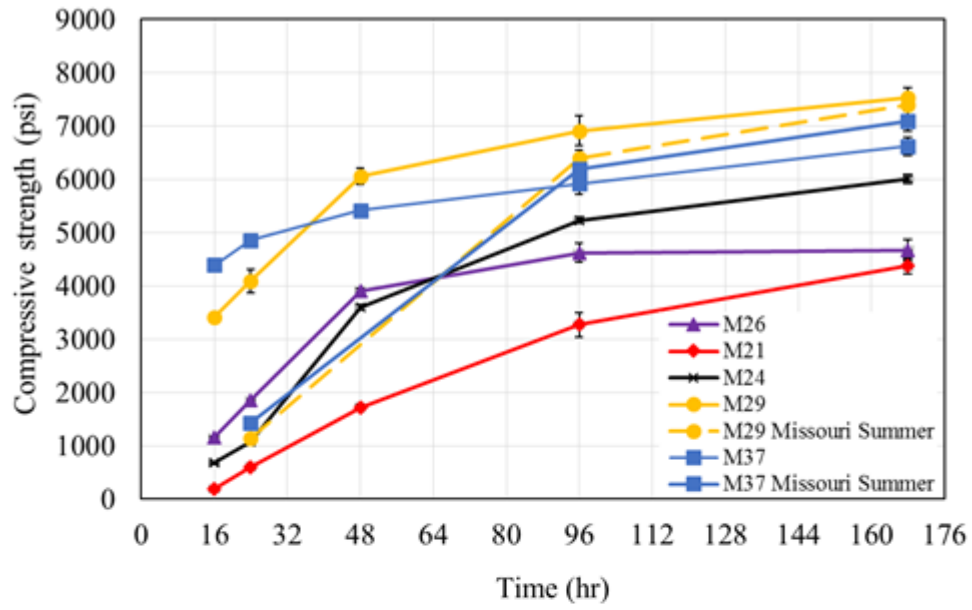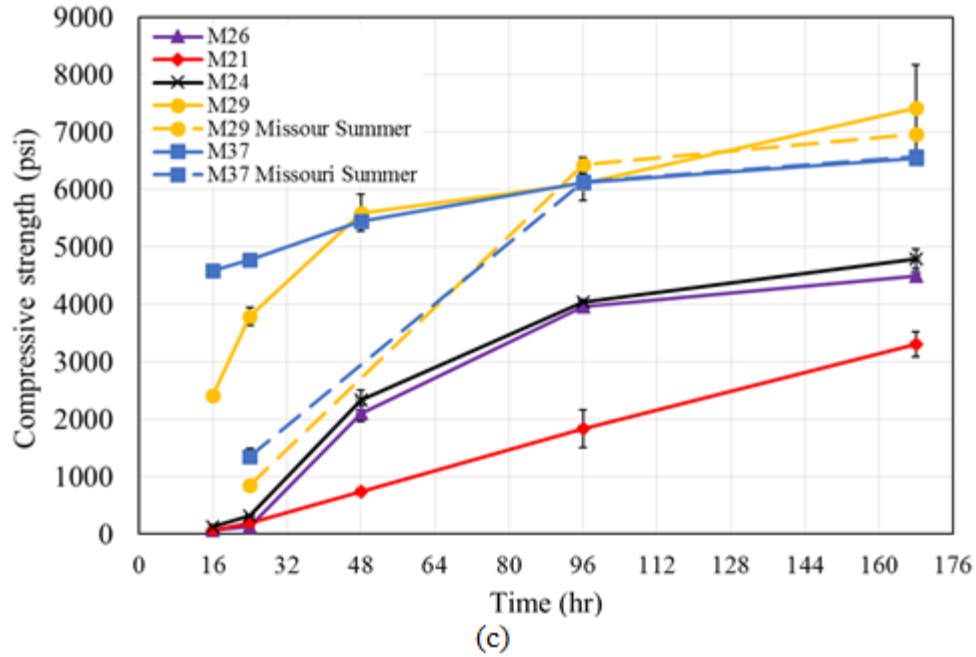
Figure 5.5: 7-day testing at 30˚C and Missouri summer conditions.

5.3.3 Energy consumption

The energy values consumed during the curing of each mixture at different temperatures and duration were recorded using a 270 kilowatt voltmeter. The recorded data can be used to find the most energy efficient curing regime for a given strength and geopolymer mixture. Therefore, for a given FA source a cost optimization can be carried out. Table 5.4 shows the energy consumption per temperature and duration. Figs. 5.6 through 5.10 show the compressive strength for FA37, FA29, FA26, FA24, and FA21, respectively, as a function of curing energy consumption. Furthermore, a correlation between the compressive strength and energy consumption is presented on each figure. The least square value (R^2) is also presented on each figure.

148

Table 5.4: Energy Consumption (kWhr).

Temp	4 hr	8 hr	16 hr	24 hr	48 hr
86 °F	2	4	8	12	24
104 °F	3	6	12	18	36
131 °F	6	12	24	36	72
158 °F	7	14	28	42	84
185 °F	10	20	40	60	120

As shown in Figs. 5.6 through 5.10, for ZC mortar synthesized using relatively higher calcium FAs such as FA37 and FA29, increasing the curing energy increased the compressive strength. However, this relationship is only valid until a relatively low energy of approximately 40 kWhr, beyond which increasing the curing energy does not significantly increase the strength. Furthermore, at low energy consumption, the mixtures displayed relatively high strength exceeding 3000 psi. Hence, FA37 and FA29 are the most energy efficient FAs. For ZC mortar synthesized using relatively low calcium FAs such as FA21, the compressive strength is more sensitive to the curing energy. At very low curing energy, the strength was quite low.
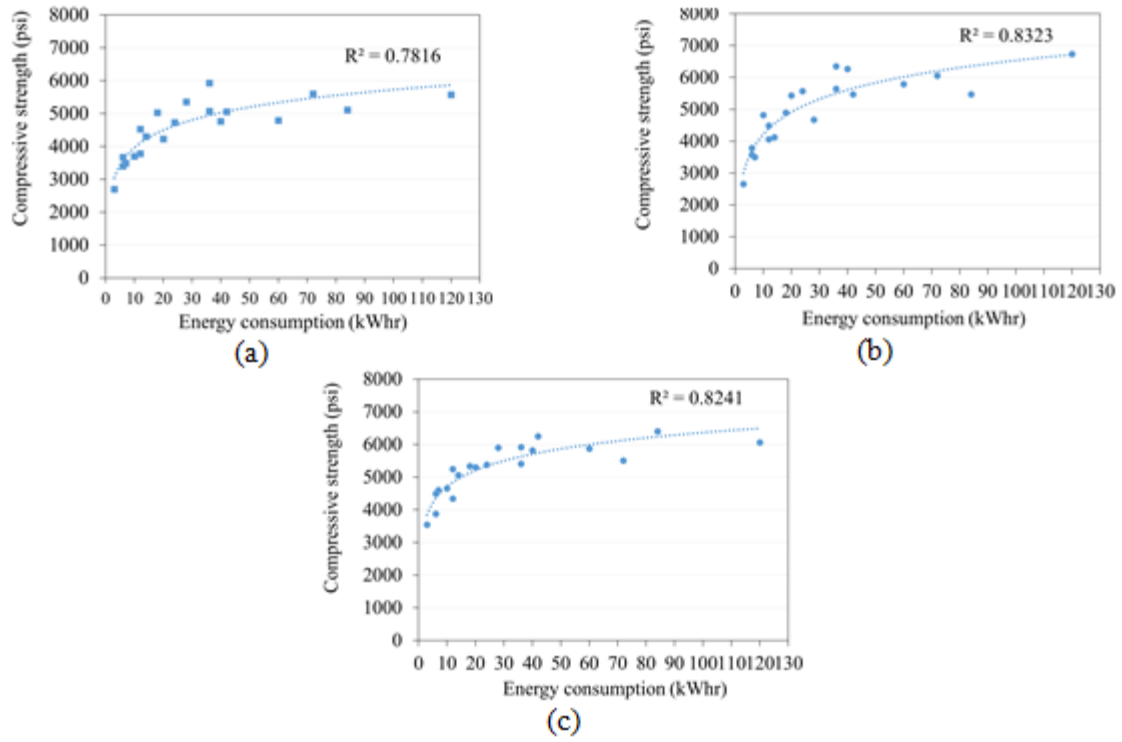
Figure 5.6: Compressive strength related to energy consumption, (a) M37-LA, (b) M37-HA, (c) M37-HS.
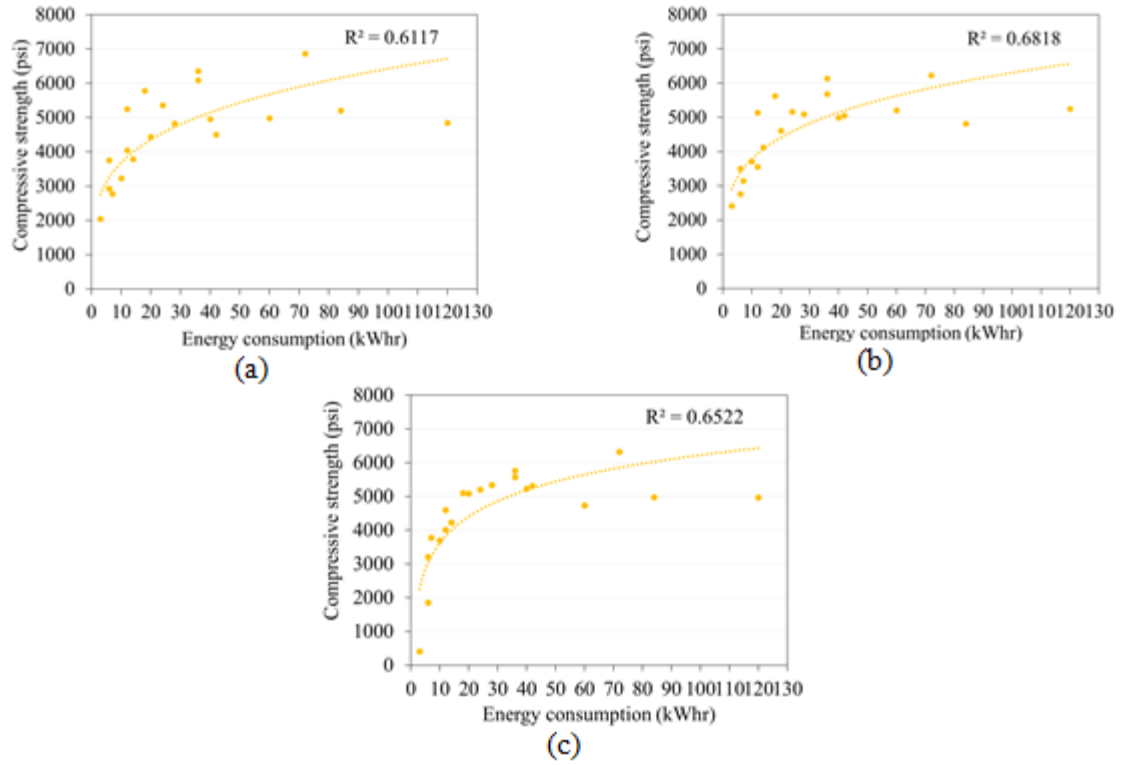
Figure 5.7: Compressive strength related to energy consumption, (a) M29-LA, (b) M29-HA, (c) M29-HS.
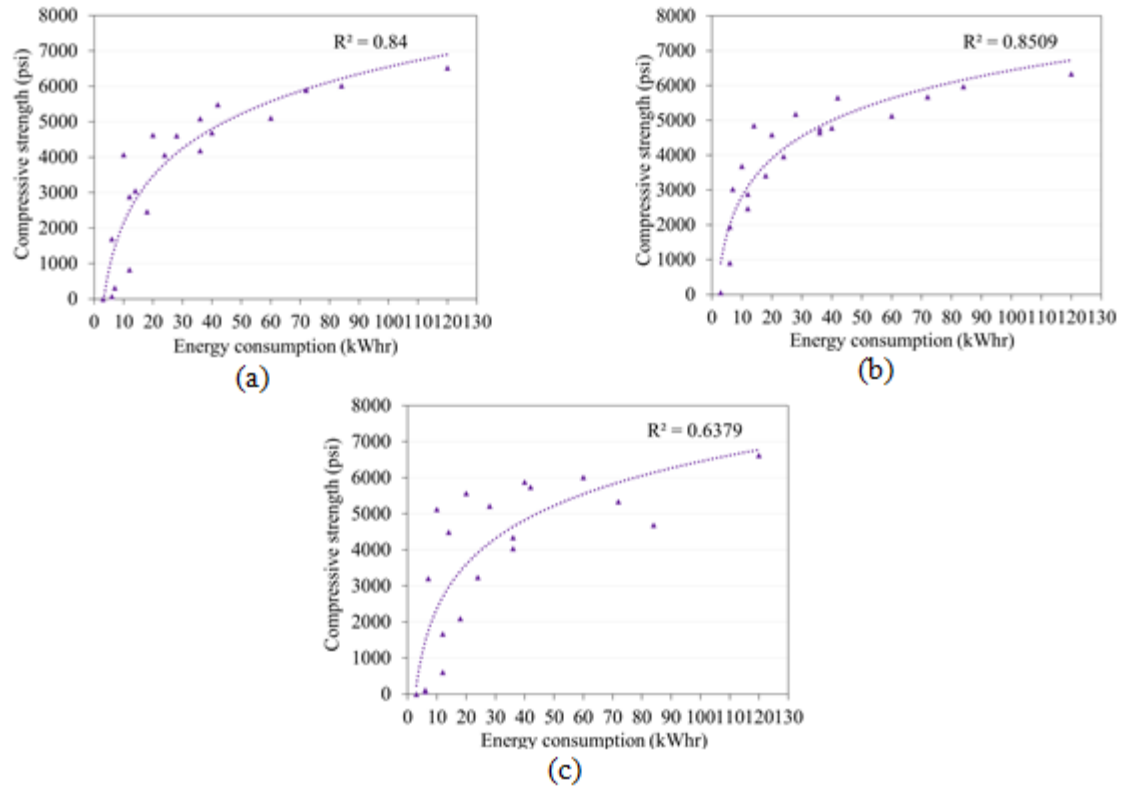
Figure 5.8: Compressive strength related to energy consumption, (a) M26-LA, (b) M26-HA, (c) M26-HS.
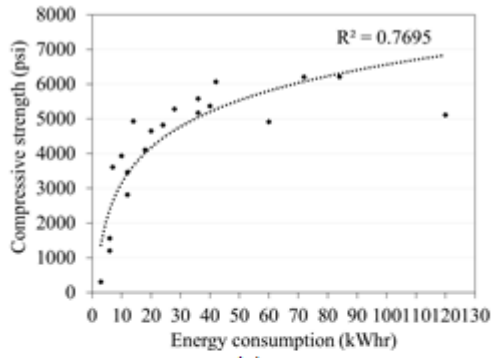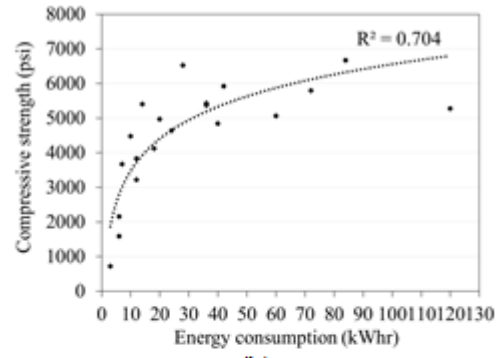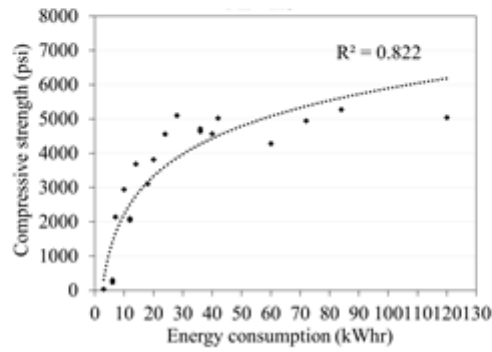
Figure 5.9: Compressive strength related to energy consumption, (a) M24-LA, (b) M24-HA, (c) M24-HS.
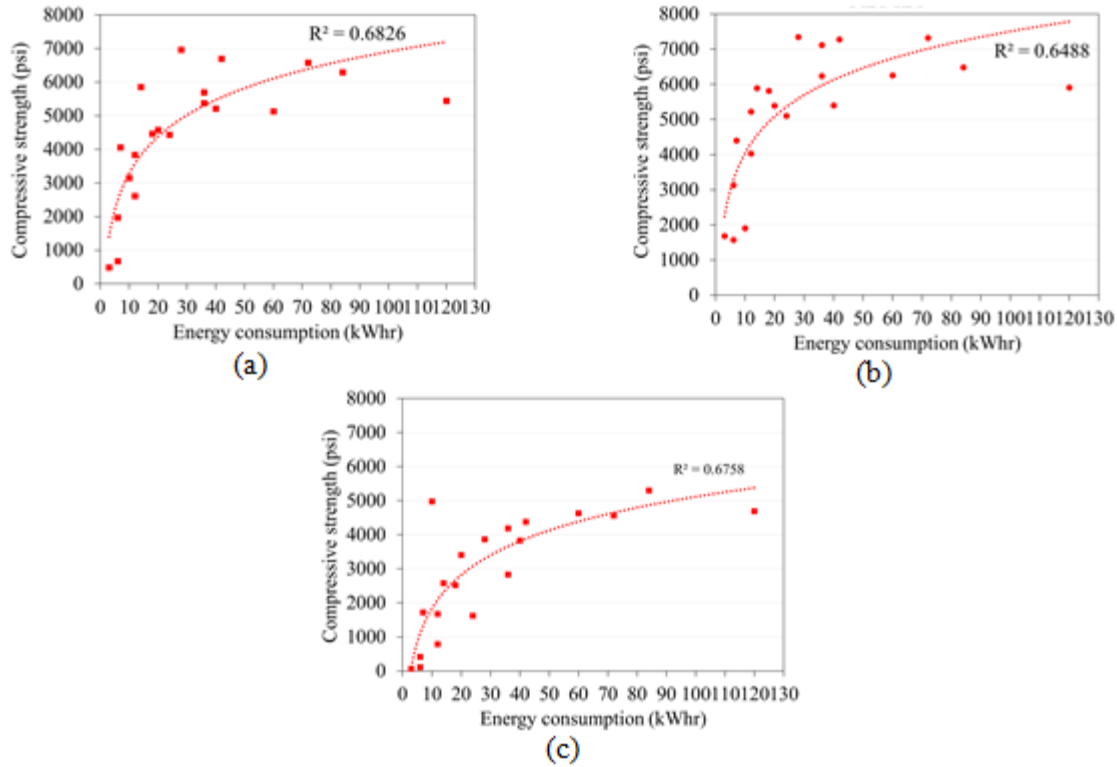
Figure 5.10: Compressive strength related to energy consumption, (a) M21-LA, (b) M21-HA, (c) M21-HS.

5.4 Findings and Conclusions

This chapter investigates the effects of different curing durations and temperatures on the strength of ZC mortar synthesized using five different types of FA. Furthermore, the effects of alkaline and silicate contents were investigated as well. Furthermore, two relatively hot weather curing regimes were investigated including an imitated Missouri summer using variable temperature (ramp type) and constant temperature. The energy consumption of each curing regime was calculated as well. Based on the investigated parameters, the following conclusions can be drawn:

- A given strength of ZC mortar can be produced using a given FA but different combinations of curing temperatures and durations. For ZC mortar synthesized using relatively high calcium content such a FA37 and FA29, a longer curing duration of approximately 24 to 48

154

hours is required in combination with curing temperatures of 86 to 185° F (30° C to 85° C) to achieve compressive strengths ranging from 3785 to 6740 psi (26.1 to 46.5 MPa). For ZC mortar synthesized using relatively lower calcium content such as FA21, a short curing duration of 16 hours is required in combination with a curing temperature of 158 to 185° F (70 to 85° C) to achieve a compressive strength ranging from 3825 to 7350 psi (26.4 to 50.7 MPa).

- Hot weather curing at 86° F (30° C) for 7 days (168 hours) or imitated Missouri summer week curing regimes were able to produce 7 days compressive strength ranging from approximately 3310 to 7530 psi (22.8 to 51.9 MPa) depending on the FA source and mixture used. Specimens prepared using FA37 and FA29, which had relatively higher calcium contents, showed the highest strengths at the hot weather curing indicating prominent hydration mechanisms.

- There was no significant difference in the 7-day compressive strength of specimens that were cured in a controlled environment at 86° F (30° C) and those cured at the imitated Missouri summer week where the curing temperature consisted of ramp up temperature from 72° F (22° C) to 97° F (36° C) over 12 hours followed by ramp down temperature from 97° F (36° C) to 72° F (22° C) over 12 hours. Hence, the variation in the temperature over nights in Missouri summer should not affect the strength of ZCC.

- There is a strong correlation between curing energy consumption and compressive strength. For a given mixture and sourced FA, there is an optimum amount of curing energy beyond which increasing the curing energy is not cost effective.

Chapter 6: Mechanical Properties and Drying Shrinkage of Zero-Cement Concrete

The mechanical properties of the optimized ZCC are presented in this chapter. The mixtures were subjected to three different curing regimes including oven, ambient, and moist curing. Then, the mechanical properties including the compressive strength, splitting tensile strength, modulus of rupture (flexural strength), and modulus of elasticity were investigated. As was concluded from Chapter 3, the best mixing procedure was no. 8, and it was used in this chapter. MoDOT Portland cement mixture B1, having a 28 day compressive strength of 5000 psi, was also investigated as a reference mixture.

6.1 Experimental Details

6.1.1 Materials

The five sourced FAs, FA37, FA29, FA26, FA24, and FA21, out of the second batch as discussed in Chapter 2 were used to prepare the ZCC mixtures presented in this chapter.

6.1.2 Packing density test

In order to optimize and maximize the compactness of the ratio between the coarse and fine aggregates that were used in the concrete mixtures, a gyratory compaction (Fig. 6.1) test was carried out. The gyratory compaction technique consists of a cylindrical mold with the simultaneous action (force) of a vertical axial static pressure and a shear force resulting from the rotation of the mold on its inclined axis. Many trials were carried out to optimize the suitable pressure to make sure that the aggregate will not be crushed under the loading pressure and the particle size distribution of the aggregates did not change. Finally, a pressure of 1.50 bar was selected to be applied to the material. The machine cylindrical mold height was 4 in. The gyrator

angle was 2.3°. The working speed was 60 rpm. A 5732 lb sample of each of the coarse aggregate and sand were dried in the oven and placed inside the cylindrical mold.
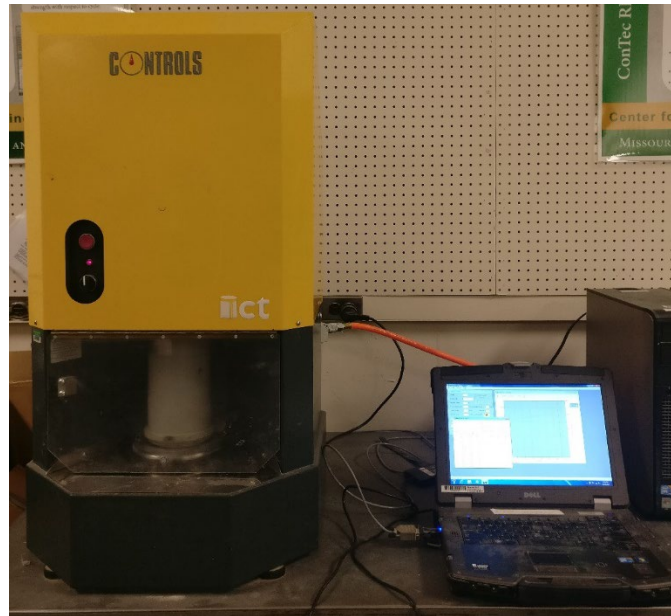
Figure 6.1: Gyratory compaction machine.

Five different aggregate combinations, including 40% to 60% coarse aggregate and from 60% to 40% sand, were tested (Table 6.1). Three different cycles of gyration of 256, 356, and 450 cycles were applied to each aggregate combination to obtain the maximum possible density of the aggregate sample.

Fig. 6.2 shows the results of the packing density test for the different aggregate combinations and different number of gyration cycles. As shown in Fig. 6.2 from the first two cycles of 256 and 356, the two aggregate combinations of 60/40 and 55/45 displayed the highest density. Hence, the third number of cycles of 450 was applied to those two aggregate combinations to select one of them for the concrete mixtures. The results revealed that the highest compaction density was achieved at aggregate combinations of 55/45. Therefore, that ratio was used for the concrete mixtures.

Table 6.1: Gyratory Compaction Test Results.

Trial No.	Coarse agg. (percentage)	Sand (percentage)	Coarse agg. (weight in lb)	Sand (weight in lb)	256 cycles (density in lb/ft^3)	356 cycles (density in lb/ft^3)	450 cycles (density in lb/ft^3)
1	40	60	2.29	3.44	122.0	124.3	-
2	45	55	2.58	3.15	126.9	125.2	-
3	50	50	2.87	2.87	125.0	127.2	-
4	55	45	3.15	2.58	126.2	128.2	129.4
5	60	40	3.44	2.29	127.4	128.2	128.8
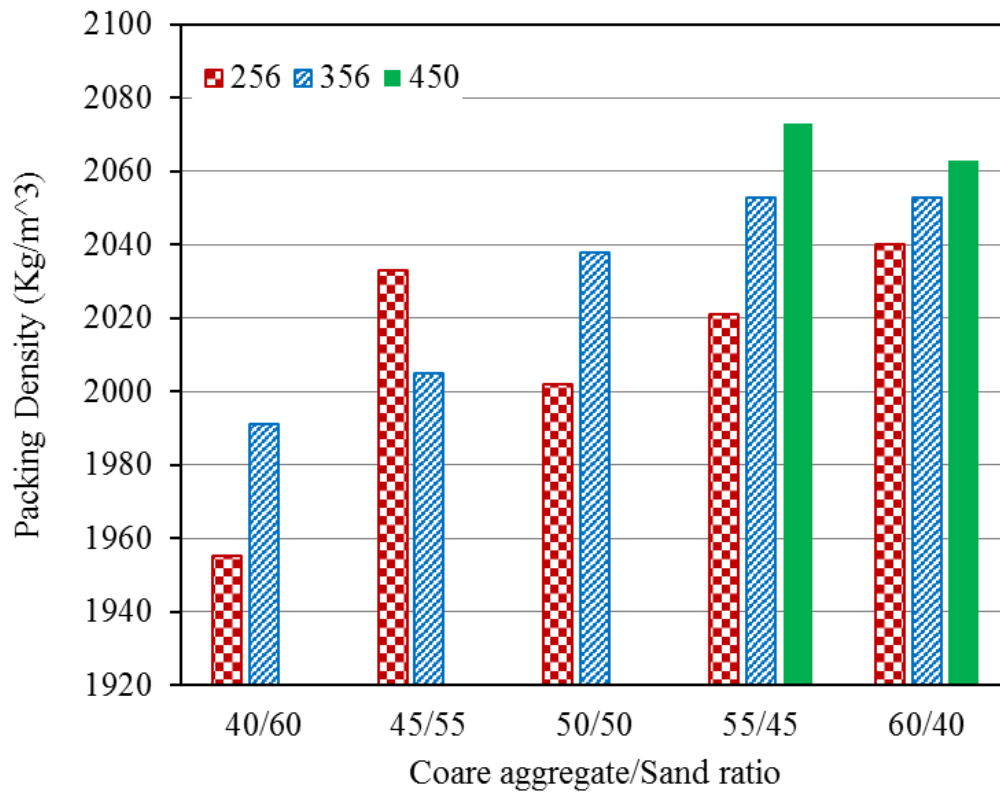
Figure 6.2: Packing density results.

6.1.3 Specimen preparation

The optimum Alk/FA, and SS/SH in ZCC were 0.30 and 1.0 as presented in Chapter 4, respectively, and they were used in the mixture investigated throughout this chapter. One mixture for each FA was prepared (Table 6.2) and their mechanical properties were determined

158

during this research. The mixtures were designed to have a target slump value of 6 – 8 in (150 – 200 mm). The W/FA was selected as either 0.34, 0.35, or 0.38, depending on the sourced FA. The two main factors that affect the required W/FA were the calcium content of the FAs and the surface area of the FAs. Both FA37, which had the highest calcium content, and FA26, which had third-highest calcium content, had W/FA of 0.35. FA29 had the second-highest calcium content combined with the highest surface area which required higher water content to improve the workability, and hence a W/FA of 0.38 was used in that mixture. The other two FAs had a slightly lower W/FA of 0.34 due to their lower calcium content. In all mixtures, the Alk/FA remained constant at 0.30 and SS/SH remained constant at 1.0.

The nomenclatures of the ZCC mixtures start with the letter "C" for a concrete followed by the calcium content percentage of the FA that was used in that concrete mixture. For example, C37 is a zero-cement concrete synthesized using a FA having a calcium content of 37%.

A MoDOT conventional concrete, i.e., ordinary Portland cement concrete mixture (B1) denoted hereafter as CC, was prepared as a reference (Table 6.2) to compare its performance with that of the five ZCC mixtures. The target slump of the CC mixture was 6 in. A water to cement ratio (W/C) of 0.54 was selected for the CC mixture to achieve a target slump of approximately 6 in.

Table 6.2: Mix Design of the ZCC and CC Mixtures (lb/ft^3).

Mix	W/FA	Alk/FA	SS/SH	W/C	C.A[a]	Sand	FA	S.S.	S.H.	W	C
C21	0.340	0.30	1	-	60.7	50.6	28.1	4.21	4.21	4.89	-
C24	0.340	0.30	1	-	60.7	50.6	28.1	4.21	4.21	4.89	-
C26	0.350	0.30	1	-	59.9	49.9	28.1	4.21	4.21	5.17	-
C29	0.380	0.30	1	-	59.0	49.2	28.1	4.21	4.21	6.01	-
C37	0.350	0.30	1	-	59.9	49.9	28.1	4.21	4.21	5.17	-
CC	-	-	-	0.540	67.9	56.6	-	-	-	10.9	19.2

[a]CA: coarse aggregate

6.1.4 Mixing procedures

A gravity mixture having a capacity of 9 ft^3 was used in mixing all mixtures (Fig. 6.3). The mixing procedure of the CC mixture per ASTM C192-16 [104], started with mixing the coarse aggregate with some of the mixing water in the mixer. Then, the sand, cement, and the rest of the mixing water were added while the mixer was running. After adding all ingredients into the mixer, it was run for three minutes followed by a three minute rest time, followed by two minutes final mixing.

Figure 6.3: ZCC mixing (a) Adding the materials to the mixer, (b) mixing process, (c) pouring the concrete, and (d) concrete ready for casting.

6.1.5 Specimen casting

The slump (Fig. 6.4), unit weight, air content (Fig. 6.5), and temperature of the each concrete mixture were determined according to ASTM C143-15 [103], ASTM C138-16 [121], ASTM C231-14 [122], and ASTM C1064 [123], respectively.
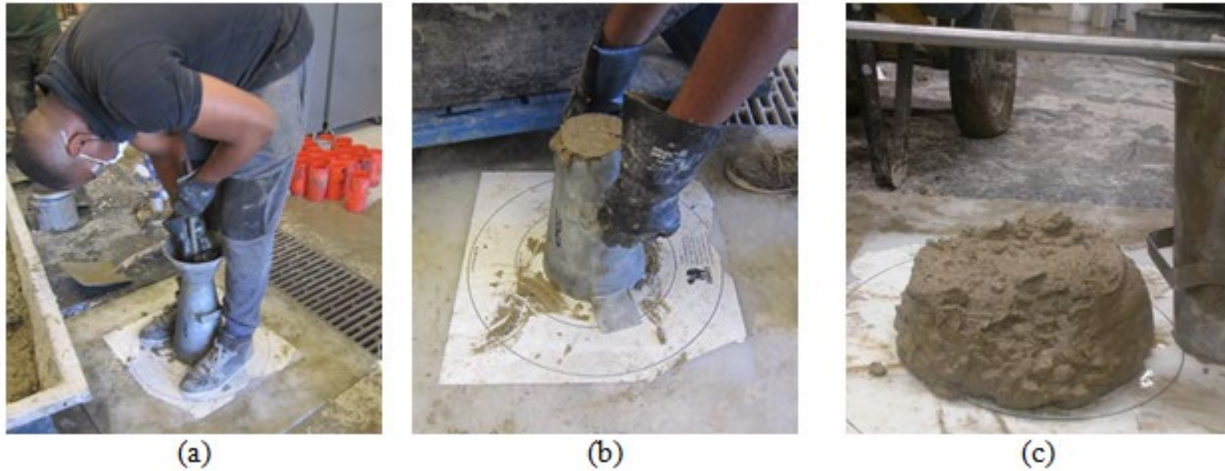
Figure 6.4: Slump test of ZCC: (a) filling the slump cone, (b) before moving the cone vertically, and (c) the slump.
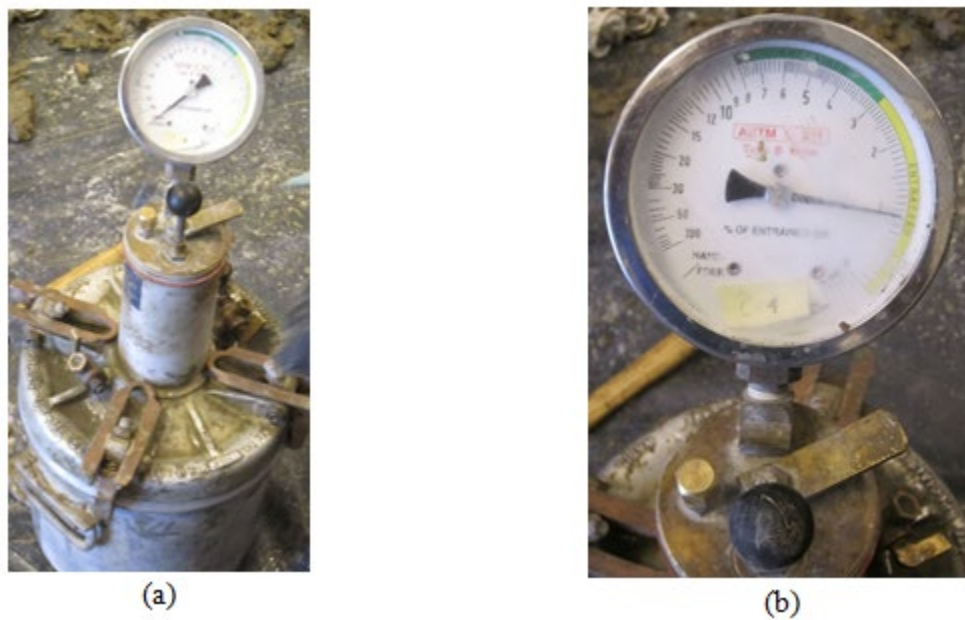
Figure 6.5: Air content test (a) before, and (b) after testing.

The fresh concrete was cast in 4 x 8 in plastic cylinders (Fig. 6.6), 3 x 3 x 11.25 in prisms, 3 x 3 x 16 in prisms (Fig. 6.7), and 6 x 6 x 24 in beams (Fig. 6.8) according to ASTM C192-16 [104]. After casting the cylinders, prisms, and beams (Fig. 6.9 and Fig. 6.10), they were encased in oven bags to prevent moisture loss during the curing period.

162

Figure 6.6: Casting 4 x 8 in cylinders.
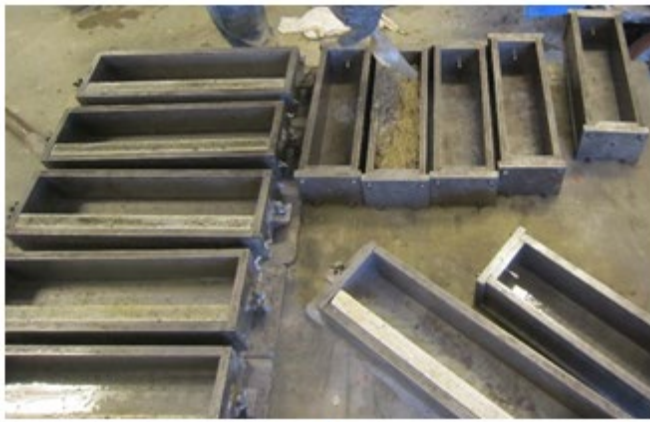
Figure 6.7: Casting 3 x 3 x 11.25 in and 3 x 3 x 16 in prisms (a) before casting and (b) surfacing the prisms.
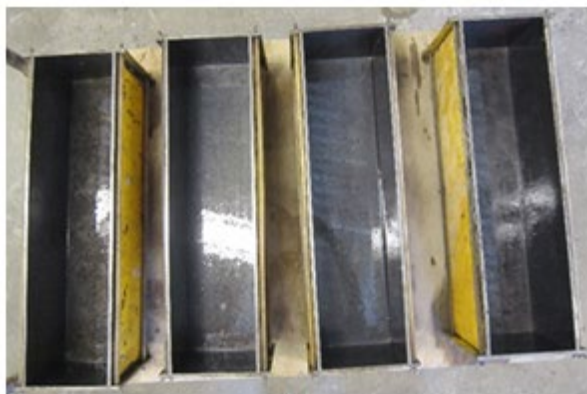
Figure 6.8: Casting 6 x 6 x 24 in beams (a) molds before casting, (b) during casting, and (c) surfacing the beams.
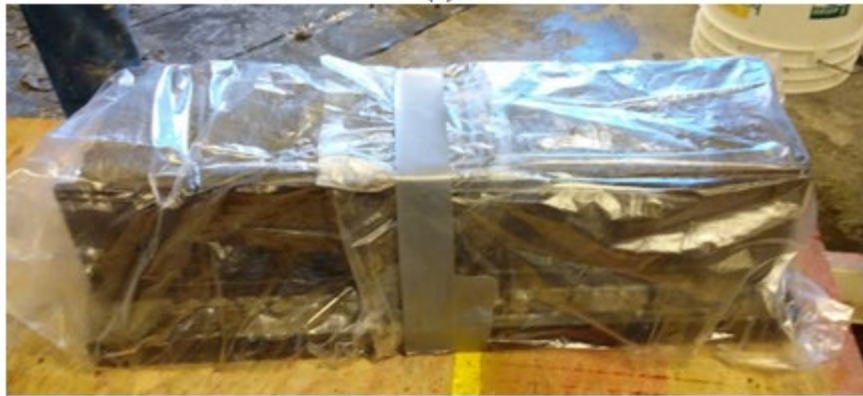
Figure 6.9: (a) During, and (b) after encasing the beams in oven bags.
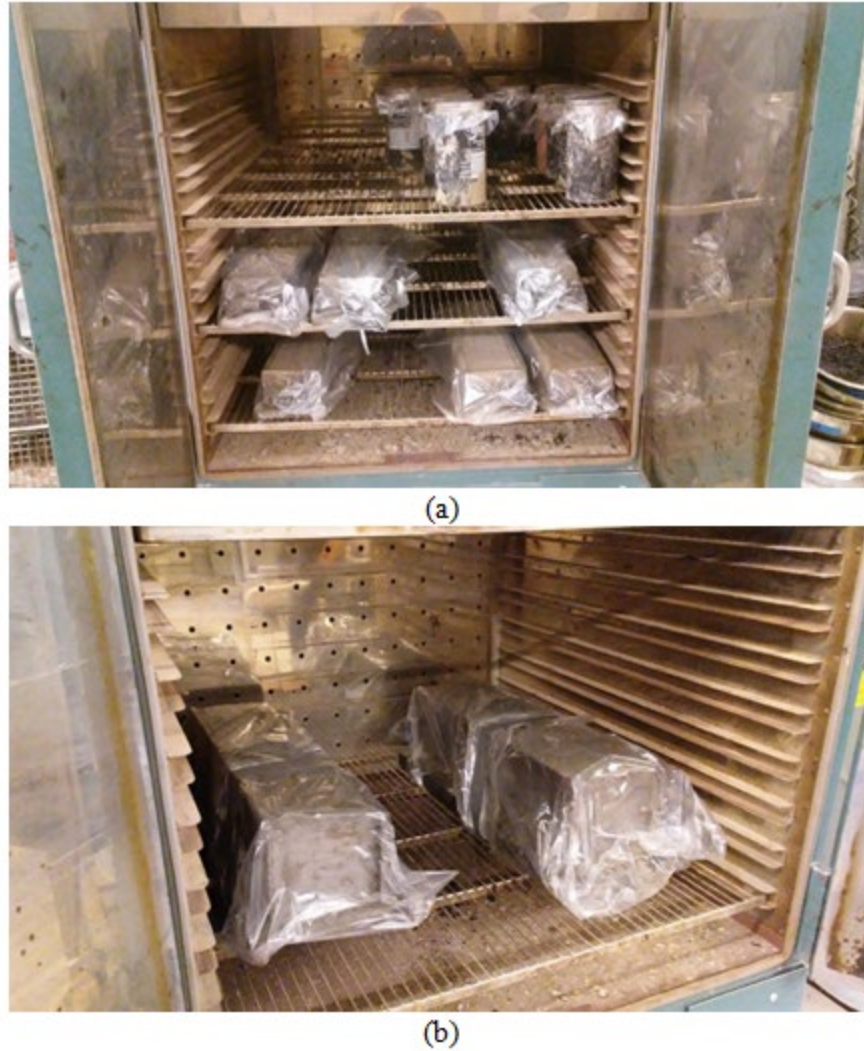
Figure 6.10: Placing the specimens in the ovens (a) cylinders and prisms, and (b) beams in oven bags.

6.1.6 Specimen curing

Three curing regimes were applied to the ZCC specimens in this study to investigate the effect of the different curing regimes on the mechanical properties. The first regime included an oven curing regime where the specimens were encased in oven bags and placed in an electrical oven at 158° F (70° C) for 24 hours. The specimens were placed in the oven after two hours rest time. After getting the specimens out of the oven, the specimens were demolded for at least 1 hour to let them cool down and avoid the sudden change in the temperature between the oven and the

ambient temperature. Thereafter the specimens were encased in plastic bags and stored in the laboratory at a temperature of 73 ± 3° F (23 ± 2° C) until the testing day.

The second curing regime included an ambient curing regime where the specimens were placed in the laboratory at the room temperature of 73 ± 3° F (23 ± 2° C). After demolding the specimens, the specimens were encased in sealed plastic bags to prevent the evaporation of the water until the testing day. The third curing regime included moist curing where the specimens were placed in the moisture room at a temperature of 73 ± 3° F ($23 \pm 2°$ C) and relative humidity of $95 \pm 5\%$ immediately after demolding the specimens until the testing day. The ambient and moist-cured specimens were demolded at two days from the casting day.

6.1.7 Mechanical properties determination

The concrete cylinders were tested to determine the compressive strength (Fig. 6.11a) per ASTM C39-17 [124], elastic modulus (Fig. 6.11b) per ASTM C496-11 [125], and splitting tensile strength (Fig. 6.12) per ASTM C469-14 [126], while the beams were tested to determine the flexural strength (Fig. 6.13) per ASTM C78-16 [127]. The compressive strengths were determined at ages of 1, 7, and 28 days for the oven-, ambient-, and moist-cured specimens. The other properties were determined at ages of 1 and 28 days for oven-cured and ages of 7 and 28 days for moist-cured specimens, including those prepared using the CC mixture.

Figure 6.11: Hardened concrete testing (a) compression, and (b) elastic modulus tests.
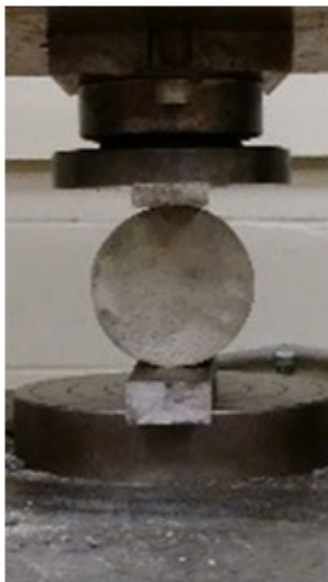
Figure 6.12: Splitting tensile testing (a) before, and (b) after splitting tensile testing.
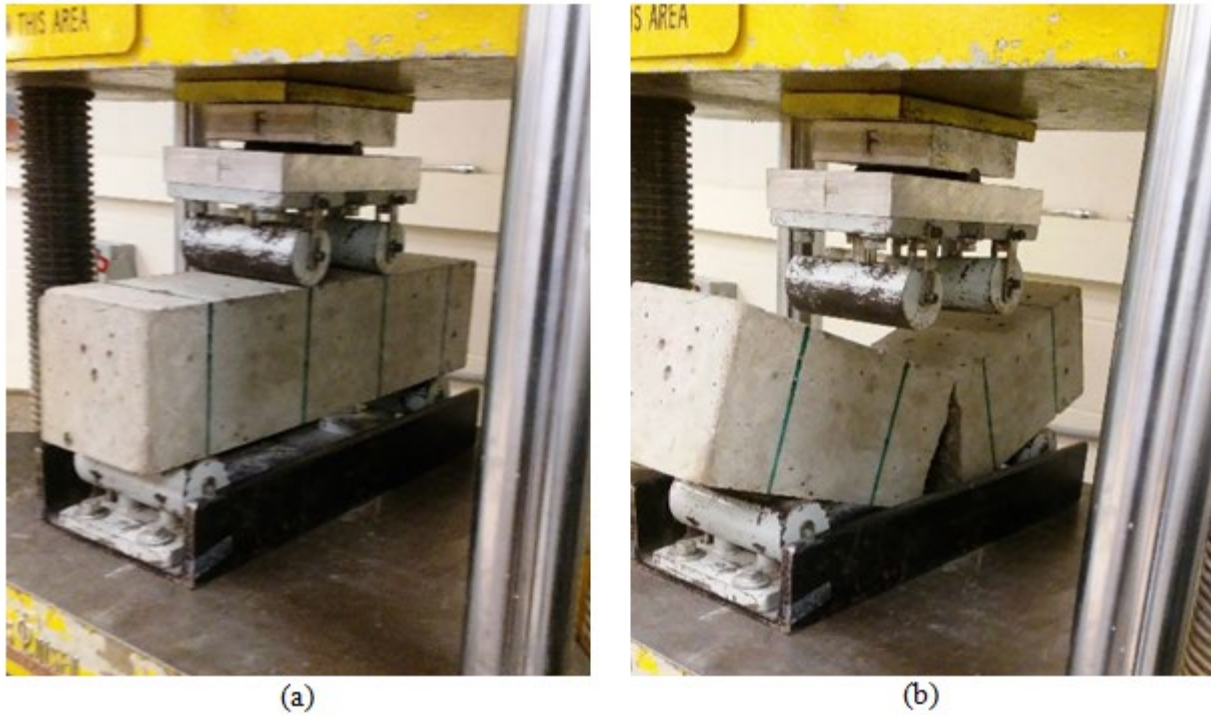
Figure 6.13: Modulus of rupture (flexural) testing (a) before, and (b) after modulus of rupture (flexural) testing.

6.1.8 Drying shrinkage determination

The drying shrinkage tests were carried out on 3 x 3 x 11.25 in concrete prisms per ASTM C157-17 [128]. The specimens were demolded at the ages of 24 hours and two days for the oven- and ambient-cured, respectively. Then, the prisms were placed in lime-saturated water for one hour. The lengths of the prisms were measured as the reference lengths.

ASTM C157-17 requires a specific curing regime including placing the demolded specimens in lime-saturated water until the specimens reach the age of 28 days; then the drying shrinkage testing started. However, ASTM does not include a procedure for oven-cured specimens. Hence, two curing regimes were carried out during this task for the ZCC specimens. First, for the moist-cured specimens, the demolded specimens were cured in the lime-saturated water at the room temperature of $73 \pm 3^{\circ}$ F ($23 \pm 2^{\circ}$ C) for 28 days (Fig 6.14); then, the drying shrinkage test

started. Second, for the oven-cured specimens, after curing the specimens in the oven for 24 hours, they were demolded, then either the shrinkage test started or they were stored in the lime-saturated water at the room temperature of 73 ± 3° F (23 ± 2° C) for a further 28 days (Fig 6.14) before the drying shrinkage test started. Curing and testing the CC specimens followed the first method.

After curing the prisms, they were placed in a room having a temperature of 70° F (21° C) and a relative humidity of 50% (Fig. 6.15). The lengths of the prisms were measured at 1, 4, 7, 14, and 28 days, and 8, 16, and 32 weeks.

Figure 6.14: Curing the ZCC in a lime-water tank.
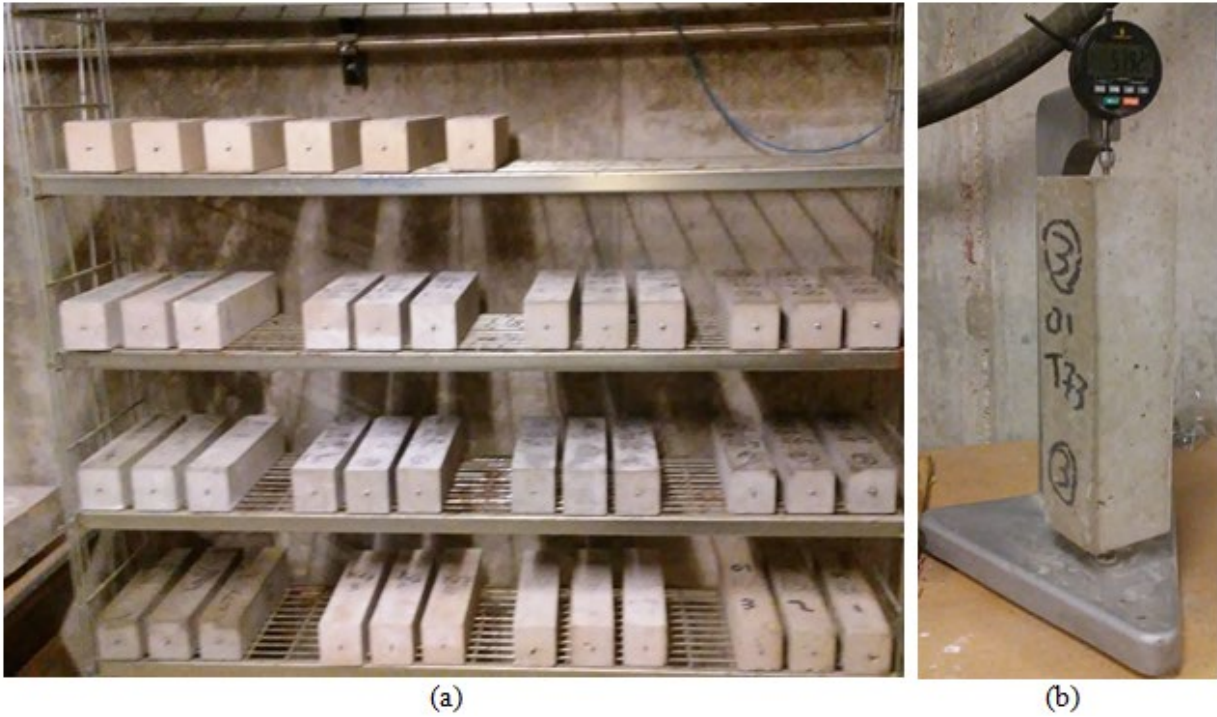
Figure 6.15: Drying shrinkage (a) storing and (b) testing the prisms of the ZCC and CC mixtures.

6.2 Results and Discussion

6.2.1 Fresh properties

Table 6.3 summarizes the results of the fresh properties of the different concrete mixtures. As shown in the table, the relative density of all the mixtures ranged from 150.5 lb/ft^3 to 154.2 lb/ft^3 which was about 2.6% to 5.1% more dense than the CC mixture. The air content of the CC mixture was the highest among the six mixtures, reaching 2% while it ranged from 1.0% to 1.9% for the ZCC. The temperature of the six mixtures was almost the same as the room temperature.

Fig. 6.16 shows the slump of the concrete mixtures. As shown in the figure, the slump of the ZCC ranged from 7 in to 8 in (175 to 200 mm). The CC displayed the lowest slump value of 6.5 in (162.5 mm) among all the mixtures despite having the highest W/C of 0.54. For the ZCC, for a given W/FA, the calcium content is inversely proportional to the slump value. For example, for

W/FA of 0.35, the slump of C37 was smaller than that of C26. Similarity, for W/FA of 0.34, the slump of C24 was smaller than that of C21.

Additional nucleation sites for precipitation of the FA dissolved species are created with higher calcium content, which accelerated the hardening process of the ZCC [129, 130]. Moreover, the reaction of the water and calcium in the presence of silica and alumina forms calcium silicate hydrate (CSH) and/or calcium aluminate silicate hydrate (CASH) faster than the relatively slower geopolymerization process of the FA [63]. Furthermore, the rapid formation of CSH and/or CASH resulted in low workability. In addition, the consumption of water in the formation of CSH and/or CASH also reduces the free water in the mixture thereby reducing the workability [59].

Although mixture C29 had the second-highest calcium content, mixture C29 required the highest W/FA of 0.38 to achieve a showed slump value of 7 in, which was the lowest among the ZCC mixtures. That occurred since FA29 had the highest surface area among the five FAs. It had approximately 60% higher surface area than the average of the other four FAs.

Table 6.3: Fresh Properties of the Different Concrete Mixtures.

	C37	C29	C26	C24	C21	CC
Relative Density (lb/ft^3)	154.2	153.6	150.5	152.3	153.6	146.7
Air content (%)	1.00	1.10	1.90	1.50	1.30	2.00
Temperature (^{o}F)	74	70	72	73	74	71
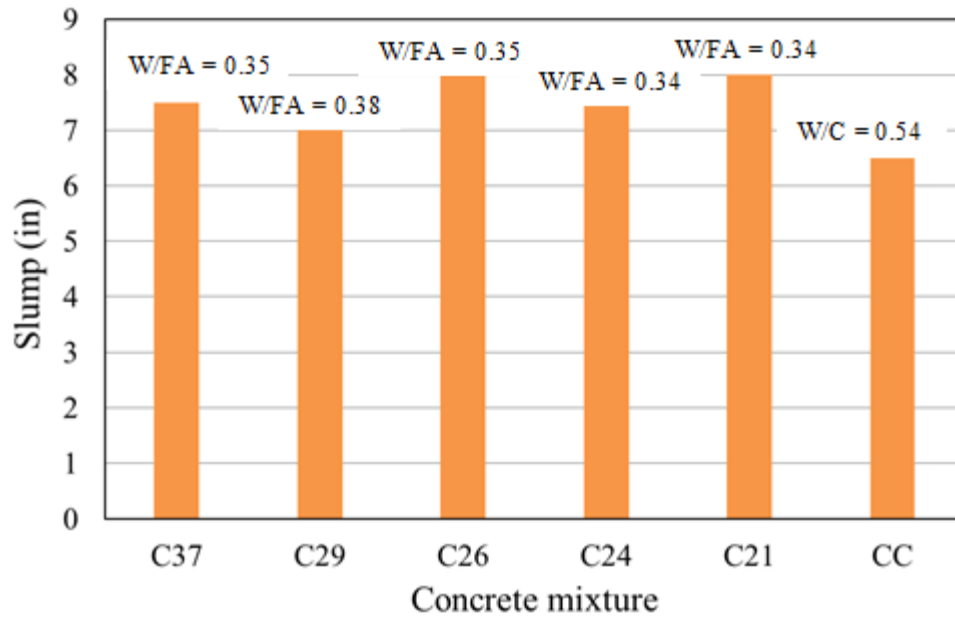
Figure 6.16: Slump of the different concrete mixtures.

6.2.2 Mechanical properties

6.2.2.1 Compressive strength

The compressive strengths of the different concrete mixtures at 1, 7, and 28 days are shown in Figs. 6.17, 6.18, and 6.19 for the oven-, ambient-, and moist-cured specimens, respectively. Although the CC mixture was moist cured, its compressive strength was presented as a reference with the three curing regimes of the ZCC. The compressive strengths of all ZCC mixtures were higher than that of the CC mixture cured in the moisture room for 28 days (Figs. 6.17 through 6.19).
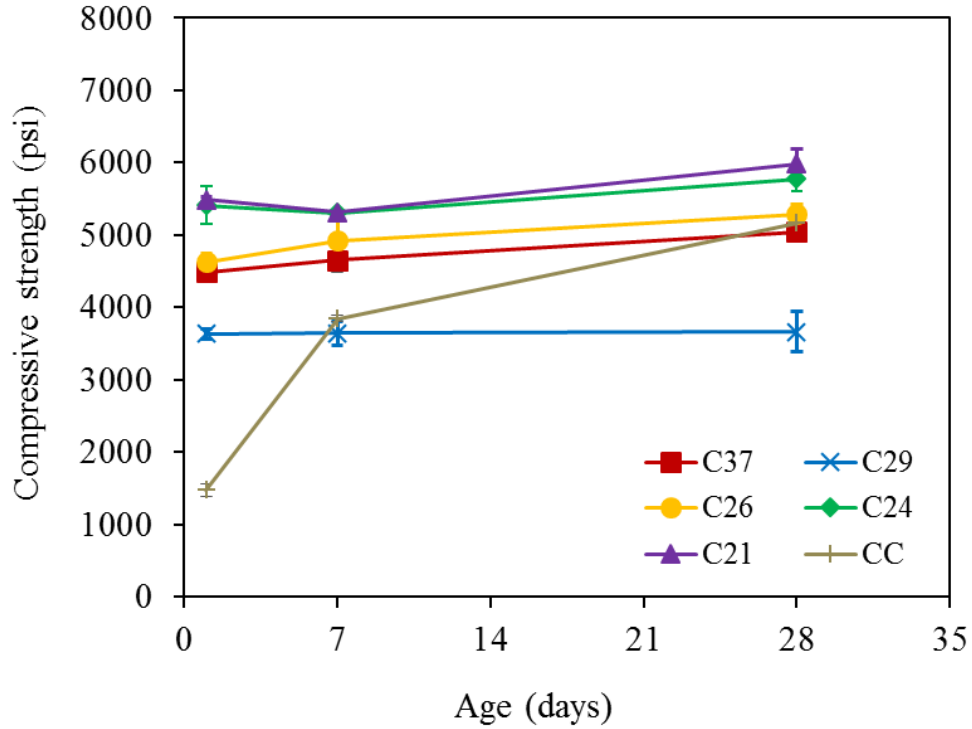
Figure 6.17: The compressive strength of the oven-cured specimens at different ages. (Note: the CC mixture was moist cured).

As shown in Fig. 6.17, at the ages of 24 hours, the compressive strengths of the oven-cured specimens ranged from 3640 psi (25.1 MPa) to 5490 psi (37.8 MPa) depending on the calcium content of the FA and its surface area. Thereafter, the compressive strength slightly increased and ranged from 3660 psi (25.2 MPa) to 5990 psi (41.28 MPa) at 28 days. The oven-cured specimens showed a slight improvement in the compressive strength with time because the majority of the reaction took place in the first 24 hours.
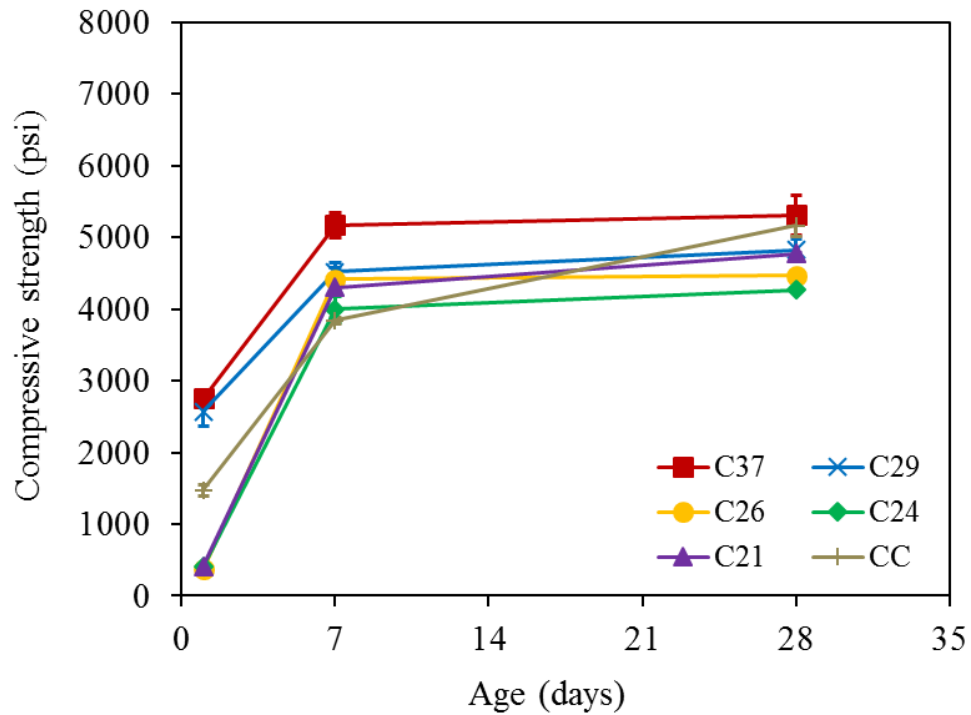
Figure 6.18: The compressive strength of the ambient-cured specimens at different ages. (Note: the CC mixture was moist cured).
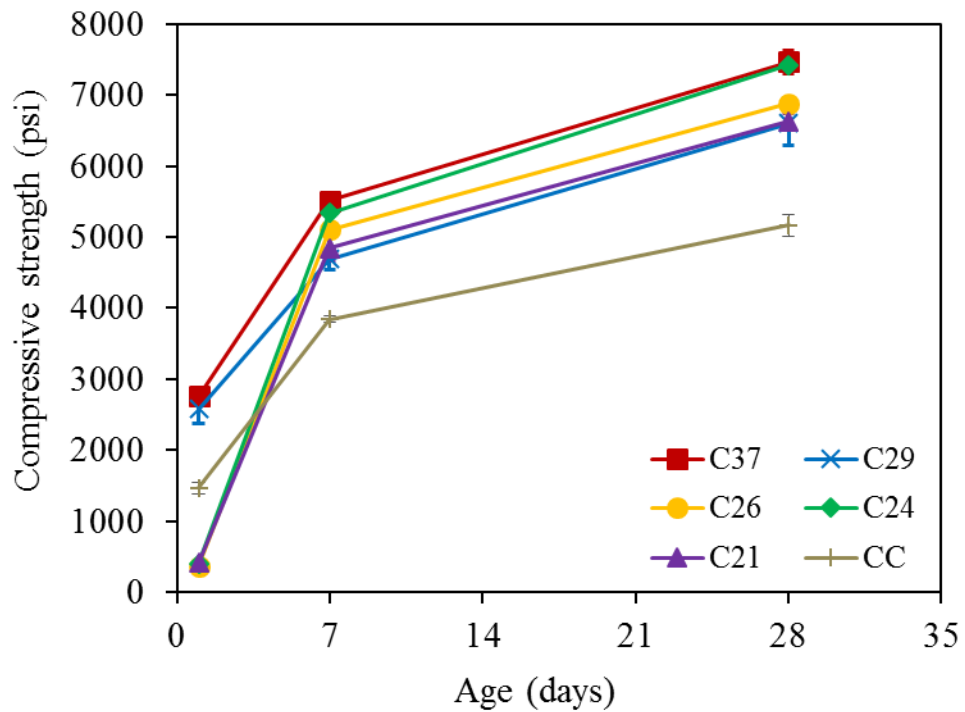
Figure 6.19: The compressive strength of the moist-cured specimens at different ages.

175

Figs. 6.18 and 6.19 show the compressive strength of the ambient- and moist-cured specimens. For all five ZCC mixtures, Figs. 6.18 and 6.19 showed a development in the strength with time from 1 day to 7 days for the ambient-cured specimens and from 1 to 28 days for the moist-cured specimens. The compressive strengths of the ambient-cured specimens ranged from 3995 psi (27.6 MPa) to 5170 psi (35.7 MPa) at the age of 7 days, depending on the calcium content and surface area. The compressive strength increased and ranged from 4270 psi (29.4 MPa) to 5310 psi (36.6 MPa) at the age of 28 days. Furthermore, the compressive strengths of the moist-cured specimens ranged from 4840 psi (33.4 MPa) to 5510 psi (38.0 MPa), depending on the calcium content and surface area. The compressive strength increased and ranged from 6630 psi (45.5 MPa) to 7465 psi (51.5 MPa) at the age of 28 days.

6.2.2.2 *Effect of calcium content of the fly ash on the compressive strength of ZCC*

The compressive strength of the different concrete mixtures with the different calcium content of the FAs are shown in Figs. 6.20, 6.21, and 6.22 for the oven-, ambient-, and moist-cured specimens, respectively. The availability of calcium, silica, and alumina contents plays an important role in the behavior of ZCC mixtures. The possible phases that form in the ZCC mixtures synthesized using high calcium FA are CSH, CASH, and sodium aluminate silicate hydrate (N-A-S-H) due to two different mechanisms, namely hydration and geopolymerization [131]. Calcium, silica, and alumina in FA can hydrate in ambient temperature forming CSH and/or CASH. However, when alkali solution is added to FA in the existence of elevated temperature a geopolymerization process takes place forming networks of mineral molecules connected by covalent bonds [45, 132]. When increasing the silica and alumina content in a FA and using oven curing, the compressive strength of the ZCC is the dominant geopolymerization mechanism. However, the presence of calcium interferes in the geopolymerization process

176

reducing the compressive strength of the ZCC. In the case of ambient curing, high calcium content was hydrated and resulted in high compressive strength.
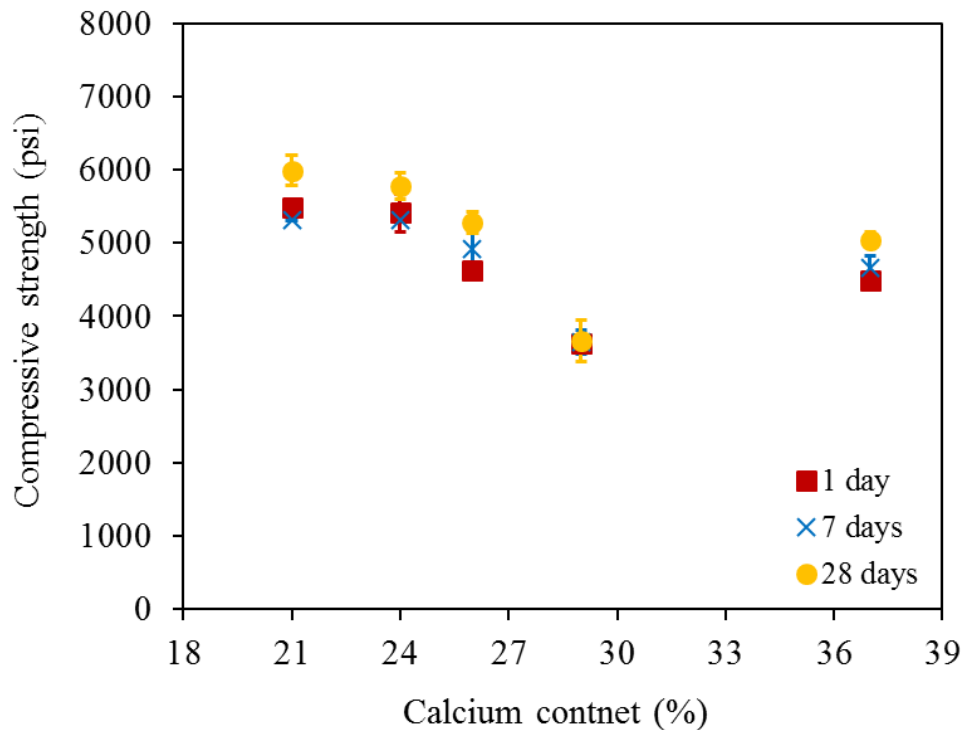
Figure 6.20: The compressive strength of the oven-cured specimens with the calcium content.

For oven-cured specimens, C21, which had the lowest calcium content, displayed the highest compressive strength while C29, which had the second-highest calcium content, showed the lowest compressive strength (Fig. 6.20). Even though C37 had a higher calcium content than C29, the oven compressive strength of C29 is lower than C37 due to the high surface area of C29. The high surface area required more W/FA to be added to enhance the workability and prevent the flash setting, which resulted in the lowest oven compressive strength among the five ZCC mixtures.
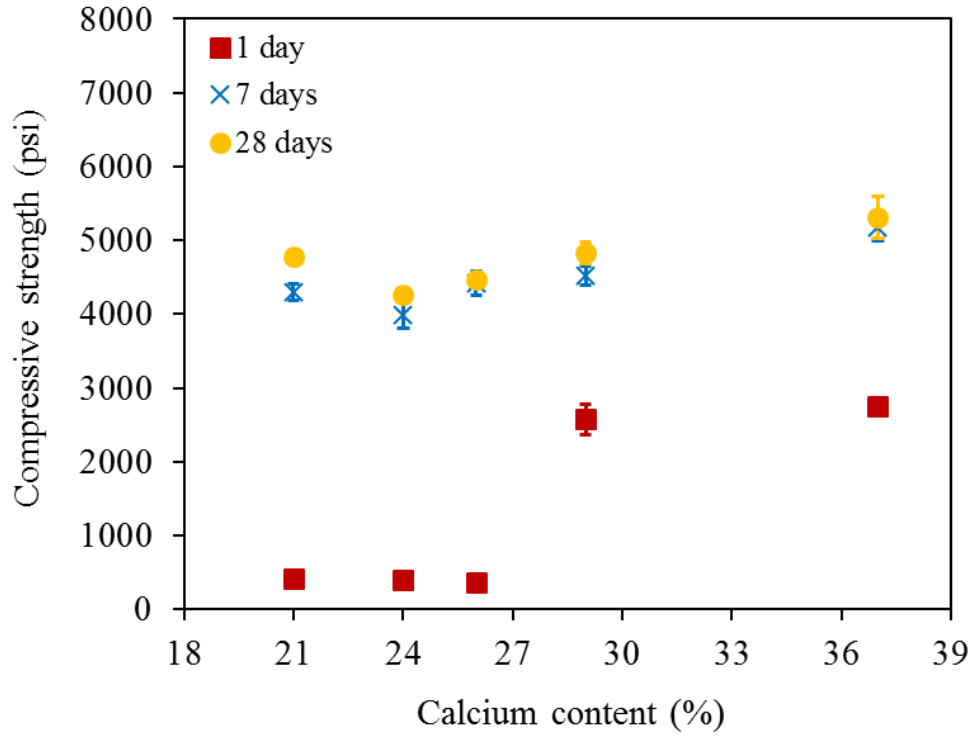
Figure 6.21: The compressive strength of the ambient-cured specimens with the calcium content.
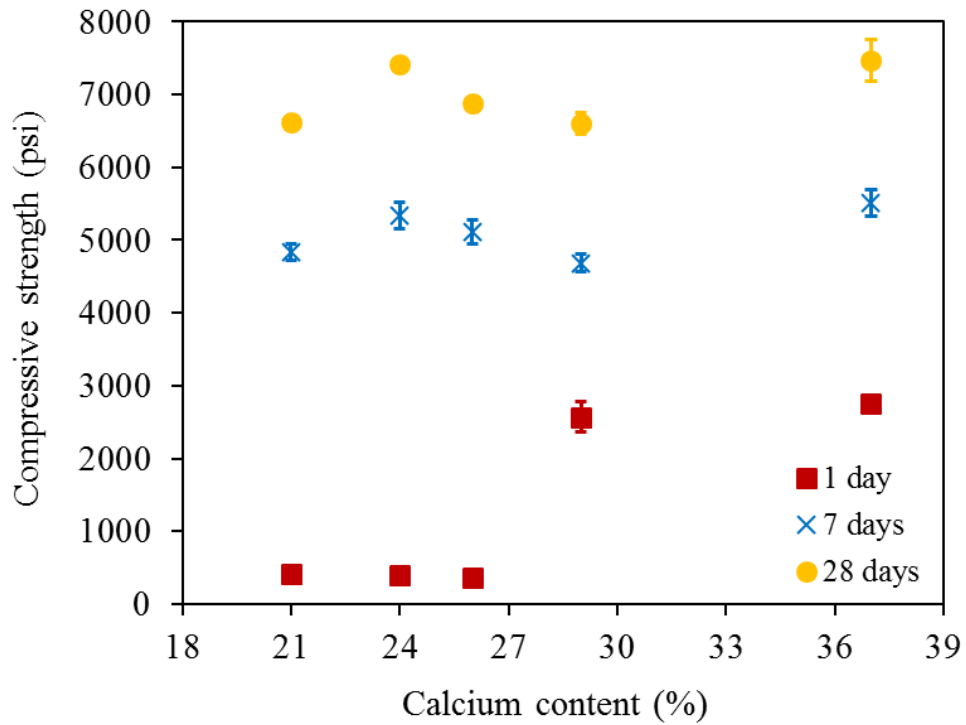
Figure 6.22: The compressive strength of the moist-cured specimens with the calcium content.

For ambient- and moist-cured specimens, C37, which has the highest calcium content, showed the highest compressive strength among the five FAs at all the different ages. With increased calcium content in the FA, more CSH and/or CASH are formed and higher compressive strength was gained, where the formation of the hydration products (CSH and CASH) do not require elevated temperature to be formed.

Although C29 has high calcium content, the compressive strength of the moist-cured specimens synthesized out of the C29 at age of 28 days was not the highest or the second-highest compressive strength among the five mixtures (Fig. 6.22). As it was mentioned earlier, the high calcium content of the C29 and the high surface area required higher W/FA than the other FAs. However, the compressive strength of C29 was the second-highest among the five ZCC mixtures at the early ages of 1 and 7 days, and the age of 28 days for the ambient-cured regimes (Fig. 6.21). That could be explained by the high calcium content and the high surface area of FA29. The high surface area provided more nuclei sites that caused more area for precipitation of CSH and CASH and increasing the growth rate.

6.2.2.3 *Effect of curing regime on the compressive strength of ZCC*

Figs. 6.23 through 6.27 show the effect of the curing regimes, namely oven, ambient, and moist, on the compressive strength developments of ZCC specimens for the five FAs.
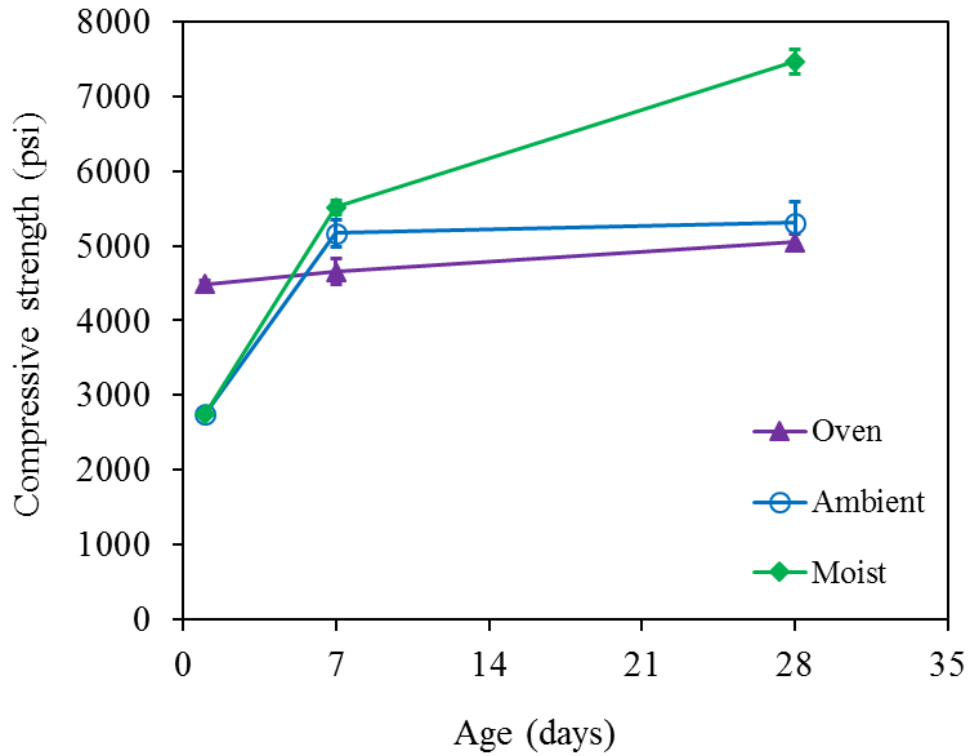
Figure 6.23: The compressive strength of differently cured ZCC synthesized using C37.
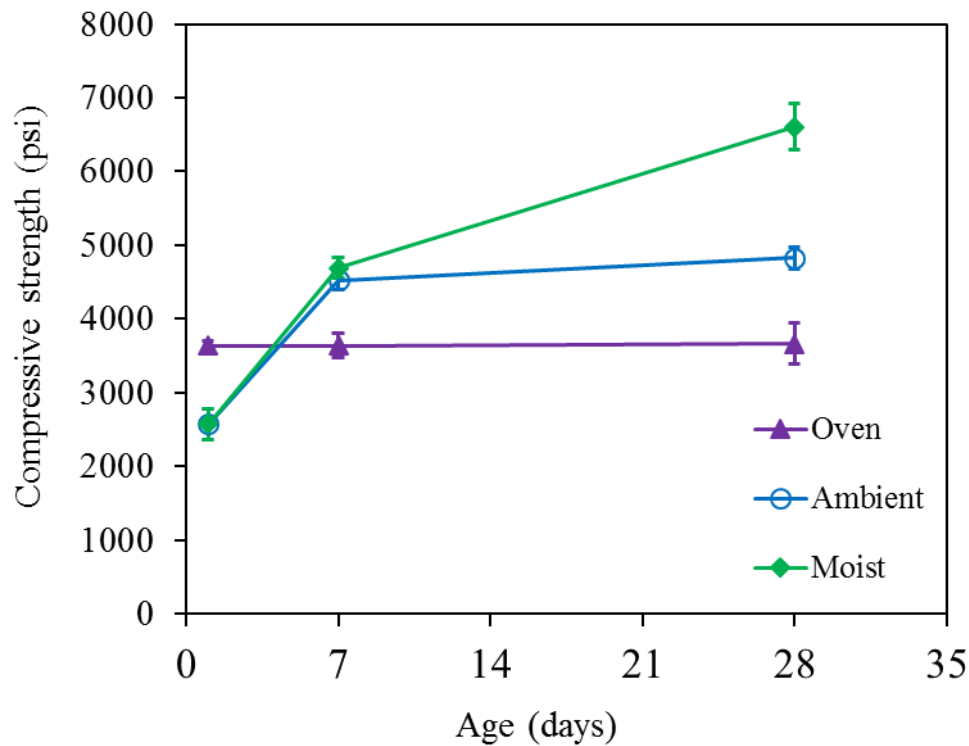
Figure 6.24: The compressive strength of differently cured ZCC synthesized using C29.
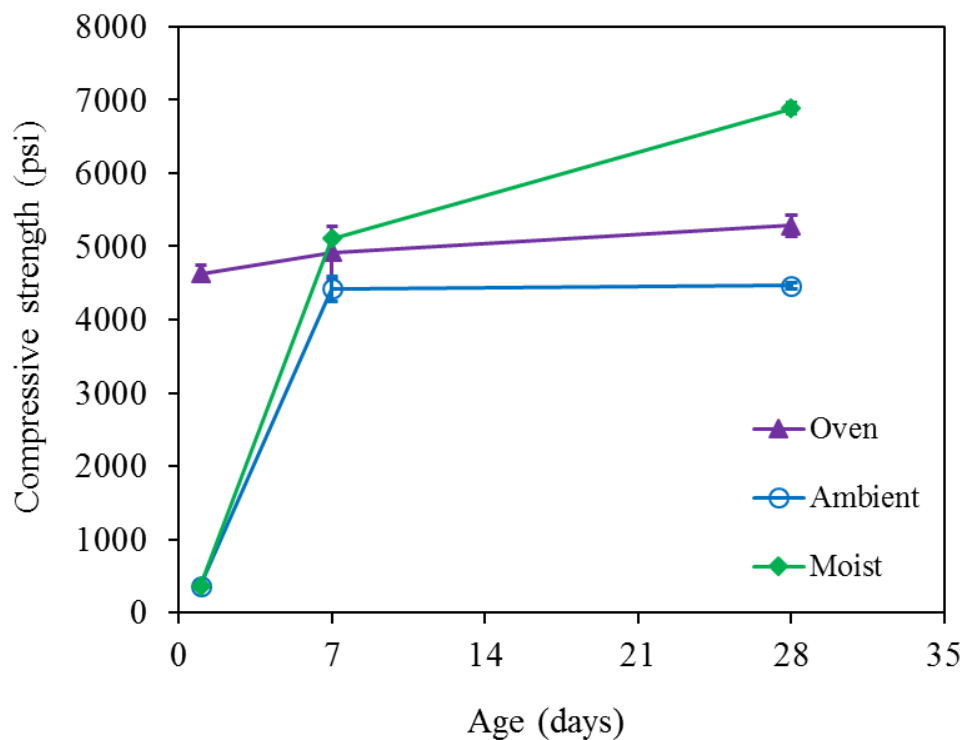
Figure 6.25: The compressive strength of differently cured ZCC synthesized using C26.
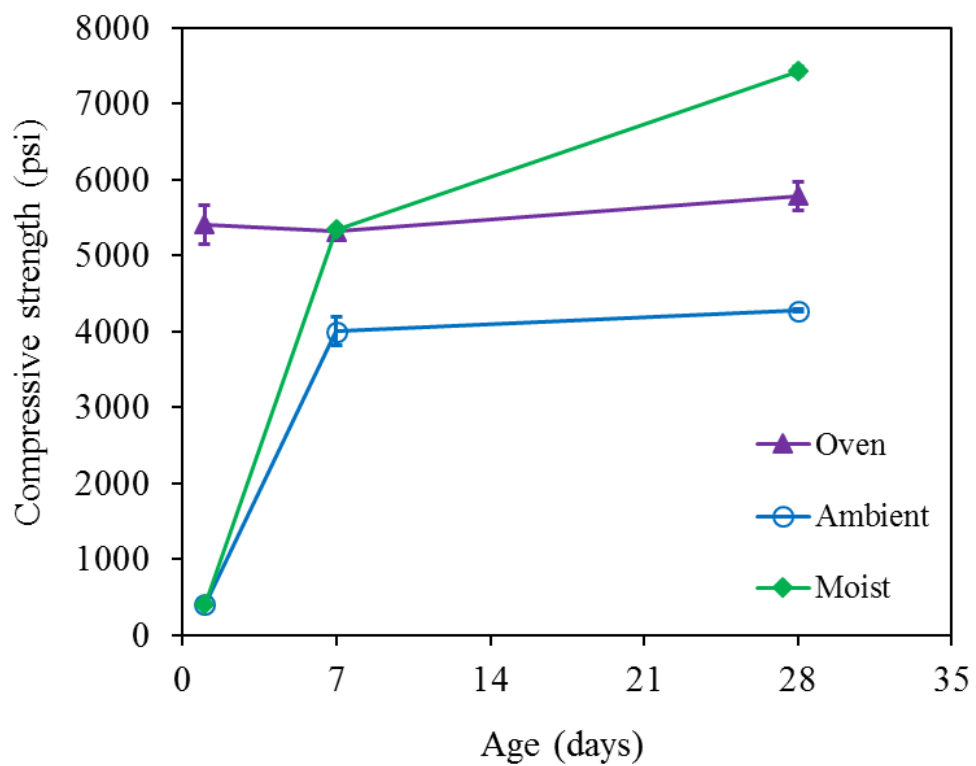
Figure 6.26: The compressive strength of differently cured ZCC synthesized using C24.

181
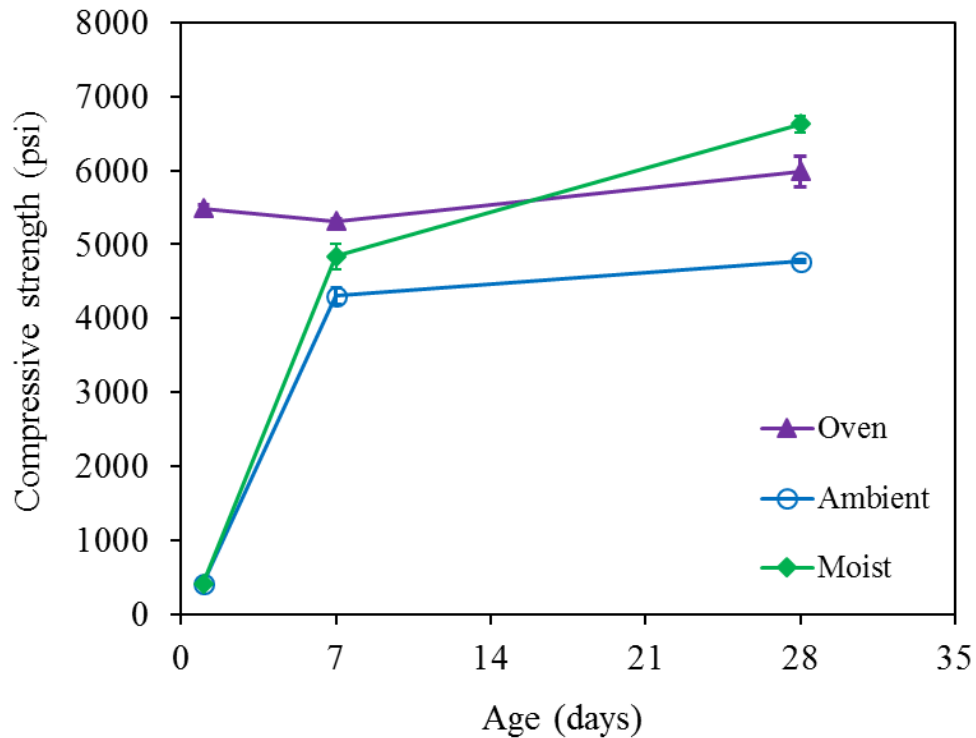
Figure 6.27: The compressive strength of differently cured ZCC synthesized using C21.

For the oven-cured specimens, the increase in strength from 1 day to 28 days was 8.4%, 12.4%, 6.4%, 0.7%, 11.0% for C21, C24, C26, C29, and C37, respectively. The maximum increase occurred for specimen C24, which had the second-lowest calcium content.

For the ambient-cured specimens, the increase in strength from 7 day to 28 days was 10.9%, 6.8%, 1.0%, 6.7%, and 2.7% for C21, C24, C26, C29, and C37, respectively. The maximum increase occurred for specimen C24, which had the lowest calcium content.

For the moist-cured specimens, the increase in strength from 7 days to 28 days was 36.9%, 39.1%, 34.8%, 40.9%, and 35.4% for C21, C24, C26, C29, and C37, respectively. The maximum increase occurred for specimen C24, which had the second-highest calcium content.

The hydration reaction that forms CSH or CASH in ZCC systems requires the presence of water and needs time to gain full strength. Hence, the moist curing displayed the highest compressive strength due to the presence of moisture during the curing period. Furthermore, the ambient-cured specimens showed a lower compressive strength compared with those moist-cured specimens due to the absence of moisture that is essential for continuous hydration. Therefore, there was an improvement in the compressive strength from 1 to 7 days due to the existence of free water in the mixture; then, the compressive strength remained constant beyond 7 days as the free water was consumed at the early age, and there was no extra water available in the ZCC specimens to allow further hydration reaction to take place.

Figs. 6.28 and 6.29 show comparison of the compressive strengths of the oven-, ambient-, and moist-cured specimens for the five ZCC mixtures and the CC mixture at the age of 7 and 28 days, respectively. As shown in Figs. 6.28 and 6.29, the compressive strengths of the moist-cured specimens were the highest strength among the three curing regimes, which indicated that the optimum curing regime for the high-calcium FAs is moist curing.
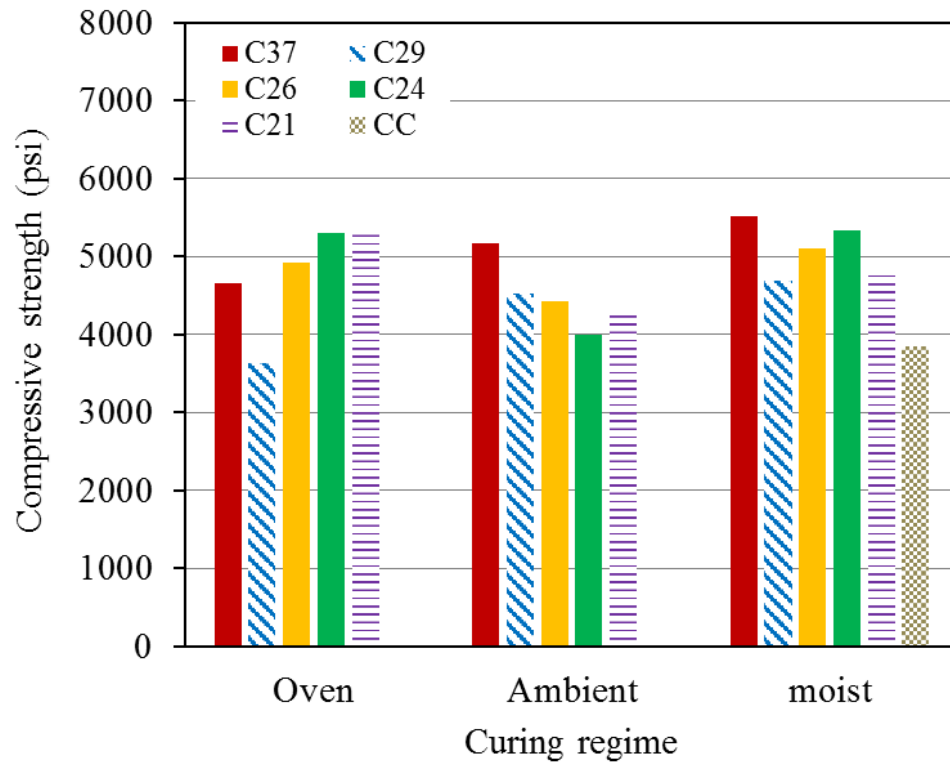
Figure 6.28: Compressive strength at the age of 7 days of three different curing regimes for the five different FA sources.
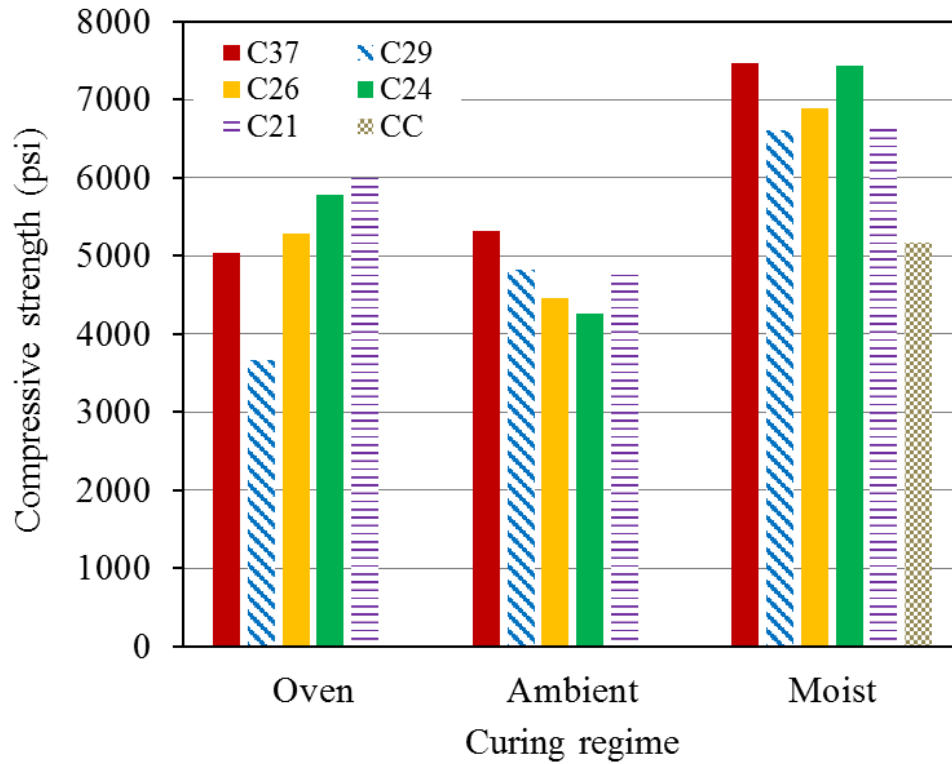
Figure 6.29: Compressive strength at the age of 28 days of three different curing regimes for the five different FA sources.

6.2.2.4 Tensile strength

Figs. 6.30 and 6.31 show the splitting tensile strength of the oven- and moist-cured ZCC specimens, respectively. Also shown in the figures is the splitting tensile strength of the CC specimen. Although the CC mixture was moist-cured only, its results were presented at both figures as a reference mixture.

The splitting tensile strength of the oven-cured specimens ranged from 270 psi (1.9 MPa) to 425 psi (2.9 MPa) and from 290 psi (2.0 MPa) to 447 psi (3.1 MPa) at the ages of 1 day and 28 days, respectively. The splitting tensile strength of the moist-cured specimens ranged from 375 psi (2.60 MPa) to 477 psi (3.3 MPa) and from 495 psi (3.4 MPa) to 585 psi (4.0 MPa) at the ages of 7 days and 28 days, respectively. The averages splitting tensile strengths of the CC specimen were 349 psi (2.4 MPa) and 445 psi (3.1 MPa) at the ages of 7 and 28 days, respectively, which

were 14% and 18% lower than the average of the corresponding moist-cured ZCC specimens at the ages of 7 and 28 days, respectively. It is worth noting that the compressive strength of the CC mixture was 23% and 22% lower than the average of the corresponding ZCC specimens at the ages of 7 and 28 days.
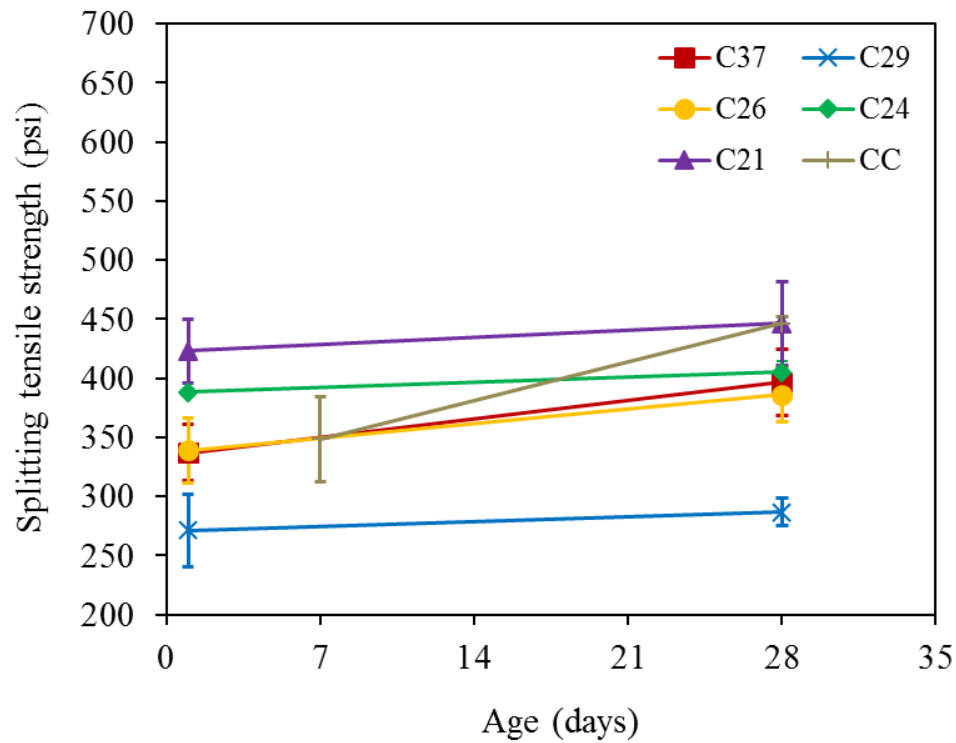
Figure 6.30: Splitting tensile strength of oven-cured ZCC specimens at different ages (Note: the CC mixture was cured in the moisture room).
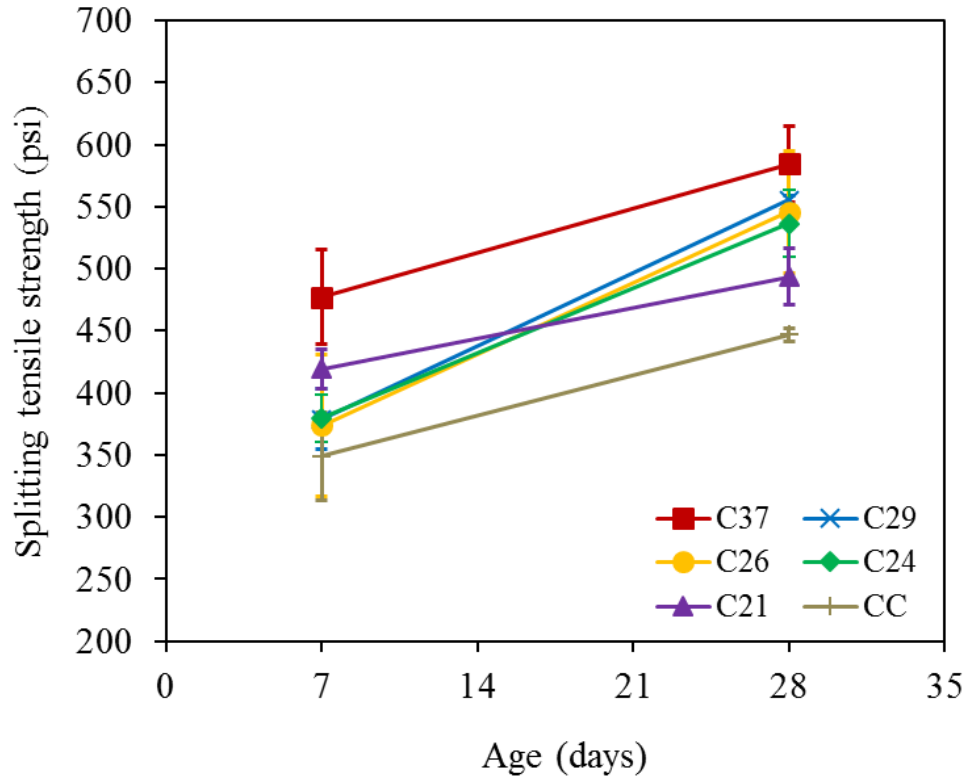
Figure 6.31: Splitting tensile strength of moist-cured ZCC specimens at different ages.

The splitting tensile strength was affected by the curing regime and the FA type. For the oven-cured specimens, C21, which had the lowest calcium content, showed the highest splitting tensile strength among the five ZCC mixtures. Hence, it had the highest flexural strength. The lowest strength was for C29 due to the high calcium content and high surface area that required higher W/FA of 0.38. The compressive strengths of the oven-cured specimens remained approximately the same or increased slightly with time. Therefore, the splitting tensile strength remained approximately constant with time.

For the moist curing regime, C37, which had the highest calcium content, showed the highest splitting tensile strength for the moist-cured specimens among the five ZCC mixtures. The splitting tensile strengths of the moist-cured specimens increased with time as explained earlier in this chapter. Therefore, the splitting tensile strength increased up to 28 days.

Codes, standards, and researchers used an empirical equation in the form of Eq. 6.1 to correlate the splitting tensile strength of concrete, f_{ct}, to its compressive strength, f_c', where k and n are constants obtained from regression analyses of experimental data. Table 6.4 summarizes the different values of k and n considered in the current research. These design codes and standards were developed based on data of CC. Fig. 6.32 presents comparisons between the experimental results of f_{ct} and those obtained using Eq. 6.1 with n and k values of the ACI 318-14 [133], AS 3600 [134], and CEB-FIP model code [135].

$$f_{ct} = k(f_c')^n \tag{6.1}$$

More recently, researchers developed similar equations for ZCC based on class F FA [36], class C FA [45], slag [57], and a combination of class F FA and slag [35, 38]. Table 6.4 summarizes the parameters n and k used by the different researchers and codes. Fig. 6.33 presents comparisons between the experimental results of f_{ct} and those obtained using Eq. 6.1 with n and k values of those researchers' equations.

Table 6.4: Splitting Tensile Strength Parameters k and n.

	k (US units)	k (SI-metric)	n	Type of binder
ACI 318 (2014)	6.7	0.560	0.50	Cement
AS 3600 (2001)	4.8	0.400	0.50	Cement
CEB-FIP model code (2010)	1.6	0.300	2/3	Cement
Sofi et al. (2007)	5.8	0.480	0.50	Class F FA + Slag
Yang et al. (2012)	1.5	0.255	0.65	Slag
Ryu et al. (2013)	0.59	0.170	0.75	Class F FA
Lee and Lee (2013)	5.4	0.450	0.50	Class F FA + Slag
Topark Ngram et al. (2015)	3.8	0.450	0.57	Class C FA
Proposed Equation	5.9	0.487	0.50	Class C FA

As shown in Figs. 6.32, the ACI 318-14 [133], AS 3600 [134], and CEB-FIP model code [135] predict quite well the trend of the experimental data. However, the ACI 318-14 [133] and CEB-

FIP model code [135] over-predicted the values of f_{ct} of the all concrete specimens (Table 6.5). Furthermore, AS 3600 [134] represents a lower bound for the experimental results (Table 6.5). Table 6.5 also shows the error, defined using Eq. 6.2, in predicting the values of f_{ct} using the different models and the coefficient of determination R^2

$$\% \ Error = \frac{Exp. - Anl.}{Anl.} \tag{6.2}$$

As shown in Table 6.5, the R^2 ranged from 0.35 to 0.98 for oven-cured and 0.45 to 0.88 for moist-cured specimens. However, when considering the results of the oven- and moist-cured specimens together, the R^2 ranged from 0.42 to 0.82. Furthermore, the k and n values proposed by Sofi et al. [35] and Yang et al. [57] resulted in the best prediction of f_{ct} with R^2 of 0.90 and 0.98 for oven-cured and 0.87 and 0.81 for moist-cured specimens, respectively. Using regression analysis, Eq. 6.3 was developed to correlate f_{ct} and f_c' of the ZCC examined in this chapter. Developed Eq. 6.3 has a coefficient of determination, R^2, of 0.82 for all of the ZCC specimens' results.

$$f_{ct} = 5.9 \ \sqrt{f_c'} \ , \text{(U.S. units, psi)} \tag{6.3a}$$

$$f_{ct} = 0.487 \ \sqrt{f_c'} \ , \text{(SI-metric, MPa)} \tag{6.3b}$$

Table 6.5: Splitting Tensile Strength Error Percentage (Experimental Results vs. Analytical Results).

Oven

	Age	Comp. (psi)	Ten. (psi)	ACI 318 2014	AS 3600 2001	CEB-FIP 2010	Sofi et al. 2007	Yang et al. 2012	Lee & Lee 2013	Ryu et al. 2013	Topark-Ngram 2015	Prop.
C21	1	5317	423	-13	21	-13	0	7	7	15	-16	-2
C21	28	5987	447	-14	20	-15	0	4	7	11	-17	-2
C24	1	5309	388	-20	11	-20	-8	-2	-1	6	-23	-10
C24	28	5780	405	-20	11	-21	-8	-3	-1	4	-24	-10
C26	1	4920	355	-24	5	-23	-13	-6	-6	2	-27	-14
C26	28	5284	386	-21	11	-20	-8	-2	-2	6	-23	-10
C29	1	3636	271	-33	-6	-28	-22	-12	-17	-2	-33	-24
C29	28	3659	287	-29	-1	-24	-18	-8	-12	3	-30	-20
C37	1	4487	337	-25	5	-23	-13	-5	-7	4	-26	-15
C37	28	5044	397	-17	16	-16	-4	4	3	12	-19	-5
R^2				0.48	0.90	0.56	0.90	0.98	0.96	0.96	0.35	0.88
R^2 of all data				0.56	0.46	0.60	0.82	0.82	0.76	0.69	0.42	0.82

Moist

	Age	Comp. (psi)	Ten. (psi)	ACI 318 2014	AS 3600 2001	CEB-FIP 2010	Sofi et al. 2007	Yang et al. 2012	Lee & Lee 2013	Ryu et al. 2013	Topark-Ngram 2015	Prop.
C21	7	4841	419	-5	33	-1	10	21	18	34	-6	8
C21	28	6627	493	7	49	9	23	34	32	46	4	21
C24	7	5339	380	-22	8	-22	-10	-4	-4	3	-25	-12
C24	28	7426	537	-7	30	-12	7	9	15	14	-12	6
C26	7	5107	374	-22	9	-21	-10	-3	-3	5	-24	-11
C26	28	6882	546	-2	37	-6	13	17	22	22	-7	12
C29	7	5513	477	-4	34	-4	11	18	19	26	-7	9
C29	28	7463	585	1	41	-4	17	18	25	23	-5	15
C37	7	4687	379	-17	15	-15	-5	4	3	13	-19	-6
C37	28	6605	555	2	42	-1	18	22	27	29	-3	16
R^2				0.88	0.45	0.87	0.87	0.81	0.75	0.67	0.82	0.89
CC	7	3843	349	-16	17	-11	-3	9	4	21	-17	-5
CC	28	5166	447	-7	29	-7	7	15	15	24	-10	5
R^2 of all data				0.56	0.46	0.60	0.82	0.82	0.76	0.69	0.42	0.82
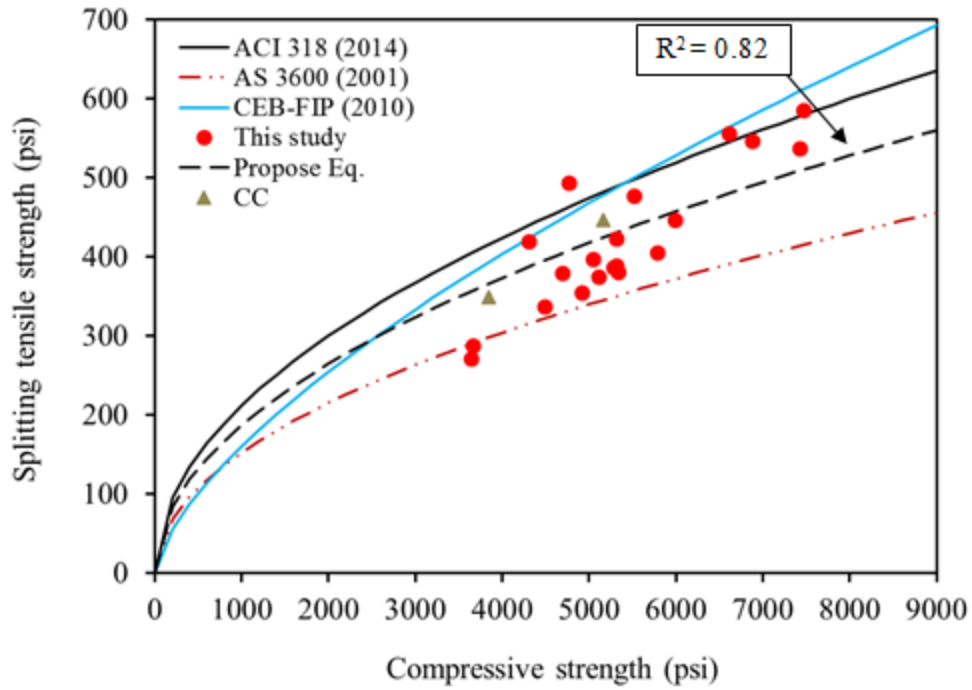
Figure 6.32: Splitting tensile strength and compressive strength of ZCC with the design codes' equations.
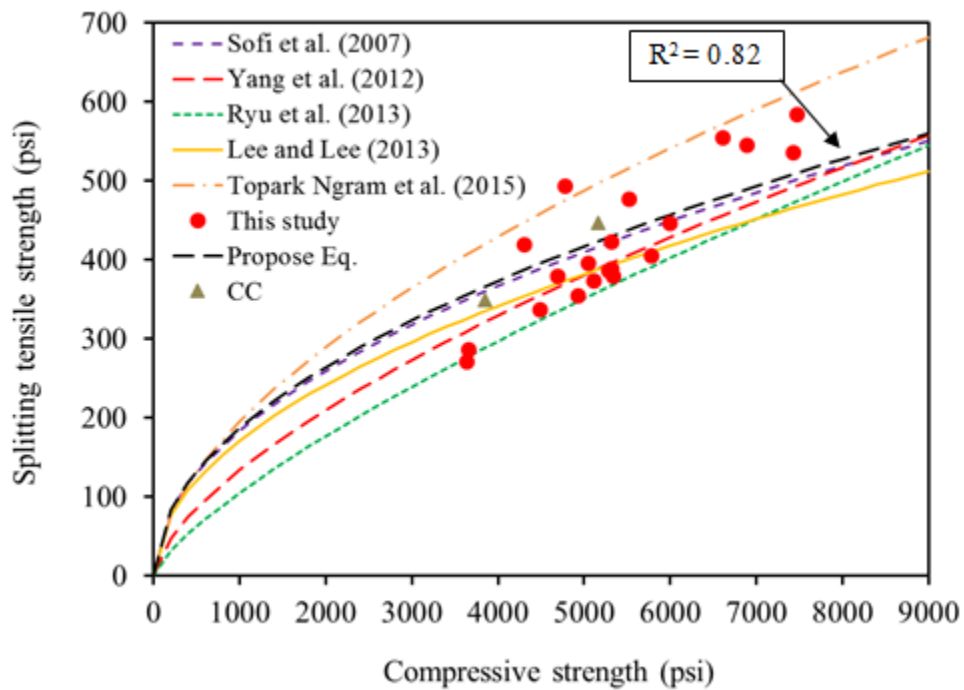
Figure 6.33: Splitting tensile strength and compressive strength of ZCC with the researchers' equations.

The proposed equation in this study and the previous studies that were conducted on class C FA and a combination of class F FA and slag all showed a higher strength than a study based on class F FA. It is known that class C FA has high calcium content, which leads to the formation of CSH and/or CASH along with the aluminosilicate network (NASH). It was suggested that the CSH and/or CASH products filled the voids of the aluminosilicate matrix, resulting in a lower porosity paste which strengthen the bond between the paste the coarse aggregate particles and leaded to a strong interfacial transition zone (ITZ) [45, 136].

6.2.2.5   *Modulus of rupture (flexural strength)*

Figs. 6.34 and 6.35 show the flexural strength of the oven- and moist-cured ZCC specimens, respectively. Also shown on the figures is the flexural strength of the CC specimen. Although the CC mixture was moist-cured only, its results were presented at both figures as a reference mixture.

The flexural strength of the oven-cured specimens ranged from 443 psi (3.1 MPa) to 675 psi (4.7 MPa) and from 465 psi (3.2 MPa) to 655 psi (4.5 MPa) at the ages of 1 day and 28 days, respectively. The flexural strength of the moist-cured specimens ranged from 525 psi (3.6 MPa) to 785 psi (5.4 MPa) and from 740 psi (5.1 MPa) to 930 psi (6.4 MPa) at the ages of 7 days and 28 days, respectively. The averages flexural strength of the CC specimens were 585 psi (4.0 MPa) and 650 psi (4.5 MPa) at the ages of 7 and 28 days, respectively, which were 9% and 19% lower than the average of those similar moist-cured ZCC specimens at the ages of 7 and 28 days, respectively. It is worth noting that the compressive strength of the CC mixture was 23% and 22% lower than the average of the corresponding ZCC specimens at the ages of 7 and 28 days.
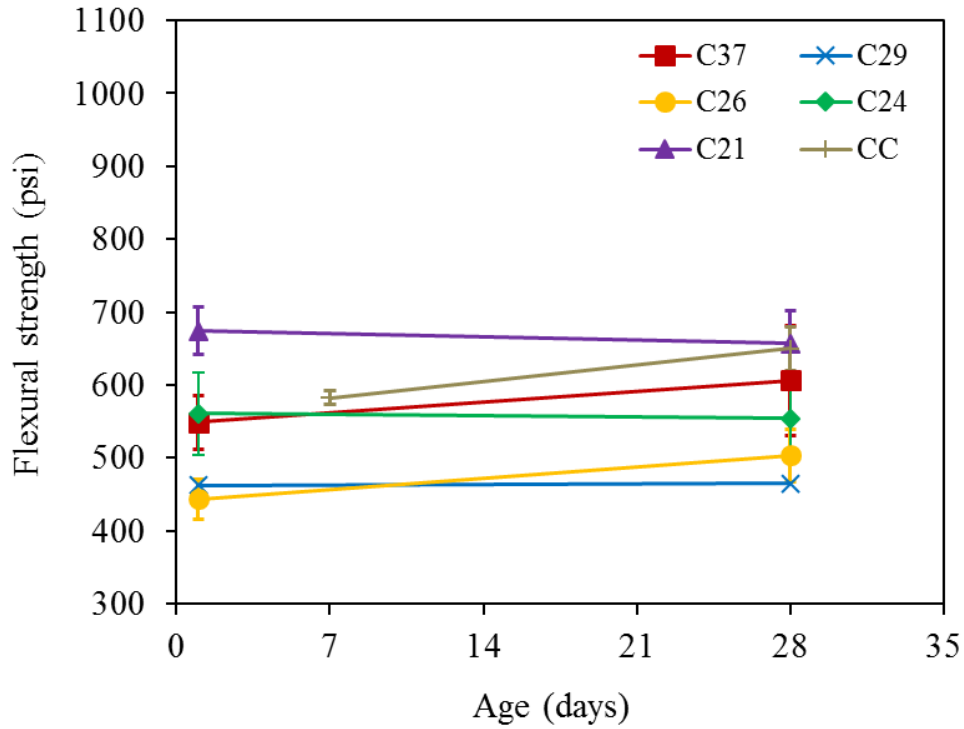
Figure 6.34: Flexural strength of oven-cured ZCC specimens at different ages (Note: the CC mixture was cured in the moisture room).
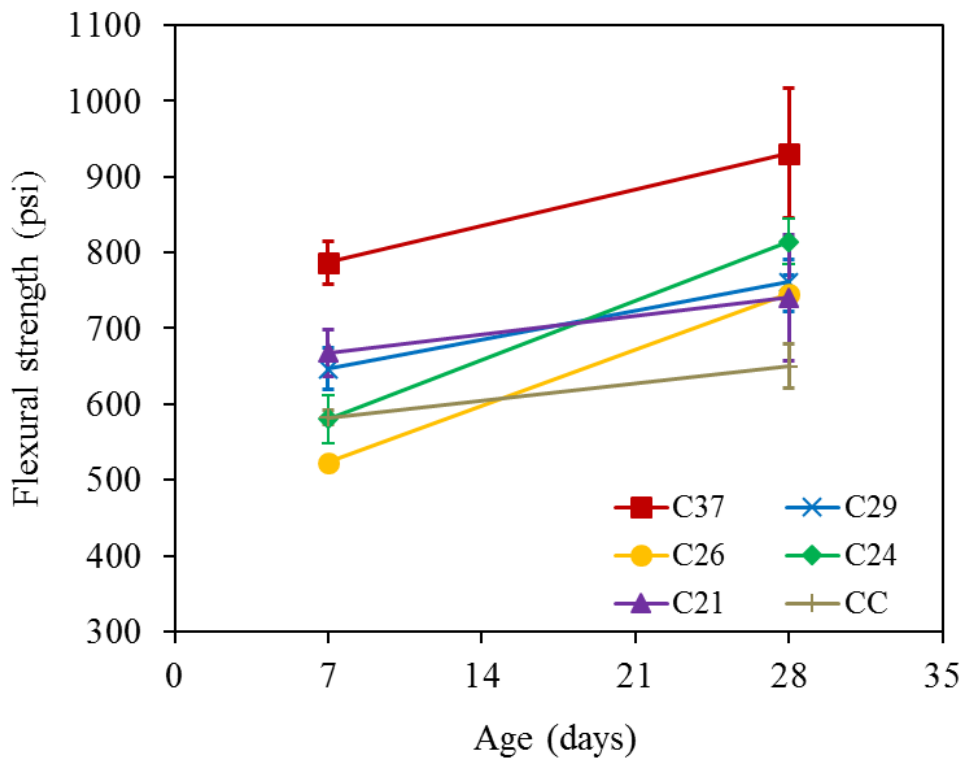
Figure 6.35: Flexural strength of moist-cured ZCC specimens at different ages.

194

The flexural strength was affected by the curing regime and the FA type. For the oven specimens, the C21 that had the lowest calcium content showed the highest flexural strength among the five ZCC mixtures. Hence, it had the highest flexural strength. The compressive strengths of the oven-cured specimens remained approximately the same with time. Therefore, the flexural strength remained constant up to 28 days.

For the moist curing regime, the C37, which had the highest calcium content, showed the highest flexural strength for the moist-cured specimens among the five ZCC mixtures. Hence, it displayed the highest flexural strength. The flexural strengths of the moist-cured specimens increased with time as explained earlier in this chapter. Therefore, the flexural strength increased up to 28 days.

Codes, standards, and researchers used an empirical equation in the form of Eq. 6.4 to correlate the flexural strength of concrete, f_r, to its compressive strength, f_c', where k and n are constants obtained from regression analyses of experimental data. Table 6.6 summarizes the different values of n and k considered in the current research. These design codes and standards were developed based on data of CC. Fig. 6.36 presents comparisons between the experimental results of f_r and those obtained using Eq. 6.4 with n and k values of the ACI 318-14 [133], AS 3600 [134], and CEB-FIP model code [135]. It is worth noting that the CEB-FIP equation that was calculated for beam had a depth of 6 in.

$$f_r = k(f_c')^n \qquad (6.4)$$

More recently, researchers developed similar equations for ZCC based on 25 different sources of FAs (13 class F FA and 12 class C FA) [48], slag [57], and a combination of class F FA and slag [35]. Table 6.6 summarizes the parameter n and k used by the different researchers and codes.

Fig. 6.37 presents comparisons between the experimental results of f_r and those obtained using

Eq. 6.4 with n and k values of those researchers' equations.

Table 6.6: Flexural Strength Parameters k and n.

	k (US units)	k (SI-metric)	n	Type of binder
ACI 318 (2014)	7.5	0.62	0.50	Cement
AS 3600 (2001)	7.2	0.60	0.50	Cement
CEB-FIP model code (2010)	2.4	0.45	2/3	Cement
Sofi et al. (2007)	8.4	0.70	0.50	Class F FA + Slag
Diaz et al. (2011)	8.3	0.69	0.50	Class F FA and Class C FA
Yang et al. (2012)	2.0	0.35	0.65	Slag
Proposed Equation	8.8	0.73	0.50	Class C FA

As shown in Fig. 6.36 and 6.37, the measured flexural strength of the ZCC are significantly

higher than those proposed by the different codes, standards, and models presented in Table 6.6.

Also, the ACI 318-14 [133] and AS 3600 [134] consistently under predicted the values of f_r of

all concrete specimens (Table 6.7). However, CEB-FIP model code [135] over predicted the

values of f_r of all concrete specimens. Table 6.7 shows also the error, defined using Eq. 6.2, in

predicting the values of f_r using the different models.

As shown in Table 6.7, the R^2 ranged from 0.88 to 0.91 for oven-cured and 0.40 to 0.77 for

moist-cured specimens. However, considering the results of the oven and moist together, the R^2

ranged from 0.40 to 0.73. Furthermore, the k and n values proposed by Sofi et al. [35] resulted in

the best prediction of E_c with R^2 of 0.89 for oven-cured and 0.77 for moist-cured specimens.

Using regression analysis, Eq. 6.5 was developed to correlate f_r and f_c' of the ZCC examined in

this chapter. Developed Eq. 6.5 has a coefficient of determination, R^2, of 0.75 for all the ZCC

specimens' results.

$$f_r = 8.8 \sqrt{f_c'} \text{ , (U.S. units, psi)} \tag{6.5a}$$

$$f_r = 0.73 \sqrt{f_c'} \text{ , (SI-metric, MPa)} \tag{6.5b}$$

Table 6.7: Flexural Strength Error Percentage (Experimental Results vs. Analytical Results).

Oven

	Age	Comp. (psi)	Flexural (psi)	ACI 318 2014	AS 3600 2001	CEB-FIP 2010	Sofi et al. 2007	Diaz et al. 2012	Yang et al. 2012	Prop.
C21	1	5317	423	23	28	-8	10	11	28	5
C21	28	5987	447	13	18	-17	1	2	15	-4
C24	1	5309	388	3	7	-23	-8	-7	6	-12
C24	28	5780	405	-3	1	-28	-13	-12	-1	-17
C26	1	4920	355	-16	-12	-36	-25	-24	-12	-28
C26	28	5284	386	-8	-4	-31	-18	-17	-4	-21
C29	1	3636	271	9	14	-16	-2	-1	16	-7
C29	28	3659	287	14	19	-14	2	3	19	-3
C37	1	4487	337	2	7	-18	-9	-8	12	-13
C37	28	5044	397	3	7	-18	-8	-7	12	-13
R^2				0.91	0.88	0.44	0.89	0.90	0.88	0.82
R^2 of all data				0.52	0.40	0.50	0.73	0.72	0.45	0.75

Moist

	Age	Comp. (psi)	Flexural (psi)	ACI 318 2014	AS 3600 2001	CEB-FIP 2010	Sofi et al. 2007	Diaz et al. 2012	Yang et al. 2012	Prop.
C21	7	4841	419	36	41	5	21	23	45	16
C21	28	6627	493	43	49	9	28	29	51	22
C24	7	5339	380	-4	0	-29	-15	-14	-1	-19
C24	28	7426	537	15	20	-18	3	4	14	-2
C26	7	5107	374	8	13	-18	-3	-2	13	-8
C26	28	6882	546	31	36	-6	17	18	31	12
C29	7	5513	477	41	47	5	26	28	46	21
C29	28	7463	585	44	50	2	28	30	41	22
C37	7	4687	379	26	31	-4	12	14	33	7
C37	28	6605	555	25	30	-10	12	13	25	6
R^2				0.51	0.40	0.83	0.77	0.75	0.46	0.84
CC	7	3843	349	25	31	-1	12	13	36	7
CC	28	5166	447	21	26	-9	8	9	25	3
R^2 of all data				0.52	0.40	0.50	0.73	0.72	0.45	0.75
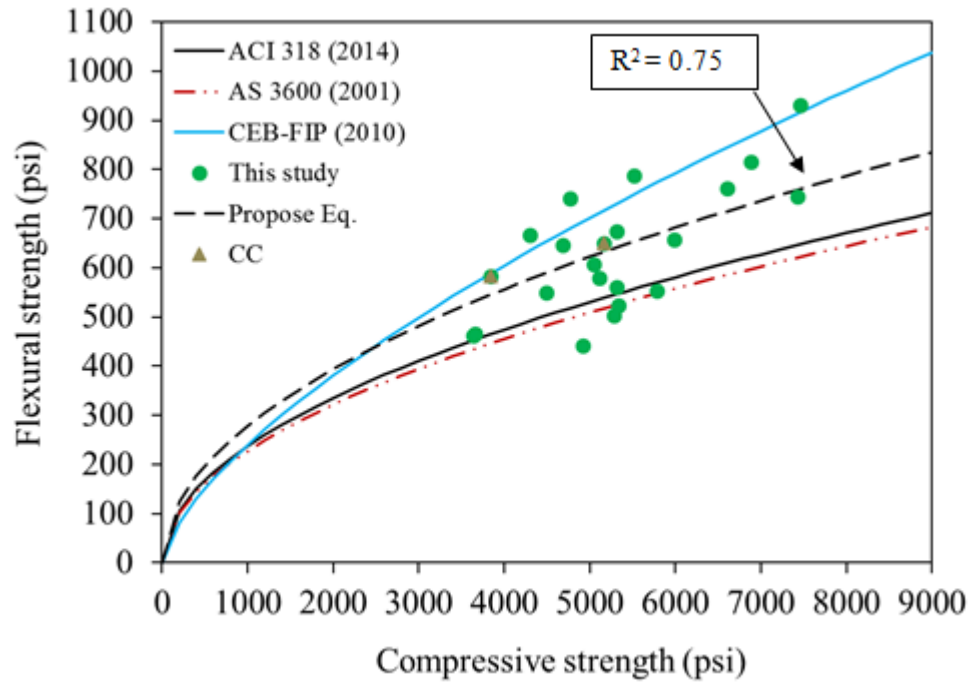
Figure 6.36: Flexural strength and compressive strength of ZCC with the design codes'
equations.
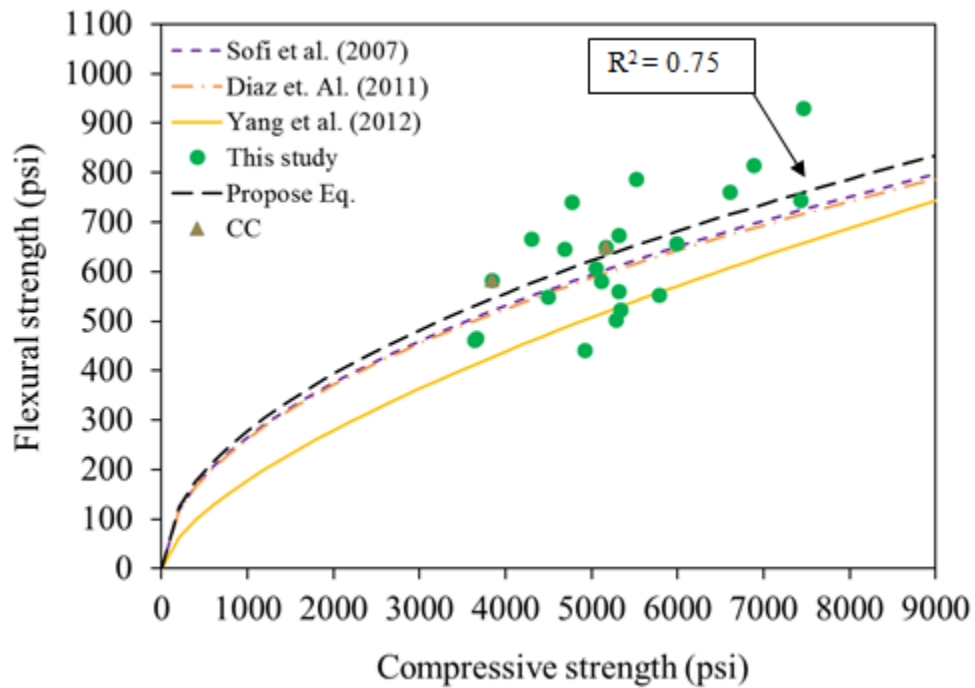
Figure 6.37: Flexural strength and compressive strength of ZCC with the researchers' equations.

6.2.2.6 *Modulus of elasticity*

The modulus of elasticity is an important factor in the design and analysis of concrete structures. It depends on the type and quality of the coarse aggregate and the paste's modulus of elasticity. Figs. 6.38 and 6.39 show the modulus of elasticity of the oven- and moist-cured ZCC specimens, respectively. Also shown on the figures are the modulus of elasticity of the CC specimen, which was moist-cured only; its results were presented at both figures as a reference mixture.

The modulus of elasticity of the oven-cured specimens ranged from 3850 psi (26.6 GPa) to 5285 psi (36.4 GPa) and from 4075 psi (28.1 GPa) to 5715 psi (39.4 GPa) at ages of 1 day and 28 days, respectively. The modulus of elasticity of the moist-cured specimens ranged from 4004 psi (27.6 GPa) to 6270 psi (43.2 GPa) and from 5185 psi (35.7 GPa) to 6825 psi (47.1 GPa) at 7 days and 28 days, respectively. The average moduli of elasticity of the CC specimens were 4550 psi (31.4 GPa) and 5100 psi (35.2 GPa) at ages of 7 and 28 days, respectively, which were 23% and 22% lower than the averages of the corresponding moist-cured ZCC specimens at the ages of 7 and 28 days, respectively, because the CC had lower compressive strength. It is worth noting that the compressive strength of the CC mixture was 23% and 22% lower than the average of the corresponding ZCC specimens at the ages of 7 and 28 days.
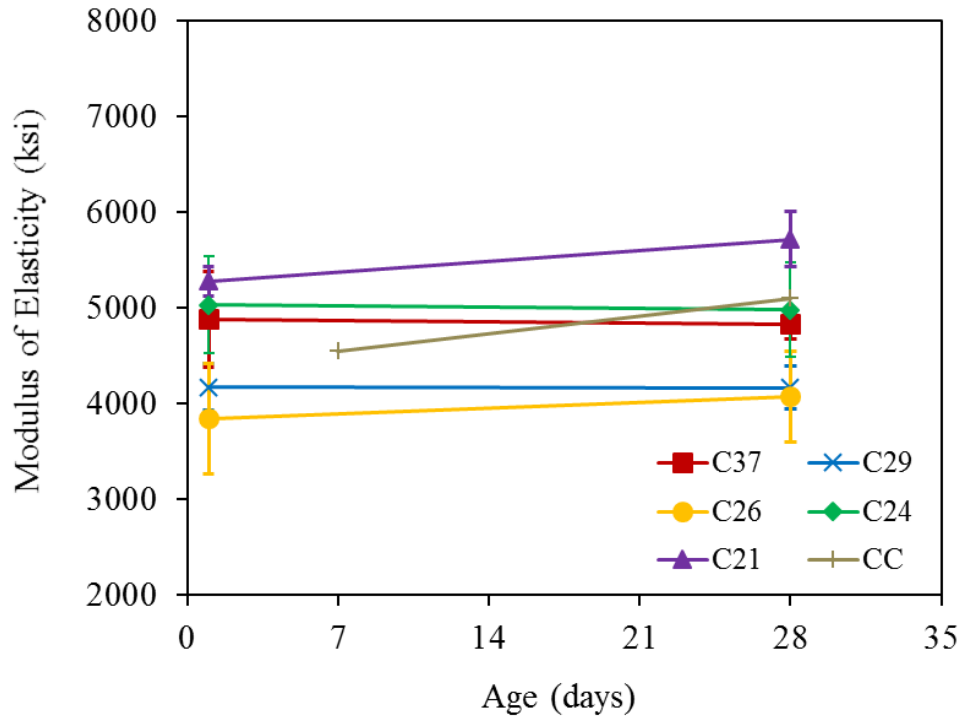
Figure 6.38: Modulus of elasticity of oven-cured ZCC specimens at different ages (Note: the CC mixture was cured in the moisture room).
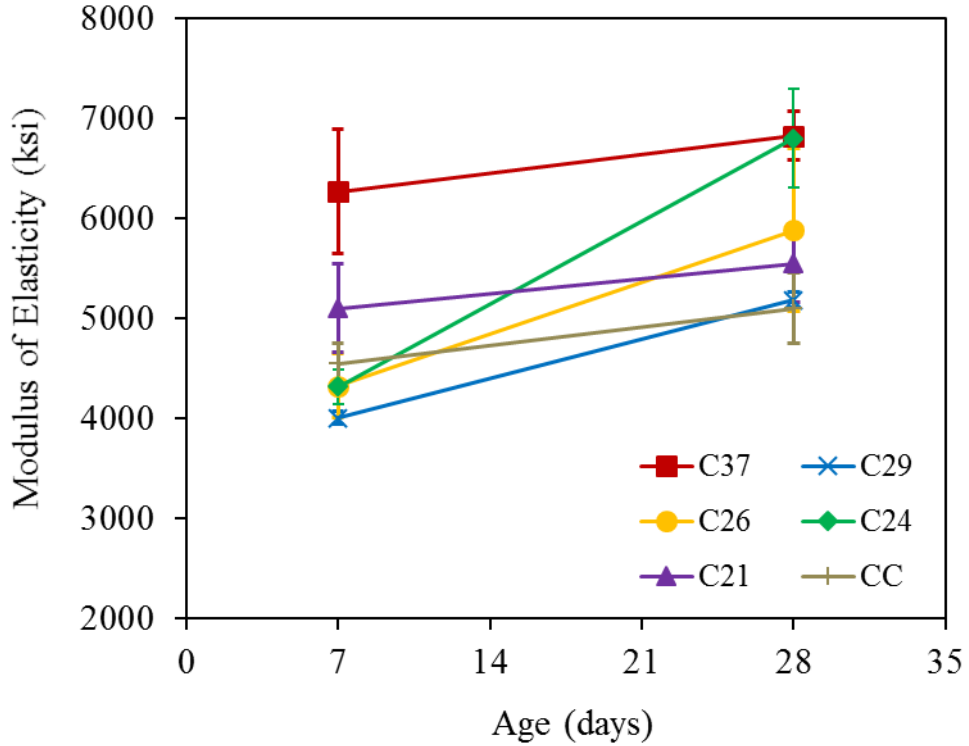
Figure 6.39: Modulus of elasticity of moist-cured ZCC specimens at different ages.

201

The modulus of elasticity was affected by the curing regime and the FA type. For the oven curing regime, the C21 that had the lowest calcium content showed the highest modulus of elasticity among the five ZCC mixtures. The moduli of elasticity of the oven-cured specimens remained approximately the same or increased slightly with time.

For the moist curing regime, C37, which had the highest calcium content, showed the highest modulus of elasticity for the moist-cured specimens among the five ZCC mixtures. The moduli of elasticity of the moist-cured specimens increased with time due to the availability of the moisture during the curing time.

Codes, standards, and researchers used an empirical equation (Eq. 6.6) to correlate the modulus of elasticity of concrete, E_c, to its compressive strength, f_c', where k and n are constants obtained from regression analyses of experimental data and w_c is the concrete density. These codes and standards were based on CC data. Fig. 6.36 presents comparisons between the experimental results of E_c and those obtained using Eq. 6.6 with n and k values of the ACI 318-14 [133] and CEB-FIP model code [135]. It worth noting that ACI 318-14 [133] presented two equations; one of them takes the concrete density into consideration and the second equation does not (Table 6.8). These design codes and standards were developed based on CC data. The modulus of elasticity of the ZCC ranged from 1450 ksi (10 GPa) to 5800 ksi (40 GPa) which is in the same range of the CC [71]. Fig. 6.40 presents comparisons between the experimental results of E_c and those obtained using Eq. 6.6 with n and k values of the ACI 318-14 [133] and CEB-FIP model code [135]. It is important to mention that the plotted equations included the concrete density in Fig. 6.40, the concrete density considered as 152.84 lb/ft^3, which was the average density of the ZCC mixtures.

$$E_c = k \, (w_c/b)^m \, (f_c'/a)^n \tag{6.6}$$

More recently, researchers developed similar equations for ZCC based on 25 different sources of FAs (13 class F FA and 12 class C FA) [48], slag [57], class C FA and slag [46], and a combination of class F FA and slag [38]. Table 6.8 summarizes the parameter n and k used by different researchers and codes. Fig. 6.41 presents comparisons between the experimental results of E_c and those obtained using Eq. 6.6 with n and k values of those researchers' equations.

Table 6.8: Modulus of elasticity parameters k and n.

	k (US units)	k (SI-metric)	m	a	b	n	Type of binder
ACI 318 (2014)	33	0.043	1.5	1	1	0.5	Cement
ACI 318 (2014)	57000	4700	-	1	1	0.5	Cement
CEB-FIP model code (2010)	535500	19400	-	1	10	1/3	Cement
Diaz et al. (2011)	580	580	-	1	1	1	Class F FA and Class C FA
Yang et al. (2012)	3530000	4600	1.5	2200	1	0.5	Slag
Lee and Lee (2013)	146300	5300	-	1	1	1/3	Class F FA + Slag
Thomas and Peethamparan (2015)	53000	4400	-	1	1	0.5	Class C FA and Slag
Proposed Equation	68600	5700	-	1	1	0.5	Class C FA

As shown in Fig. 6.40 and 6.41, the measured modulus of elasticity of the ZCC are significantly higher than those proposed by the different codes, standards, and models presented in Table 6.8. Also, the ACI 318-14 [133] and CEB-FIP model code [135] consistently under predicted the

203

values of E_c of all concrete specimens (Table 6.9). Table 6.9 also shows the error, defined using Eq. 6.2, in predicting the values of E_c using the different models.

As shown in Table 6.9, the R^2 ranged from -0.93 to 0.91 for oven-cured and -1.37 to 0.78 for moist-cured specimens. However, with considering the results of the oven and moist together, the R^2 ranged from -2.46 to 0.75. Furthermore, the k and n values proposed by Yang et al. [57] resulted in the best prediction of E_c with R^2 of 0.91 for oven-cured and 0.78 for moist-cured specimens. Using regression analysis, Eq. 6.7 was developed to correlate E_c and f_c' of the ZCC examined in this chapter. Developed Eq. 6.7 has a coefficient of determination, R^2, of 0.81 for all the ZCC specimens' results.

$$E_c = 68600\sqrt{f_c'} \text{ , (U.S. units, psi)} \tag{6.7a}$$

$$E_c = 5700\sqrt{f_c'} \text{ , (SI-metric, MPa)} \tag{6.7b}$$

Table 6.9: Modulus of Elasticity Error Percentage (Experimental Results vs. Analytical Results).

Oven

	Age	Comp. (psi)	Modulus (ksi)	ACI 318 2014	CEB-FIP 2010	Diaz et al. 2011	Yang et al. 2012	Lee & Lee 2013	Thomas and Peethamparan 2015	Prop.
C21	1	5317	5284	14	18	42	11	52	27	5
C21	28	5987	5717	16	21	39	13	54	28	7
C24	1	5309	5033	10	14	39	6	49	23	1
C24	28	5780	4983	5	10	33	1	47	19	-5
C26	1	4920	3851	-14	-10	26	-18	35	3	-25
C26	28	5284	4075	-11	-6	25	-15	37	5	-22
C29	1	3636	4873	14	16	47	11	50	27	6
C29	28	3659	4834	8	12	39	5	48	22	-1
C37	1	4487	4175	10	8	49	7	46	23	1
C37	28	5044	4167	9	8	49	6	46	23	0
R^2				0.88	0.83	-0.34	0.91	-0.93	0.56	0.92
R^2 of all data				0.67	0.49	-1.07	0.75	-2.46	0.07	0.81

Moist

	Age	Comp. (psi)	Modulus (ksi)	ACI 318 2014	CEB-FIP 2010	Diaz et al. 2011	Yang et al. 2012	Lee & Lee 2013	Thomas and Peethamparan 2015	Prop.
C21	7	4841	5099	20	21	51	17	53	32	12
C21	28	6627	5550	22	25	50	20	56	34	15
C24	7	5339	4316	-6	-1	28	-9	41	10	-16
C24	28	7426	6801	21	29	37	18	58	33	13
C26	7	5107	4325	-3	1	32	-7	42	12	-13
C26	28	6882	5884	12	20	32	9	53	25	3
C29	7	5513	6267	26	30	49	23	59	37	19
C29	28	7463	6825	21	29	37	18	58	33	13
C37	7	4687	4004	-7	-4	32	-11	39	9	-17
C37	28	6605	5183	2	10	26	-1	47	17	-8
R2				0.72	0.56	-0.29	0.78	-1.37	0.30	0.85
CC	7	3843	4550	15	14	51	12	50	28	7
CC	28	5166	5100	12	16	41	9	50	25	3
R2 of all data				0.67	0.49	-1.07	0.75	-2.46	0.07	0.81
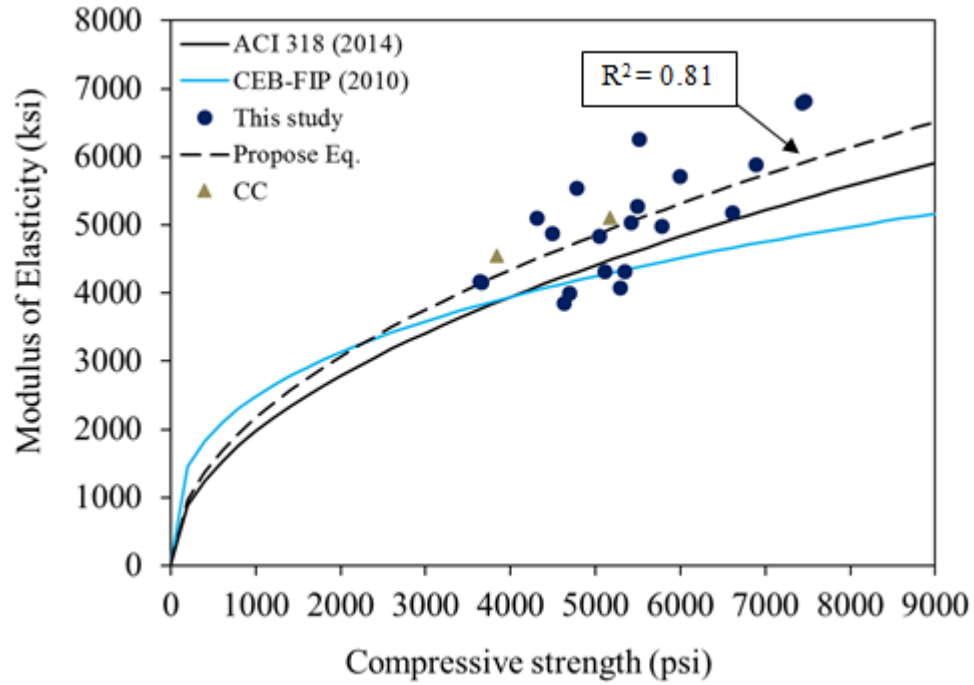
Figure 6.40: Modulus of elasticity and compressive strength of ZCC with the design codes'
equations.
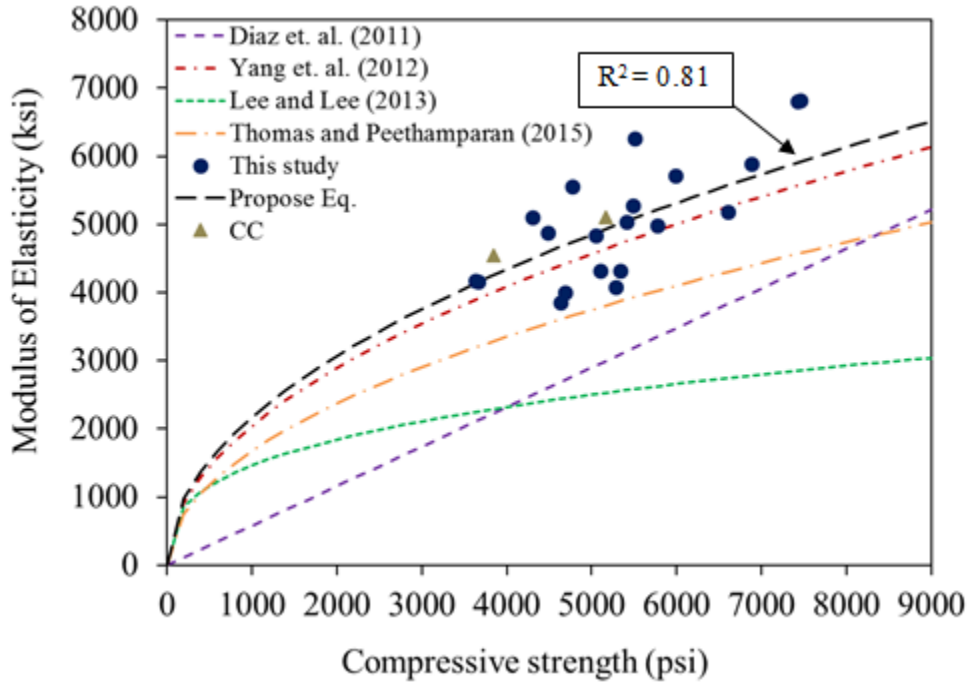
Figure 6.41: Modulus of elasticity and compressive strength of ZCC with the researchers'
equations.

6.2.2.7 *Drying shrinkage*

Figs. 6.42, 6.43, and 6.44 show the drying shrinkage values of three curing and storing methods; the oven-cured specimens that were tested directly after 24 hours of oven curing, the oven-cured specimens that were stored for 28 days then tested, and the moist-cured specimens that were stored for 28 days then tested, respectively. The drying shrinkage values of the CC mixture is also shown in the figures. The CC was moist-cured only and stored for 28 days then tested.
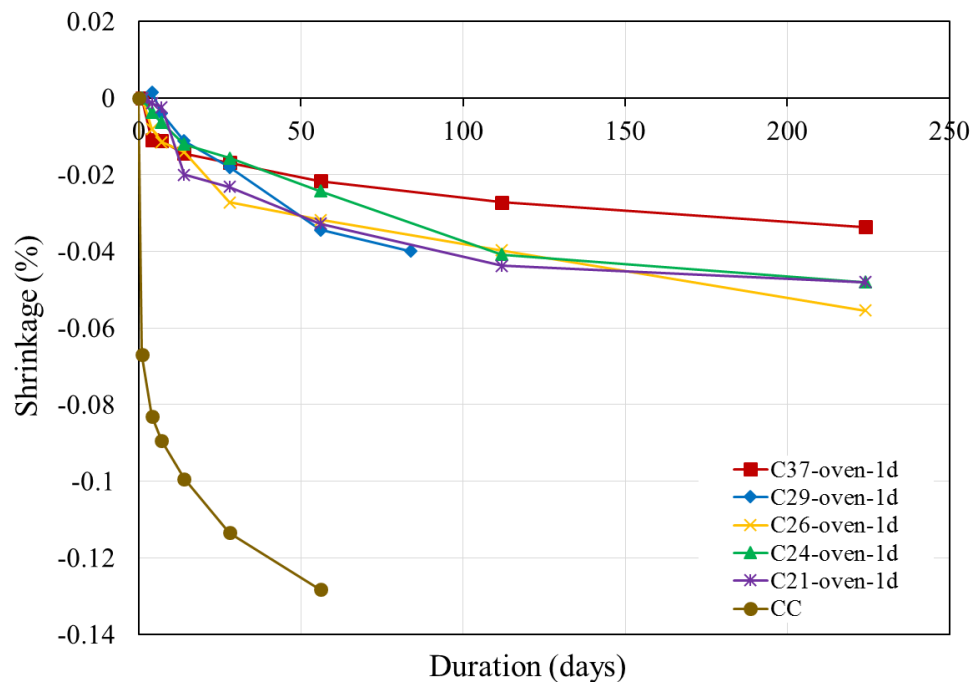
Figure 6.42: Shrinkage results of the oven-cured specimens tested directly after 24 hours of oven curing.
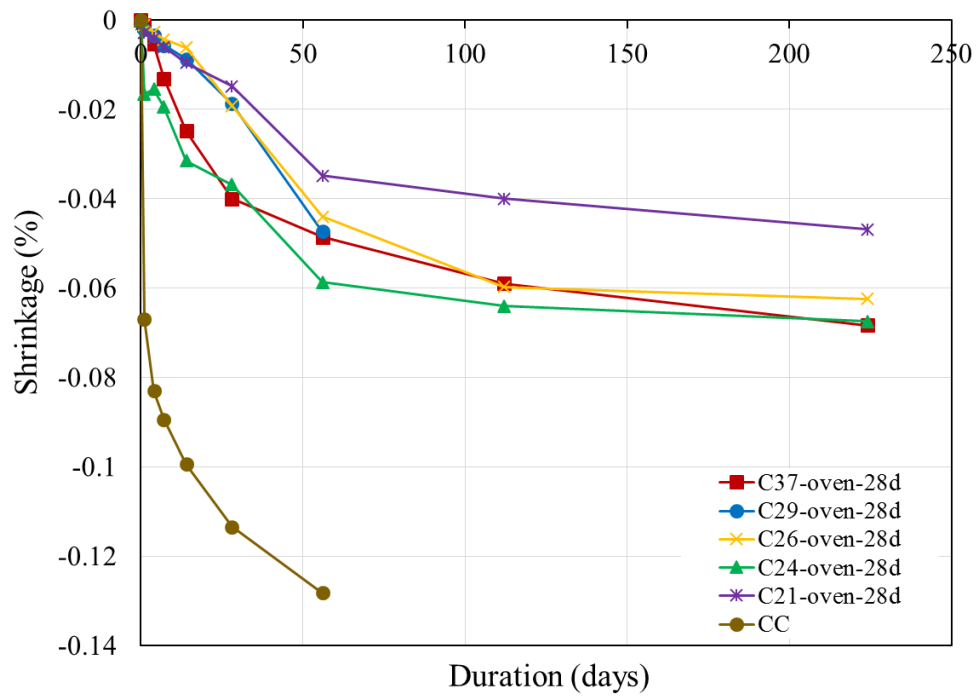
Figure 6.43: Shrinkage results of the oven-cured specimens stored for 28 days then tested.
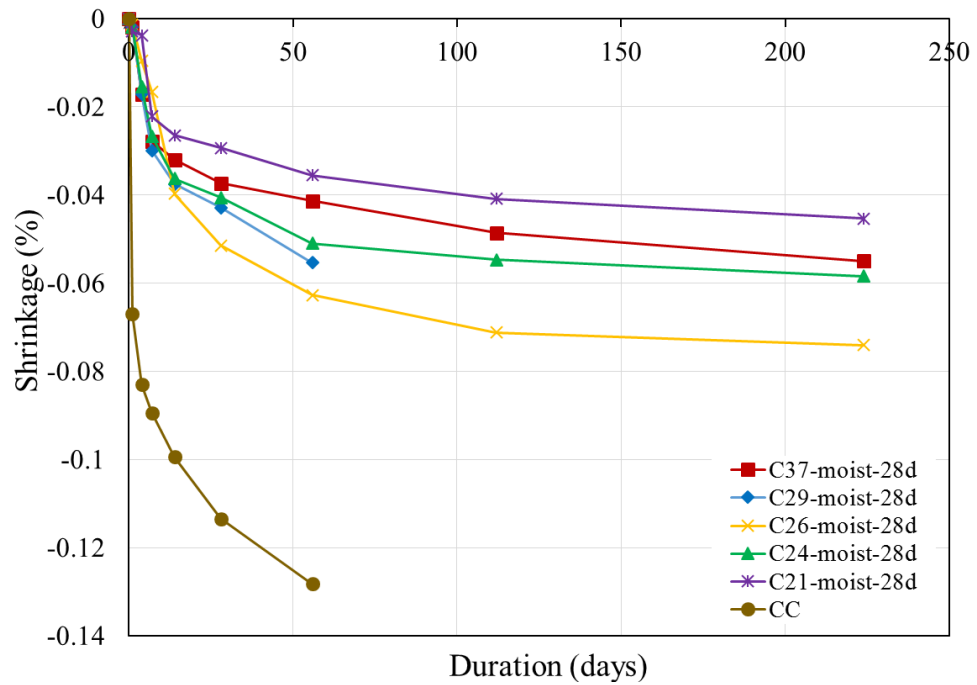
Figure 6.44: Shrinkage results of the moist-cured specimens stored for 28 days then tested.

As shown in the figure, the drying shrinkage values of the oven-cured ZCC specimens were significantly less than those of the CC mixture. At 56 days, the drying shrinkage values of the ZCC mixtures ranged from 0.0216% to 0.0344% with an average of 0.029%, from 0.0348% to 0.0587% with an average of 0.0467%, and from 0.0355% to 0.0627% with an average of 0.0491%, for the oven-cured specimens that were tested directly after 24 hours of oven curing, the oven-cured specimens that were stored for 28 days then tested, and the moist-cured specimens that were stored for 28 days then tested, respectively. However, at 56 days, the drying shrinkage of the CC mixture was 0.1282%. Hence the drying shrinkage of the ZCC mixtures at 56 days are 77%, 64%, and 62% lower than that of the CC mixture.

The curing regime was also a prominent influential parameter on the drying shrinkage. At 224 days, the drying shrinkage values ranged from 0.0336% to 0.0555% with an average of 0.0463%, from 0.0468% to 0.0683% with an average of 0.0613%, and from 0.0453% to 0.074% with an average of 0.0582% for the oven-cured specimens that were tested directly after 24 hours of oven curing, the oven-cured specimens that were stored for 28 days then tested, and the moist-cured specimens that were stored for 28 days then tested, respectively.

6.3 Findings and Conclusions

This chapter presents the mechanical properties of ZCC mixtures synthesized from FA sourced from five different locations in Missouri. A reference CC mixture was prepared and tested as well. The ZCC mixtures were subjected to three curing regime namely oven, ambient, and moist. The compressive strength, splitting tensile, modulus of rupture, modulus of elasticity, and drying shrinkage of each ZCC mixture were determined. The following conclusions can be drawn from this investigation:

- The oven curing regime is more suitable for the ZCCs that were synthesized using FA having a lower calcium content while ambient and moist curing are more suitable for ZCC that were synthesized using FA having a high calcium content. C21, C24, C26, C29, and C37 displayed compressive strengths of 5485, 5410, 4630, 3635, and 4485 psi after curing at 158° F (70 ^{o} C) for 24 hours. However, C21, C24, C26, C29, and C37 displayed compressive strengths of 4305, 3995, 4420, 4525, and 5170 psi after 7 days and 4770, 4270, 4465, 4825, and 5310 psi after 28 days of ambient curing. Furthermore, C21, C24, C26, C29, and C37 displayed compressive strengths of 4840, 5340, 5105, 4685, and 5510 psi after 7 days and 6625, 7425, 6880, 6605, and 7465 psi after 28 days of moist curing, respectively.

- The compressive strength significantly increased from 1 to 7 days for moist and ambient-cured specimens while it remained approximately constant for oven curing beyond 1 day. The increases in compressive strength of the ZCC from 1 day to 7 days were 976%, 902% 1079%, 72%, and 88% for ambient-cured and 1110%, 1238%, 1299%, 88%, and 100% for moist-cured specimens for C21,C24, C26, C29, and C37 respectively. Beyond 7 days, the rates of increase in the strength decreased. The increases in compressive strength from 7 days to 28 days were 10.9%, 6.8%, 1.0%, 6.7%, and 2.7% for ambient-cured and 36.9%, 39.1%, 34.8%, 40.9%, and 35.4% for moist-cured specimens for C21, C24, C26, C29, and C37, respectively. For oven curing, the compressive strength increased by 8.4%, 12.4%, 6.4%, 0.7%, 11.0% for C21, C24, C26, C29, and C37, respectively, from the age of 1 day to 28 days.

- The relationships between the compressive strength of ZCC and splitting tensile strength, flexural strength, and modulus of elasticity are similar to those used by ACI 318-14 [133], AS 3600 [134] design code, and CEB-FIP model code [135].

- The ACI 318-14 [133] and CEB-FIP model code [135] overestimated the splitting tensile strength of ZCC by an average of 9% and 11%, respectively, while AS 3600 [134] underestimated the splitting tensile strength by 27%. Furthermore, the ACI 318-14 [133] and CEB-FIB [135] also overestimated the splitting tensile strength of CC by 12% and 9%, respectively.

- The CEB-FIP model code [135] overestimated the flexural strength of ZCC by an average of 9%, while ACI 318-14 [133] and AS 3600 [134] underestimated the flexural strength by 24% and 29%, respectively. Furthermore, CEB-FIB [135] also overestimated the splitting tensile strength of CC by 5%.

- The ACI 318-14 [133] and CEB-FIP model code [135] underestimated the modulus of elasticity of ZCC by an average of 12% and 20%, respectively.

- The drying shrinkage values of the ZCC specimens with different curing regimes at all ages were significantly lower than those of the CC specimens. At 56 days, the average shrinkage values of ZCC were 0.029%, 0.0467%, and 0.0491% for the oven-cured specimens that were tested directly after 24 hours of oven curing, the oven-cured specimens that were stored for 28 days then tested, and, the moist-cured specimens that were stored for 28 days then tested, respectively, while it was 0.1282% for the moist-cured CC specimens. This indicates that the ZCC would display fewer cracks during its service life, resulting in less penetration of any deicing or other harmful salts that could cause deterioration.

Chapter 7: Durability of Zero-Cement Concrete

With an average of 110 days with temperatures below 32° F (0° C), freeze-thaw durability is a crucial issue in the state of Missouri, as there is considerable degradation of concrete pavements and roads.

The durability of zero-cement concrete (ZCC) is presented in this chapter. Durability was investigated by testing freeze-thaw resistance, surface resistivity, bulk electrical conductivity, and rapid chloride ion penetration per ASTM C666-15 [74], AASHTO TP 95 [137], ASTM C1760-12 [138], and ASTM C1202-17 [139], respectively.

Freeze-thaw damage is caused by unreacted free water molecules that freeze and expand at low temperatures, breaking the cementitious binders[140]. There are two possible solutions to this issue: either reduce free water in the matrix, or introduce admixtures that control air voids to dissipate the stress from free water expansion that leads to disintegration of the paste structure [141-143]. However, all admixtures are designed specifically for OPC, which behaves considerably differently to FA. Hence, this chapter focuses mainly on investigating the performance of ZCC without any admixtures. The results are compared to those of CC without any admixtures as well.

7.1 Experimental Program

7.1.1 Materials

Chapter 2 of this report details the materials used for the concrete mixtures presented in this chapter including the alkali activators, sand, coarse aggregate, FAs, and slag. As discussed in Chapter 2, different batches of FA were received and used during the course of this project. Five

FAs, FA37, FA29, FA26, FA24, and FA21 of the second batch, were used to prepare the concrete mixtures presented in this chapter. A 5000 psi MoDOT conventional concrete (CC) mixture was also prepared and tested along with the ZC concrete mixtures for comparison purpose.

7.1.2 Mix design

The optimum Alk/FA, and SS/SH in ZCC were 0.30 and 1.0 as presented in Chapter 4, respectively, and they were used in the mixture investigated throughout this chapter. The W/FA was adjusted in each mixture based on the FA chemical composition and physical properties to have good workability. The mixtures used in this chapter are shown in Table 7.1. As shown in the table, those mixtures are similar to those used and presented in Chapter 4. Furthermore, the literature proposes that adding slag to the FA improves the freeze and thaw resistance of ZCC [39]. Hence, two types of slags, S1 and S2, were used as a partial replacement of the FA in C26 mixture which was prepared using FA26, which has medium calcium content. Similarly, a crumb rubber was added to mixture C37 as an additive with volume equals to 4% of the total volume of the mixture for investigating the effect of the rubber on the freeze and thaw resistance of ZCC. In addition, an air entraining admixture (AEA), BASF Master AE200, was added to mixture C21 to study its effect on the freeze and thaw resistance of ZCC. The AEA dosage was 0.51 mft^3/100lb (32 mL/100 kg) of the FA.

The nomenclatures of the ZCC mixtures start with the letter "C" for concrete, followed by "S" for a mixture with slag as a partial replacement, followed by the calcium content percentage of the FA used, followed by 1 or 2 to indicate which type of slag was used in that mixture, followed by O for oven curing or M for moist curing. For example, CS26-1M is a ZCC made of an FA

having a calcium content of 26%, a slag S1 as a replacement, and moist curing. Table 7.1 shows the mix proportions of the nine mixtures investigated in this chapter.

Table 7.1: Mix Design of ZC Concrete Mixtures for Durability Testing (lb/ft^3).

Mix	W/FA	Alk/FA	SS/SH	W/C	C.A^a (lb/ft^3)	Sand (lb/ft^3)	FA (lb/ft^3)	S.S. (lb/ft^3)	S.H. (lb/ft^3)	W (lb/ft^3)	Slag (lb/ft^3)	C (lb/ft^3)
C21	0.34	0.30	1.0	-	60.7	50.6	28.1	4.21	4.21	4.89	-	-
CA21	0.34	0.30	1.0	-	60.7	50.6	28.1	4.21	4.21	4.89	-	-
C24	0.36	0.30	1.0	-	59.9	49.9	28.1	4.21	4.21	5.43	-	-
CS26-1	0.40	0.30	1.0	-	58.2	48.4	19.7	4.21	4.21	6.43	8.43	-
CS26-2	0.39	0.30	1.0	-	58.2	484	19.7	4.21	4.21	6.31	8.43	-
C29	0.38	0.30	1.0	-	59.0	49.2	28.1	4.21	4.21	5.99	-	-
C37	0.40	0.30	1.0	-	58.2	48.4	28.1	4.21	4.21	6.43	-	-
CR37	0.40	0.30	1.0	-	58.2	48.4	28.1	4.21	4.21	6.43	-	-
CC	-	-	-	0.54	67.9	56.6	-	-	-	10.9	-	19.2

^{a}CA: coarse aggregate

7.1.3 Mixing procedure

Mixing procedure no. 8 was used in this chapter as described in Chapter 3. When the slag was used, it was added to the mixer after adding the FA and before adding the water.

7.1.4 Casting and curing conditions

Cylinders measuring 4 x 8 in and prisms measuring 3 x 3 x 16 in and 3 x 4 x 16 were cast and cured to determine the compressive strength and the durability of the ZCC specimens. The specimens were either oven or moist cured; both curing regimes are explained in detail in Chapter 6. The cylinders, 3 x 3 x 16 in prisms, and 3 x 4 x 16 in prisms were cured for 28 days, 28 days, and 35 days, respectively, before subjecting them to freezing and thawing cycles. The oven-cured specimens were cured in the oven for 24 hours, then stored in the moisture room until testing commenced.

The ZCC mixtures that were synthesized using relatively low-calcium-content FA, FA21 and FA24, were oven cured. Those that were synthesized using FA29 and FA37 were moist cured. Two identical sets of specimens were prepared using the mixtures that included the slag. One set was oven cured and the other set was moist cured. Furthermore, the rubber and the AEA were added to ZCC mixtures synthesized using FA37 and FA21, respectively. The former mixture was moist cured while later mixture was oven cured.

7.1.5 Fresh and mechanical properties testing

Both the slump and air content of the prepared mixtures were measured per ASTM C143-15 [103], and ASTM C231-14 [122], respectively. The compressive strength of each mixture at the age of 28 days was measured for each curing regime.

7.1.6 Freeze and thaw test

The 3 x 3 x 16 in prisms were tested according to testing procedure A per ASTM C666-15 [74] at Missouri University of Science and Technology while the 3 x 4 x 16 in prisms were tested according to testing procedure B per ASTM C666-15 [74] at the MoDOT Construction and Materials Testing Laboratory in Jefferson City, Missouri. For procedure A, the prisms were completely immersed in water while they were subjected to freezing and thawing cycles. For procedure B, the prisms were left in the air during the freezing phase of each cycle while immersed in water during the thawing phase of each cycle. Before subjecting the prisms to the freezing and thawing cycles, the fundamental transverse frequency of the specimens was measured using the ultrasonic pulse velocity test (Fig. 7.1).

Figure 7.1: Ultrasonic pulse velocity test.

The specimens that were tested under procedures A and B conditions were subjected to sets of freezing and thawing cycles. For procedure A, each set consisted of 36 cycles; however, for procedure B, each set consisted of 9 to 35 cycles. After each set, each specimen was taken out of the chamber, and its fundamental transverse frequency was measured, and the dynamic modulus of elasticity calculated; then, the specimen was placed back in the chamber for another set of cycles. Testing continued until 300 cycles of freeze and thaw or the tested specimen lost more than 40% of its original relative dynamic modulus of elasticity. The relative dynamic modulus of elasticity and durability factor for each specimen were calculated as described in Eqs.7.1 and 7.2, respectively [74]. Fig. 7.2 shows specimens in the freeze and thaw chamber before starting the test.

$$P_c = (n_1^2/n^2) \; x \; 100 \qquad\qquad (7.1)$$

$$DF = PN/M \qquad\qquad (7.2)$$

Where: P_c is the relative dynamic modulus of elasticity, after c cycles of freezing and thawing, n is the fundamental transverse frequency at 0 cycles of freezing and thawing, and n_1 is the fundamental transverse frequency after c cycles of freezing and thawing. DF is the durability

factor, P is the relative dynamic modulus of elasticity at N cycles, N being the number of cycles at which P reaches the specified minimum value for discontinuing the test or the specified number of cycles at which the exposure is to be terminated, whichever is less, and M being the specified number of cycles at which the exposure is to be terminated [74].

Figure 7.2: Freeze and thaw chamber for procedure A of ASTM C666-15 [74].

7.1.7 Surface resistivity

The concrete is a porous material, and the solid part of the concrete has a high surface resistivity. However, capillary pores that are fully or partially saturated with water have a lower relative resistivity as the electrical current can flow through these pores. Therefore, the surface resistivity can indicate the quality of the concrete, where low resistivity indicates more porous concrete. Low permeability results from a small pore network with low connectivity leading to high electrical resistivity.

The electrical resistivity ρ (Eq. 7.3) is a function of the applied voltage V by the instrument on the specimen, the resulting current flow I intensity due to the applied voltage on the specimen, and the specimen constant k which is the geometrical parameter (Eq. 7.4) that is a function of the size and the shape of the specimen γ (dimensionless factor) as well as the distance between the electrodes a (Eq. 3) [144].

$$\rho = k \cdot \left(\frac{V}{I}\right) \tag{7.3}$$

$$k = \gamma \cdot a \tag{7.4}$$

The surface resistivity per AASHTO TP 95 [137] of each mixture was determined using a Respiod resistivity meter with a uniform electrode spacing of 1.5 in to assess the surface resistivity of the cylinders (Fig. 7.3). The Respiod resistivity meter was designed based on a Wenner probe (Fig. 7.4) [145]. The cylinder specimens were stored in lime-water until the testing age. Then, the specimens were taken directly and tested. For each concrete mixture, two 4x8 in cylinders were tested. For each specimen, four different readings at angles of 0°, 90°, 180°, and 270° around the circumference were measured and their average value was calculated. Furthermore, the reported results are the average of readings of the two specimens per mixture. The evaluation of the surface resistivity test was according to AASHTO TP 95 [137] assessments (Table 7.2).

Figure 7.3: Surface resistivity test.
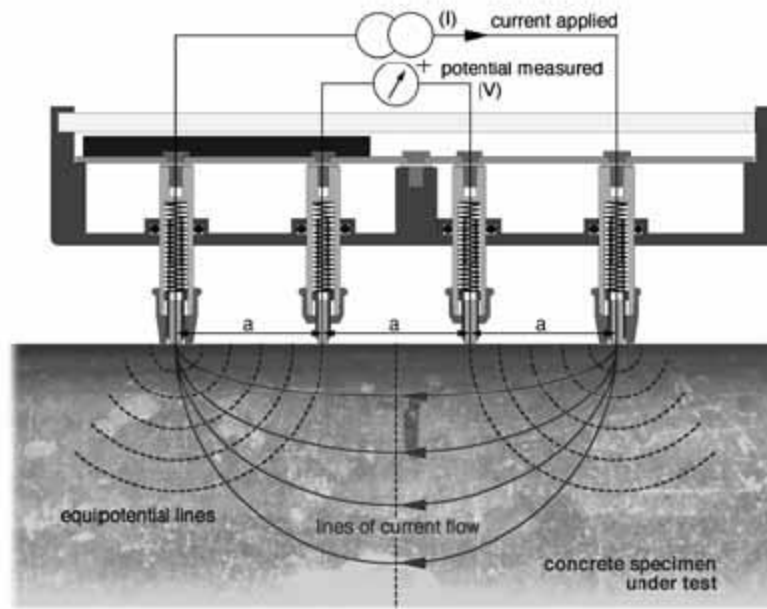
Figure 7.4: Principles of surface resistivity test [145].

Table 7.2: Surface Resistivity Test Results Assessment.

Permeability class	AASHTO TP 95 (kohm-cm)
High	< 12
Moderate	12-21
Low	21-37
Very Low	37-254
Negligible	>254

7.1.8 Bulk electrical conductivity

The cylinders that were used for the surface resistivity were also used to measure the bulk electrical conductivity per ASTM C1760-12 [138]. The two ends of each specimen had to be grinded to provide a flat and smooth surface prior to measuring the bulk electrical conductivity (Fig. 7.5). The setup consisted of two steel plates and two pieces of foam in wet condition. The two pieces of foam were placed on the top and bottom of each test cylinder. The steel plates were then placed so that they sandwiched the foam pieces and test cylinders (Fig. 7.6). The bulk resistivity ρ is a function in applied voltage and the current flow I and the geometrical parameter

k (Eq. 7.3). However, k in function is the cross sectional area A perpendicular to the current, which is the cross sectional area of the cylinders and the height of the specimen L (Eq. 7.5). The reported results were the average readings of two specimens.

$$k = \frac{A}{L} \tag{7.5}$$

Figure 7.5: Grinded surfaces of the test specimens prior to the bulk electrical conductivity test.

Figure 7.6: Bulk electrical conductivity testing.

7.1.9 Rapid chloride ion penetration (RCIP)

A rapid chloride ion penetration (RCIP) test was carried out on the ZCC to assess the durability of the concrete per ASTM C1202-17 [139]. A two in thick concrete disk was cut from each cylinder cast out of the different ZCC mixtures (Fig. 7.7). The test started with coating the sides of the disk with a non-permeable epoxy to prevent the penetration of any liquid through the disk sides during the testing process, i.e., to ensure a unidirectional flow through the surfaces of the disks. Each disk was placed inside a vacuum desiccator; then, the desiccator was sealed, and a vacuum pump was started applying a pressure of 6650 Pa for 3 hours. Thereafter, while the vacuum pump was still running, the water stopcock was opened, and sufficient water was drained into the desiccator until the specimens were fully covered by the water. The water stopcock was closed, and the vacuum pump was allowed to run for one additional hour; then, the pump was turned off. The specimens were soaked under water for 18 hours (Fig. 7.8a). The disks were placed between two cells (Fig. 7.8b). One of the cells was filled with a 0.3N NaOH solution and the other cell was filled with a 3% NaCl solution. Thereafter, the disks were subjected to 60 volts and tested for 6 hours (Fig. 7.8c). The performance of each test specimen under the rapid chloride ion penetration test was assessed per ASTM C1202-17 [139] (Table 7.3) [139].

Figure 7.7: 2 in. high disks for RCIP test.

Table 7.3: Rapid chloride ion penetration test results assessment.

Chloride ion penetrability	Charge passed (ASTM C1202 (Coulombs))
High	>4000
Moderate	2000-4000
Low	1000-2000
Very Low	100-1000
NE	<100
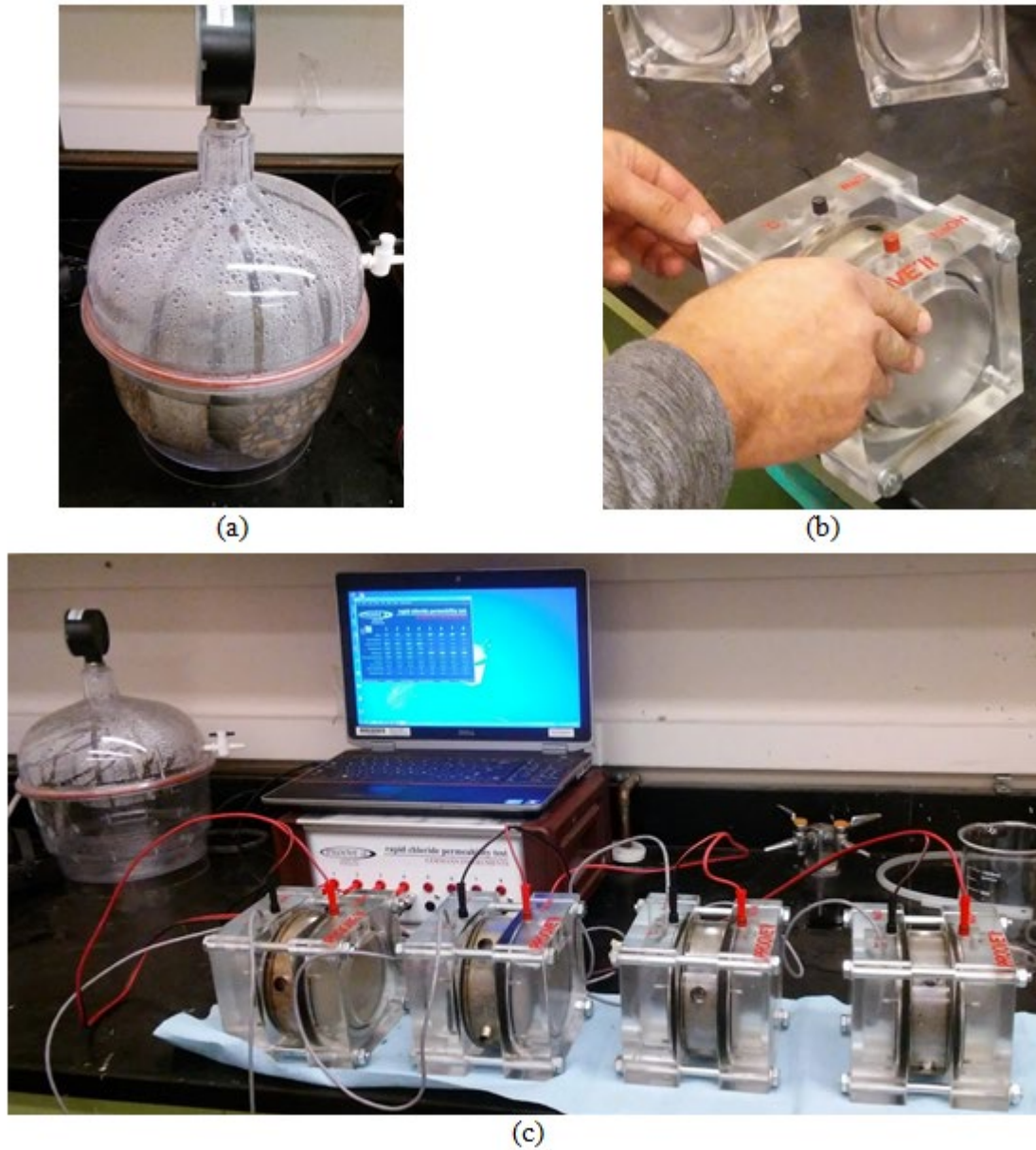
Figure 7.8: Chloride ion penetration test (a) soaking a disk under water, (b) placing a disk between two cells, and (c) running the test.

7.2 Results and Discussion

7.2.1 Fresh and mechanical properties

Fig. 7.9 shows the slump values of the different ZCC mixtures. The slump values ranged from 6.0 to 10.0 in for all the different mixtures. For the slag mixtures, a higher W/FA ratio was required to achieve workability comparable to those of the other mixtures. This occurred as the

slag had a high calcium content which resulted in lower workability. In addition, the slag had an irregular particle shape which added to the lower workability. Adding the rubber and the AEA resulted in lower and higher workability, respectively, with keeping the W/FA constant compared with their reference mixtures.
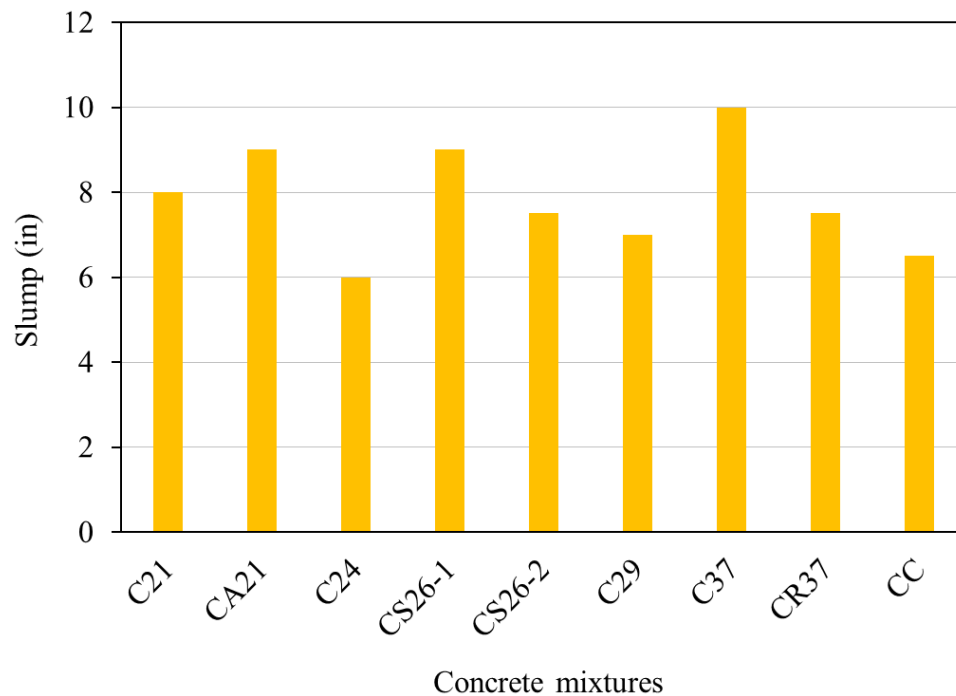
Figure 7.9: Slump values of the different mixtures.

Fig. 7.10 shows the air content of the different mixtures. As shown in the figure, the air content values of all ZCC were lower than that of the CC. The air content of the ZCC mixtures ranged from 0.9% to 3.0% while it was 2.0% for the CC mixture. Generally, Adding the rubber and AEA resulted in higher air content comparing with their reference mixtures.
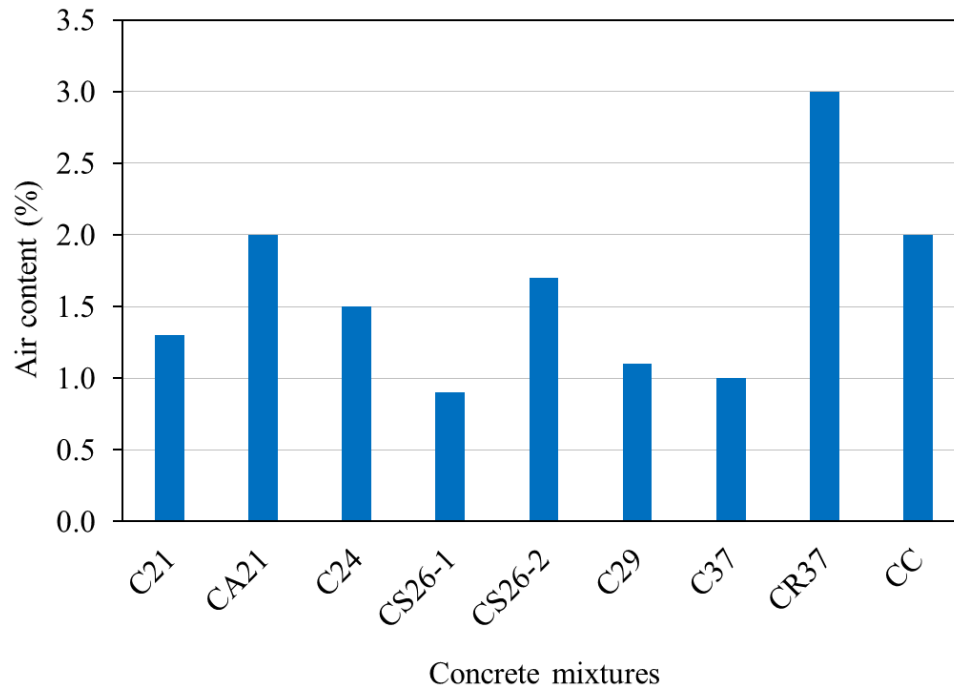
Figure 7.10: Air content of the different mixtures.

Fig. 7.11 shows the compressive strength of the different mixtures. The compressive strength of the ZCC mixtures ranged from 4780 psi to 8010 psi. The compressive strength of the CC mixture was 4775 psi. The compressive strengths of the FA mixtures that had the slag as an additive, CS26-1M and CS26-2M, were 7620 psi and 8010 psi, respectively, which showed the highest compressive strength among the ZCC mixtures in the case of the moist-cured specimens. However, the compressive strengths of these two mixtures, CS26-1O and CS26-2O, were 2475 and 4875 psi, respectively, when they were oven cured, which indicates that the addition of slag is more favorable for the specimens that cured in the moist room at ambient temperature. Since the compressive strength of CS26-1(O) was less than 4000 psi, it was not tested for durability resistance. Adding the rubber and the AEA resulted in lower compressive strength compared with their reference mixtures.

226
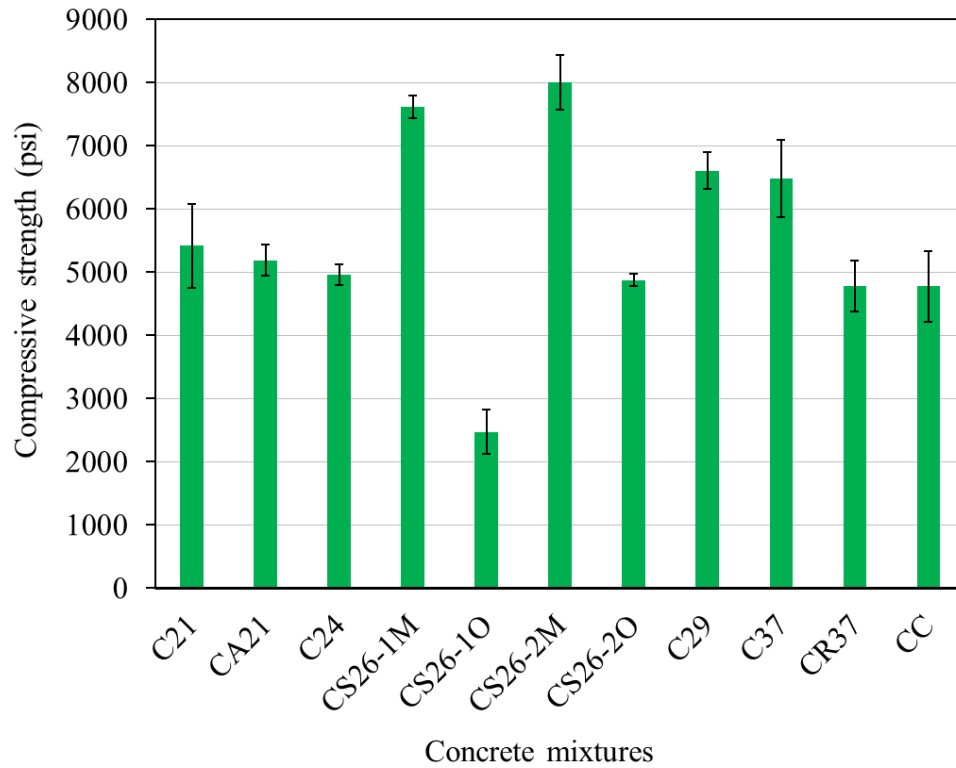
Figure 7.11: Compressive strength of the different mixtures.

7.2.2 Freeze and thaw performance

7.2.2.1 Procedure A

Tables 7.4 and 7.5 show the fundamental transverse frequency and the relative dynamic modulus of elasticity measured for each mixture at the end of each loading set (i.e., 36 cycles), as well as the end of the test at which point the specimen had either been subjected to 324 cycles or had lost 40% of its dynamic modulus of elasticity.

Table 7.4: Fundamental Transverse Frequency (1/µs) and Relative Dynamic Modulus of Elasticity (%).

Mix	C21	C21	CA21	CA21	C24	C24	CS26-1M	CS26-1M	CS26-2O	CS26-2O
No. of cycles	$1/FTF_a$	P_c^b	$1/FTF_a$	P_c^b	$1/FTF_a$	P_c^b	$1/FTF_a$	P_c^b	$1/FTF_a$	P_c^b
0	92.1	100.0	86.0	100.0	92.2	100.0	78.3	100.0	83.4	100.0
36	92.3	99.6	88.7	94.0	139	44.0	78.8	98.7	89.8	86.4
72	93.4	97.2	148.5	33.5	-	-	79.9	96.0	91.4	83.4
108	94.8	94.3	-	-	-	-	78.0	100.8	89.2	87.5
144	102.3	80.9	-	-	-	-	79.2	97.6	85.8	94.5
180	109	71.3	-	-	-	-	79.6	96.8	87.9	90.1
216	375	6.0	-	-	-	-	80.1	95.6	88.1	89.6
252	-	-	-	-	-	-	80.7	94.0	88.7	88.5
288	-	-	-	-	-	-	80.9	93.6	89.3	87.2
324	-	-	-	-	-	-	82.6	89.9	95.7	76.0

[a]FTF: Fundamental transverse frequency
[b]P_c: Relative dynamic modulus of elasticity

Table 7.5: Fundamental Transverse Frequency (1/µs) and Relative Dynamic Modulus of Elasticity (%).

Mix	CS26-2M	CS26-2M	C29	C29	C37	C37	CR37	CR37	CC	CC
No. of cycles	$1/FTF^a$	P_c^b	$1/FTF^a$	P_c^b	$1/FTF^a$	P_c^b	$1/FTF^a$	P_c^b	$1/FTF^a$	P_c^b
0	80.9	100.0	82.6	100.0	80.1	100	91.2	100	82.5	100
36	84.3	92.1	84.5	95.4	87.1	84.6	91.6	99.1	346	5.7
72	83.5	93.9	93.6	77.8	89.1	80.8	90.1	102.5	-	-
108	82.2	96.9	74.1	77.0	93.2	73.9	88.4	106.4	-	-
144	84.8	91.0	346	5.7	94.7	71.5	90.4	101.8	-	-
180	97.4	69.1	-	-	103	60.5	90.4	101.8	-	-
216	346	5.5	-	-	-	-	89.6	103.6	-	-
252	-	-	-	-	-	-	87.9	107.7	-	-
288	-	-	-	-	-	-	88.6	106.0	-	-
324	-	-	-	-	-	-	89.2	104.5	-	-

[a]FTF: Fundamental transverse frequency
[b]P_c: Relative dynamic modulus of elasticity

Figs. 7.12 through 7.13 show the relative dynamic modulus of elasticity and the durability factor of the different mixtures. As shown in the figures, the durability factor of the CC mixture was the lowest among all the mixtures. Although the CC mixture had a similar compressive strength with five (C21, CA21, C24, CS26-O1, and CR37) ZCC mixtures, the CC specimens were damaged after only 36 cycles. It is worth noting that MoDOT requires a minimum air content of 5%; however, for comparison purposes only, neither the CC nor the ZCC mixtures were provided any air content except mixture CA21.
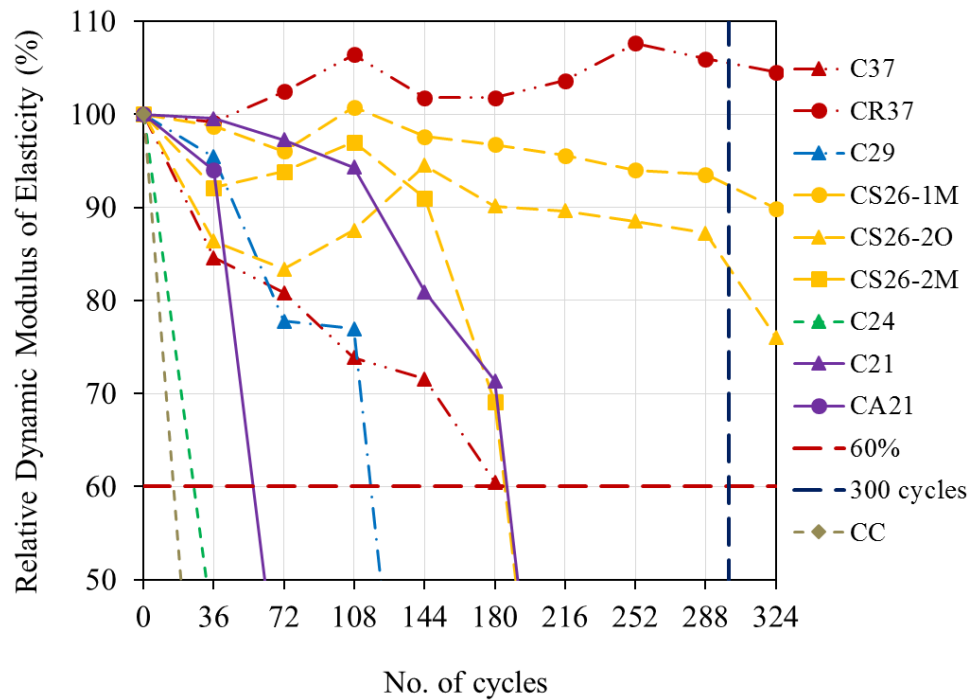
Figure 7.12: Dynamic modulus of elasticity vs. time for specimens subjected to freeze and thaw cycles following procedure A of ASTM C666-15 [74].
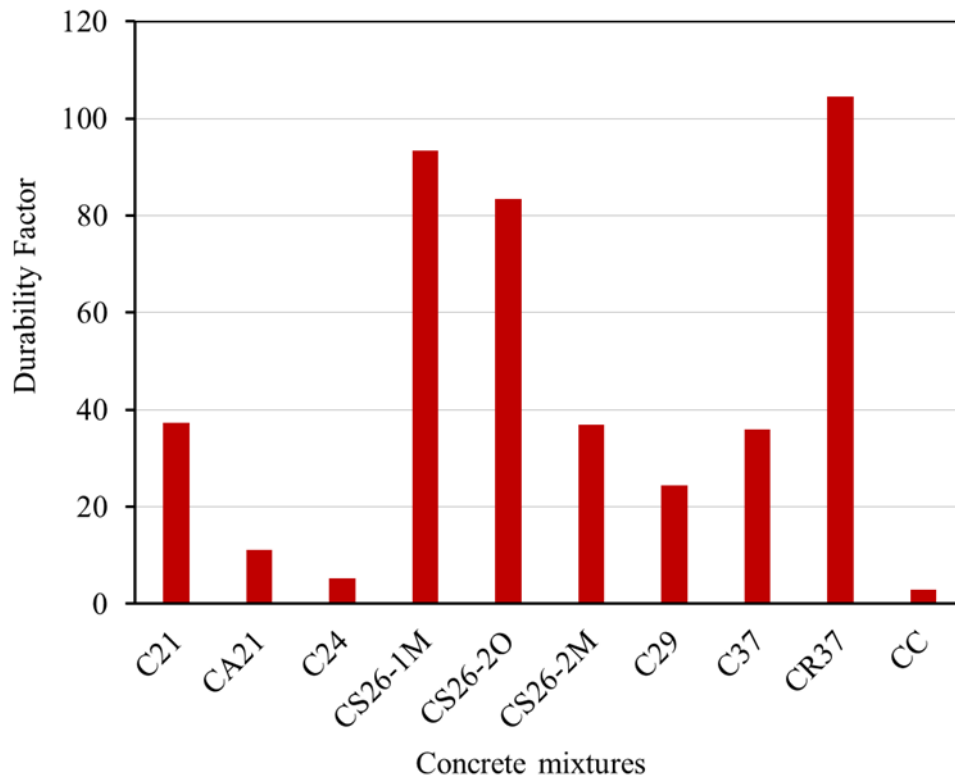
Figure 7.13: Durability factor for the different specimens subjected to freeze and thaw cycles following procedure A of ASTM C666-15 [74].

As shown in Figs. 7.12 and 7.13, mixtures CS26-1M, CS26-2O, and CR37 which included slag and rubber, outperformed all specimens and passed the 300 cycles with a relative dynamic modulus of elasticity of 93.3%, 83.4%, and 104.5% and with a durability factor of 93.3, 83.4, and 104.5, respectively, which exceeded the 60% relative dynamic modulus of elasticity required by ASTM C666-15 [74]. Mixture CS26-2M specimens displayed relative dynamic modulus of elasticity of 91% up to 144 cycles; beyond that a gradual degradation occurred, and all specimens failed at approximately 180 cycles and showed a durability factor of 37. Similarly, specimens C21 and C37 showed degradation in the relative dynamic modulus of elasticity reaching failure, i.e., reduction of 40% in the relative dynamic modulus of elasticity at approximately 180 cycles. Specimens CA21, C24, and C29 were less successful and failed at 56, 26, and 117 cycles, respectively. Specimens C21, CA21, C24, C29, and C37 displayed durability

230

factors of 37.2, 11.2, 5.2, 24.4, and 36, respectively, at failure. Figs. 7.14 and 7.15 show the shape of the ZCC samples after the cycles of freezing and thawing for the test specimens.

| 0 cycle | 216 cycles | 0 cycle | 72 cycles | 0 cycle | 36 cycles |
| (a) C21 | | (b) CA21 | | (c) C24 | |

| 0 cycle | 324 cycles | 0 cycle | 324 cycles | 0 cycle | 216 cycles |
| (d) CS26-1(M) | | (e) CS26-2(O) | | (f) CS26-2(M) | |
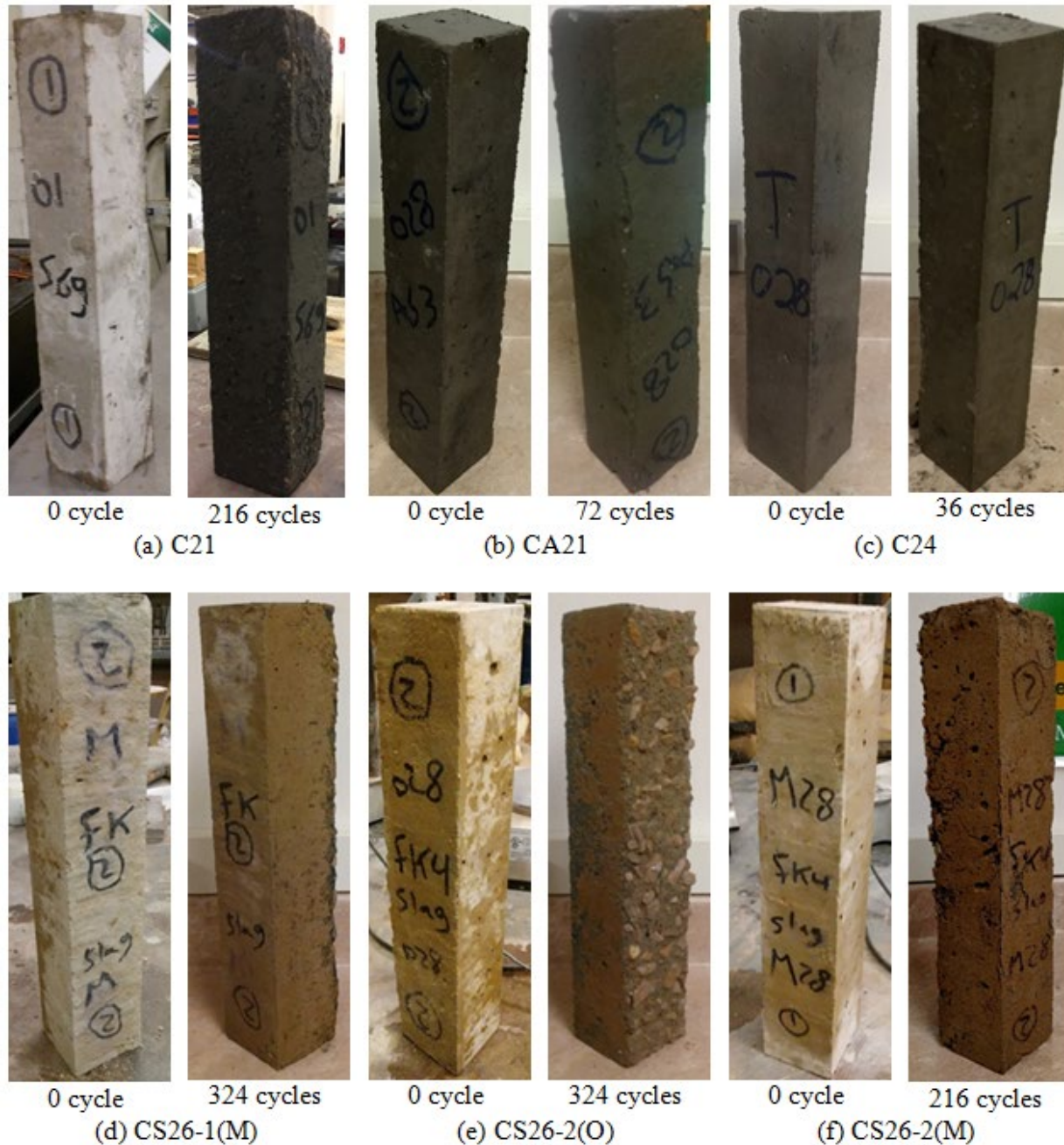
Figure 7.14: ZCC mixtures after freeze and thaw cycles for specimens subjected to freeze and thaw cycles following procedure A of ASTM C666-15 [74].
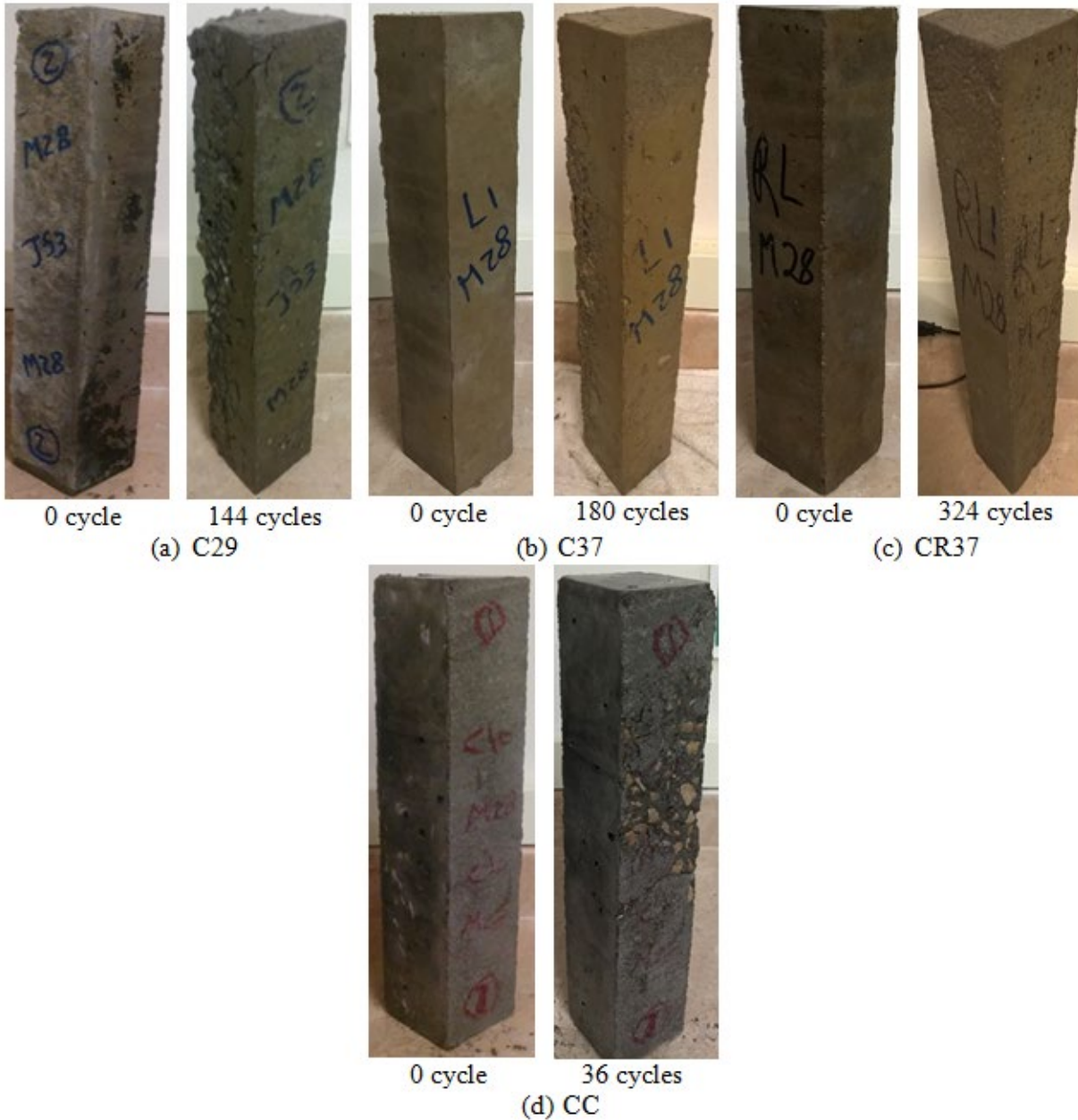
Figure 7.15: (a, b, c) ZCC mixtures, and (d) CC before and after freeze and thaw cycles for specimens subjected to freeze and thaw cycles following procedure A of ASTM C666-15 [74].

7.2.2.2 Procedure B

Only five mixtures were tested following procedure B of ASTM C666-15 [74] included C21, CA21, C37, CR37, and CC. Table 7.6 shows the fundamental transverse frequency and the relative dynamic modulus of elasticity measured for each mixture at the end of each loading set

(i.e., ranged from 9 to 35 cycles), as well as the end of the test at which point the specimen had either been subjected to 311 cycles or had lost 40% of its dynamic modulus of elasticity.

Table 7.6: Fundamental Transverse Frequency (1/µs) and Relative Dynamic Modulus of Elasticity (%).

Mix	C21	C21	CA21	CA21	C37	C37	CR37	CR37	CC	CC
No. of cycles	FTF[a]	P_c[b]	FTF[a]	P_c[b]	FTF[a]	P_c[b]	FTF[a]	P_c[b]	FTF[a]	P_c[b]
0	2184	100.0	2153	100.0	2342	100.0	2205	100.0	2288	100.0
9	1983	82.4	1907	78.5	2284	95.1	2138	94.0	1205	27.7
27	1866	73.0	1446	45.1	2275	94.4	2119	92.4	-	-
62	1438	43.4	-	-	2251	92.4	2115	92.0	-	-
91	-	-	-	-	2182	86.8	2114	91.9	-	-
126	-	-	-	-	2092	79.8	2104	91.0	-	-
135	-	-	-	-	2044	76.2	2103	91.0	-	-
144	-	-	-	-	2025	74.8	2100	90.7	-	-
153	-	-	-	-	1973	71.0	2094	90.2	-	-
188	-	-	-	-	1699	52.6	2089	89.8	-	-
197	-	-	-	-	-	-	2079	88.9	-	-
214	-	-	-	-	-	-	2056	86.9	-	-
249	-	-	-	-	-	-	2016	83.6	-	-
278	-	-	-	-	-	-	1960	79.0	-	-
311	-	-	-	-	-	-	1886	73.2	-	-

[a]FTF: Fundamental transverse frequency
[b]P_c: Relative dynamic modulus of elasticity

Figs. 7.16 through 7.17 show the relative dynamic modulus of elasticity and the durability factor of the different mixtures. As shown in the figures, the durability factor of the CC mixture was the lowest among all the mixtures. Although the CC mixture had a compressive strength similar to that of the three ZCC mixtures (C21, CA21, and CR37), the CC specimens were damaged after only 9 cycles. It is worth noting that MoDOT requires a minimum air content of 5%; however, for comparison purposes only, neither the CC nor the ZCC mixtures were provided any air content except mixture CA21.
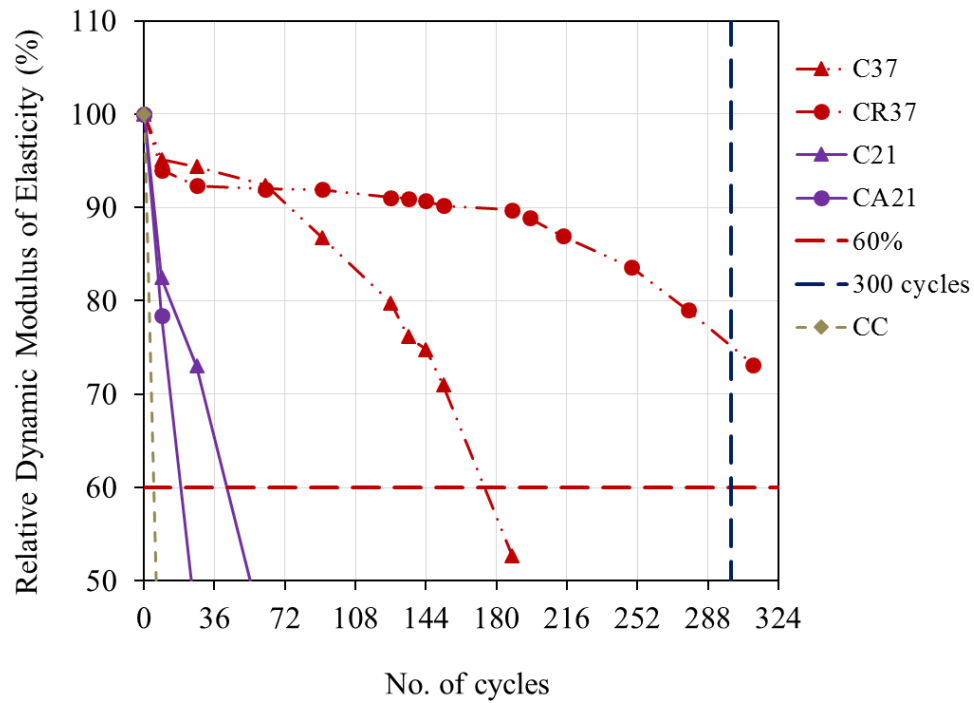
Figure 7.16: Dynamic modulus of elasticity vs. time for the different mixtures for specimens subjected to freeze and thaw cycles following procedure B of ASTM C666-15 [74].
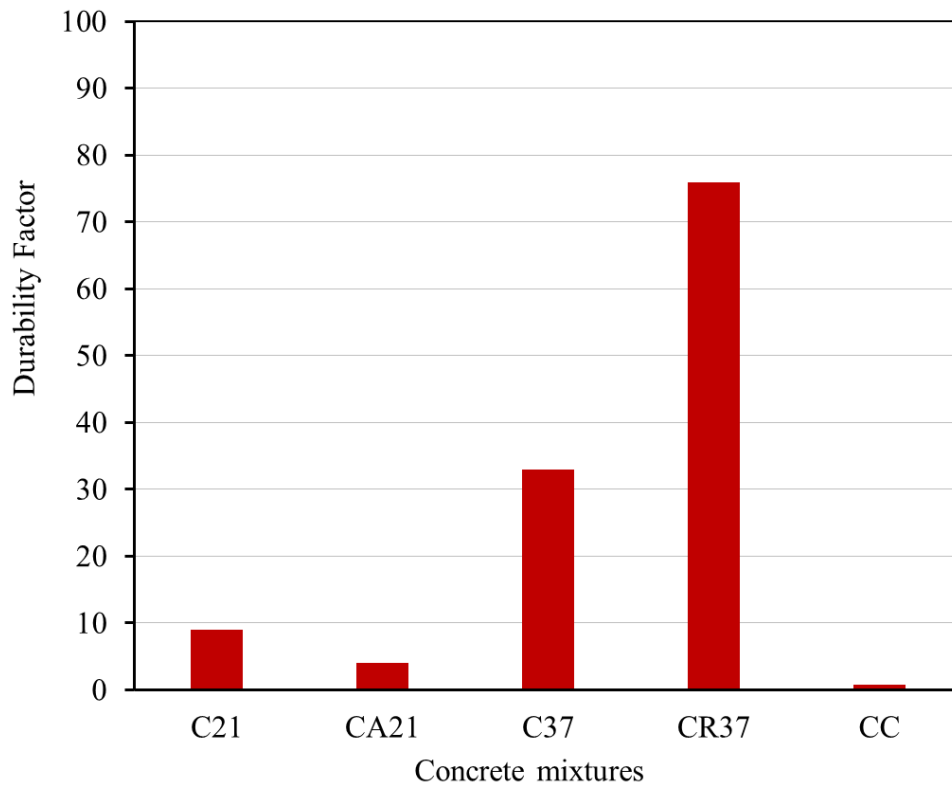
Figure 7.17: Durability factor for the different specimens subjected to freeze and thaw cycles following procedure B of ASTM C666-15 [74].

234

As shown in Figs. 7.16 and 7.17, mixture CR37 which included rubber, outperformed all specimens and passed the 300 cycles with a relative dynamic modulus of elasticity of 75.9% and with a durability factor of 75.9 which exceeded the 60% relative dynamic modulus of elasticity required by ASTM C666-15 [74]. Specimens C37 showed degradation in the relative dynamic modulus of elasticity reaching failure, i.e., reduction of 40% in the relative dynamic modulus of elasticity at approximately 174 cycles. Specimens C21, and CA21 were less successful and failed at 42 and 19 cycles, respectively. Specimens C21 and CA21 displayed durability factors of 9 and 4, respectively, at failure.

7.2.3 Surface resistivity, bulk electrical conductivity, and rapid chloride ion penetration

The ZCC significantly outperformed the CC in surface resistivity, bulk electrical conductivity, and rapid chloride ion penetration. Tables 7.7 and 7.8 as well as Figs. 7.18 through 7.20 show the results summary of the surface resistivity, bulk electrical conductivity, and chloride ion penetration tests. The surface resistivity values of the oven- and moist-cured ZCC specimens ranged from 11.6 to 35.1 kΩ.cm and from 10.3 to 19.9 kΩ.cm, respectively. The bulk electrical conductivity values of the oven- and moist-cured ZCC specimens ranged from 31.4 to 79.8 kΩ.cm and from 29.8 to 62.1 kΩ.cm, respectively. The surface resistivity and bulk electrical conductivity of the CC mixture values were 9.2 and 29.5 kΩ.cm. The CC mixture showed the lowest surface resistivity and bulk electrical conductivity value among all the mixtures. The surface resistivity of the CC mixture represents approximately 26.2% to 89.3% of that of the ZCC mixture values. Similarly, the bulk electrical resistivity of the CC mixture represents approximately 34.0% to 99.0% of that of the ZCC mixture values. Furthermore, surface

resistivity and bulk electrical conductivity values of the oven-cured specimens were higher than those of the moist-cured specimens.

The rapid chloride ion penetration values (charge passed) of the oven- and moist-cured ZCC specimens ranged from 1578 to 4219 coulombs and from 2459 to 5152 coulombs, respectively. The rapid chloride ion penetration value (charge passed) of the CC mixture was 6964 coulombs. The CC mixture showed the highest rapid chloride ion penetration value among all the mixtures. The rapid chloride ion penetration value (charge passed) of the CC mixture represents approximately 135.2% to 441.3% of that of the ZCC mixture values.

There was a good correlation between the surface resistivity and chloride ion penetration test results. Evaluation of the specimens were the same from both tests except for one specimen, the moist-cured C37 mix, which was assessed as a high-corrosion-risk concrete according to the surface resistivity test but was assessed as a moderate-corrosion-risk concrete per the chloride penetration test.

Table 7.7: Surface Resistivity and Bulk Electrical Conductivity Tests Results and Evaluation.

Mix	Curing regime	Surface resistivity (kΩ.cm)	Bulk electrical conductivity (kΩ.cm)	Evaluation
C21	Oven	35.1	79.8	Low
C21	Moist	14.7	42.4	Moderate
C24	Oven	14.9	40.7	Moderate
C24	Moist	13.8	41.4	Moderate
C26	Oven	22.3	65.2	Low
C26	Moist	19.9	62.1	Moderate
C29	Oven	11.6	31.4	High
C29	Moist	10.3	29.8	High
C37	Oven	27.5	78.3	Low
C37	Moist	10.8	34.6	High
CC	Moist	9.2	29.5	High

Table 7.8: Rapid Chloride Ion Penetration Test Results and Evaluation.

Mix	Curing regime	Chloride ion penetration (charge passed) (coulomb)	Evaluation
C21	Oven	1578	Low
C21	Moist	2459	Moderate
C24	Oven	2176	Moderate
C24	Moist	2719	Moderate
C26	Oven	2615	Moderate
C26	Moist	2531	Moderate
C29	Oven	4219	High
C29	Moist	5152	High
C37	Oven	1689	Low
C37	Moist	3473	Moderate
CC	Moist	6964	High
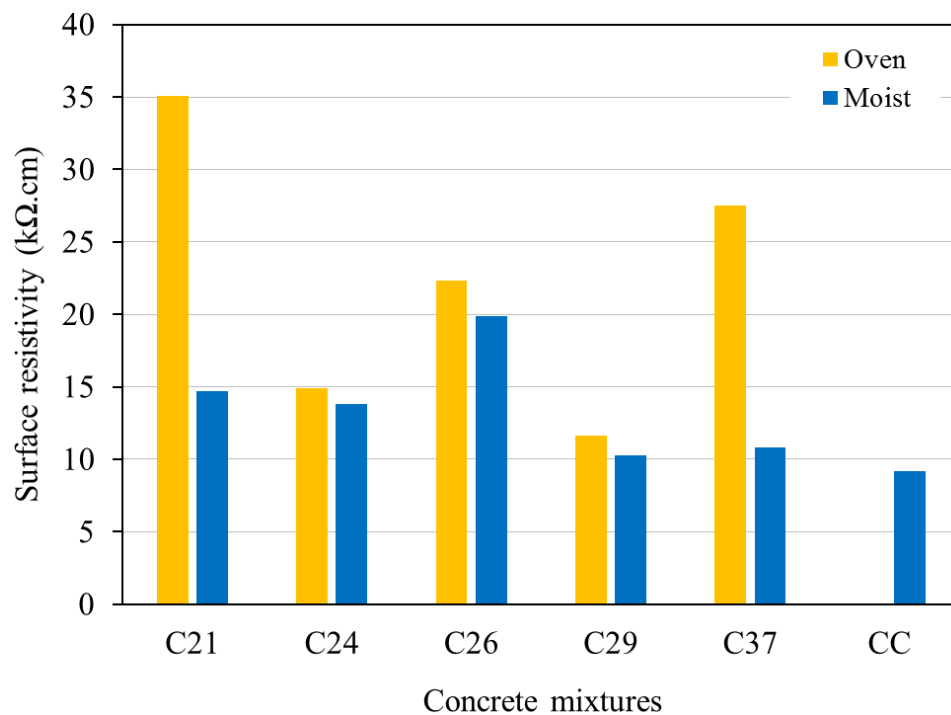
Figure 7.18: Surface resistivity of the different oven- and moist-cured mixtures.
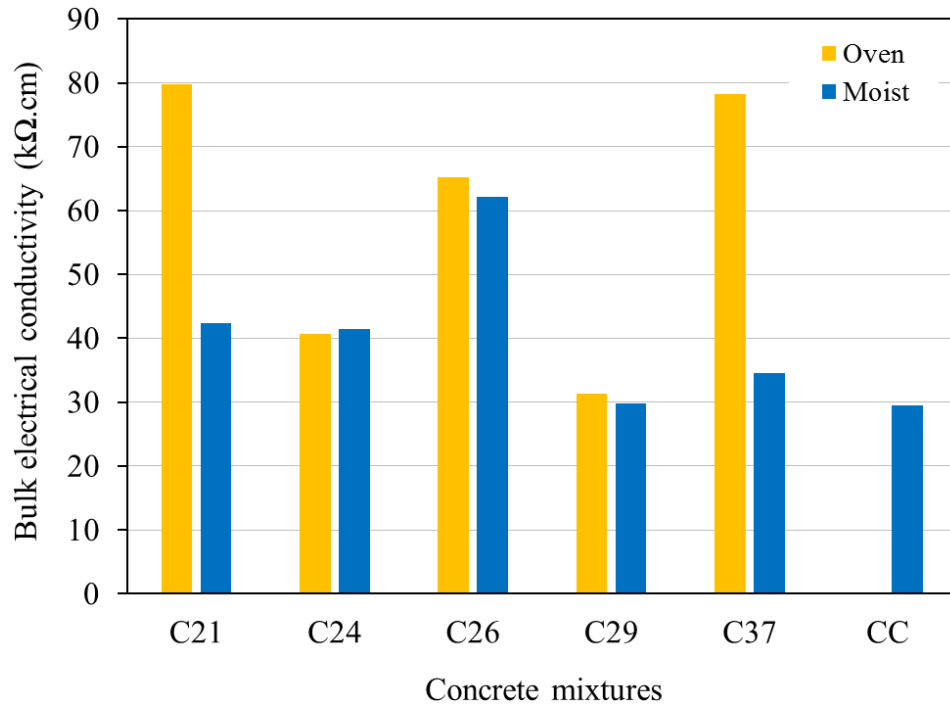
Figure 7.19: Bulk electrical resistivity of the different oven- and moist-cured mixtures.
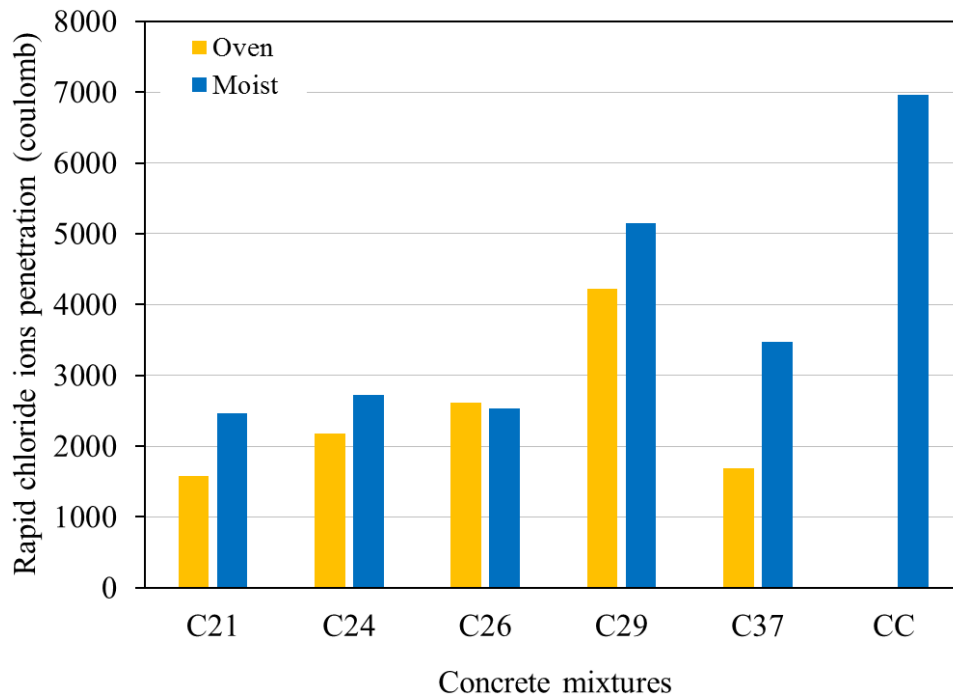
Figure 7.20: Rapid chloride ion penetration of the different oven- and moist-cured mixtures.

7.3 Findings and Conclusions

This chapter presents the durability results of C21, C24, CS26, CS26-1, CS26-2, C29, and C37 ZCC mixtures and a CC mixture. Durability was determined in terms of freeze-thaw resistance, surface resistivity, bulk electrical conductivity, and rapid chloride ion penetration tests per ASTM C666-15 [74], AASHTO TP 95 [137], ASTM C1760-12 [138] , and ASTM C1202-17 [139], respectively.

To improve the durability, CS26-1 and CS26-2 ZCC mixtures were prepared using slag as an additive to replace FA26. Using slag in ZCC mixtures required adding more water, compared to other ZCC mixtures, to keep the mixture slump the same as in ZCC mixtures without slag. The air content of the FA mixtures including slag was almost the same as that of the other FA mixtures. However, the compressive strength of the moist-cured mixtures improved and reached 8010 psi, but the strength of the oven-cured mixture decreased compared with that of the reference mixtures. The following points can be concluded:

- All the ZCC mixtures displayed higher freeze-thaw resistance compared with that of the CC mixture

- The CC mixture failed after only 36 and 9 cycles following procedure A and B per ASTM C666-15 [74], respectively. All other ZCC mixtures were able to resist from 19 to 324 cycles of freeze-thaw for both procedures A and B per ASTM C666-15 [74].

- Among all ZCC mixtures, specimens synthesized using FA21 and FA37 showed the highest freeze-thaw resistance while specimens synthesized using FA24 showed the lowest resistance.

- The durability of the ZCC was improved significantly by adding the slag as a partial replacement and the rubber as an additive to the FA. Two out of three slag specimens

239

successfully passed the 324 cycles of ASTM C666-15 procedure A with durability factor of 93.3 and 83.4 for the moist-and oven-cured specimens, respectively. The rubber specimens successfully passed 324 cycles with a durability factor of 104.5 following ASTM C666-15 procedure A and 311 cycles with a durability factor of 75.9 following C666-15 procedure B, respectively.

- There was a good agreement between the results of the chloride ion penetrability and that of surface resistivity.

- Based on the surface resistivity and chloride ion penetration tests, most of the ZCC mixtures had a low to moderate permeability and chloride ion penetrability. However, the CC mixture showed a high permeability and chloride ion penetrability.

- The results of the rapid chloride ion penetration test showed lower values in the case of most of the ZCC mixtures compared to that of CC. The rapid chloride ion penetration (charge passed) ranged from 0.23 to 0.61 and 0.35 to 0.74 times that of CC for thermally cured and moist-cured. For thermal curing, the rapid chloride ion penetration (charge passed) were 1578, 2176, 2615, 4219, and 1689 coulomb for C21, C24, C26, C29, and C37, respectively. For moist curing, the rapid chloride ion penetration (charge passed) were 2459, 2719, 2531, 5152, and 3473 coulomb for C21, C24, C26, C29, and C37, respectively.

- The results of the surface resistivity test showed higher values in the case of most of the ZCC mixtures compared with CC. The surface resistivity of ZCC ranged from 1.3 to 3.8 and 1.1 to 2.2 times that of CC for thermally cured and moist-cured, respectively. For oven curing, the surface resistivity values were 35.1, 14.9, 22.3, 11.6, and 27.5 kΩ.cm for

C21, C24, C26, C29, and C37, respectively. For moist curing, the surface resistivity values were 14.7, 13.8, 19.9, 10.3, and 10.8, respectively.

- The results of the bulk electrical conductivity test showed higher values in the case of most of the ZCC mixtures compared to that of CC. The bulk resistivity of ZCC ranged from 1.1 to 2.7 and 1.0 to 2.1 times that of CC for thermally cured and moist-cured, respectively. For oven curing, the bulk electrical conductivities were 79.8, 40.7, 65.2, 31.1, and 78.3 kΩ.cm for C21, C24, C26, C29, and C37, respectively. For moist curing, the bulk electrical conductivities were 42.4, 41.4, 62.1, 29.8, and 34.6 kΩ.cm for C21, C24, C26, C29, and C37, respectively.

Chapter 8:   Zero-Cement Concrete as a Repair Material

Slant shear and pull-off tests were carried out to examine the bond between zero-cement concrete (ZCC) and conventional concrete (CC). Adequate bond is required for successful use of ZCC in repairing structures that are constructed out of conventional concrete (CC). During both tests, specimens had been constructed out of CC mixtures representing the host structure, i.e., the existing concrete structural elements. The specimens had been then left to cure. Then, ZCC was used as a repair material by placing it against the CC specimens. Hence, both tests examine the bond between the newly placed ZCC and the existing CC. This chapter reports the material characterization, repair procedure, and results of both tests.

8.1 Experimental Program

8.1.1 Materials

The four FAs, FA21, FA24, FA29, and FA37, obtained from the second batch as explained in Chapter 2 were used throughout this chapter. As explained in Chapter 2, two of the FAs had high calcium content, FA29 and F37, and the other two had relatively low calcium content, FA21 and FA24. The details of the FAs chemical composition, the coarse aggregate, the fine aggregate, and alkali activators were discussed in Chapter 2 of this report.

8.1.2 Mixture design and procedure

Six mixtures were prepared and used during this chapter; this included four ZCC mixtures and two CC mixtures. The four ZCC mixtures were similar to those described and used in Chapter 4. They had Alk/FA of 0.30 and SS/SH of 1.0 (Table 8.1). Mixing procedure no. 8 was used for mixing the concrete as discussed in detail in Chapter 3. Two CC mixtures were used as reference

mixtures with slightly different water-to-cement ratios of 0.50 and 0.54 (Table 8.1). The mixing

procedure of the CC mixture is discussed in Chapter 6.

Table 8.1: Design of ZCC and CC Mixtures (lb/ft^3).

Mix	W/FA	Alk/FA	SS/SH	W/C	C.A^a	Sand	FA	S.S.	S.H.	W	C^b
C21	0.380	0.30	1.0	-	59.0	49.2	28.1	4.21	4.21	6.01	-
C24	0.355	0.30	1.0	-	59.9	49.9	28.1	4.21	4.21	5.31	-
C29	0.390	0.30	1.0	-	58.2	48.4	28.1	4.21	4.21	6.29	-
C37	0.355	0.30	1.0	-	59.9	49.9	28.1	4.21	4.21	5.31	-
CC1	-	-	-	0.540	66.7	55.6	-	-	-	10.8	18.9
CC2	-	-	-	0.500	67.9	56.6	-	-	-	10.1	19.2

^{a}CA: coarse aggregate
^{b}C: cement

8.1.3 Casting and curing of the test specimens

8.1.3.1 Slant shear specimens

To prepare a test specimen, the CC1 mixture representing the host material was placed in a 4 x 8

in cylinder to fill one half of the cylinder. While the concrete was still fresh, the cylinders were

then placed on a wooden form that was designed to make the cylinders set on an angel of 45°

(Fig. 8.1). Therefore, the final surface of each cylinder was inclined at an angel of 45°. After

casting the half-cylinder specimens, the curing regime was applied. The curing regime was moist

curing where the half-cylinder specimens were stored, still in the plastic molds, in a moisture

room having a relative humidity of 95 ± 5% for 28 days (Fig. 8.2). Fig. 8.3 shows the CC half-

cylinder specimens after 28 days of moist curing.

Figure 8.1: Preparing the test specimens for the slant shear test (a) form work inclined at 45°, and (b) applying oil to the plastic cylinders.

Figure 8.2: Storing the half cylinders of the CC specimens in the moisture curing room.

(a)   (b)
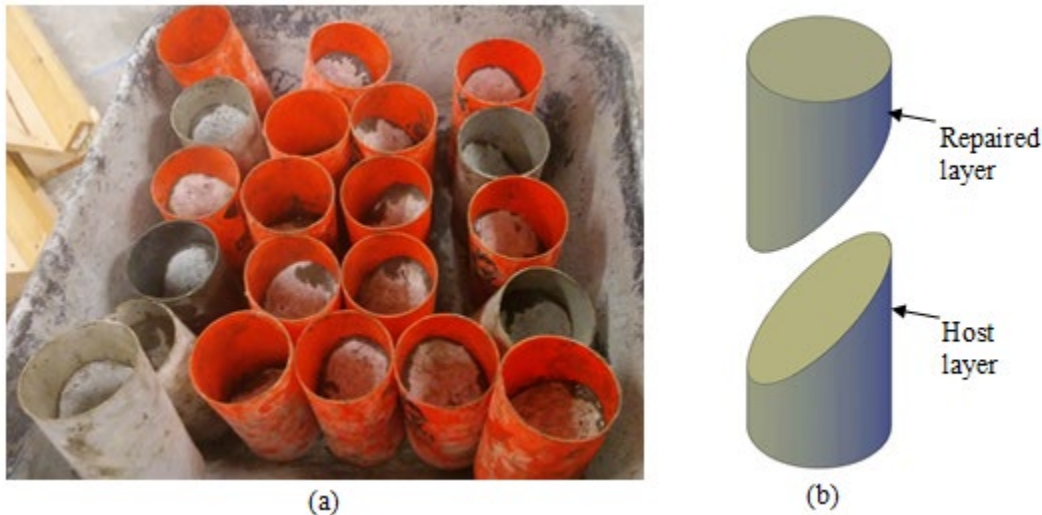
Figure 8.3: (a) Half cylinders of the CC mixture after moisture curing and (b) schematic for the host and repaired layers.

After curing the CC specimens, which represent the host structure, the ZCC, which represents the repair material, was placed against the CC specimens to fill the second half of each plastic cylinder. Neither surface treatment nor bond agent was applied to any of surfaces of the CC half-cylinder specimens before placing the ZCC. This was carried out to examine the friction and adhesion between the ZCC and CC. After placing the ZCC on top of the CC, two curing regimes were applied to each one of the full cylinders. The first curing regime was oven curing after two hours of rest time. The cylinders then were encased in plastic oven bags to prevent moisture loss before placing them in an electrical oven at a temperature of 158° F (70° C) for 24 hours. More details about the oven curing details are presented in Chapter 6. Then, the cylinders were

demolded and left in the laboratory temperature to cool down until the testing day. The second curing regime was moist curing where after two days of rest time, the cylinders were demolded and stored in the moisture room at temperature of $73 \pm 3^{\circ}$ F ($23 \pm 2^{\circ}$ C) and relative humidity of $95 \pm 5\%$ for 28 days.

In addition to ZCC-CC specimens, other specimens were prepared using CC materials, for the purpose of comparison. Two different CC mixtures were placed against the host CC specimens to fill the second half of each plastic cylinder, CC1 and CC2. After placing the CC repair, the specimens were cured following two curing regimes based on the CC mixture, i.e., CC1 and CC2. The first curing regime was ambient curing where the specimens were covered with a top plastic lid to prevent moisture loss. Then, the specimens were placed in the laboratory, while still in the plastic molds, at a room temperature of $73 \pm 3^{\circ}$ F ($23 \pm 2^{\circ}$ C) for 28 days. The ambient curing regime was applied to specimens constructed out of mixture CC2. The second curing regime was moist curing where the specimens, still in the plastic molds, were stored in a moisture room having a relative humidity of $95 \pm 5\%$ for 28 days. The moist curing regime was applied to specimens constructed out of mixture CC1. Furthermore, full-height cylinders of each of the ZCC and CC mixtures were cast as reference specimens to compare their failure loads to that of the repaired cylinders.

8.1.3.2 Pull-off specimens

The pull-off specimen preparation was similar to that of the slant shear test with one single difference, the size and shape of the specimens. The specimens that were used during this test were beams having dimensions of 6 x 6 x 24 in. To prepare the test specimens, a layer of CC was poured to fill one half, which was equal to three inches of the depth of the beam, as a host material. Thereafter, the specimens were cured for 28 days in the moisture room. Fig. 8.4 shows

the one-half-deep test specimens after curing and before placing the repairing ZCC. After curing, the ZCC was placed against the host material, i.e., the CC, followed by two curing regimes: oven and moist as discussed in the previous section. As discussed in the previous section, no surface treatment or bond agent was applied to the CC surface before placing the ZCC.

Figure 8.4: Half beams constructed out of the host material, i.e., CC after curing and before placing the ZCC repair.

In addition to the ZCC/CC specimens, other specimens were prepared using CC materials, for a comparison purpose. Two different CC mixtures were placed against the host CC specimens to fill the second half of each plastic cylinder, CC1 and CC2.

After placing the CC repair material, the specimens were either cured under ambient conditions or in the moisture room. After placing the CC repair, the specimens were cured following two curing regimes based on CC mixture, i.e., CC1 and CC2. The first curing regime was ambient curing where the specimens were covered with a top plastic sheet to prevent moisture loss. Then, the specimens, still in the molds, were placed in the laboratory at a room temperature of $73 \pm 3^{\circ} \mathrm{F}$

(23 ± 2° C) for 28 days. The ambient curing regime was applied to specimens constructed out of mixture CC2. The second curing regime was moist curing where the specimens were stored, still in the molds, in a moisture room having a relative humidity of 95 ± 5% for 28 days. The moist curing regime was applied to specimens constructed out of mixture CC1. Furthermore, full-depth beams of each of the ZCC and CC mixtures were cast to compare their failure loads to those of the repaired beams.

8.1.4 Testing

8.1.4.1 Slant shear specimens

After curing the specimens, they were tested for compression per ASTM C39-17 [124] (Fig. 8.5). The details of the test were similar to those described for compression testing of the ZCC specimens in Chapters 3 and 6. The reported results are the average of three specimens. Two failure modes would occur during testing. If the bond between the host concrete and repair concrete is strong enough to transfer the full shear along the inclined 45° surface, compression failure of the cylinder will happen. Otherwise, the specimen would fail in sliding shear.

Figure 8.5: Slant shear test for the repaired cylinders.

8.1.4.2 *Pull-off specimen*

After curing the beam specimens, the pull-off test started by forming six cores in each beam. Fig. 8.6 shows the wet drilling process that was used to form the cores in the pull-off beams. The depth of drilling was selected to pass the bonding surface between the host and the repair material, so the bond strength could be tested. Then, aluminum disks were attached to the top of each drilled core using an epoxy. A commercially available epoxy which sets in five minutes, having bond strength of 3200 psi, was used during this test. After 24 hours of epoxy curing at the laboratory temperature of 73 ± 3° F (23 ± 2° C), the pull-off device was installed on top of the test specimen (Fig. 8.7). Once it was installed, the level of the device was adjusted using the three legs in the device. Then, the handle of the device was slowly and carefully rotated with a maximum pulling speed of 0.183 inch/minute (4.65 mm/minute) until failure occurred in the test specimen.

It is worth noting that, for the oven-cured specimens, after 24 hours curing in the oven, the specimens were left for 24 hours in the laboratory temperature of 73 ± 3° F (23 ± 2° C) followed by drilling the core. Then the beams were left to dry for 24 hours since the drilling process was performed at wet condition. Thereafter, the aluminum disks were attached to the top of each beam and left to be cured for 24 hours. Then the pull-off tests were carried out. For the moist-cured specimens, the same steps were followed except that the curing was for 28 days in the moisture room.

Figure 8.6: Core preparation processes (a) before drilling, (b) during drilling, and (c) the beams after drilling all the cores.

Figure 8.7: Pull-off test procedures (a) placing the pull-off device on top of the beams, (b) adjusting the levels of the pull-off device legs before testing, and (c) leveling and pull-off readings.

Fig. 8.8 shows the typical modes of failure of a pull-off test specimen [146]. Four individual modes of failure or a combination of them are expected to take place during the pull-off test, as follows: (1) tensile failure in the host material, (2) bond failure at the interface between the two

materials, (3) tensile failure in the repair material, and (4) failure at the top surface of the repaired material. The occurrence of the first or third modes of failure indicates that the bond between the repair and host materials is stronger than the tensile strengths of the repair or host material. The occurrence of the second mode of failure indicates that the bond between the repair and host materials is weaker than the tensile strengths of the repair and/or host material, which is not a desired mode of failure. One of the criteria for using a repair material is to assure that the repair material has a strong bond with the host material to avoid any debonding between the two materials. Occurrence of the fourth mode of failure, which takes place in the paste, indicates that the paste of the repair material is weak due to entrapped and excessive water in the top paste layer during the surfacing or curing process, which is not a desired mode of failure. Should failure have occurred in the interface between the aluminum disk and repair material, the test would be considered as a failed test. Failure modes of the full-depth beams were two: (1) failure in the host concrete at any depth of the beam, except the surface, which was named as a pull-off failure, and (2) failure at the top surface of the beam, which was similar to the fourth mode of failure in the repaired beams (Fig. 8.8) [146].
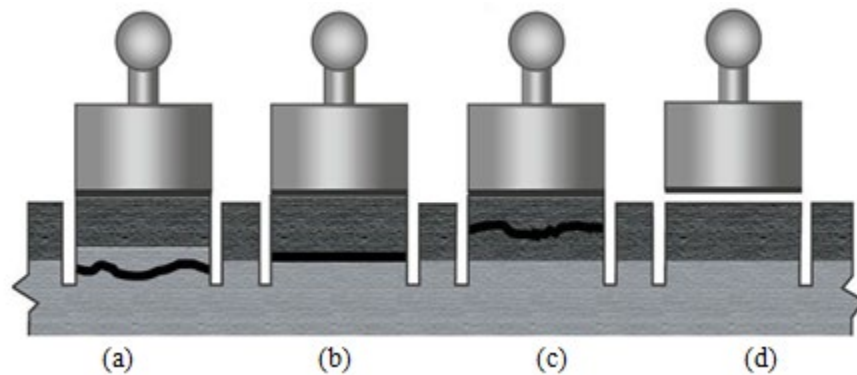
Figure 8.8: Modes of failure of the pull-off test, failure (a) in bottom layer, (b) at the interface between the two layers, (c) in top layer, and (d) at the top surface of the beam [146].

8.1.5 Results and discussion

8.1.5.1 Slant shear test

Figs. 8.9 and 8.10 show the failure modes of the full-height and oven-cured ZCC-repaired cylinders, as well as full-height and moist-cured ZCC specimens, respectively. As shown in the figures, the bond between the ZCC repair and CC host material was quite adequate to trigger compression failure in the repair or host material. Failure was not observed in the any of bond surfaces and consistently occurred in a typical compression failure of the cylinders.

| C21-Full-height | C24- Full-height | C29- Full-height | C37- Full-height | CC2- Full-height |
| C21-Repaired | C24-Repaired | C29-Repaired | C37-Repaired | CC2-Repaired |
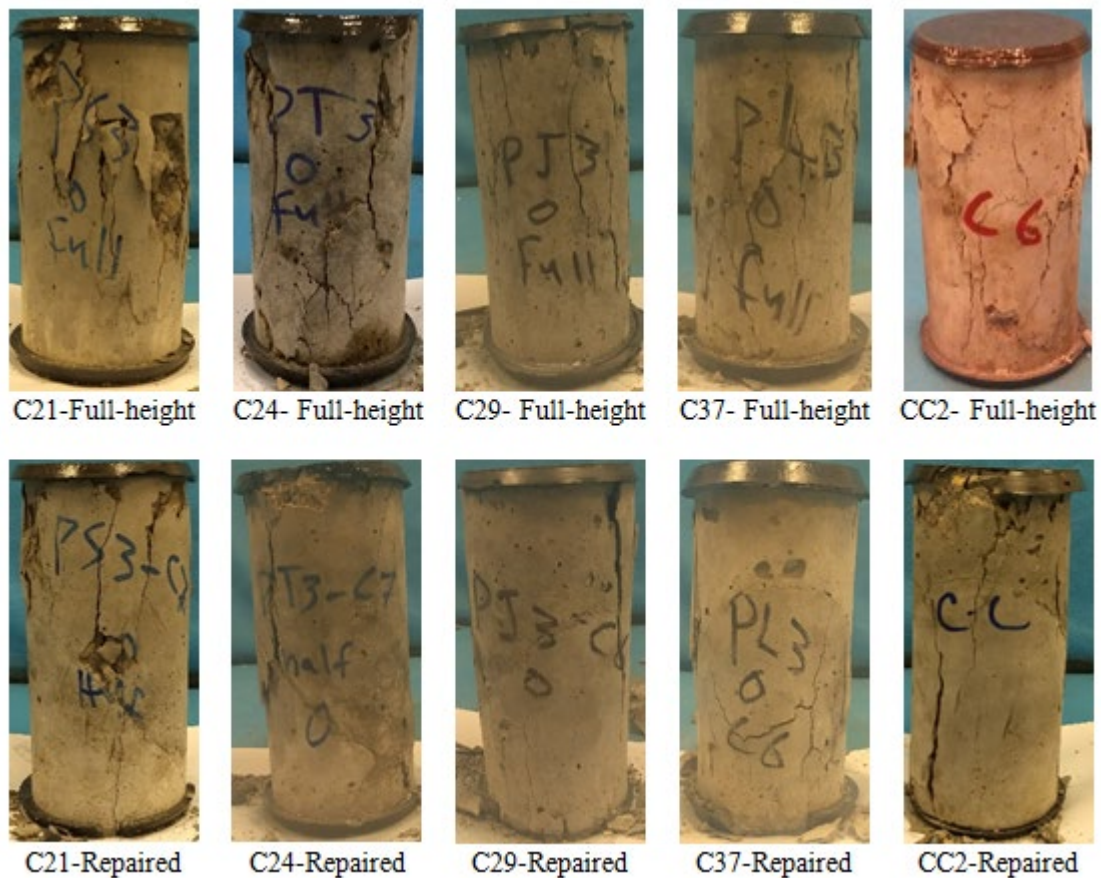
Figure 8.9: Failure modes of the full-height and repaired cylinders for the oven-cured specimens.

Fig. 8.11 shows the failure loads of the oven-cured ZCC-repaired and full-height cylinders. Also shown in the figures are the strength and normalized strength of the repaired and full-height CC

cylinders despite being ambient-cured for comparison purposes. Fig. 8.12 shows the compressive strength of the repaired cylinders normalized by the compressive strength of the corresponding full-height cylinders. Similarly, Figs. 8.13 and 8.14 show the failure loads and normalized loads of the moist-cured ZCC-repaired and full-height cylinders. Similarly shown in the figures are the strength and normalized strength of the moist-cured CC repaired and full-height CC cylinders. Figs. 8.15 and 8.16 show the compressive strength of the ZCC-repaired specimens normalized by the compressive strength of the CC repaired specimens for oven and moist curing, respectively. The data shown in Figs. 8.11 through 8.16 represent the average of three replicate specimens for each mixture. The range of the measured data for each mixture is also shown on each figure using vertical lines.

C21- Full-height   C24- Full-height   C24- Full-height   C29- Full-height   CC- Full-height

C21-Repaired   C24-Repaired   C26-Repaired   C29-Repaired   CC1-Repaired

Figure 8.10: Failure modes of the full-height and repaired cylinders for the moist-cured specimens.
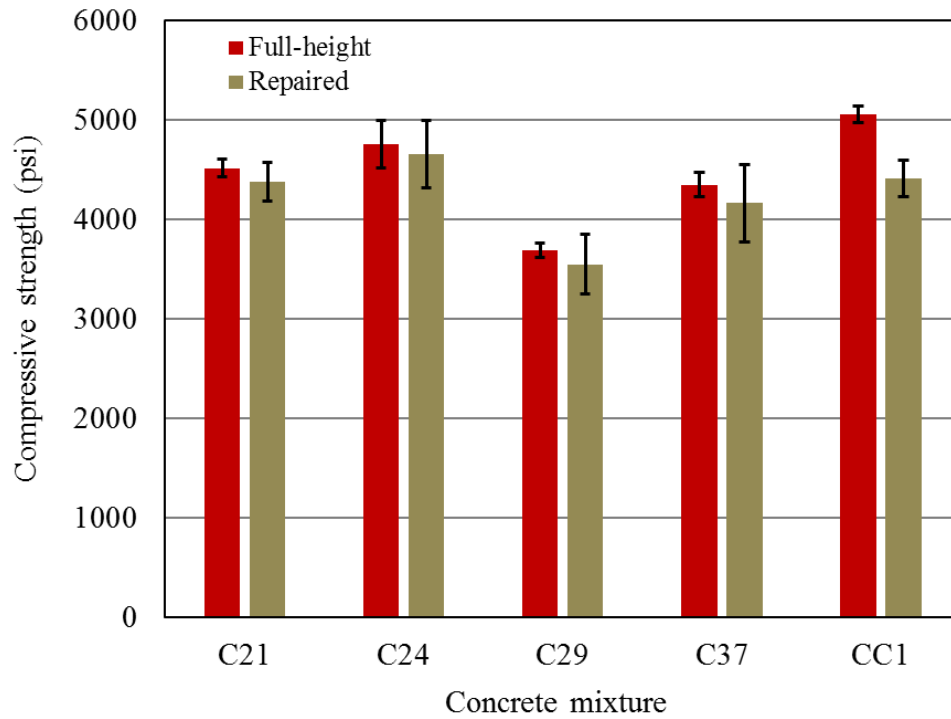
Figure 8.11: Compressive strength of the oven-cured repaired and full-height ZCC specimens (Note: repaired and full-height ambient-cured CC cylinders are shown as a reference).
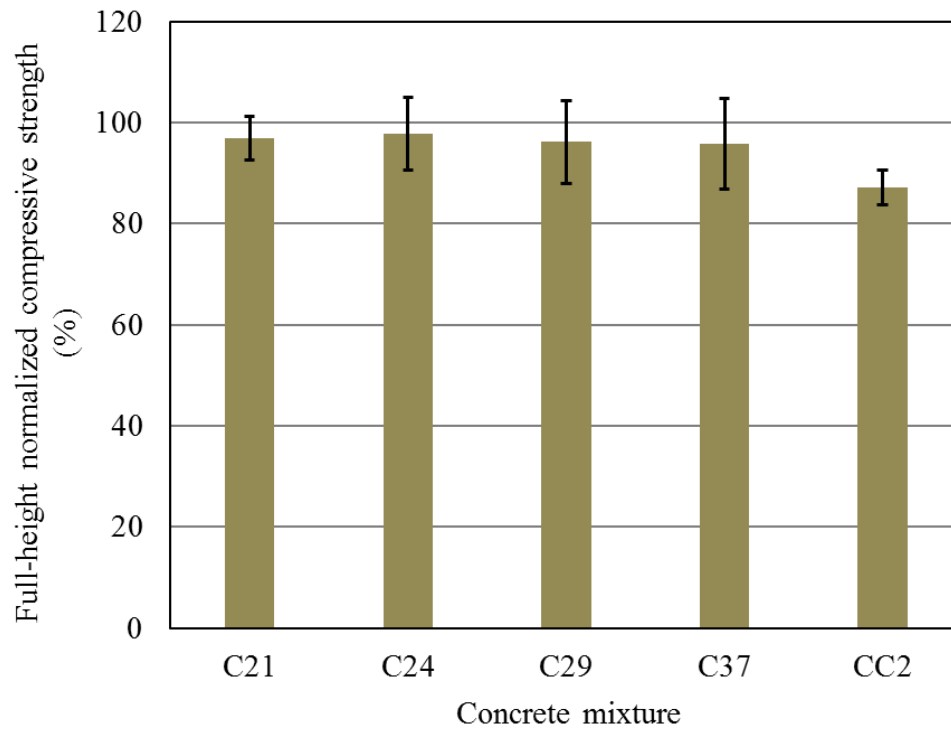
Figure 8.12: Full-height normalized compressive strength of the oven-cured repaired and full-height ZCC specimens (Note: repaired and full-height ambient-cured CC cylinders are show as a reference).
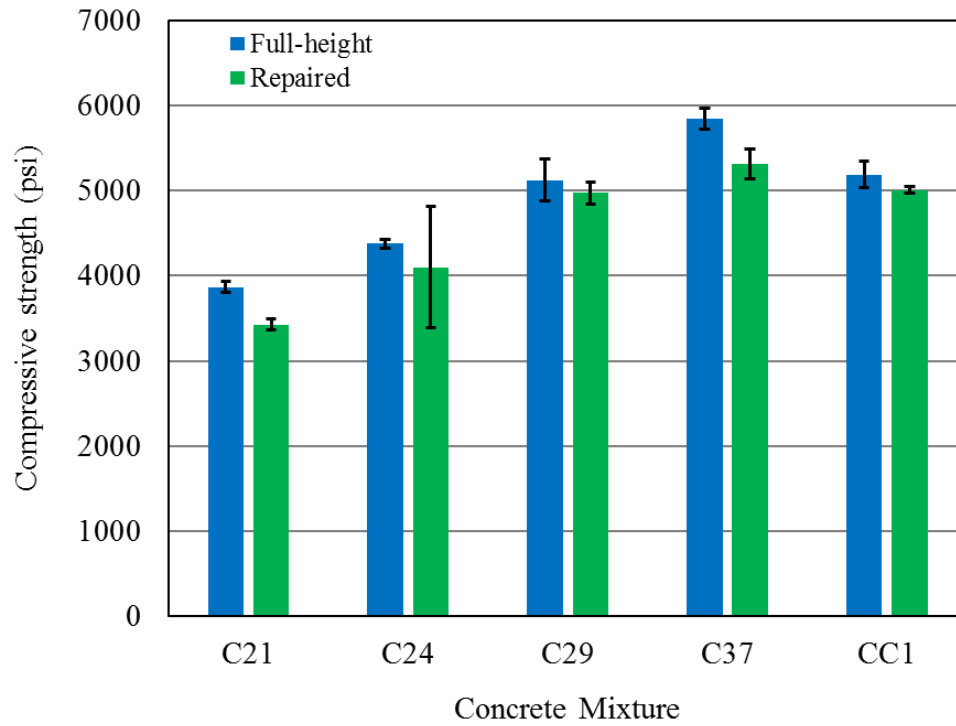
Figure 8.13: Compressive strength of the moist-cured repaired and full-height ZCC specimens (Note: repaired and full-height moist-cured CC cylinders are shown as a reference).
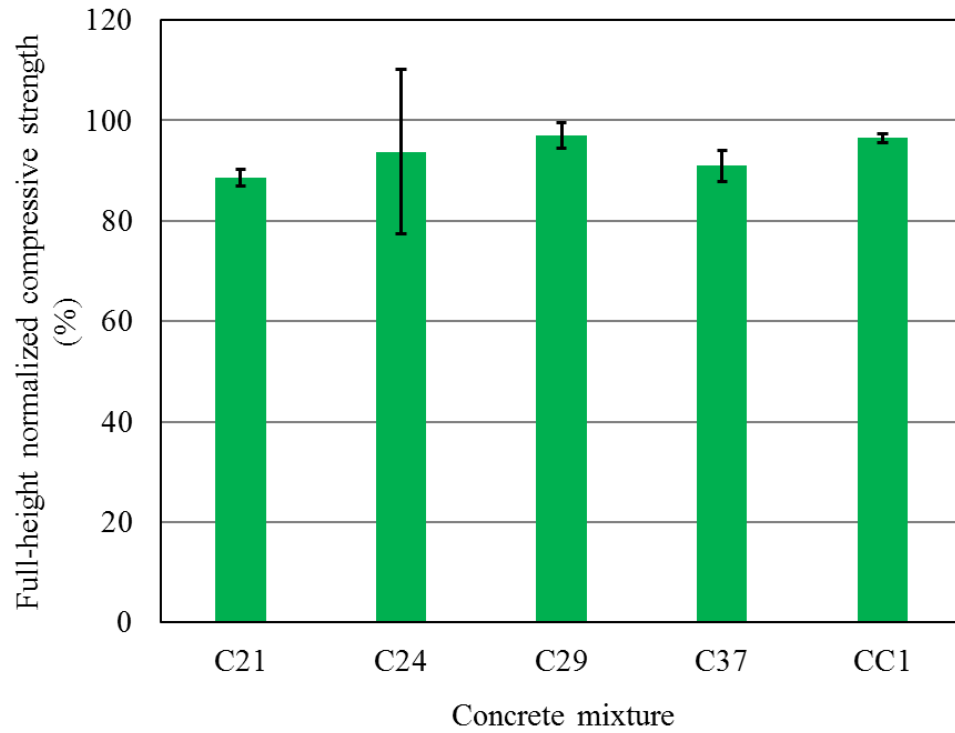
Figure 8.14: Full-height normalized compressive strength of the moist-cured repaired and full-height ZCC specimens (Note: repaired and full-height moist-cured CC cylinders are shown as a reference).
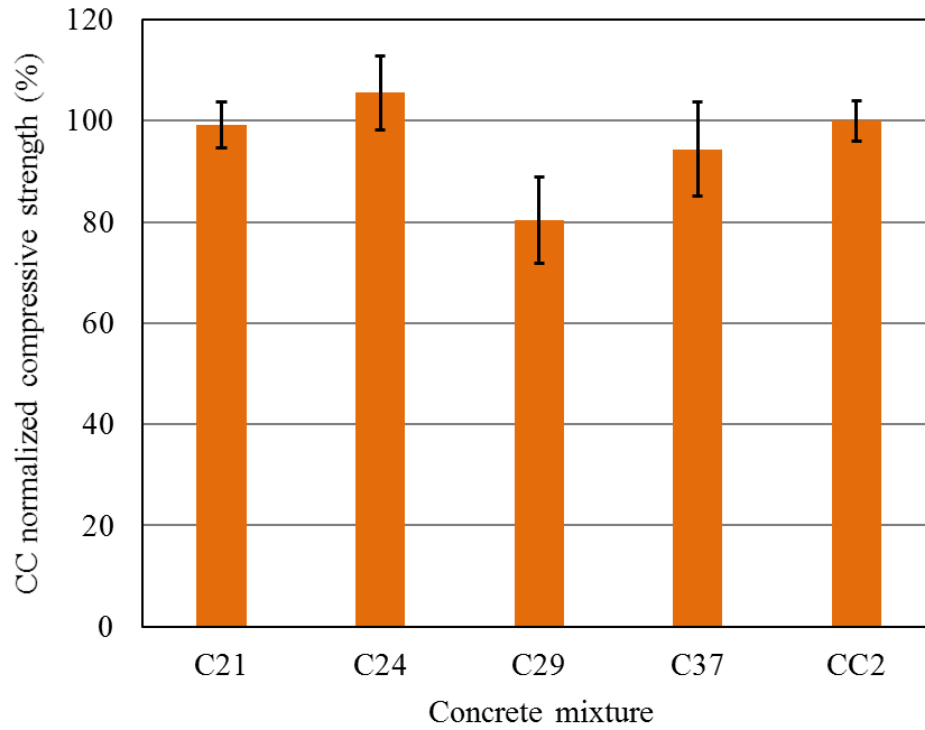
Figure 8.15: CC normalized compressive strength of the oven-cured repaired specimens (Note: repaired ambient-cured CC cylinders are shown as a reference).
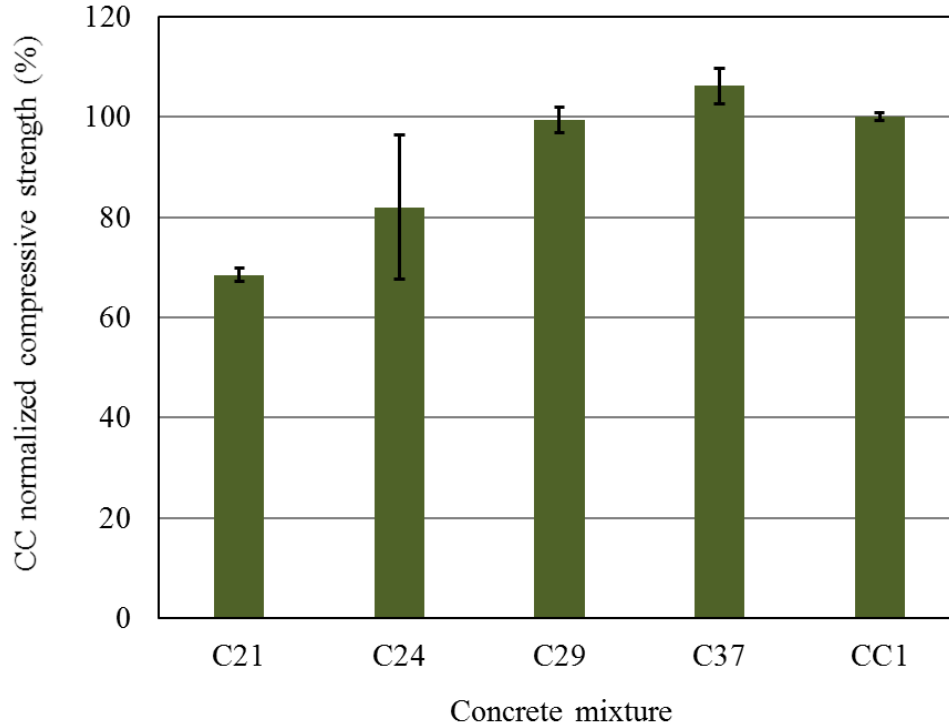
Figure 8.16: CC normalized compressive strength of the moist-cured repaired specimens (Note: repaired moist-cured CC cylinders are shown as a reference).

As shown in Figs. 8.11 through 8.16, repairing CC using ZCC was quite successful, and the ZCC repair developed an adequate bond with the host CC material. The failure loads of the full-height cylinders were higher than those of the repaired cylinders only by up to approximately 13%. The failure loads of the oven-cured repaired specimens were 3.1%, 2.1%, 3.8%, 4.2%, and 12.7% lower than those of the full-height specimens constructed using C21, C24, C29, C37, and CC2 mixtures. Similarly, the failure loads of the moist-cured repaired specimens were 11.4%, 6.2%, 3.0%, 9.1%, and 3.5% lower than those of the full-height specimens constructed using C21, C24, C29, C37, and CC1 mixtures, respectively. Therefore, improving the bond between the ZCC repair material and CC concrete using a bonding agent or sand blasting would have a limited effect on the strength of the test specimens.

Curing slightly affected the bond between the ZCC repair material and host CC concrete (Figs. 8.15 and 8.16). Oven-cured ZCC repair developed, on average, 97% of the strength of that of the full-height specimens while the moist-cured ZCC repair developed, on average, 93% of the strength of that of the full-height specimens. The results of both curing regimes were very consistent. The average standard deviation and coefficient of variation were 295 psi and 7.1% for oven-cured repair and 300 psi and 6.9% for moist-cured repair, respectively.

As shown in Figs. 8.15 and 8.16, repairing using ZCC was capable of achieving failure loads similar to that of the CC repair. The oven-cured ZCC repair strengths normalized by CC repair strength were 99%, 106%, 80%, and 94% for C21, C24, C29, and C37, respectively, with an average of 95% and standard deviation of 295 psi. Similarly, the moist-cured ZCC strengths normalized by CC repair strength were 68%, 82%, 99%, and 106% for C21, C24, C29, and C37, respectively, with an average of 89% standard deviation of 300 psi. As indicated earlier, no bond failure occurred in any of the test specimens. Hence, the failure loads were controlled by those of

the strength of the ZCC or CC mixtures. Hence, in some cases where the ZCC repair displayed repair strength smaller than that of the CC repair strength, the strength of the ZCC mixture can be adjusted to achieve the required repair strength.

8.1.6 Pull-off test

Fig. 8.17 shows a summary of the failure modes of the different repaired beams. Four failure modes took place as follows: 1) Direct tensile failure in the host material, 2) Bond failure at the interface surface between the host and repair material, 3) Direct tensile failure in the repaired material, and 4) Failure at the top surface of the beam.

(a) Failure in the host CC material

(b) Failure at the interface between the host and repair material

(c) Failure in repair material

(d) Failure at top surface of the repair material

Figure 8.17: Different failure modes of the reference and repaired specimens.

Table 8.2 listed the modes of failure of each beam. The common failure mode of the full-depth beams was a pull-off. Out of the eight ZCC beams and two CC beams, 87.5% failed due to the pull-off 12.5% due to top surface for the oven-cured ZCC, 50% failed due to pull-off and 50% failed due to top surface for the moist-cured ZCC, however, 100% of the CC failed due to pull-off. However, the most common mode of failure of the repaired beams was bond failure at the

interface between the two materials being CC on CC or ZCC on CC. It is worth noting that there

was not any kind of surface treatment applied to the concrete surface before placing the repair

material. Applying surface treatment may improve pull-off loads. However, the two curing

regimes that were applied for the ZCC and CC specimens made a difference in the failure load.

The ZCC specimens that were cured in the oven were compared with the CC specimens that

were cured at the ambient temperature in the laboratory which represented the dry curing

condition for both regimes. However, the ZCC specimens that were cured in the moisture room

were compared with the CC specimens that were also cured in the moisture room which

represented the wet curing condition. Furthermore, the pull-off test does measure the direct

tensile capacity of the bond between the two surfaces; however, under service loads, the interface

between the repair and host material is rarely subjected to direct tension and it is always

subjected to indirect tension, shear, or a combination of them. In addition, it is well documented

in the literature that the pull-off test results display a high variation [147]. Fig. 8.18 shows the

beams that were tested in this section of the chapter.

Table 8.2: Failure Modes of the Different Mixtures.

Oven-cured beams

Mixes	Full-depth	Repaired
C21	Pull-off	-
C24	Pull-off	-
C29	Pull-off	Top surface/bond
C37	Top surface/ Pull-off	Bond
CC1/CC2	Pull-off	Bond

Moist-cured beams

Mixes	Full-depth	Repaired
C21	Top surface	ZCC repair /bond
C24	Top surface	Bond/Host material
C29	Pull-off	Bond
C37	Pull-off	Bond
CC1/CC2	Pull-off	Bond

Figure 8.18: Beams tested for the pull-off test.

Fig. 8.19 shows the failure loads of the oven-cured ZCC full-depth and repaired beams. Fig. 8.20 shows the compressive strength of the repaired beams normalized by the compressive strength of the corresponding full-depth beams. Also shown in the figures are the strength and normalized strength of the full-depth and repaired CC beams despite being ambient-cured for comparison purposes. It is worth noting that during the drilling process of beams repaired using oven-cured mixtures C21 and C24, the cores were broken; hence, there was no pull-off test results for both cases shown in Figs. 8.19 and 8.20. Similarly, Figs. 8.21 and 8.22 show the failure loads and normalized loads of the moist-cured ZCC full-depth and repaired beams. Similarly shown in the figures are the strength and normalized strength of the moist-cured CC full-depth and repaired CC beams. Figs. 8.23 and 8.24 show the compressive strength of the ZCC-repaired specimens

normalized by the compressive strength of the CC repaired specimens for oven and moist curing, respectively.
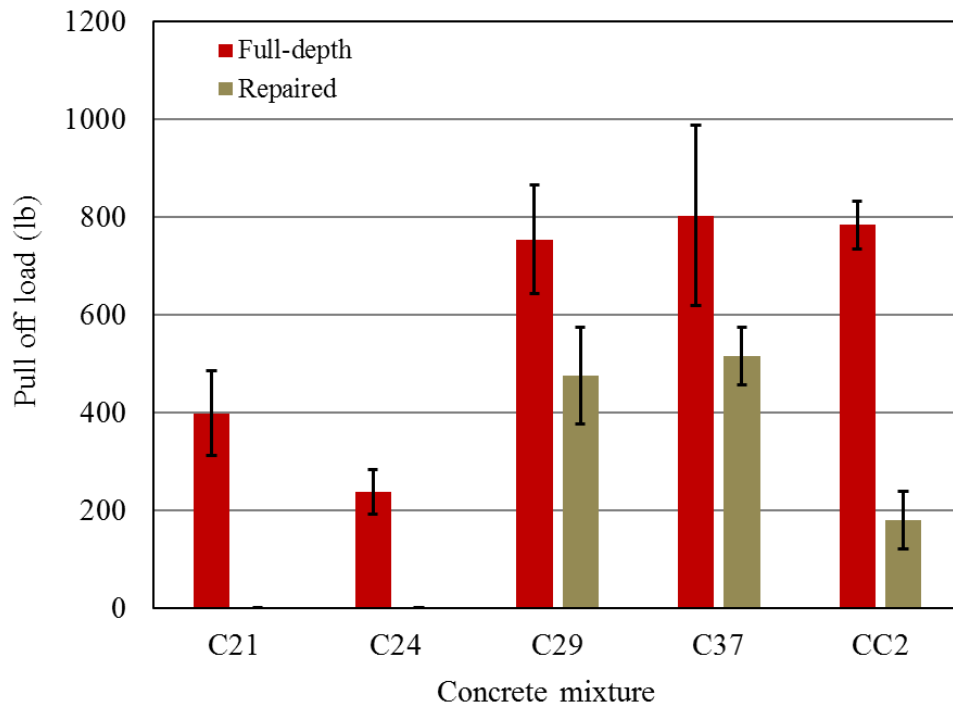
Figure 8.19: Pull-off load of the oven-cured repaired and full-depth ZCC specimens (Note: repaired and full-depth ambient-cured CC beams are shown as a reference).
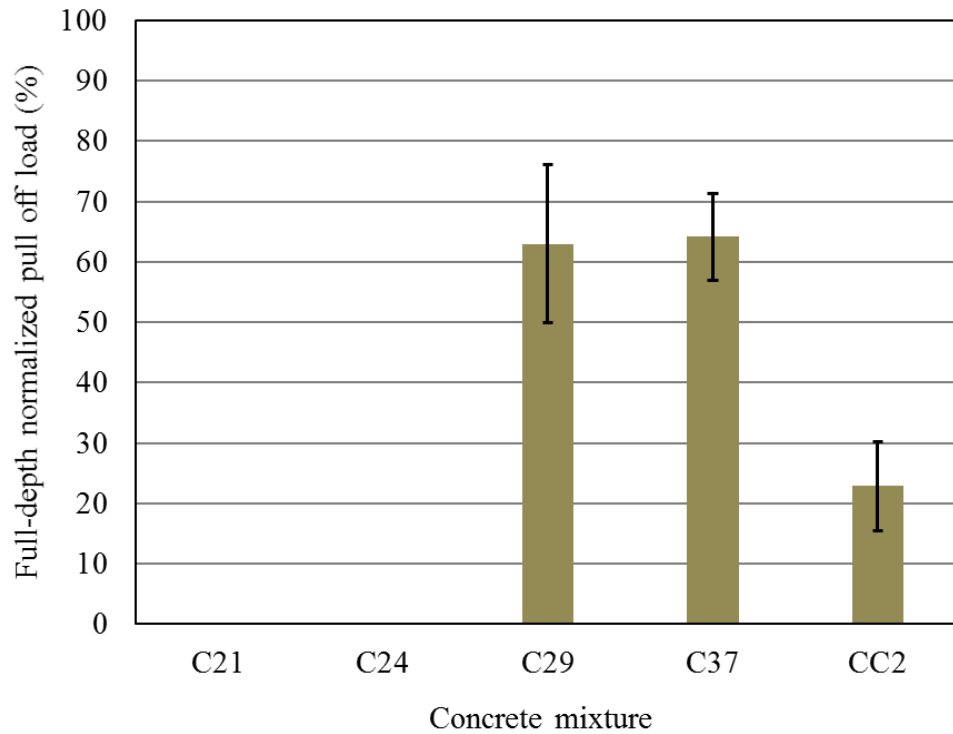
Figure 8.20: Full-depth normalized pull-off load of the oven-cured repaired (Note: repaired and full-depth ambient-cured CC beams are shown as a reference).
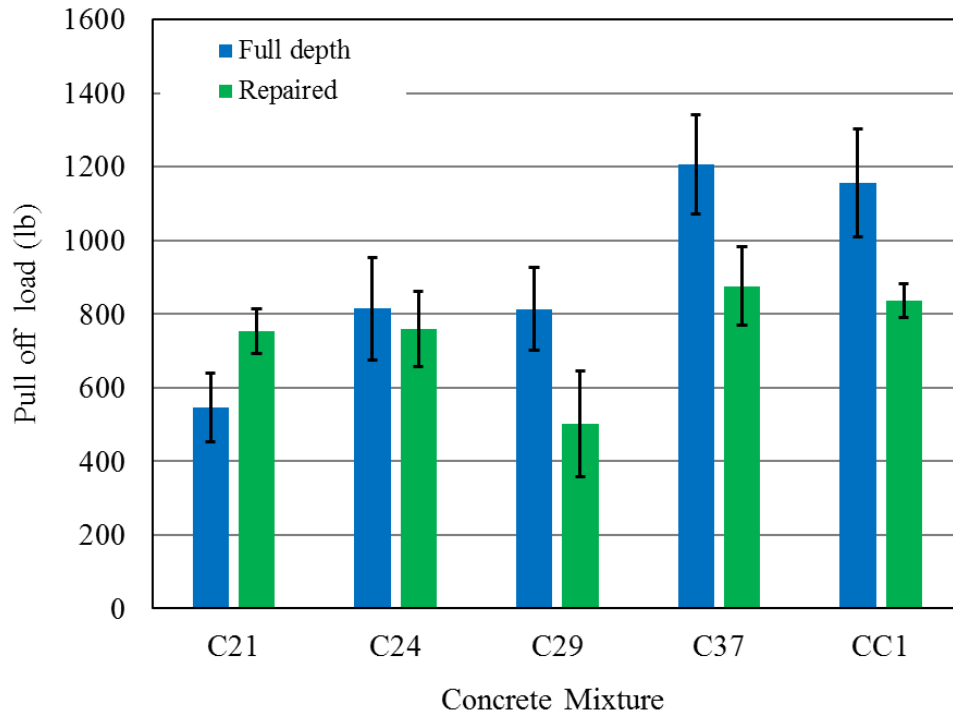
Figure 8.21: Pull-off load of the moist-cured repaired and full-depth ZCC specimens (Note: repaired and full-depth moist-cured CC cylinders are shown as a reference).
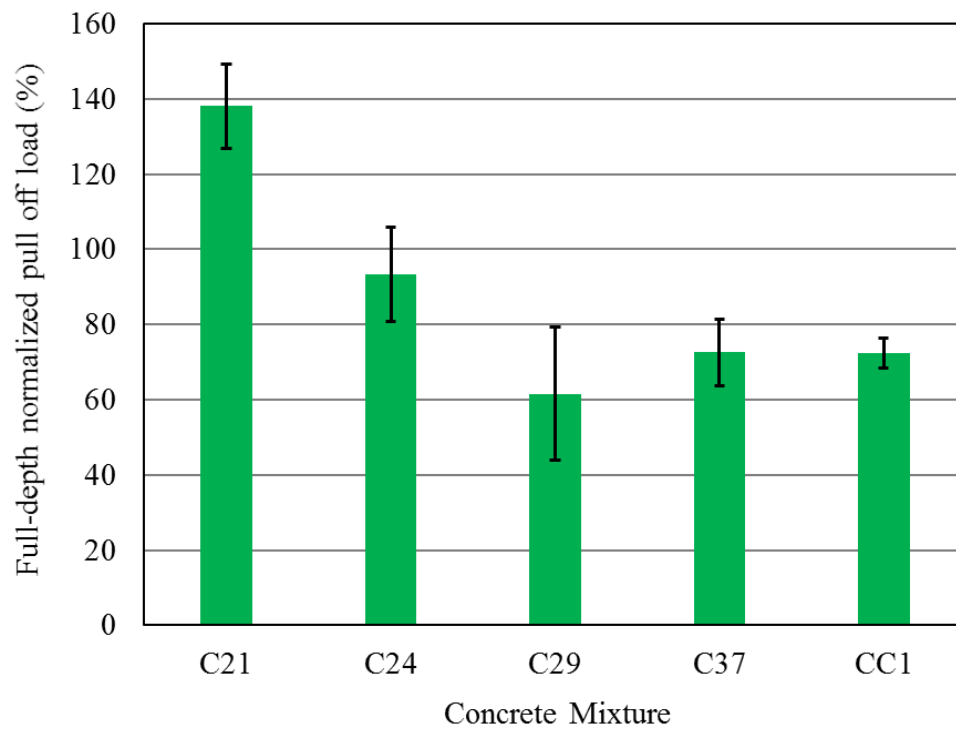
Figure 8.22: Full-depth normalized pull-off load of the moist-cured repaired specimens (Note: repaired and full-depth moist-cured CC cylinders are shown as a reference).
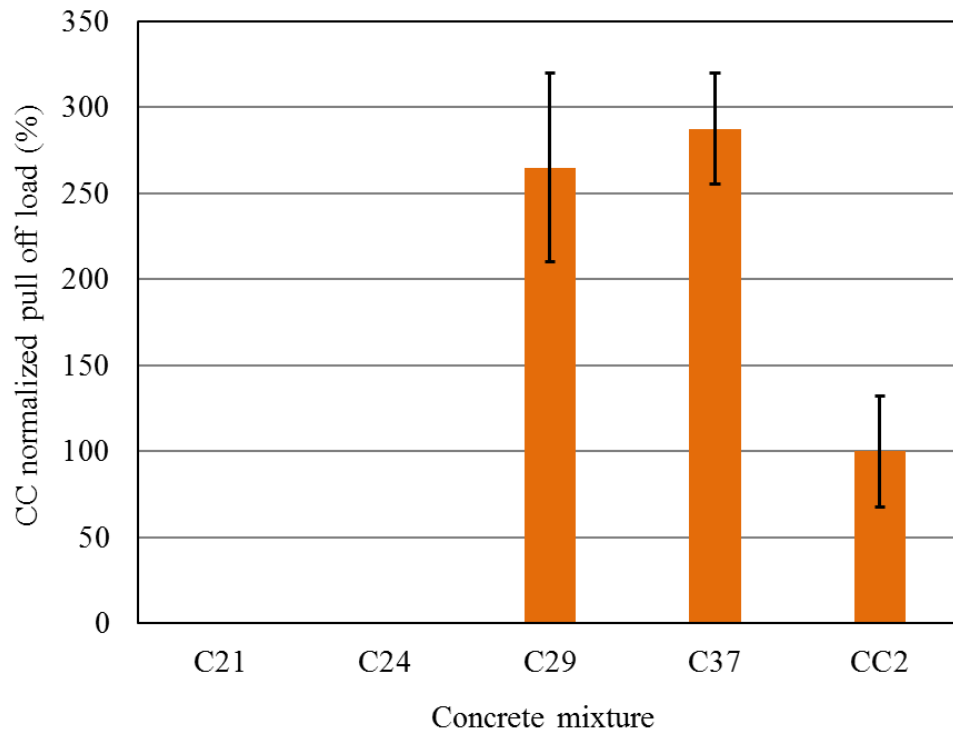
Figure 8.23: CC normalized pull-off load of the oven-cured repaired specimens (Note: repaired ambient-cured CC beams are shown as a reference).
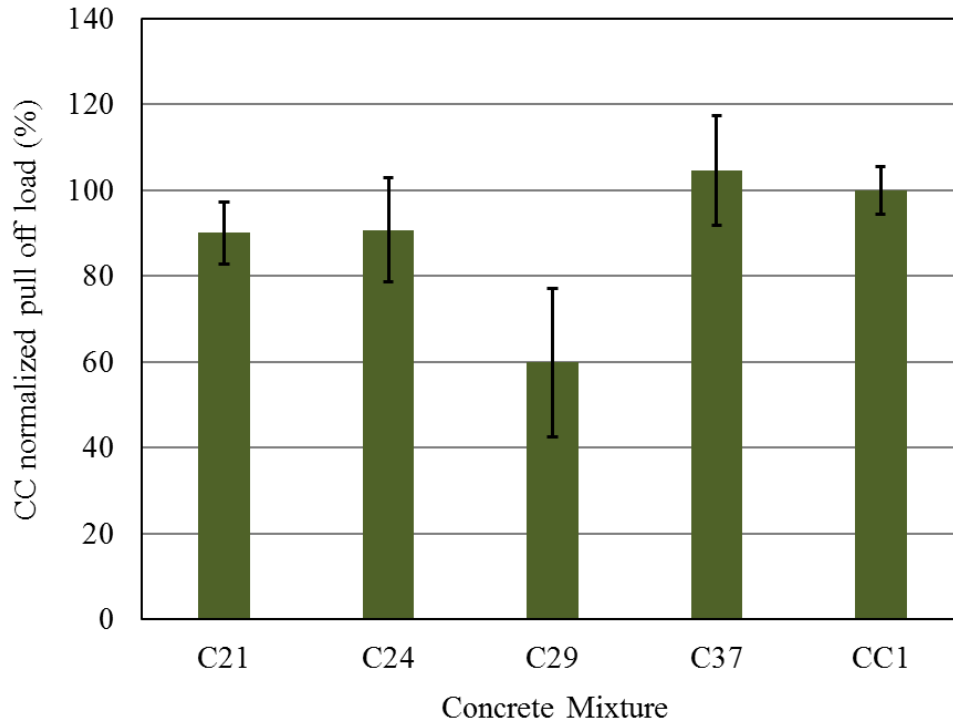
Figure 8.24: CC normalized pull-off load of the moist-cured repaired specimens (Note: repaired moist-cured CC cylinders are shown as a reference).

As shown in Figs. 8.19 through 8.24, repairing CC using either CC or ZCC was not able to develop an adequate bond with the host CC material. This contradicted the results from the slant shear. This may be attributed to the absence of surface treatment as well as the concept of the test where direct tensile strength is applied to the bond between the repair and host materials. The failure loads of the repaired beams were 63%, 64%, and 23% of the full-depth beams for the oven-cured specimens constructed using C29, C37, and CC1 mixtures, respectively. Similarly, the failure loads of the moist-cured repaired specimens were 93%, 62%, 73%, and 72% of the full-depth specimens constructed using C24, C29, C37, and CC2 mixtures. However, for beams repaired using mixture C21, the pull-off of the repaired specimen was higher than that of the full-depth specimens. This indicated that the bond between the host and repair material was enough to trigger failure in the ZCC itself. Furthermore, the failure mode of the pull-off cores of the full-

depth beams was mainly at the top surface and pull-off (Table 8.2) indicating that the paste at the top surface of the beam was weak due to the surfacing process that may have entrapped some excessive water in the top paste layer. However, failure in the corresponding repaired specimens was either at the top layer, bond, or bottom layer (Table 8.2).

Curing significantly affected the bond between the ZCC repair material and host CC concrete. Oven-cured ZCC repair developed an average 63.6% of the strength of that of the full-depth beams while the moist-cured ZCC repair developed an average 91.4% of the strength of that of the full-depth beams. Therefore, it can be concluded that curing the repaired specimens under wet conditions resulted in higher bond strength than curing under dry conditions. The results of both curing regimes were relatively consistent. The standard deviation and coefficient of variation were 125 lb and 17.6% for oven-cured repair and 115 lb and 17.2% for moist-cured repair, respectively.

As shown in Figs. 8.23 and 8.24, repair using ZCC was capable of achieving performance different than that of CC repair in the case of the oven-cured specimens; however, it was similar in the case of the moist-cured specimens. The oven-cured ZCC repair strength normalized by that of the ambient-cured CC repair was 265.0%, and 287.5% for repairing using C29 and C37, respectively, with an average of 276.3%. Hence, oven cure repair outperformed the CC repair in the case of curing under the dry conditions. However, the moist-cured ZCC repair strength normalized by that of the moist-cured CC repair was 90.1%, 90.8%, 59.9%, and 104.7% for repairing using C21, C24, C29, and C37, respectively, with an average of 86.4%. Hence, moist cure repair was similar to that of the CC repair.

8.2 Findings and Conclusions

This chapter presents the results of slant shear and pull-off tests that were carried out to characterize the bond between the CC as a host material and ZCC as a repair material. The bond between CC as a host material and CC as a repair material was also investigated as a reference. In addition to the slant and pull-off tests, compression load tests were carried out on full-height ZCC and full-height CC specimens. Pull-off tests were also carried out on full-depth ZCC and CC beams. The following can be concluded:

- The bond between ZCC concrete and CC was adequate to trigger compression damage in the host CC material or the ZCC repair material rather than shear sliding along the interface surface.

- The compressive strengths of the repaired cylinders were slightly less than that of the full-height cylinders since bond failure did not occur. The reduction in the failure load from the full-height to the repaired ZCC cylinders ranged from 2.1% to 4.2% for the oven-cured specimens and from 3.0% to 11.4% for the moist-cured specimens.

- In the case of testing the cylinders under compression for the slant shear test, both curing regimes showed high bond strength between the CC host concrete and ZCC repair, which indicated that the curing at the elevated temperature of 158° F (70° C) did not adversely weaken the bond between the two materials.

- The slant shear tests showed that both CC and ZCC repairing performed very similarly. The cylinders that were repaired using ZCC achieved compressive strength ranging from 68.4% to 106.2% with an average of 91.9% of that of the specimens repaired using CC. However, since bond failure did not occur; failure was controlled by the compressive strength of the host CC material and repair ZCC material.

271

- Most of the failure mode of the full-depth beams was a pull-off, where the failure took place within the beam itself not at the surface. However, the most common mode of failure of the repaired beams was at the interface between the host and repair materials. This occurred whether the repair was carried out using CC or ZCC. Surface treatment such as sand blasting and/or a bonding agent may improve the bond between the two materials. Furthermore, the pull-off test is a measure of the direct tensile capacity of the bond between the two surfaces; however, under service loads, the interface between the repair and host material is rarely subjected to direct tension and it is more common to be subjected to indirect tension, flexural tension, shear, or a combination of them.

- The pull-off strengths of the repaired beams (whether the repair was CC or ZCC) were less than that of the full-depth beams. The curing regime played an important role in the bond strength, where the moist-cured specimens showed higher bond strength than the oven-cured specimens. For the thermally cured specimens, the pull-off strengths of the repaired beams ranged from 66% to 67% of the full-depth beams. However, for the moist-cured specimen, the pull-off strength of the repaired beams ranged from 62% to 93% of the full-depth beams. For the CC specimens, the pull-off strengths of the repaired CC beams ranged from 23% to 72% of the full-depth beams.

Chapter 9:   Cost Analysis

The cost analysis of zero-cement concrete (ZCC) is presented in this chapter and compared to that of conventional Portland cement concrete. Producing sustainable and durable concrete such as ZCC is important and desired by different stockholders; however, the cost of the mixture is a crucial factor for selecting a construction material.

9.1 Mixture Cost

Table 9.1 shows the price of each ton of the coarse aggregate, sand, fly ash, sodium silicate, sodium hydroxide, and cement. The prices do not include the freight cost. As shown in the table, the most expensive components in producing ZCC are the sodium silicate and sodium hydroxide. The variations in the cost of both components are based on the purchase quantity, purity, and producer. Further, the price also depends on whether the user will acquire the material in a solid state and create the solution before preparing the concrete mixture or it will be acquired in solution form.

Table 9.1: Material Prices for Each Ton.

Material	Price per Ton
Coarse aggregate	$10
Sand	$8.5
Fly ash	$20 (assumed)
Sodium silicate	$400-$100
Sodium hydroxide (10M)	$147-$44
Water	Free
Cement	$120

Table 9.2 shows a comparison between the price of the ZCC and CC mixtures. The mixtures' proportions were mentioned in detail in Chapter 6. As shown in the table, the cost of the ZCC

273

mixtures ranged from 60% to 112% that of the CC mixture depending on many factors as described earlier in this chapter. The authors believe that once ZCC becomes a mainstream construction material, the cost can drop to 50% of that of conventional concrete. Furthermore, the ZCC mixtures presented in Table 9.2 had strengths ranging from 6600 to 7500 psi compared to 5200 psi of the conventional concrete. Finally, for a more common compressive strength in the order of 4000 psi, the fly ash quantity in ZCC can be reduced which will trigger a reduction in the required sodium silicate and sodium hydroxide, therefore producing a cheaper mixture. For example, reducing the fly ash by 10% would reduce the mixture cost by approximately 10%.

Table 9.2: ZCC and CC Mixture Prices/ft^3.

ZCC mixture (C21, C24, C26, C29, and C37)

Component	Weight (lb)	Price ($)
Coarse aggregate (lb/ft^3)	59.9	0.60
Sand (lb/ft^3)	49.9	0.42
Fly ash (lb/ft^3)	28.1	0.56
Cement (lb/ft^3)	-	-
Sodium silicate (lb/ft^3)	4.21	1.68-0.42
Sodium hydroxide (10M) (lb/ft^3)	4.21	0.62-0.19
Water	4.89-6.01	-
Total Price($/ft^3)		*3.88-2.19*
Slump (in)	7 - 8	
Strength (moist) 28 days (psi)	6600- 7500	

CC mixture

Component	Weight (lb)	Price ($)
Coarse aggregate (lb/ft^3)	67.9	0.68
Sand (lb/ft^3)	56.6	0.48
Fly ash (lb/ft^3)	-	-
Cement (lb/ft^3)	19.2	2.30
Sodium silicate (lb/ft^3)	-	-
Sodium hydroxide (10M) (lb/ft^3)	-	-
Water	10.92	-
Total Price($/ft^3)		*3.46*
Slump (in)	6.5	
Strength (moist) 28 days (psi)	5200	

It is worth noting that ZCC can reach its designed compressive strength relatively quickly as presented in Chapter 6. For examples, oven-cured specimens such as C21, C24, and C26 reached compressive strengths of 5485 psi, 5410 psi, and 4630 psi, respectively, at the age of 24 hours. Ambient-cured specimens such as C37 and C29 reached their compressive strengths of 5170 psi and 4524 psi, respectively, at the age of seven days. Moist-cured specimens such as C37 and C26 reached compressive strengths of 5510 psi and 5340 psi, respectively, at the age of seven days. This feature is very advantageous in terms of cost saving, especially for precast concrete producers and contractors with a tight project schedule.

9.2 Findings and Conclusions

- The ZCC mixtures had prices ranging from 60% to 112% of that of the CC. The cost of ZCC ranged from $59/yd^3 ($2.19/ft^3) to $105/yd^3 ($3.88/ft^3) while that of CC is approximately $93/yd^3 ($3.46/ft^3).

- The price of ZCC can be further optimized for a strength range of 3500 psi to 4500 psi and for larger quantities.

- Structural elements made using ZCC can reach their designed compressive strengths faster than conventional Portland cement concrete where oven-, ambient-, and moist-cured specimens can reach their specified compressive strength at 24 hours, seven days, and seven days respectively.

Chapter 10:   Conclusions, Recommendations, and Future Work

The main objective of this research study was to investigate the feasibility of using locally available fly ashes (FAs) to synthesize zero-cement concrete (ZCC) for different structural and repair applications. ZCC is a relatively new class of concrete that does not include any ordinary Portland cement (OPC) and relies on other alternative materials such as fly ash, slag, etc. as the binder material.

Five different types of class C FAs sourced from Labadie (FA37), Jeffrey Energy Center (FA29), Kansas City (FA26), Thomas Hill (FA24), and Sikeston (FA21) power plants, in the state of Missouri, were used to synthesize the ZCC used in this report. Two different alkali activators (Alk) were used in this study as aggregates: sodium silicate (SS), Na_2SiO_3, and sodium hydroxide (SH), NaOH, with a fixed molarity of 10M. River sand and dolomite were used for synthesizing mortar and concrete. Slag, crumb rubber, and air-entraining admixture (AEA) were used in few mixtures as additives to improve the durability of ZCC.

The mixing procedure, water (W)/FA, Alk/FA, SS/SH, curing regime, fresh properties, mechanical properties, durability, repair applicability, and cost analysis of the ZCC were investigated in this study. To address these parameters and properties, approximately 300 mortar and concrete mixtures were investigated. A 5000 psi MoDOT conventional concrete (CC) mixture was prepared and tested for comparison purposes.

Twelve different mixing procedures (four for mortar and eight for concrete) were investigated. W/FA ranging from 0.26 to 0.60, Alk/FA ranging from 0.2 to 0.4, and SS/SH ranging from 0.0 to 2.5 was examined. The investigated fresh properties included the slump, unit weight, air content,

and temperature. The investigated mechanical properties included the compressive strength, splitting tensile strength, modulus of rupture (flexural strength), and modulus of elasticity, as well as the drying shrinkage. The durability testing included the freeze-thaw resistance, surface resistivity, bulk electrical conductivity, and rapid chloride ion penetration. The ZCC repair applicability tests included the slant shear and pull-off tests to examine the bond between ZCC and CC.

This study applied three curing regimes to the ZCC specimens to investigate the effect of the different curing regimes on the mechanical properties ZCC. The first curing regime included oven curing where the specimens were encased in oven bags and placed in an electric oven at different curing temperatures and curing periods with 158° F (70° C) for 24 hours being the most common thermal curing regime. The second curing approach included ambient curing in the laboratory at the room temperature of 73° F (23 ± 2° C). The third curing approach included moist curing in the moisture room at a temperature of 73° F ($23 \pm 2^{\circ}$ C) and relative humidity of $95 \pm 5\%$ until the testing day.

10.1 Findings and Conclusions

Based on the main findings of this study, the following conclusions can be drawn:

10.1.1 Mixing procedures

- Mixing the water with all the ZC mortar/concrete solid ingredients before adding the alkali activators was essential where it prevented flash setting and poor workability. In addition, it resulted in a good workability, setting time, and compressive strength.

- Mixing at higher speed, adding the alkali activators gradually over five minutes rather than one minute, and mixing the SS and SH before adding them to the mixer increased the workability, setting times, and the compressive strength.

10.1.2 Mixing design

- ZCC having W/FA of 0.34, 0.34 , 0.35 , 0.380, and 0.350 for FA21, FA24, FA26, FA29, and FA37, respectively, Alk/ FA of 0.300, SS/SH of 1.0, and FA content of 759 lb/yd^3 (28.1 lb/ft^3) resulted in workable ZCC with a compressive strength exceeding 4000 psi and hence adequate for most structural applications.

10.1.3 Curing regimes

- The three curing regimes applied to ZCC, namely, oven, ambient, and moist curing regimes resulted in compressive strengths ranging from 3660 psi to 5985 psi, 4270 psi to 5310 psi, and 6605 psi to 7465 psi, respectively, based on the chemical and physical properties of the FA as well as mixture design.

- A given strength of ZC mortar can be produced using a given FA and different combinations of thermal curing temperatures and durations.

- A thermal curing regime is more suitable for the ZCCs that were synthesized using FA having relatively a lower calcium content while ambient and moist curing are more suitable for ZCC that were synthesized using FA having a relatively high calcium content. C21, C24, C26, C29, and C37 displayed compressive strengths of 5485, 5410, 4630, 3635, and 4485 psi after curing at 158° F (70° C) for 24 hours. However, C21, C24, C26, C29, and C37 displayed compressive strengths of 4305, 3995, 4420, 4525, and 5170 psi after 7 days and 4770, 4270, 4465, 4825, and 5310 psi after 28 days of ambient

curing. Furthermore, C21, C24, C26, C29, and C37 displayed compressive strengths of 4840, 5340, 5105, 4685, and 5510 psi after 7 days and 6625, 7425, 6880, 6605, and 7465 psi after 28 days of moist curing, respectively.

- The compressive strength significantly increased from 1 to 7 days for moist- and ambient-cured specimens while it remained approximately constant for thermal curing beyond 1 day. The increases in compressive strength of the ZCC from 1 day to 7 days were 976%, 902% 1079%, 72%, and 88% for ambient-cured and 1110%, 1238%, 1299%, 88%, and 100% for moist-cured specimens for C21,C24, C26, C29, and C37 respectively. Beyond 7 days, the rates of increase in the strength decreased. The increases in compressive strength from 7 days to 28 days were 10.9%, 6.8%, 1.0%, 6.7%, and 2.7% for ambient-cured and 36.9%, 39.1%, 34.8%, 40.9%, and 35.4% for moist-cured specimens for C21, C24, C26, C29, and C37, respectively. For thermal curing, the compressive strength increased by 8.4%, 12.4%, 6.4%, 0.7%, 11.0% for C21, C24, C26, C29, and C37, respectively, from the age of 1 day to 28 days.

- Hot weather curing at 86° F (30° C) for 7 days (168 hours) or imitated Missouri summer week curing regimes were able to produce 7-day compressive strengths ranging from approximately 3310 to 7530 psi depending on the FA source and mixture design. Specimens prepared using FA37 and FA29, which had relatively higher calcium contents, showed the highest strengths at the hot weather curing indicating prominent hydration mechanisms.

- There was no significant difference in the 7-day compressive strength of specimens that were cured in a controlled environment at 86° F (30° C) and those cured at the imitated Missouri summer week where the curing temperature consisted of ramped up temperature

from 72° F (22° C) to 97° F (36° C) over 12 hours followed by ramped down temperature from 97° F (36° C) to 72° F (22° C) over 12 hours. Hence, the variation in the temperature overnights in Missouri summer should not affect the strength of ZCC.

- There is a strong correlation between curing energy consumption, i.e., curing duration and temperature and compressive strength. For a given mixture and sourced FA, there is an optimum amount of curing energy beyond which increasing the curing energy is not cost effective.

10.1.4 Mechanical properties

- The relationships between the compressive strength of ZCC and splitting tensile strength, flexural strength, and modulus of elasticity are similar to those used by ACI 318-14 [133], AS 3600 design code [134], and CEB-FIP model code [135].

- The ACI 318-14 [133] and CEB-FIP model code [135] overestimated the splitting tensile strength of ZCC by an average of 9% and 11%, respectively, while AS 3600 [134] underestimated the splitting tensile strength by 27%. Furthermore, the ACI 318-14 and CEB-FIB model code [135] also overestimated the splitting tensile strength of CC by 12% and 9%, respectively.

- The CEB-FIP model code [135] overestimated the flexural strength of ZCC by an average of 16%, while ACI 318-14 [133] and AS 3600 [134] underestimated the flexural strength by 24% and 29%, respectively. Furthermore, CEB-FIB model code [135] also overestimated the splitting tensile strength of CC by 5%.

- The ACI 318-14 [133] and CEB-FIP model code [135] underestimated the modulus of elasticity of ZCC by an average of 12% and 20%, respectively.

- The drying shrinkage values of the ZCC specimens with different curing regimes at all ages were significantly lower than those of the CC specimens. At 56 days, the average shrinkage values of ZCC were 0.029%, 0.0467%, and 0.0491% for the oven-cured specimens that were tested directly after 24 hours of oven curing, the oven-cured specimens that were stored for 28 days then tested, and, the moist-cured specimens that were stored for 28 days then tested, respectively, while it was 0.1282% for the moist-cured CC specimens. This indicates that the ZCC would display fewer cracks during its service life, resulting in less penetration of any deicing or other harmful salts that could cause deterioration.

10.1.5 Durability

- The durability of the ZCC was improved significantly by adding slag as a partial replacement and the rubber as an additive to the FA. Two out of three slag specimens successfully passed the 300 cycles of ASTM C666-15 [74] with durability factor of 93.3 and 83.4 for the moist- and oven-cured specimens following procedure A, respectively. The rubber specimens successfully passed the 300 cycles with durability factor of 104.5 and 75.9 following procedures A and B per ASTM C666-15, respectively.

- Based on the surface resistivity and chloride ion penetration tests, most of the ZCC mixtures had a low to moderate permeability and chloride ion penetrability. However, the CC mixture showed a high permeability and chloride ion penetrability. Therefore, ZCC presents higher corrosion resistance compared to CC.

- The results of the rapid chloride ion penetration test showed lower values in the case of most of the ZCC mixtures compared to that of CC. The rapid chloride ion penetration (charge passed) ranged from 0.23 to 0.61 and 0.35 to 0.74 times that of CC for thermally

cured and moist-cured. For thermal curing, the rapid chloride ion penetration (charge passed) were 1578, 2176, 2615, 4219, and 1689 coulomb for C21, C24, C26, C29, and C37, respectively. For moist curing, the rapid chloride ion penetration (charge passed) were 2459, 2719, 2531, 5152, and 3473 coulomb for C21, C24, C26, C29, and C37, respectively.

- The results of the surface resistivity test showed higher values in the case of most of the ZCC mixtures compared with CC. The surface resistivity of ZCC ranged from 1.3 to 3.8 and 1.1 to 2.2 times that of CC for thermally cured and moist-cured, respectively. For oven curing, the surface resistivity values were 35.1, 14.9, 22.3, 11.6, and 27.5 kΩ.cm for C21, C24, C26, C29, and C37, respectively. For moist curing, the surface resistivity values were 14.7, 13.8, 19.9, 10.3, and 10.8, respectively.

- The results of the bulk electrical conductivity test showed higher values in the case of most of the ZCC mixtures compared to that of CC. The bulk resistivity of ZCC ranged from 1.1 to 2.7 and 1.0 to 2.1 times that of CC for thermally cured and moist-cured, respectively. For oven curing, the bulk electrical conductivities were 79.8, 40.7, 65.2, 31.1, and 78.3 kΩ.cm for C21, C24, C26, C29, and C37, respectively. For moist curing, the bulk electrical conductivities were 42.4, 41.4, 62.1, 29.8, and 34.6 kΩ.cm for C21, C24, C26, C29, and C37, respectively.

10.1.6 Repair

- During a slant shear test, the bond between ZCC concrete as a repair material and CC as a host material was adequate to trigger compression damage in the host CC material or the ZCC repair material rather than shear sliding along the interface surface.

- The compressive strengths of the repaired cylinders, i.e., ZCC placed over CC, was slightly less than that of the full-height cylinders constructed out of the corresponding ZCC concrete mixture. The reduction in the failure load from the full-height to the repaired cylinders ranged from 2.1% to 4.2% for the thermally cured specimens and from 3.0% to 11.4% for the moist-cured specimens.

- In the case of slant shear test, both curing regimes showed high bond strength between the CC host concrete and ZCC repair, which indicated that the curing at the elevated temperature of 158° F (70° C) did not adversely weaken the bond between the two materials.

- For the pull-off test, the failure loads of the ZCC and the CC were comparable to each other, which prove that the ZCC can be successfully used as a repair material.

- Most of the failure mode of the reference full-depth ZCC or CC beams was a pull-off, where the failure took place within the beam itself, not at the surface. However, the most common mode of failure of the repaired beams was at the interface between the host and repair materials. This occurred whether the repair was carried out using CC or ZCC. Surface treatment such as sandblasting and/or a bonding agent may improve the bond between the repair and host materials. Furthermore, the pull-off test is a measure of the direct tensile capacity of the bond between the two surfaces; however, under service loads, the interface between the repair and host material is rarely subjected to direct tension and it is more common to be subjected to indirect tension, flexural tension, shear, or a combination of them.

- The pull-off strengths of the repaired beams (whether the repair was CC or ZCC) were less than that of the full-height beams. The curing regime played an important role in the

bond strength, where the moist-cured specimens showed higher bond strength than the oven-cured specimens. For the thermally cured specimens, the pull-off strengths of the repaired beams ranged from 66% to 67% of the full-depth beams. However, for the moist-cured specimens, the pull-off strength of the repaired beams ranged from 62% to 93% of the full-depth beams. For the CC specimens, the pull-off strengths of the repaired CC beams ranged from 23% to 72% of the full-depth beams.

10.1.7 Cost analysis

- The cost of ZCC mixtures ranged from 60% to 112% of that of the CC. The cost of ZCC ranged from $59/yd^3 to $105/yd^3 while that of CC is approximately $93/yd^3. The price of ZCC can be further optimized for strength range of 3500 psi to 4500 psi and for larger quantities.

- Structural elements made using ZCC can reach their designed compressive strengths faster than conventional Portland cement concrete where thermal, ambient, and moist-cured specimens can reach their specified compressive strengths at 24 hours, seven days, and seven days respectively.

10.2 Recommendations

The five sourced FAs that were investigated during the course of this study can be used to produce ZCC and ZC mortar. Based on the extensive and comprehensive experimental work presented in this report the following recommendations are presented:

1. The best ZCC mixing procedure is as follows: (1) the coarse and fine aggregate were mixed for one minute. (2) The FA was added and mixed with the aggregates for one minute. (3) The water was gradually added over one minute. (4) The alkali activator was

gradually added over five minutes. (5) Once all ingredients were added, the mixing procedure continued for another five minutes.

2. Table 10.1 summarizes mix design proposals for each sourced FA that is capable of producing structural ZCC with a good workability and strength. These design mixtures need to be considered carefully based on the performance required in different projects, and trial mixtures need to be carried out due to variations in different material, chemical, and physical properties.

Table 10.1: Mix Design of the ZCC and CC Mixtures.

Mix	W/FA	Alk/FA	SS/SH	CA[a] (lb/yd³)	Sand (lb/yd³)	FA (lb/yd³)	SS (lb/yd³)	SH (lb/yd³)	W (lb/yd³)
C21	0.340	0.30	1	1638	1365	758	114	114	132
C24	0.340	0.30	1	1638	1365	758	114	114	132
C26	0.350	0.30	1	1616	1347	758	114	114	140
C29	0.380	0.30	1	1593	1328	758	114	114	162
C37	0.350	0.30	1	1616	1347	758	114	114	140

[a]CA: coarse aggregate

3. Different curing regimes and durations can be applied to ZCC to achieve different performances. For relatively low calcium FAs such as FA21, FA24, and FA26 thermal curing for 24 hours at 158° F (70° C) can produce ZCC having a compressive strength of 5285 psi or higher. For relatively high calcium FAs such as FA37 and FA29, ambient curing and moist curing for 7 days at 73 ± 3° F (23 ± 2° C) can produce ZCC having a compressive strength of 4525 psi or higher.

4. Eq. 6.3a, repeated here for convenience, was developed to correlate the tensile splitting stress, f_{ct}, and compressive strength, f_c', of ZCC.

$$f_{ct} = 5.9 \sqrt{f_c'} \text{ , (U.S. units, psi)} \tag{6.3a}$$

5. Eq. 6.5a, repeated here for convenience, was developed to correlate the modulus of rupture, f_r, and f_c' of ZCC.

$$f_r = 8.8 \sqrt{f_c'} \text{, (U.S. units, psi)} \tag{6.5a}$$

6. Eq. 6.7a, repeated here for convenience, was developed to correlate the modulus of elasticity, E_c, and f_c' of the ZCC examined in this chapter.

$$E_c = 68600\sqrt{f_c'} \text{, (U.S. units, psi)} \tag{6.7a}$$

10.3 Future Work

While this study showed the feasibility and advantages of using the locally available class C FAs to synthesize ZCC concrete, further studies are still required to fine-tune the characterization long term durability of ZCC. This includes the following issues:

1. The durability of ZCC under the effects of deicing salts, which is a major issue in the transportation infrastructure in the U.S.

2. The durability of ZCC subjected to an acid solution.

3. The abrasion resistance of ZCC. Abrasion resistance is a crucial characteristic for transportation infrastructure.

4. The effects of different superplasticizers on slump retention, workability, and strength of ZCC.

5. The rheological properties of ZCC, especially the workability retention.

6. Trial placement of large-scale ZCC deck and footing in the laboratory to explore the performance of ZCC.

7. Repair of RC beams using ZC mortar. Both slant tests and pull-off tests showed the potential of using ZCC in repair. However, both tests do not represent the realistic conditions and state of stresses that ZCC repair will sustain during service, hence it needs to be investigated.

The development of one-part ZCC, where the alkali activators would be prepared in powder form instead of the liquid used during this project. This is a tremendous development as the powder will reduce the freight cost and risk associated with transporting the liquid activator. It also reduces the risk of handling the liquid activator at the construction site. Furthermore, the fly ash and activator are mixed together in dry conditions and packed in one bag that acts as a substitute for the conventional Portland cement bag.

Chapter 11: References

1.   Kosmatka, S.H. and M.L. Wilson, *Design and Control of concrete Mixtures*. 16th Edition ed. 2016: Portland Cement Association, Sokie, Illinois, USA. 632.
2.   Development, W.B.C.f.S., *The Cement Sustainability Initiative*. 2009.
3.   Edwards, P., *The Rise and Potential Peak of Cement Demand in the Urbanized World*, G.C. Magazine, Editor. 2016: CORNERSTONE, The official journal of the world coal industry
4.   Glavind, M., *5 - Sustainability of cement, concrete and cement replacement materials in construction A2 - Khatib, Jamal M*, in *Sustainability of Construction Materials*. 2009, Woodhead Publishing. p. 120-147.
5.   Temuujin, J., et al., *Utilization of radioactive high-calcium Mongolian flyash for the preparation of alkali-activated geopolymers for safe use as construction materials.* Ceramics International, 2014. **40**(10, Part B): p. 16475-16483.
6.   Provis, J.L. and S.A. Bernal, *Geopolymers and Related Alkali-Activated Materials.* Annual Review of Materials Research, 2014. **44**: p. 299-327.
7.   Okoye, F.N., J. Durgaprasad, and N.B. Singh, *Mechanical properties of alkali activated flyash/Kaolin based geopolymer concrete.* Construction and Building Materials, 2015. **98**(Supplement C): p. 685-691.
8.   Nabil Bouzoubaa, M.-H.Z.V.M.M. and M.G. Dean, *Blended Fly Ash Cements A Review.* Materials Journal, 1999. **96**(6).
9.   J. Geiseler, H.K. and E. Lang, *Influence of Blast Furnace Cements on Durability of Concrete Structures.* Materials Journal, 1995. **92**(3).
10.   Wongkeo, W., et al., *Compressive strength and chloride resistance of self-compacting concrete containing high level fly ash and silica fume.* Materials & Design, 2014. **64**: p. 261-269.
11.   Davidovits, J., *Geopolymer chemistry and application*, ed. t. Edition. 2015, Saint-Quentin, France: Geopolymer Institute.
12.   Blissett, R.S. and N.A. Rowson, *A review of the multi-component utilisation of coal fly ash.* Fuel, 2012. **97**: p. 1-23.
13.   Djwantoro Hardjito, S.E.W.D.M.J.S. and B.V. Rangan, *On the Development of Fly Ash-Based Geopolymer Concrete.* Materials Journal, 2004. **101**(6).
14.   Kong, D.L.Y. and J.G. Sanjayan, *Effect of elevated temperatures on geopolymer paste, mortar and concrete.* Cement and Concrete Research, 2010. **40**(2): p. 334-339.
15.   S.E., W., *Creep Behaviour of Fly Ash-Based Geopolymer Concrete*. 2010. Vol. 12. 2010.
16.   Thokchom, S., P. Ghosh, and S. Ghosh, *Resistance of fly ash based geopolymer mortars in sulfuric acid.* arPN Journal of engineering and applied Sciences, 2009. **4**.
17.   Association, A.R.T.B., *Production and use of coal combustion products in the U.S.* 2015, American Coal Ash Association.
18.   Administartion, *U.S.E.I. Missouri State Profile and Energy Estimates*. 2015.
19.   Agency, *U.S.E.P. National Primary Drinking Regulation*. 2017.
20.   Sturgis, S. *Disaster in east Tennessee*. 2010; Available from: https://grist.org/article/disaster-in-east-tennessee/full/.
21.   Diaz, E.I., E.N. Allouche, and S. Eklund, *Factors affecting the suitability of fly ash as source material for geopolymers.* Fuel, 2010. **89**(5): p. 992-996.

22.   Ahmaruzzaman, M., *A review on the utilization of fly ash.* Progress in Energy and Combustion Science, 2010. **36**(3): p. 327-363.
23.   *Standard Specification for Coal Fly Ash and Raw or Calcined Natural Pozzolan for Use in Concrete*, in *American Society for Testing Materials, ASTM C618*. 2015.
24.   Association, C.S., *Cementitious materials for use in concrete.* CAN/CSA A3001, 2008.
25.   Somna, K., et al., *NaOH-activated ground fly ash geopolymer cured at ambient temperature.* Fuel, 2011. **90**(6): p. 2118-2124.
26.   Zhu, J.P., et al. *Influence of particle size distribution of fly ash on compressive strength and durability of Portland cement concrete*. in *Materials Science Forum*. 2011. Trans Tech Publ.
27.   Davidovits, J., *Geopolymers.* Journal of thermal analysis, 1991. **37**(8): p. 1633-1656.
28.   Davidovits, J., *High-Alkali Cements for 21st Century Concretes.* Special Publication, 1994. **144**.
29.   Van Jaarsveld, J.G.S., J.S.J. Van Deventer, and L. Lorenzen, *The potential use of geopolymeric materials to immobilise toxic metals: Part I. Theory and applications.* Minerals Engineering, 1997. **10**(7): p. 659-669.
30.   Komnitsas, K. and D. Zaharaki, *Geopolymerisation: A review and prospects for the minerals industry.* Minerals Engineering, 2007. **20**(14): p. 1261-1277.
31.   Davidovits, J. *Chemistry of geopolymeric systems, terminology*. in *Geopolymer*. 1999.
32.   Hardjito, H. and R.V. Rangan, *Development and properties of low-calcium fly ash based geopolymer concrete.* 2005, Research Report GC1, Faculty of Engineering, Curtin University of Technology, Perth, Australia.
33.   Bakharev, T., *Geopolymeric materials prepared using Class F fly ash and elevated temperature curing.* Cement and Concrete Research, 2005. **35**(6): p. 1224-1232.
34.   Ana M. Fernandez-Jimenez, A.P. and L.-H. Cecilio, *Engineering Properties of Alkali-Activated Fly Ash Concrete.* Materials Journal, 2006. **103**(2).
35.   Sofi, M., et al., *Engineering properties of inorganic polymer concretes (IPCs).* Cement and Concrete Research, 2007. **37**(2): p. 251-257.
36.   Ryu, G.S., et al., *The mechanical properties of fly ash-based geopolymer concrete with alkaline activators.* Construction and Building Materials, 2013. **47**(Supplement C): p. 409-418.
37.   Nagalia, G., et al., *Compressive Strength and Microstructural Properties of Fly Ash–Based Geopolymer Concrete.* Journal of Materials in Civil Engineering, 2016. **28**(12): p. 04016144.
38.   Lee, N.K. and H.K. Lee, *Setting and mechanical properties of alkali-activated fly ash/slag concrete manufactured at room temperature.* Construction and Building Materials, 2013. **47**: p. 1201-1209.
39.   Puertas, F., et al., *Mechanical and durable behaviour of alkaline cement mortars reinforced with polypropylene fibres.* Cement and Concrete Research, 2003. **33**(12): p. 2031-2036.
40.   Li, X., et al., *Mechanical properties and microstructure of class C fly ash-based geopolymer paste and mortar.* Materials, 2013. **6**(4): p. 1485-1495.
41.   Gourley, J. *Geopolymers; opportunities for environmentally friendly construction materials*. in *Materials 2003 Conference: Adaptive Materials for a Modern Society, Sydney, Institute of Materials Engineering Australia*. 2003.

42. Chindaprasirt, P., et al., *High-Strength Geopolymer Using Fine High-Calcium Fly Ash.* Journal of Materials in Civil Engineering, 2011. **23**(3): p. 264-270.

43. Guo, X., H. Shi, and W.A. Dick, *Compressive strength and microstructural characteristics of class C fly ash geopolymer.* Cement and Concrete Composites, 2010. **32**(2): p. 142-147.

44. Chindaprasirt, P., T. Chareerat, and V. Sirivivatnanon, *Workability and strength of coarse high calcium fly ash geopolymer.* Cement and Concrete Composites, 2007. **29**(3): p. 224-229.

45. Pattanapong, T.-N., C. Prinya, and S. Vanchai, *Setting Time, Strength, and Bond of High-Calcium Fly Ash Geopolymer Concrete.* Journal of Materials in Civil Engineering, 2015. **27**(7).

46. Thomas, R.J. and S. Peethamparan, *Alkali-activated concrete: Engineering properties and stress–strain behavior.* Construction and Building Materials, 2015. **93**(Supplement C): p. 49-56.

47. Bakharev, T., *Thermal behaviour of geopolymers prepared using class F fly ash and elevated temperature curing.* Cement and Concrete Research, 2006. **36**(6): p. 1134-1147.

48. Diaz-Loya, E.I., E.N. Allouche, and V. Saiprasad, *Mechanical Properties of Fly-Ash-Based Geopolymer Concrete.* Materials Journal, 2011. **108**(3).

49. Temuujin, J., R.P. Williams, and A. van Riessen, *Effect of mechanical activation of fly ash on the properties of geopolymer cured at ambient temperature.* Journal of Materials Processing Technology, 2009. **209**(12): p. 5276-5280.

50. Duxson, P., et al., *Geopolymer technology: the current state of the art.* Journal of Materials Science, 2007. **42**(9): p. 2917-2933.

51. Singh, B., et al., *Effect of activator concentration on the strength, ITZ and drying shrinkage of fly ash/slag geopolymer concrete.* Construction and Building Materials, 2016. **118**: p. 171-179.

52. Sabitha, D., et al., *Reactivity, workability and strength of potassium versus sodium-activated high volume fly ash-based geopolymers.* Current Science, 2012. **103**(11): p. 1320-1327.

53. van Jaarsveld, J.G.S. and J.S.J. van Deventer, *Effect of the Alkali Metal Activator on the Properties of Fly Ash-Based Geopolymers.* Industrial & Engineering Chemistry Research, 1999. **38**(10): p. 3932-3941.

54. Abdullah, M., et al. *The relationship of NaOH molarity, Na2SiO3/NaOH ratio, fly ash/alkaline activator ratio, and curing temperature to the strength of fly ash-based geopolymer.* in *Advanced Materials Research.* 2011. Trans Tech Publ.

55. Görhan, G. and G. Kürklü, *The influence of the NaOH solution on the properties of the fly ash-based geopolymer mortar cured at different temperatures.* Composites Part B: Engineering, 2014. **58**: p. 371-377.

56. Muthadhi, A. and V. Dhivya, *Investigating Strength Properties of Geopolymer Concrete with Quarry Dust.* Materials Journal, 2017. **114**(3).

57. Yang, K.-H., A.-R. Cho, and J.-K. Song, *Effect of water–binder ratio on the mechanical properties of calcium hydroxide-based alkali-activated slag concrete.* Construction and Building Materials, 2012. **29**: p. 504-511.

58. Deb, P.S., P. Nath, and P.K. Sarker, *The effects of ground granulated blast-furnace slag blending with fly ash and activator content on the workability and strength properties of*

geopolymer concrete cured at ambient temperature. Materials & Design (1980-2015), 2014. **62**: p. 32-39.

59. Zhang Hongen, J.F.W.Q.T.L. and X. Shi, *Influence of Cement on Properties of Fly-Ash-Based Concrete.* Materials Journal, 2017. **114**(05).

60. Rattanasak, U. and P. Chindaprasirt, *Influence of NaOH solution on the synthesis of fly ash geopolymer.* Minerals Engineering, 2009. **22**(12): p. 1073-1078.

61. Rattanasak, U., K. Pankhet, and P. Chindaprasirt, *Effect of chemical admixtures on properties of high-calcium fly ash geopolymer.* International Journal of Minerals, Metallurgy, and Materials, 2011. **18**(3): p. 364.

62. Chamila Gunasekara, S.S. and W.L. David, *Long-Term Mechanical Properties of Different Fly Ash Geopolymers.* Structural Journal, 2017. **114**(3).

63. Chindaprasirt, P., et al., *Effect of SiO2 and Al2O3 on the setting and hardening of high calcium fly ash-based geopolymer systems.* Journal of Materials Science, 2012. **47**(12): p. 4876-4883.

64. Kotwal, A.R., et al., *Characterization and Early Age Physical Properties of Ambient Cured Geopolymer Mortar Based on Class C Fly Ash.* International Journal of Concrete Structures and Materials, 2015. **9**(1): p. 35-43.

65. Palacios, M. and F. Puertas, *Effectiveness of Mixing Time on Hardened Properties of Waterglass-Activated Slag Pastes and Mortars.* ACI Materials Journal, 2011. **108**(1).

66. Chindaprasirt, P., P. De Silva, and S. Hanjitsuwan, *Effect of High-Speed Mixing on Properties of High Calcium Fly Ash Geopolymer Paste.* Arabian Journal for Science and Engineering, 2014. **39**(8): p. 6001-6007.

67. Lowke, D. and P. Schiessl, *Effect of mixing energy on fresh properties of SCC.* Paper, Technical University of Munich, Centre of Building Materials, 2005: p. 1-8.

68. Pan, Z., J.G. Sanjayan, and B.V. Rangan, *An investigation of the mechanisms for strength gain or loss of geopolymer mortar after exposure to elevated temperature.* Journal of Materials Science, 2009. **44**(7): p. 1873-1880.

69. Swanepoel, J.C. and C.A. Strydom, *Utilisation of fly ash in a geopolymeric material.* Applied Geochemistry, 2002. **17**(8): p. 1143-1148.

70. Sindhunata, et al., *Effect of Curing Temperature and Silicate Concentration on Fly-Ash-Based Geopolymerization.* Industrial & Engineering Chemistry Research, 2006. **45**(10): p. 3559-3568.

71. Ding, Y., J.-G. Dai, and C.-J. Shi, *Mechanical properties of alkali-activated concrete: A state-of-the-art review.* Construction and Building Materials, 2016. **127**(Supplement C): p. 68-79.

72. Deb, P.S., *Durability of Fly Ash Based Geopolymer Concrete*, in *Civil Engineering.* June 2013, Curtin University. p. 178.

73. E. Douglas, A.B. and V.M. Malhotra, *Properties and Durability of Alkali-Activated Slag Concrete.* Materials Journal, 1992. **89**(5).

74. *Standard Test Method for Resistance of Concrete to Rapid Freezing and Thawing.* 2015.

75. Škvára, F., T. Jílek, and L. Kopecký, *Geopolymer materials based on fly ash.* Ceram.-Silik, 2005. **49**(3): p. 195-204.

76. Škvára, F., et al., *Concrete based on fly ash geopolymers.* Proceedings of 16th IBAUSIL, 2006. **1**: p. 1079-1097.

77. Sun, P. and H.-C. Wu, *Chemical and freeze–thaw resistance of fly ash-based inorganic mortars.* Fuel, 2013. **111**: p. 740-745.

78. Sun, P., *Fly ash based inorganic polymeric building material.* 2006.
79. Brooks, R., et al., *Properties of alkali-activated fly ash: high performance to lightweight.* International Journal of Sustainable Engineering, 2010. **3**(3): p. 211-218.
80. Rostami, H. and W. Brendley, *Alkali Ash Material: A Novel Fly Ash-Based Cement.* Environmental Science & Technology, 2003. **37**(15): p. 3454-3457.
81. Cyr, M. and R. Pouhet, *The frost resistance of alkali-activated cement-based binders*, in *Handbook of Alkali-Activated Cements, Mortars and Concretes*. 2015, Woodhead Publishing: Oxford. p. 293-318.
82. DEGIRMENCI, F.N., *Freeze-thaw and fire resistance of geopolymer mortar based on natural and waste pozzolans.* Ceramics–Silikáty, 2018. **62**(1): p. 41-49.
83. Davalos, J., *Advanced materials for civil infrastructure rehabilitation and protection.* Seminar at The City College of New York, New York, 2012.
84. Pacheco-Torgal, F., et al., *23 - Performance of alkali-activated mortars for the repair and strengthening of OPC concrete*, in *Handbook of Alkali-Activated Cements, Mortars and Concretes*. 2015, Woodhead Publishing: Oxford. p. 627-641.
85. Yan, L. and N. Chouw, *Behavior and analytical modeling of natural flax fibre-reinforced polymer tube confined plain concrete and coir fibre-reinforced concrete.* Journal of Composite Materials, 2013. **47**(17): p. 2133-2148.
86. Pacheco-Torgal, F., J.P. Castro-Gomes, and S. Jalali, *Adhesion characterization of tungsten mine waste geopolymeric binder. Influence of OPC concrete substrate surface treatment.* Construction and Building Materials, 2008. **22**(3): p. 154-161.
87. Phoo-ngernkham, T., et al., *Adhesion characterisation of Portland cement concrete and alkali-activated binders.* Advances in Cement Research, 2017. **0**(0): p. 1-11.
88. McLellan, B.C., et al., *Costs and carbon emissions for geopolymer pastes in comparison to ordinary portland cement.* Journal of Cleaner Production, 2011. **19**(9): p. 1080-1090.
89. Mathew, M.B.J., M.M. Sudhakar, and D.C. Natarajan, *Strength, economic and sustainability characteristics of coal ash–GGBS based geopolymer concrete.* International Journal of Computational Engineering Research, 2013. **3**(1): p. 207-212.
90. *Standard Test Method for Relative Density (Specific Gravity) and Absorption of Coarse Aggregate*. 2015.
91. *Standard Specification for Concrete Aggregates*. 2016, ASTM International.
92. *Standard Test Method for Relative Density (Specific Gravity) and Absorption of Fine Aggregate*. 2015.
93. *Standard Specification for Standard Sand*. 2017.
94. *Standard Test Method for Major and Minor Elements in Coal and Coke Ash by X-Ray Fluorescence*, in *American Society for Testing Materials, ASTM D4326*. 2013.
95. BRUKER, *X-Ray Radiattion Safety-Manual for Operator Training*. 2010.
96. Arvaniti, E.C., et al., *Physical characterization methods for supplementary cementitious materials.* Materials and Structures, 2015. **48**(11): p. 3675-3686.
97. *Standard Test Method for True Specific Gravity of Refractory Materials by Gas-Comparison Pycnometer*. 2012.
98. *Standard Specification for Flow Table for Use in Tests of Hydraulic Cement*. 2014.
99. *Standard Test Method for Flow of Hydraulic Cement Mortar*, in *American Soceity for Testing Materials, ASTM C1437*. 2015.
100. *Standard Test Methods for Time of Setting of Hydraulic Cement by Vicat Needle*, in *American Soceity for Testing Materials, ASTM C191*. 2013.

101.   *Standard Test Method for Compressive Strength of Hydraulic Cement Mortars (Using 2-in. or [50-mm] Cube Specimens)*, in *American Soceity for Testing Materials, ASTM C109*. 2016.

102.   *Standard Specification for Portland Cement*, in *American Society for Testing Materials, ASTM C150*. 2016.

103.   *Standard Test Method for Slump of Hydraulic-Cement Concrete*. 2015.

104.   *Standard Practice for Making and Curing Concrete Test Specimens in the Laboratory*. 2016, ASTM International.

105.   *Standard Test Method for Compressive Strength of Cylindrical Concrete Specimens*. 2016.

106.   *Standard Test Method for Compressive Strength of Hydraulic Cement Mortars (Using 2-in. or [50-mm] Cube Specimens)*. 2016, ASTM International.

107.   *Standard Test Methods for Time of Setting of Hydraulic Cement by Vicat Needle*. 2013.

108.   Kumar, S. and R. Kumar, *Mechanical activation of fly ash: Effect on reaction, structure and properties of resulting geopolymer.* Ceramics International, 2011. **37**(2): p. 533-541.

109.   Siyal, A.A., et al., *Effects of Parameters on the Setting Time of Fly Ash Based Geopolymers Using Taguchi Method.* Procedia Engineering, 2016. **148**: p. 302-307.

110.   Gomaa, E., et al., *Fresh properties and compressive strength of high calcium alkali activated fly ash mortar.* Journal of King Saud University - Engineering Sciences, 2017.

111.   Temuujin, J., A. van Riessen, and R. Williams, *Influence of calcium compounds on the mechanical properties of fly ash geopolymer pastes.* Journal of Hazardous Materials, 2009. **167**(1–3): p. 82-88.

112.   Puertas, F., et al., *Alkali-activated fly ash/slag cements.* Cement and Concrete Research, 2000. **30**(10): p. 1625-1632.

113.   Guo, X., et al., *Alkali-activated complex binders from class C fly ash and Ca-containing admixtures.* Journal of Hazardous Materials, 2010. **173**(1–3): p. 480-486.

114.   Yip, C.K., G.C. Lukey, and J.S.J. van Deventer, *The coexistence of geopolymeric gel and calcium silicate hydrate at the early stage of alkaline activation.* Cement and Concrete Research, 2005. **35**(9): p. 1688-1697.

115.   Morsy, M.S., et al., *Effect of Sodium Silicate to Sodium Hydroxide Ratios on Strength and Microstructure of Fly Ash Geopolymer Binder.* Arabian Journal for Science and Engineering, 2014. **39**(6): p. 4333-4339.

116.   Part, W.K., M. Ramli, and C.B. Cheah, *An overview on the influence of various factors on the properties of geopolymer concrete derived from industrial by-products.* Construction and Building Materials, 2015. **77**: p. 370-395.

117.   Yip, C.K., et al., *Effect of calcium silicate sources on geopolymerisation.* Cement and Concrete Research, 2008. **38**(4): p. 554-564.

118.   van Deventer, J.S.J., et al., *Reaction mechanisms in the geopolymeric conversion of inorganic waste to useful products.* Journal of Hazardous Materials, 2007. **139**(3): p. 506-513.

119.   Panias, D., I.P. Giannopoulou, and T. Perraki, *Effect of synthesis parameters on the mechanical properties of fly ash-based geopolymers.* Colloids and Surfaces A: Physicochemical and Engineering Aspects, 2007. **301**(1): p. 246-254.

120.   Cho, H., et al., *Solution state structure determination of silicate oligomers by 29Si NMR spectroscopy and molecular modeling.* Journal of the American Chemical Society, 2006. **128**(7): p. 2324-2335.

121. *Standard Test Method for Density (Unit Weight), Yield, and Air Content (Gravimetric) of Concrete.* 2016.

122. *Standard Test Method for Air Content of Freshly Mixed Concrete by the Pressure Method.* 2014.

123. *Standard Test Method for Temperature of Freshly Mixed Hydraulic-Cement Concrete.* 2017.

124. *Standard Test Method for Compressive Strength of Cylindrical Concrete Specimens.* 2017, ASTM International.

125. *Standard Test Method for Splitting Tensile Strength of Cylindrical Concrete Specimens.* 2011, ASTM International.

126. *Standard Test Method for Static Modulus of Elasticity and Poisson’s Ratio of Concrete in Compression.* 2014.

127. *Standard Test Method for Flexural Strength of Concrete (Using Simple Beam with Third-Point Loading).* 2016, ASTM International.

128. *Standard Test Method for Length Change of Hardened Hydraulic-Cement Mortar and Concrete.* 2017.

129. Pangdaeng, S., et al., *Influence of curing conditions on properties of high calcium fly ash geopolymer containing Portland cement as additive.* Materials & Design, 2014. **53**: p. 269-274.

130. Lee, W.K.W. and J.S.J. van Deventer, *The effects of inorganic salt contamination on the strength and durability of geopolymers.* Colloids and Surfaces A: Physicochemical and Engineering Aspects, 2002. **211**(2–3): p. 115-126.

131. Garcia-Lodeiro, I., et al., *Compatibility studies between N-A-S-H and C-A-S-H gels. Study in the ternary diagram Na2O–CaO–Al2O3–SiO2–H2O.* Cement and Concrete Research, 2011. **41**(9): p. 923-931.

132. Davidovits, J. and M. Davidovics, *Geopolymer: Room-Temperature Ceramic Matrix for Composites*, in *Proceedings of the 12th Annual Conference on Composites and Advanced Ceramic Materials: Ceramic Engineering and Science Proceedings.* 2008, John Wiley & Sons, Inc. p. 835-841.

133. ACI, A., *318-14.* Building Code Requirements for Structural Concrete, American Concrete Institute, Farmington Hills, Michigan, 2014.

134. AS, A.S., *Concrete structures.* AS3600-2001. Sydney (Australia): Standards Australia, 2001.

135. CEB-FIP, C., *Model code 2010.* Comite Euro-International du beton, 2010.

136. Hanjitsuwan, S., et al., Cem. Concr. Compos., 2014. **45**: p. 9.

137. AASHTO, T., *95-11 "Standard Method of Test for Surface Resistivity Indication of Concrete's Ability to Resist Chloride Ion Penetration.".* AASHTO Provisional Standards, 2011 Edition, 2011.

138. *Standard Test Method for Bulk Electrical Conductivity of Hardened Concrete.* 2012.

139. *Standard Test Method for Electrical Indication of Concrete's Ability to Resist Chloride Ion Penetration.* 2017.

140. Beaudoin, J.J. and C. MacInnis, *The mechanism of frost damage in hardened cement paste.* Cement and Concrete Research, 1974. **4**(2): p. 139-147.

141. Shi Yan, Y.H., *Aging Mechanism of Dam Concrete under the action of Freeze-Thaw Damage* Applied Mechanics and Materials 2014.

142. Fan, L., *Research into the concrete freeze-thaw damage mechanism based on the principle of thermodynamics.* Applied Mechanics and Materials 2013.

143. Ben Li, K.W., *STUDY ON THE DAMAGE MECHANISM OF PORE STRUCTURE IN CONCRETE SUBJECTED TO FREEZE-THAW CYCLES.* THE CIVIL ENGINEERING JOURNAL, 2015.

144. Azarsa, P. and R. Gupta, *Electrical Resistivity of Concrete for Durability Evaluation: A Review.* Advances in Materials Science and Engineering, 2017. **2017**: p. 30.

145. *Resipod Family Operating instructions, concrete durability testing, Proceq SA.* 2017 [cited 2017.

146. PCTE. *Dy-2 Pull Off Tester*. 2017 [cited 2018 04/11/2018]; Available from: http://www.pcte.com.au/dy-2-pull-off-tester.

147. Bonaldo, E., J.A.O. Barros, and P.B. Lourenço, *Bond characterization between concrete substrate and repairing SFRC using pull-off testing.* International Journal of Adhesion and Adhesives, 2005. **25**(6): p. 463-474.